11-1-2014

Condition Monitoring System of Wind Turbine Generators

Khaled Bubaker Abdusamad
University of Denver

CONDITION MONITORING SYSTEM OF WIND TURBINE GENERATORS

A Dissertation

Presented to

The Faculty of the Daniel Felix Ritchie School of Engineering and Computer Science

University of Denver

_____

In Partial Fulfillment

of the Requirements for the Degree

Doctor of Philosophy

_____

by

Khaled B. Abdusamad

November 2014

Advisor: David Wenzhong Gao

Author: Khaled B. Abdusamad
Title: CONDITION MONITORING SYSTEM OF WIND TURBINE GENERATORS
Advisor: David Wenzhong Gao.
Degree Date: November, 2014

Abstract

The development and implementation of the condition monitoring systems (CMS) play a significant role in overcoming the number of failures in the wind turbine generators that result from the harsh operation conditions, such as over temperature, particularly when turbines are deployed offshore. In order to increase the reliability of the wind energy industry, monitoring the operation conditions of wind generators is essential to detect the immediate faults rapidly and perform appropriate preventative maintenance. CMS helps to avoid failures, decrease the potential shutdowns while running, reduce the maintenance and operation costs and maintain wind turbines protected. The knowledge of wind turbine generators' faults, such as stator and rotor inter-turn faults, is indispensable to perform the condition monitoring accurately, and assist with maintenance decision making.

Many techniques are utilized to avoid the occurrence of failures in wind turbine generators. The majority of the previous techniques that are applied to monitor the wind generator conditions are based on electrical and mechanical concepts and theories. An advanced CMS can be implemented by using a variety of different techniques and methods to confirm the validity of the obtained electrical and mechanical condition monitoring algorithms.

This thesis is focused on applying CMS on wind generators due to high temperature by contributing the statistical, thermal, mathematical, and reliability analyses, and mechanical concepts with the electrical methodology, instead of analyzing the electrical signal and frequencies trends only. The newly developed algorithms can be compared with previous condition monitoring methods, which use the electrical approach in order to establish their advantages and limitations. For example, the hazard reliability techniques of wind generators based on CMS are applied to develop a proper maintenance strategy, which aims to extend the system life-time and reduce the potential failures during operation due to high generator temperatures. In addition, the use of some advanced statistical techniques, such as regression models, is proposed to perform a CMS on wind generators. Further, the mechanical and thermal characteristics are employed to diagnose the faults that can occur in wind generators. The rate of change in the generator temperature with respect to the induced electrical torque; for instance is considered as an indicator to the occurrence of faults in the generators. The behavior of the driving torque of the rotating permanent magnet with respect to the permanent magnet temperature can also utilize to indicate the operation condition. The permanent magnet model describes the rotating permanent magnet condition during operation in the normal and abnormal situations. In this context, a set of partial differential equations is devolved for the characterization of the rotations of the permanent. Finally, heat transfer analysis and fluid mechanics methods are employed to develop a suitable CMS on the wind generators by analyzing the operation conditions of the generator's heat exchanger. The proposed methods applied based on real data of different wind turbines, and the obtained results were very convincing.

Acknowledgements

The completion of my doctoral degree was possible with the support of several people. First and foremost, I would like to give greatest thanks to my supervisor, Dr. Wenzhong Gao, for his support, encouragement, expert advice, understanding, and coordination of my research. I would also like to thank Dr. Kathryn Johnson, who collects the data measurements of my research from Colorado School of Mines and National Renewable Energy Laboratory. I owe a great deal of thanks to Dr. Yun Bo Yi and Dr. Mohammad Matin, the members of my supervisory committee. I would like also to thank the Libyan Ministry of Higher Education and Scholarship Program and the Canadian Bureau for International Education (CBIE) for funding my Ph.D. study. Thanks to Dr. Matt Gordon, the chair of the Mechanical and Material department for his support, help, and great advice. Special thanks to Renee Carvalho and Elizabeth Buckius from the Engineering Office and Office of Graduate Studies for their support with paperwork. I most want to thank my wife Hana Tmomen and my kids Muad, Malek, Nader, and Lamar for their love, enormous support and countless sacrifices to help me get to this point. This dissertation is dedicated to my parents Abubaker Abdusamad and Salwa Al-Kome for their love, endless support and encouragement.

Table of Contents

List of Figures

List of Tables

Nomenclature

Chapter 4

τ_{ripp}	-The ripple torque
τ_{cog}	-The cogging torque
$\emptyset_g$	-The air-gap flux
R_g	-The air-gap reluctance
φ	-The position of the rotor
B_r	-The remanent magnetic densities at temperature T
$B_{r_{amb}}$	-The remanent magnetic densities at the ambient temperature
α_B	-The temperature coefficients for the remanent magnetic density
α_H	-The temperature coefficients for the coercive field intensity
T_G	-The generator temperature
T_{amb}	-The ambient temperature
H_c	-The forced or coercive field intensities at the operation temperature
$H_{c_{amb}}$	-The forced or coercive field intensities at the ambient temperature
P_{el}	-The electrical power
P_{mech}	-The mechanical power
P_{loss}	- The frictional losses power
P_{SL}	-The stray losses
$P_{F\&W}$	-The friction and windage losses
P_{CL}	-The core losses
P_{cu}	-The copper losses
R_A	-The armature resistance (the generator stator resistance)
I_A	-The armature current flow (the phase current)
R_{th1}	-The thermal resistance from the windings to the case
R_{th2}	-The thermal resistance case to the ambient
τ_{el}	-The electromagnetic torque
K_M	-The generator torque constant
E_a	-The internal generated voltage
$V_\emptyset$	-The output phase voltage
X_s	-The synchronous reactance of the generator
ω_s	-The generator synchronous speed
δ	-The torque angle of synchronous generator
τ_m	-The mechanical torque
τ_{lacc}	-The acceleration torque
J	-The combined generator rotor and wind turbine inertia coefficient
τ_{Ls}	-The low-speed side shaft torque
τ_{Hs}	-The high-speed side shaft torque
ω_t	-The rotational angular speed of the low speed shaft
ω_r	-The rotational angular speed of the high speed shaft

$J_{B,H}$	-The moment of inertia of the turbine
J_B	-The turbine blades moment of inertia
J_H	-The turbine hub moment of inertia
J_g	-The moment of inertia of the generator's rotor
D_1	-The diameter of the hub
D_2	-The diameter of the generator's rotor
l	-The blades measured length
b	-The average width of the blades
θ	-The blade angle
d	-The center of mass displacement of the blades
m_H	- The hub weight
m_g	-The generator's rotor weight
t_1	-The number of teeth on the output gear
t_2	-The number of teeth on the input gear
$\emptyset$	-The magnetic flux
N_C	-The coil turns of stator
f_e	-The electrical frequency
p	-The number of pole pairs
$\forall$	-The cylindrical volume of the permanent magnet
L	-The length of the permanent magnet
r	-The radius of the permanent magnet
ρ	-The density of the permanent magnet
m	-The total mass of the of the permanent magnet
A	-The cross section area of
n	-The normal vector at a point of the permanent magnet boundary ∂A
T	-The temperature in the cylindrical volume of the permanent magnet
c	-The specific heat of the permanent magnet air
λ	-The thermal conductivity of the permanent magnet
T_0	-The initial temperature of the surrounding
α	-The heat transfer coefficient
ω	-The velocity of a point in the $x - y$ plan
t	-The time
h	-The convection heat transfer coefficient
F	-The total levitation force in three dimensions of the permanent magnet
B	-The magnetic field due to the induced currents in the permanent magnet
m_z	-The permanent magnet mass in the $z -$ direction
ξ	-Abbreviation symbol

Chapter 5

Q_h	-The heat loss of the hot fluid
Q_c	-The heat gain of the cold fluid
$\dot{m}_h$	-The mas flow rate of the hot fluid
$\dot{m}_c$	-The mass flow rate of the cold fluid
$c_{p,h}$	-The specific heat of the hot fluid
$c_{p,c}$	-The specific heat of the cold fluid
$T_{h,i}$	-The inlet temperature of the hot fluid
$T_{c,i}$	-The inlet temperature of the cold fluid
$T_{h,o}$	-The outlet temperature of the hot fluid
$T_{c,o}$	-The outlet temperature of the cold fluid
LMTD = ΔT_m	-The logarithmic average of the temperature difference
q	-The heat flow per unit of mass (kJ/kg)
A	-The area pf the wind generator's heat exchanger
U	-The overall heat transfer coefficient
h_i	-The internal heat coefficient
h_o	-The external heat coefficient
ΔP	-The pressure drops of the flow streams through the heat exchanger
L	-The effective pipe length of the heat exchanger
d	-The pipe internal diameter
N	-The number of pipes inside the heat exchanger
V_C	-The cold fluid velocity
ρ_c	-The cold fluid density
R_e	-The shell-side Reynolds number
μ_T	-The cold fluid viscosity
ρ_0	-The cold fluid density at $T_0 = 20$C°

Chapter 6

$h(t)$	-Hazard function
$\underline{T}$	-The failure time
β	-The Weibull distribution shape parameter
α	-The Weibull distribution scale parameter
$f(t, \alpha, \beta)$	-The Weibull probability density function
$R(t, \alpha, \beta)$	-The Weibull survival function
σ_x	-The standerd deviation of the group of data (x);
μ_x	-The average value of the group of data (x);
$S(t)$	-The survival function
$E(T)$	-The mean of the Weibull probability density function
$S.D$	-The standard deviation of the Weibull probability density function
$F(t, \alpha, \beta)$	-The Weibull cumulative distribution function
$F(t)$	-The cumulative distribution function

MTTF	-The mean time to failure
$R_m(t)$	-The reliability of the maintained system at time t
$MTTF_{var}$	- The variance of MTTF
$MTTF_{ML}$	-The median Life of the MTTF
$MTTF_{S.D.}$	- The standard deviation of the MTTF

Chapter 7

GP	-Generator power
OT	-Ambient or outside temperature
NT	-Nacelle temperature
CT	-Generator cooling temperature
y	-Dependent variable (experimental value).
$\hat{y}$	-Dependent variable (predicted by a regression model)
$\bar{y}$	-The experimental value mean (mean value of y)
n	-Number of independent variables (number of coefficients)
$X_i\ (i = 1,2, \dots, n)$	-The i^{th} independent variable from total set of n variables
$\beta_i\ (i = 1,2, \dots, n)$	-i^{th} coefficient corresponding to X_i
β_0	-The intercept coefficient (or constant)
i=1,2,3,….,n	-Independent variables' index
k	-The regression degree of freedom = The number of the independent variables
N	-Number of observations (experimental data points)
ε	-Residual (the difference between the experimental and predicted value)
σ^2	-The error variance of term y
SS_{RES}	-The residual sum square
SS_R	-The regression sum square
SS_T	-The total sum of squares
MS_{RES}	-The residual mean sum square
MS_R	-The regression mean sum square
γ	-The confidence interval percent
ϑ^2	-The residual mean square
β_{jj}	-The j^{th} diagonal element of the $(\beta'\ \beta\ )^{-1}$ matrix
C_{jj}	-The j^{th} diagonal element of the $(X'\ X\ )^{-1}$ matrix
F_0	-The significance of regression statistical value.
R^2	-The coefficient of determination.
$S_{ii}, i = 1,2,,,.,n$	-The corrected sum of squares for regressor X_i
$S_{jj}, j = 1,2,,,.,N$	-The corrected sum of squares for regressor X_j
r_{ij}	-The correlation between the regressor X_i and X_j
$\hat{b}_i$, i=1,2,….,n	-The standardized regression coefficients.
$w_i, i = 1,2, \dots, k$	-The new length standardized regression scaling.
SS_{LOF}	-The lack-of-fit sum of squares.

SS_{PE}	-The pure-error sum of squares.
F_{LOF}	-The Lack-of-fit statistical value.
df_{LOF}	-The lack-of-fit degree of freedom.
df_{PE}	-The pure error degree of freedom.
h_{ij}	-The ij^{th} element of the hat matrix H.
VIF	-The variance inflation factor.
$\hat{T}_G$	-The predicted generator temperature.
$\overline{X}_{i_{old}}$,i= 1,2,…,k	-The mean value of the old data
P	-The degree of significant
H	-The hat matrix
p	-The regression degree of freedom-1
t_0	-The significance of the regression coefficient's statistical value

Chapter 1. Introduction

1.1. Theoretical Background

The transition to using the wind energy remarkably was a very significant trend since the massive amount of the kinetic energy in the wind can be captured and converted to electrical power, which can be used in many purposes. Therefore, the rapid expansion of wind farms has drawn attention to operational and maintenance issues. The technology used in the manufacture and design of wind turbines has been developed dramatically, such as decreasing the weights of the turbine, reducing the undesirable noise, and achieving the maximum power tracking by applying felicitous control methods. Consequently, the captured annual output power increases with advanced wind turbines [1-4].

Increasing the number of wind monitoring stations and applying an advanced condition monitoring techniques lead to generating more power and reducing maintenance and operation costs from the wind energy. Checking the system components' health, either by human-based resources or smart systems, helps to prevent and bring down the number of major breakdowns. CMS is one of the efficient methods that can be used in the wind energy application for early failure detection in order to prevent the turbine components from breakdown and reduce the cost for corrective maintenance. Detecting the failures at

an early stage leads to decreasing the downtimes, and revenue losses. Therefore, the maintenance schedule can be more accurate, and the possibility of increasing the system reliability can be available [5-8].

CMS provides detailed information about the wind turbine components' condition by analyzing measured signals to predict and avoid the imminent failures that occur in the wind turbines' components. The monitoring process involves sensor measurements to determine the operation condition of the system parts. Analyzing the measured signals is very significant in order to define their behavior during the operation, which helps to take appropriate action to prevent the occurrence of technical problems. Within the control part of the CMS, regulation of the processes is considered, which requires variables and various models to identify the system condition [5-11].

CMS plays a substantial role in establishing condition-based maintenance and repair, which can be applied to determine the appropriate time to replace a component such as the wind generator and considered more beneficial than corrective and preventive maintenance. CMS therefore, provides motivation to rethink the method of wind turbine maintenance by utilizing many different techniques for monitoring the health of the wind turbine components. This benefits the most from the fact that with early failure detection in particular, for the offshore wind turbines since their farthest locations and the difficulty of conducting maintenance operations losses.

Different CMSs which have been applied on wind turbines components provide a suitable opportunity for a wide research area to develop in the field of wind turbine structural health monitoring and onsite CMSs. Autonomous online CMSs with integrated fault detection algorithms allow early warnings of mechanical and electrical defects to avoid major component failures, and side effects on other components can be reduced significantly [12, 13,]. Several faults can be detected while the defective component is still operational. Thus, essential repair actions can be planned in time and need not be taken immediately, and this fact is of special importance for offshore plants where bad conditions, such as storm or high tide, can prevent any repair actions for several weeks [10, 14,]. Evaluating significant system component conditions, therefore, leads to improved recognition of faulty parts and will simplify the reduction in time and cost within maintenance.

In general, applying a modern condition monitoring on the parts that permanently faced failures such as gearboxes and generators of the wind turbines amplifies the generated wind power and helps to reduce the operation and maintenance costs particularly which increases the reliability of the wind energy. There is a need, therefore, to develop active fault prediction algorithms, and those algorithms can be utilized to implement CMS on the wind generators.

1.2. Motivation

Condition monitoring of wind turbine generators can greatly reduce the maintenance cost and downtime for a wind turbine. Furthermore, an accurate maintenance plan can be applied by adopting the policy of CMS in order to increase the system reliability. The wind generator is one of the most significant parts of a wind turbine that are exposed to failures due to various causes such as high temperatures while running. Therefore, applying condition monitoring on these active components is very beneficial. Increased attention has been given to the manufacturers, and engineers to avoid the technical problems that occurred by wind generators during running. Various research concentrates on applying CMS on wind generators by creating different algorithms based on electrical methodologies. However, almost none of the studies have looked to use the statistical, mechanical, and thermal theories to apply an effective CMS on wind generators.

The thesis's main objective is presenting different techniques and algorithms, such as statistical, mechanical, reliability, and thermal analyses in order to apply CMS on wind generators due to different reasons, such as high temperatures of wind generators. In addition, the research presents on the types of wind generators' failures in order to study the causes and effects of such failures and develop the proposed techniques that are used in CMS of wind generators.

This research is not only general research about the application of classic methods of CMS on wind turbine generators field but also is the implementation of modern

algorithms to apply a CMS on wind turbine generators effectively. Previous research utilizes some methods to apply a condition monitoring on the wind turbine generator. In this research, various techniques are created to apply an effective CMS on the wind turbine generator.

1.3. Thesis Organization

This report is arranged and organized as follows: Chapter two provides a theoretical background about the CMS and the fault detection mechanism. Further, this chapter presents an overview of the most important previous literature that is interested in applying CMS on wind generators. Through this chapter, different algorithms and techniques are presented in the field of the wind generator's CMS. Chapter three describes the synchronous generator and induction motors failure modes. This chapter demonstrates the differences and similarities in the structure and faults for both induction and synchronous generators, which are the most widespread generators that are used in the wind turbines industry.

The thesis presents four different methods to apply CMS on the wind generators. Chapter four introduces the first method, which consists of three different algorithms are used to explain the application of CMS on the wind generators. The first algorithm concentrates on the use of the electrical torque pulsations as an indicator to monitor the generator health under different operation conditions. The mechanical torque is utilized to

evaluate accurate values of the electrical torque with respect to the acceleration torque. Through the second algorithm of the first method, the rate of change in the generator temperature with respect to the induced electrical torque is utilized to determine the faults in the wind generators. The last proposed algorithm of the first method links the mathematical, thermal, and mechanical analyses with the electrical methodology to apply CMS on the wind generators. The proposed approach is based on determining the torque of the permanent magnet of the generator with respect to the temperature of the permanent magnet, which is slightly higher than the generator temperature to implement CMS on the wind generators. The application of heat transfer analysis through wind generator's heat exchangers to apply CMS on wind generators is presented in Chapter five. The proposed method discusses the use of the heat transfer and fluid mechanics relations to indicate the faults that occur on the wind generators due to the increase in the heat loss. The heat loss parameter with respect to the logarithmic average of the temperature difference of the generator's heat exchanger is a significant indicator to define the generator operation condition. Chapter six presents the application of Hazard reliability analysis method to implement a proper maintenance strategy of wind generators based on CMS. The proposed technique is utilized to estimate the failure rates, survival rates, and the mean time to failures parameter based on the expended operating hours of the wind turbines. The use of the statistical regression models to apply a suitable CMS on the wind generators is presented in Chapter seven. The proposed method shows two types of regression models. The first type is the standard multiple linear regression model, which can be used in the linear pattern between the response and the independent variables of the model. The second

type is the polynomial regression model, which can be applied when a curvilinear relationship is existent between the response and the model's independent variables. In addition, the influence of the heat loss on the generator's temperatures is presented based on the utilization of the regression technique. The final chapter contains a conclusion of the work and a number of recommendations for future research.

Chapter 2. Condition Monitoring System Background and Literature Review.

The failures of wind generators, which occur in various forms have increased remarkably. External factors—such as harsh climate and variable electrical loads—cause abnormal operation conditions. However, wind energy shows a growing reliability due to advanced implementation of the monitoring systems recently. The development of the electric wind generators is one of the most robust accomplishments of the modern energy conversion industry. However, due to the primary restrictions of material lifetime, impairment, manufacturing deficiency, or damages in running, an electrical generator certainly will face unexpected failure, and applying a condition monitoring technique before the occurrence of failure is required. With the help of condition monitoring and fault diagnostic techniques, therefore, the proper maintenance can be scheduled to avoid the imminent failures and the operation cost could be reduced. This chapter is divided into two main parts. The first part submits a theoretical background about the CMS process. Then, a review of the most important research which is related to the implementation of CMS on the wind generators is presented [6], [15-18].

2.1. Condition Monitoring System Theoretical Background

Condition monitoring system for wind turbine components is significant for developing an effective maintenance program, which increases the generated wind power and reduces operation and maintenance expenses. An inclusive monitoring system provides diagnostic information on the health of the turbine components, and issues warnings to the maintenance crew that potential failures or critical malfunctions might be imminent. CMS, therefore, can be used to schedule maintenance tasks or repairs before a technical problem causes downtime in the whole wind turbine. Further, CMSs focus on the most expensive components, such as the generator, gearbox, and blade. However, high-level knowledge on component condition monitoring cannot be accessed quickly because of the difficulty in conducting fault experiments and the lack of field failure records. On one hand, wind farm operators are wary of adopting expensive technologies without reasonable economic justification. On the other hand, wind turbine generators (WTGs) and their associated equipment in wind farms are connected to a supervisory control and data acquisition (SCADA) system, which archives comprehensive historical signals, fault information, environmental conditions, and operational conditions [13, 14]. Using the monitoring parameters of an SCADA system is the most feasible and economical approach to assessing WTGs conditions.

The CMS techniques can be divided into two categories: off-line monitoring and on-line monitoring. The wind turbine must be taken out of service in order to allow the maintenance crew to inspect the conditions through the off-line monitoring. Usually this monitoring technique is applied as routine or scheduled maintenance at regular intervals. The maintenance includes verification of the oil condition and inspection of the functioning of the system components and the control systems. The on-line monitoring, on the other hand, provides enough details about the performance of the turbine subsystems performance while they rotate under different loading conditions. In recent years, many advanced on-line monitoring systems have been introduced to wind generators. The most common ones are vibration monitors, temperature monitors, electrical current monitors, and fluid contamination monitors [6, 7,], [9-12], [19].

The most important components of a wind generator, which faced failures are the bearing, stator, and rotor. Table 2.1 presents the failures proportions of the induction generator components. The table emphasizes that the technical faults, which occur due to the stators and bearings of the wind turbine's induction generators are very significant [20]. In general, the most failures that occur in the wind generators are due to the bearing, stator, and rotor, which requires the attention to understanding the causes of these failures.

Table 2. 1 The failures proportions of the induction generator components, [20]

Generator Components	Failure Percentage
Bearing	40%
Stator	38%
Rotor	10%
Other parts	12%

On the other hand, the implementation of the fault detection system, such as SCADA is very sensitive since it should have appropriate actions in a limited time to analyze the collected signals. SCADA system in turn, provides remote monitoring by collecting data from the system and sending them to a central computer for monitoring and control usages. Most likely, the faults in generators can be detected by several methods like current measurement and Fast Fourier Transformer [20-23]. The basic fault detection framework of wind generators can be presented as shown in Fig. 2.1. The collected data, which are related to the system physical conditions, must be analyzed through the signal processing phase. Through this phase, the signals are converted into digital numeric values, which can be manipulated by a computer. Then, noise reduction process is necessary to remove the noise from the signals. After that, classification process is required in order to categorize the signals based on the operation condition.

The faults can be categorized in different levels of urgency and system responses; for instance, they can be a caution, warning, or alarm. The caution condition indicates that there is a need of service or adjustment of the generator. However, the system will not be affected when the maintenance does not perform within a specified period. The warning condition denotes that there are some measurements within the generator system are not acceptable, and their trend is outside of the normal operating limits. Continuing in this situation will lead to serious damages or failures in the generator system. An imminent failure might occur in the alarm condition. In general, this condition indicates that the situation is very critical for the whole system as well as to the personnel. Instantaneous

shutdown is the common action in this emergency case [16], [25-30]. A number of practical approaches are available to identify the faults which are listed and explained briefly as follows:

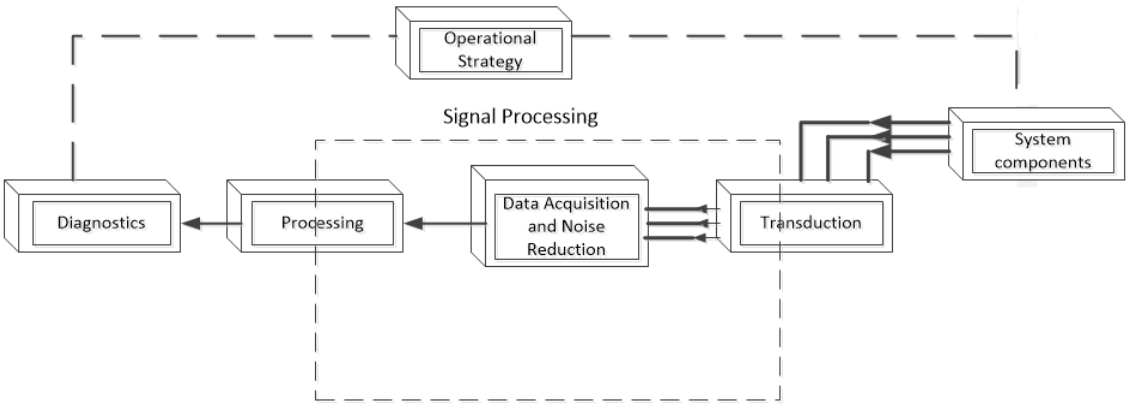

Figure 2. 1. The framework of wind generators fault detection, [20-24]

- System identification approach (Estimated parameters):

In this approach, the system identification parameters are considered in set values. The set values are compared with inputs and outputs in order to detect the faults. This method is successfully used, especially in the accurate linear processes [16], [25-30]. Figure 2.2 illustrates the system identification approach.

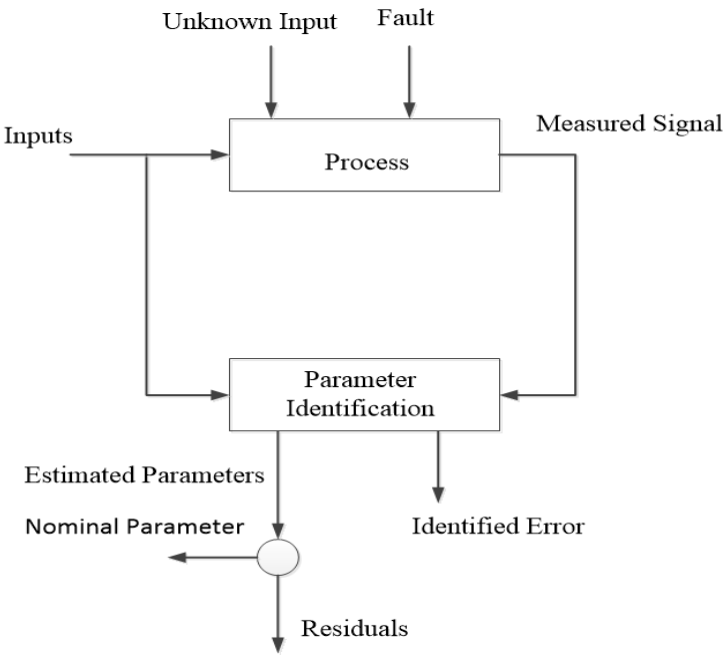

Figure 2. 2 The system identification approach [16], [25-30]

- Observer-based approach:

The observer-based approach is based on Kalman filter (recursive estimators), which is utilized in order to calculate the residuals that are the observation error. This algorithm uses a series of measurements observed over time, containing noise (random variations), which results in estimations of unknown variables that seem to be more accurate than those based on a single measurement [16], [25-30]. Figure 2.3 shows the mechanism of the observer-based approach.

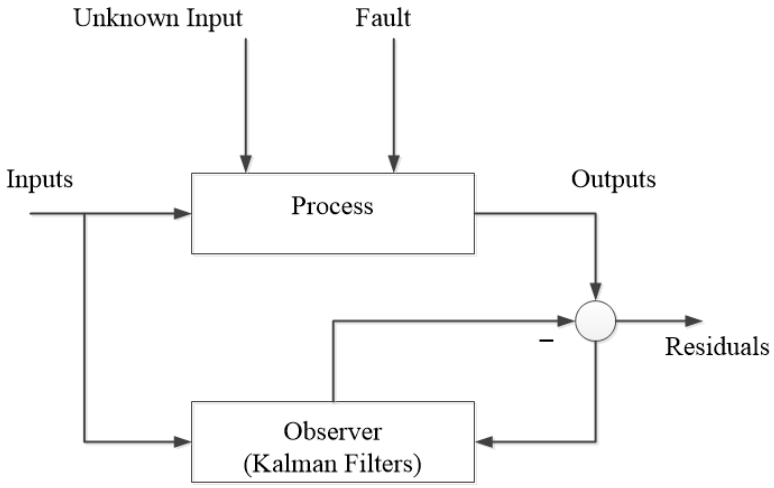

Figure 2. 3 The Observer-based approach [16], [25-30].

- Signal analysis approach:

This model is based on time and frequency signal analysis. Spectrum analysis methods are used in this approach, such as Cepstrum (includes Fourier Transformer) and envelope curve, which derive faults. This approach has successfully been applied to estimate the lifetime and other diagnosis purposes, especially in the rotating machinery [16], [25-30]. Figure 2.4 shows the mechanism of the signal analysis approach.

- Artificial intelligent (AI) and expert systems approach:

In the complex processes, an expert system can be used to model and evaluate the current conditions along as measured signals. Fuzzy techniques and Neural Networks have also been considered in the fault detection systems [16], [25-30]. Figure 2.5 shows the mechanism of the Expert system approach.

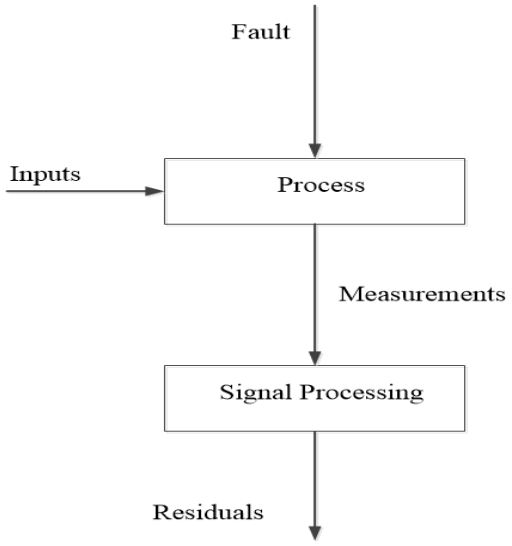

Figure 2. 4 The Signal analysis approach [16], [25-30].

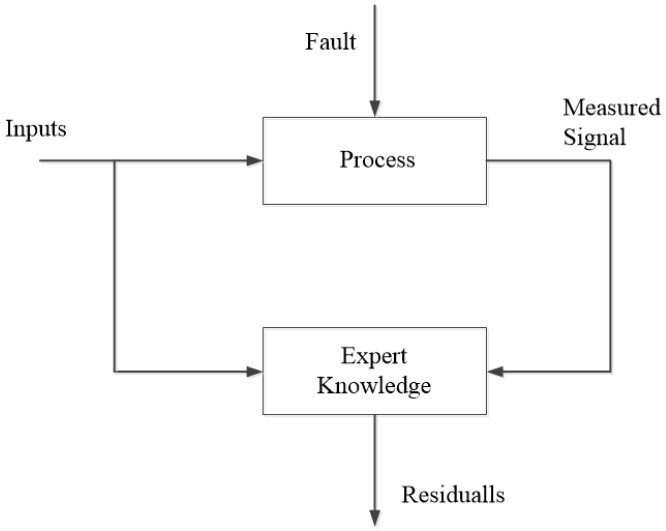

Figure 2. 5 The Expert system approach [16], [25-30].

In general, there are various techniques, which can be applied to diagnose and provide signs of the imminent failures that occur on the wind generators in order to

implement preventive maintenance opportunely. Table 2.2 displays a classification of the fault diagnosis techniques based on different methods.

Table 2. 2 The type of faults of electrical generators, [16, 20], [26-31]

Fault diagnosis Technique	Fault Description
Signal-based fault diagnosis	Mechanical vibration analysis. Shock pulse monitoring. Temperature measurement. Acoustic noise analysis. Electromagnetic field monitoring through inserted coil. Instantaneous output power variation analysis. Infrared analysis. Gas analysis. Oil analysis. Motor current signature analysis. Statistical analysis of relevant signals. Radio-frequency emission monitoring.
Model-based fault diagnosis	Neural network. Fuzzy logic analysis. Genetic algorithm. Artificial intelligence. Finite-element magnetic circuit equivalents. Linear-circuit-theory-based mathematical models.
Machine-theory-based fault analysis	Winding function approach. Modified winding function approach. Magnetic equivalent circuit.
Simulations-based fault analysis	Finite-element analysis. Time-step coupled finite element state space analysis

2.2. Literature Review

Condition monitoring and fault diagnosis of the wind generators have been covered in past literature. Researchers have improved several condition-monitoring techniques that

can apply on the wind generators and increase the reliability of the wind energy industry. For instance, the analysis of the generator temperature trend based on the Nonlinear State Estimate Technique (NSET) is proposed to apply a CMS on wind generators [15]. The differences between the estimated generator temperatures values of the proposed model and the generator temperatures, which are measured by SCADA can be used as an important indicator to identify the faults that occur due to the elevated temperatures of the wind generators. When the generator experiences a fault, new observation vectors will deviate from the standard working space, and the NSET estimate of the residual distribution and its time development will change. The moving window averaging approach is used to find out the statistically significant changes of the residual mean value and standard deviation in an efficient manner. An incipient failure will be flagged when the residual mean value and standard deviation exceed previously the specified thresholds. The results of the proposed method emphasize that the initial failure can be defined when the residuals between model estimates and the measured generator temperature become significant. The method identifies the generator over temperatures before the damage is occurred, which results in a complete shutdown of the turbine. Figure 2.6 shows the residual between the NSET technique and real generator temperatures is almost zero, which confirms the validity of the proposed model.

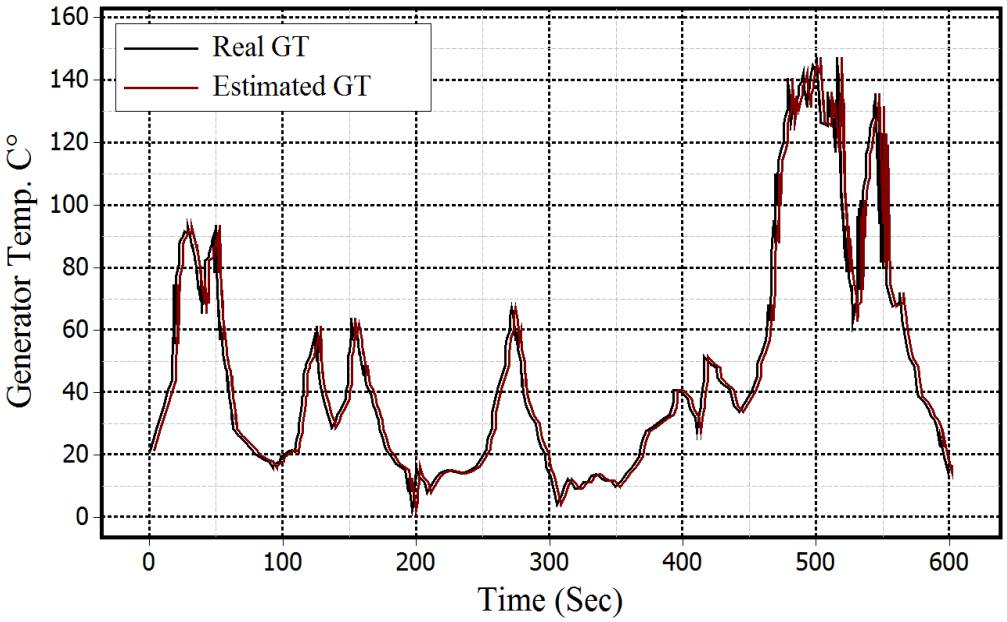

Figure 2. 6 The validation result for NSET model [15].

Yang Wenxian, P. J. Tavner, and Michael Wilkinson discussed the use of the mechanical characters to diagnose the electrical faults that occur in the wind generators when they operate under different conditions [16]. The authors proposed the use of the Continuous Wavelet Transform function (CWT) to analyze the power signal based on a valid signal processing technique, which helps to detect the mechanical and electrical faults in the wind generators. They assumed that when the electrical torque varies slowly relative to the electrical grid frequency, a steady-state condition (the mechanical torque is equivalent approximately to the electric torque) might be taken for the analysis. A stator winding fault in the generator is simulated on the test rig by simultaneously shorting three coils, which are installed on the stator of the generator. When the connection state of the coils changes periodically, the behavior of the produced electrical torque with respect to

the rotational speed of the generator's rotor will change dramatically, which determine the generator operation condition.

The torque/speed signals will significantly increase when the coils of the stator are shorted, and the corresponding synchronous reactance of the generator decreases remarkably (fault condition). On the other hand, when the coils of the stator are well-connected, the torque/speed signals will significantly decrease and the corresponding synchronous reactance of the generator increases as shown in the Fig. 2.7, which presents the time-waveforms of the torque speed signals. The drawback of the proposed work is limited in the assumption of balancing the mechanical and electrical torque. In the real conditions, the generator torque is reduced by the acceleration torque, which needs to be estimated to evaluate accurate electrical torque values.

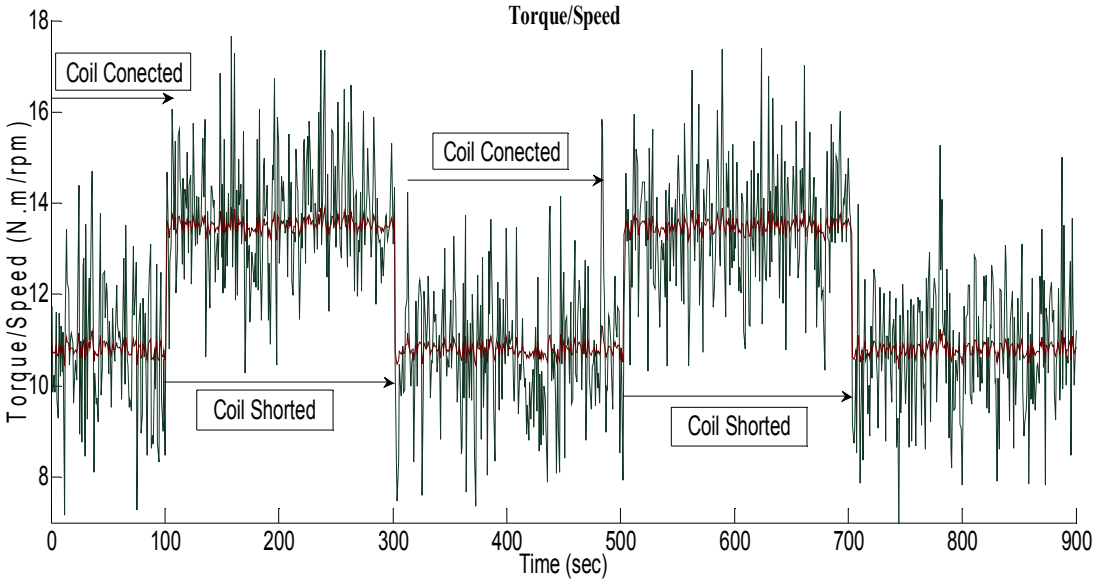

Figure 2. 7 The torque/speed signals trend when the coil is connected/shorted [16].

Condition monitoring of the power output of the wind turbine generators by using the wavelets is discussed in another paper [17]. The mechanism of the work supposes that by monitoring the power at modest frequencies and by applying a CWT to the resulting data, the magnitude of the component at twice slip frequency divided by pole pairs (2sf1 /p) might be tracked a rotor eccentricity. Rotor eccentricity is often the result of increased bearing wear and can be determined by monitoring the power of the variable-speed wind turbines at reasonable frequencies based on the application of the CWT. The proposed technique applied on two Doubly Fed Induction Generators (DFIGs) that have 1.5 rated power. The use of the CWT to extract the strength of the frequency components and the bearing's faults characteristic. The trend of the Root Mean Square wavelet power amplitude (RMS) of a 1.5 MW wind turbine with respect to the frequency of 2*sf*1 */p* is shown in Fig. 2.8.

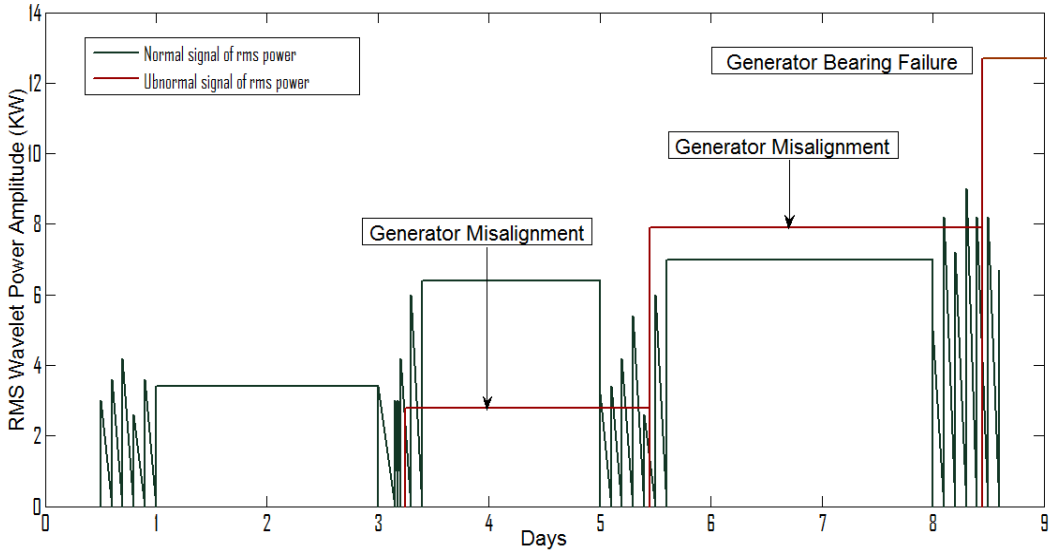

Figure 2. 8 Daily root mean square value of the CWT of the 1.5-MW wind turbine power corresponding to a frequency of $2sf_1$ /p [17].

The obtained results of the proposed techniques show a sudden increase in the RMS power amplitude leads to a failure in the generator's bearing through the 5th day of the applied experiment.

In Ref. [18], an assessment of the failure detection techniques is applied in order to detecting the faults of the wind turbine generator' bearings based on the homopolar current component of the stator of the induction generators. The proposed technique adopts the use of the Ensemble Empirical mode Decomposition (EEMD) as a method for detecting the failures, which occur due to the bearings of the wind generators in the stationary and non-stationary cases steady without requiring any training database. The homopolar current component decomposes into substantial mode functions through the EEMD, which is the Empirical Mode Decomposition (EMD) free mixed mode version. The authors found out that the 4th Intrinsic Mode Function (IMF) is the most energized mode, which can be utilized for bearing health monitoring based on the statistical criterion of the experimental data as shown in Fig. 2.9. The achieved results clearly demonstrate that the 4th IMF can be used as an indicator for bearing health monitoring.

Additional research spotlights on the failures that occur on the wind generators due to the bearing faults [32]. Gong Xiang and Wei Qiao present a condition monitoring technique, which is based on monitoring and analyzing the stator current Power Spectral Density (PSD), for bearing fault detection of direct-drive WTGs. In order to convert the variable fundamental frequency of the stator current to a fixed frequency, an appropriate

interpolation/up-sampling and down-sampling algorithms are designed according to the estimated primary speed of the WTG. The characteristic frequencies of bearing faults, consequently, can be clearly identified from the resulting stator current PSD. The approach of the proposed method can be summarized in Fig. 2.10.

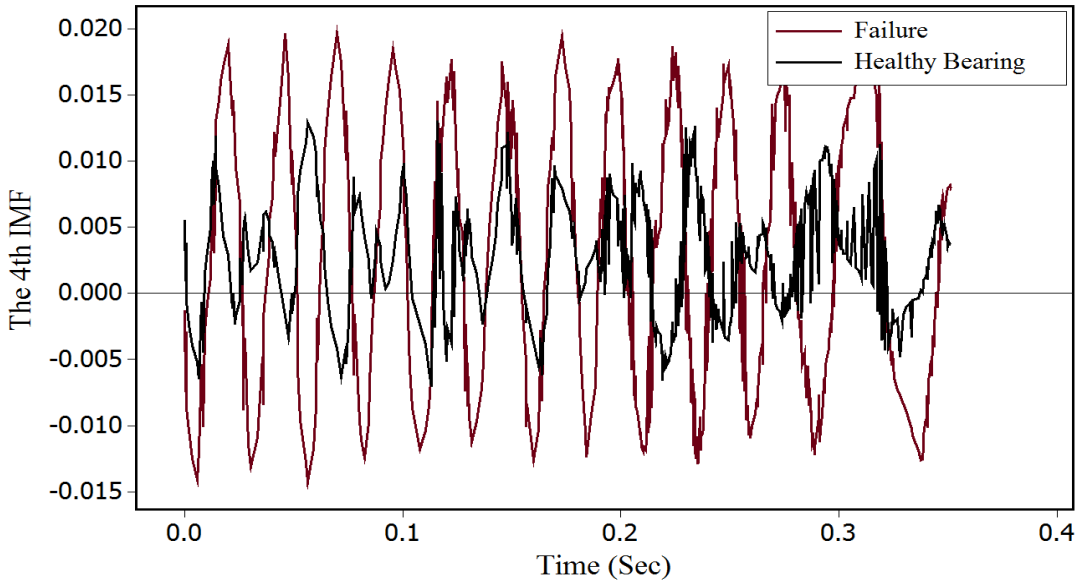

Figure 2. 9 Current homopolar component 4th IMF for healthy and faulty bearings [18]

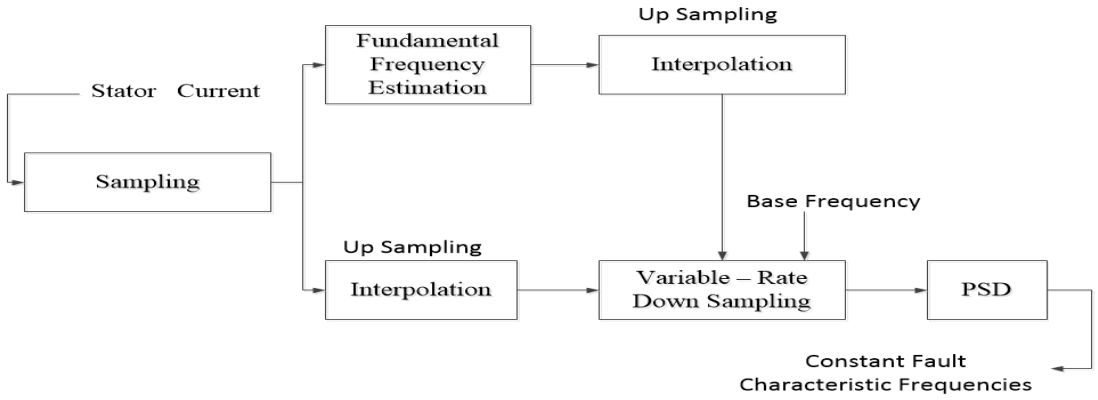

Figure 2. 10 The schematic diagram of the stator current spectrum analysis method [32].

The results of the proposed experiment show that the detection of the bearing outer-race and inner race defects for a direct-drive WTG is possible. Figure 2.11 presents the pulsation of the PSD of the stator currents for the wind generator with the healthy and outer-race faulted bearings.

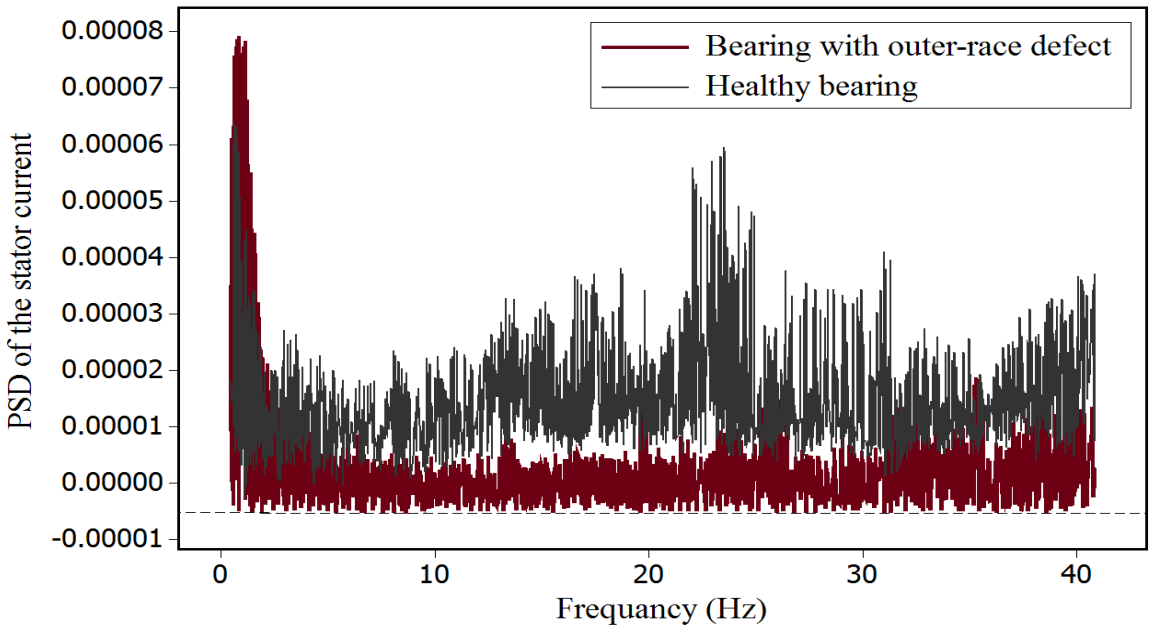

Figure 2. 11 Comparison of the PSD of the stator currents for the WTG with the healthy and outer-race faulted bearings [32].

Damian S. et al. propose a model in order to detect the wound rotor induction generator bearing faults based on the stator current analysis [33]. The main concept of the proposed work is based on the analysis of the produced electrical signal, which can be used to localize the outer race bearing faults in the wound rotor of a 30 KW induction machine. The technique first establishes a time-steeped simulation, which is an analytical machine model in order to detect the faults of the induction generator's bearings. Then, the results of the time-stepped simulation are utilized to test the stator current spectral signatures of

the typical bearing faults. The initial bearing fault causes air-gap variations, which produce numbers of low magnitude faults in the frequency components that appear in the current signal. In fact, the use of the conventional current signature analysis techniques creates a difficulty for detecting the bearing faults since the complexity of the current. Therefore, the authors suggest an alternative technique based on the spectral analysis of the complex current in order to improve fault detection. A test rig is performed on the wound rotor of the induction machine to introduce the severity of the bearing faults and confirm the model validity. Figure 2.12 shows the variation of the fault frequency amplitude with respect to the defect width for the machine, which operates at 1630 rpm. The collected results demonstrate the suitability of the use of complex signals as fault severity trend indicators since the amplitude of the fault frequency linearly increases with the fault severity.

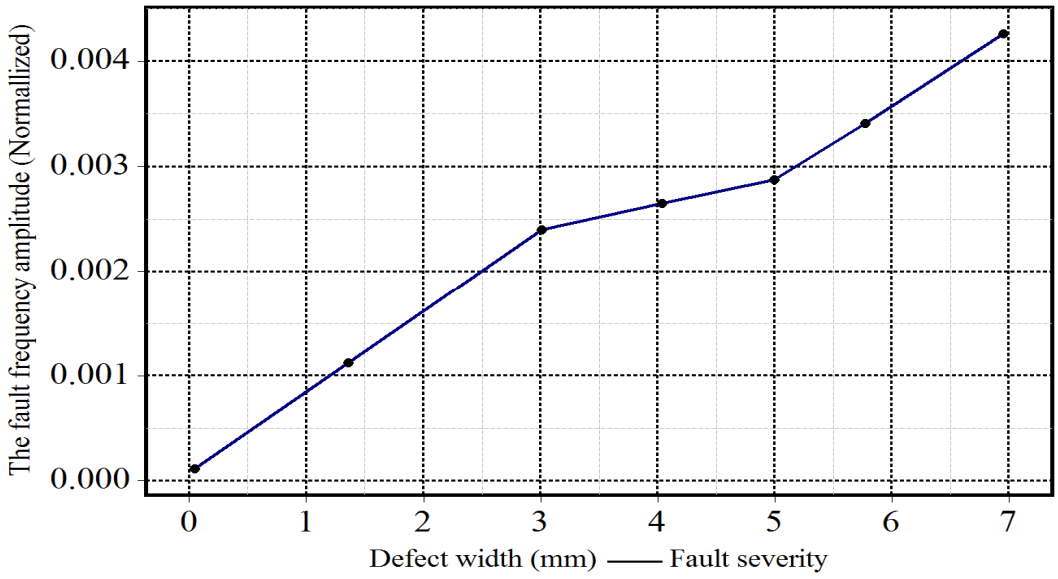

Figure 2. 12 The fault frequency amplitude against fault severity [33].

Condition Based Maintenance (CBM) strategy can be used in order to decrease the operation and maintenance costs of wind power systems. Wu Bairong et al. propose a CBM optimization approach based on the Artificial Neural Network (ANN) prediction information [34]. The component such as the wind generator can be monitored at different inspection points in order to estimate the predicted failure probability with respect to the turbine levels. The optimal threshold failure probability values can be determined by applying the CBM optimization. Thus, at each inspection point, a decision needs to be made in order to determine the component condition. The proposed maintenance policy is defined by two failure likelihood threshold values at the wind turbine level. The use of the Artificial Neural Network-based health condition prediction is for determining the lifetime distribution of the component. Based on the simulation of the proposed technique, the maintenance type can be specified. The methodology of the proposed method is presented in Fig. 2.13, which includes three proposed phases. The goal of the first phase is determining the ANN lifetime prediction distribution. Evaluating the optimal failure probability of the component is defined in the second phase. Then, the proper maintenance type that should be applied on the component is specified through the third phase.

The generator output power and rotational speed can be utilized to derive the fault signal and apply efficient CMS on the wind generators. Wenxian Yang et al. present a detection algorithm based on the continuous-wavelet-transform and adaptive filter to track the energy in the specified time-varying fault-related frequency bands in the power signal [35].

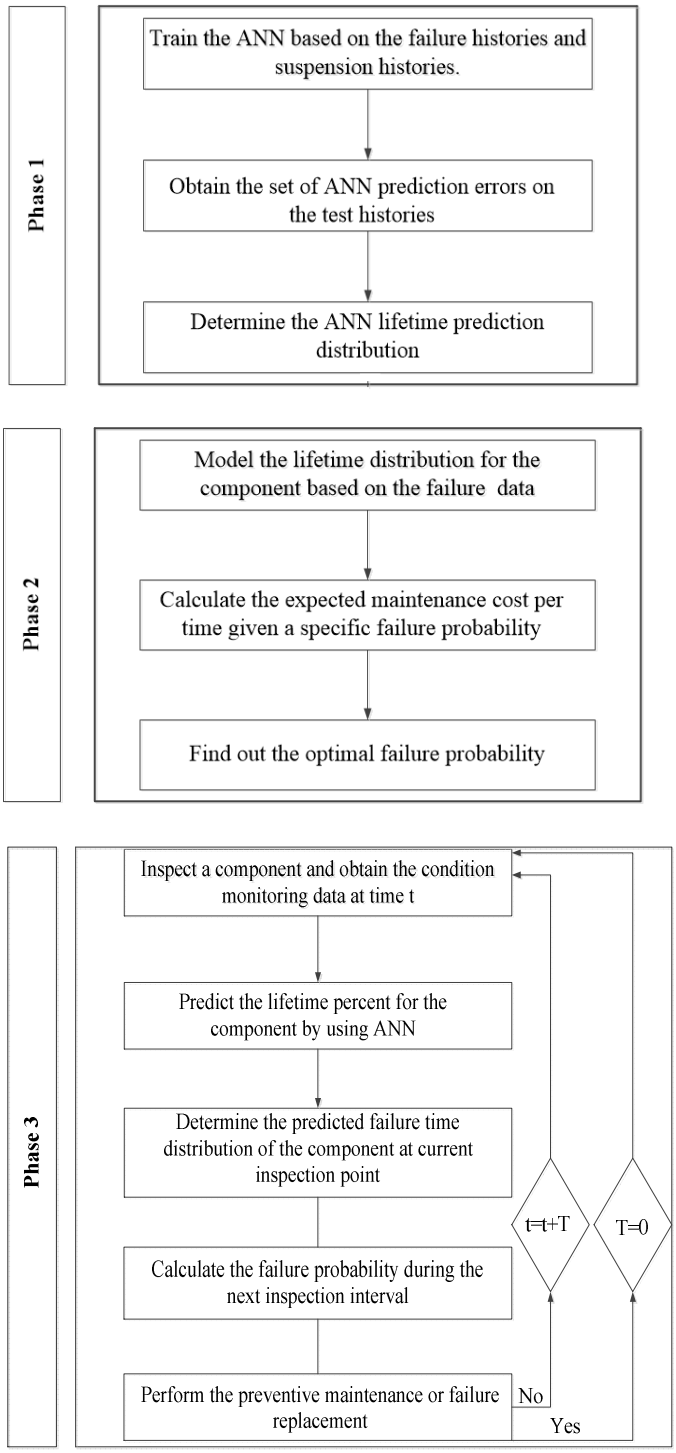

Figure 2. 13 The proposed methodology of the CBM approach by using ANN prediction technique [34].

The central frequency of the filter is controlled by the generator speed since the filter bandwidth is adapted to the speed fluctuation. The proposed method is applied on a wind turbine drive train with the aim of the test rig to achieve satisfactory results. Figures 2.14 and 2.15 illustrate schematic diagrams of the test rig of a wind turbine drive train with permanent-magnet synchronous generator and induction generator respectively. The proposed test rig is applied with synchronous and induction generators, which are installed in order to determine the differences of both the mechanical and electrical faults due to the mechanical unbalance faults of the generator' rotor.

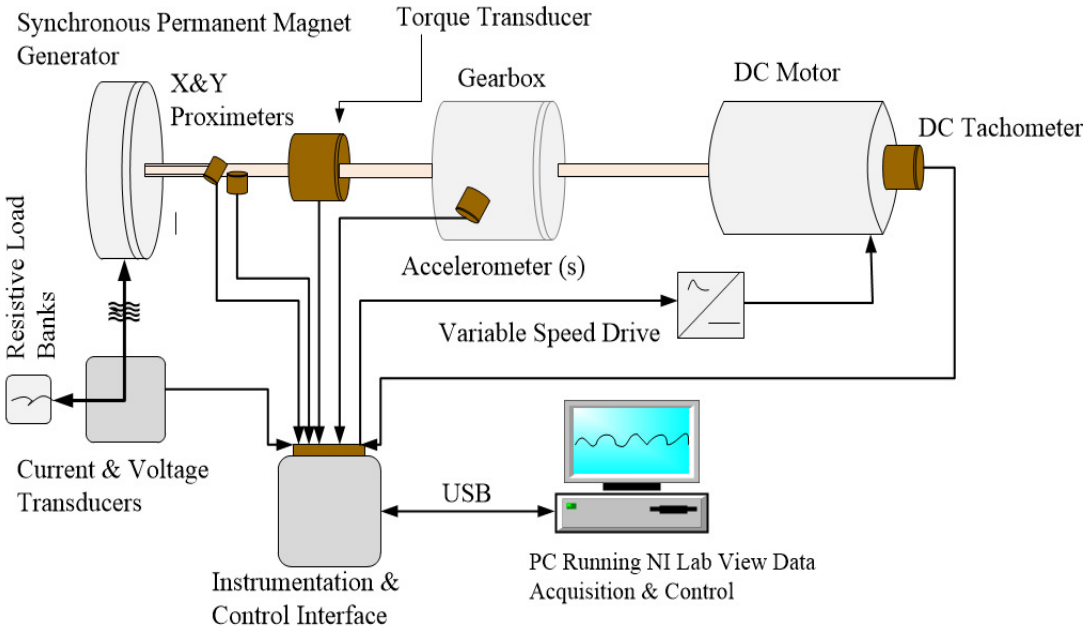

Figure 2. 14 Schematic diagram of a wind turbine drive train test rig with permanent-magnet synchronous generator [35].

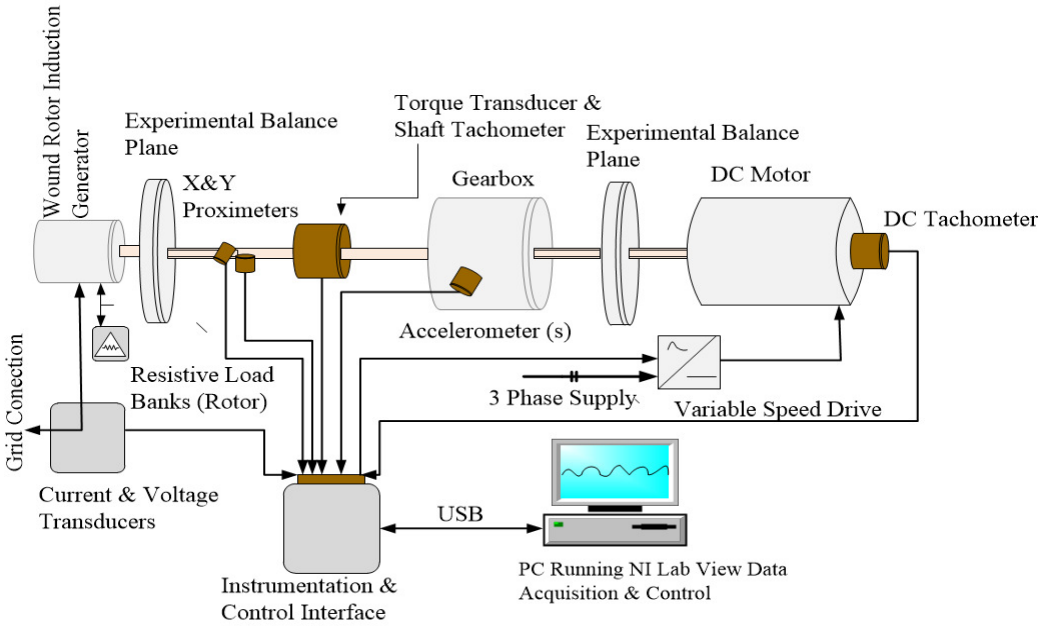

Figure 2. 15 Schematic diagram of a wind turbine drive train test rig with induction generator [35].

Additional research can be reviewed quickly suggests different techniques to apply CMS on the wind generators. For instance, using the analysis of the time and frequency domain to apply CMS on the wind generators is presented in Ref [36]. The authors emphasize that by monitoring the stator and rotor current line trend when both the stator and rotor of the generator are under unbalanced force, the detection of the generator faults is possible. In order to diagnosis the faults in the generators—such as turn-to turn fault, broken rotor bars— and static or dynamic eccentricity, the authors apply the Machine Current Signature Analysis (MCSA) method—which is employed as a noninvasive online or offline monitoring technique.

Li Yanyong presented the principles of the CMS that can be applied on the components of the wind turbines [7]. The root reasons of the failures that occur in the wind turbine components are reviewed to implement the CMS properly in the wind farms. In addition, the important requirements to apply an effective CMS on the wind turbine's components, such as understanding the component structure and the mechanism of work of the component are presented. The author pointed to the need for an accurate analysis of the data to assess and determine the machine condition properly

A. Yazidi et al. present a simulation to design efficient diagnostic systems oriented to the wind turbines that are working with the Doubly-Fed Induction Generator (DFIG) [37]. For this purpose, a complete system has been analyzed to study the influence of the electrical faults on the induction machine, which aims to implement the proper maintenance that can be applied. The proposed simulation is based on different experiments, which are accomplished to examine the electrical trend of the DFIG. These experiments describe different electrical faults, such as the stator phase unbalance faults, rotor phase unbalance faults, and turn-to-turn faults. For instance, the rotor phase unbalance is simulated with different resistances in the machine rotor phases, and the fault can be detected in the control system rotor voltages, which are unbalanced if the system is current-controlled. The study helps to increase the time of the produced energy by reducing the undesirable load operating time and the incidences of the faults.

As reported by Kevin Alewine, and William Chen at the Electrical Insulation Conference 2011, several widespread failure types have been specified [38]. They reviewed the failures for over 1200 of wind turbine generators and discovered that half of the failures were electrical in nature due to mechanical failures of the insulation structure. The authors confirm that the electrical failures occur because the wind generators are commonly exposed to voltage irregularities, mechanical stresses, and sometimes are effected by poor power quality from the IGBT based convertors, which used in the most wind turbines. Furthermore, they investigate that many of the failures occur due to the improper lubrication methods that are used in the maintenance operations and poor insulated materials. The authors confirm that the high quality of materials, which are used in the insulation and the appropriate maintenance can reduce the most electrical failures once a machine is operated.

Condition monitoring techniques for the electrical equipment are also presented in Ref. [25]. The study describes some of the monitoring methods that are used to perform CMS on the generators, and induction motors. The authors demonstrate in detail the causes and effects of the stator-winding faults**,** rotor body faults, rotor winding faults, and stator–core faults for the electrical generators. In addition, some general monitoring techniques for the induction motors, such as vibration monitoring, and current monitoring are proposed in this study. The study also points out to the benefits that could be obtained through the utilization of advanced signal processing and artificial techniques in developing CMS.

Analyzing the total power signals, which are measured from the terminals of the wind generator based on the approach of Empirical Mode Decomposition (EMD) is proposed in Ref. [39] in order to detect the generator faults. The authors emphasize that the EMD technique, which are attributed to its intrinsic locally adaptive property can show a great success in dealing with the non-stationary and the nonlinear wind turbine signals. In addition, the EMD can be considered as a tool to monitor the produced power of the wind generators based on analyzing the power signal into a finite number of Intrinsic Mode Functions (IMFs), which are able to indicate the change of the machine running condition. Finally, the authors confirm that the computational algorithm of the EMD is more efficient than the traditional wavelet analysis in online CMS since the EMD can be utilized for detecting the drive train mechanical faults and the generator electrical faults.

Using Fourier transform and the wavelet analysis techniques are very common for detecting the generator rotor misalignment and bearing faults. H. A. et al. propose the use of Fourier analysis technique for detecting the abnormal signals such as seen in the variable speed electrical generators, based on the analysis of the generator power signals [28]. In addition, the authors point out to the use of the wavelets transform in the analysis of the generator current waveforms for the fault diagnosis of the generator broken rotor bars. The authors present an example of broken rotor bars and air-gap eccentricity faults, which are very widespread and required applying vibration monitoring based on the analysis of the current signals [26].

The condition assessment of wind turbine generator systems (WTGSs) requires comprehensive information on most components. It is very obvious that the majority of the aforementioned papers, which are interested in the implementation of the CMS on wind generators, deal with the analytical electrical methodologies and theories to create suitable algorithms and techniques. Through this literature, the electrical faults and failure modes of the induction and synchronous generators are presented. However, this research suggests different techniques and methods, which carry diverse analyses, such as statistical, mechanical, electrical, reliability, and thermal analyses to apply CMS on the wind generators. [8], [40-44].

Chapter 3. Faults in the Synchronous Generator and Induction Generator.

In order to implement an effective CMS on wind generators, knowledge of the wind generators' failure modes is required. This chapter presents two types of the most popular generators used in the wind industry; synchronous and induction generators. The construction of each wind generator is explained; then, the faults that are related to each type are presented.

3.1. Introduction to the AC Generators

The most used generators in wind energy systems include doubly-fed induction generators and direct-drive permanent-magnet synchronous generators. Even though wound-rotor synchronous generator is not so common, it is becoming an available alternative because of grid-code requirements, such as voltage support during fault situations, control of reactive power in a given range, limiting maximum power generation, and start-up current transients [45, 46,]. In general, AC motors are classified in three categories: synchronous motors, induction motors (asynchronous motors), and the series wound-motors. This research is concentrated on the first two types synchronous and induction generators.

The synchronous generator is the most common type used in large wind turbines. This generator operates at synchronous speed regardless of the electric load's volume, and it does not have any self-starting torque. The synchronous generator is defined as a double machine; whereas, the rotor field winding is excited using the DC source, and the stator field winding is excited using the AC source. In the synchronous generator, a DC current is provided to the rotor winding to produces a rotor magnetic field, which in turns, induces a three-phase voltage within the stator winding. Furthermore, the synchronous motor runs at the leading power factor from the lagging power factor by changing the excitation [26-28], [31, 38,]. On the other hand, the three-phase set of the stator currents generates a rotating magnetic field, which causes the rotor magnetic field to align with it. Synchronous generators can be classified based on how the rotor is magnetized. There are two types of synchronous generators. The first type is called the Stationary Field Synchronous Generator (SFSG), in which the winding field on the stator incorporates the DC to create a stationary magnetic field. The Permanent Magnet Synchronous Generator (PMSG) represents the SFSG type. The second type is called the Revolving Field Synchronous Generator (RFSG), in which the rotating magnetic field is induced by the DC field winding on the rotor that is powered by slip-rings/brushes.

The most common synchronous generator used in the wind energy industry is the Permanent Magnet Synchronous Generator (PMSG), since this type does not require a DC supply for the excitation circuit, nor does it have slip rings and contact brushes. It operates at low speed and can attach to the wind turbine without a gearbox as shown in Fig. 3.1.

This figure illustrates a scheme of wind turbine that works with PMSG, and a rectifier to convert the Alternating Current (AC) to Direct Current (DC). The inverter takes the DC power that is supplied by the storage battery bank and electronically converts it to the AC power. In order to increase the voltage to a suitable level for transmitting the produced energy to the connection point, there is a transformer between the wind turbine terminals and the power grid [29].

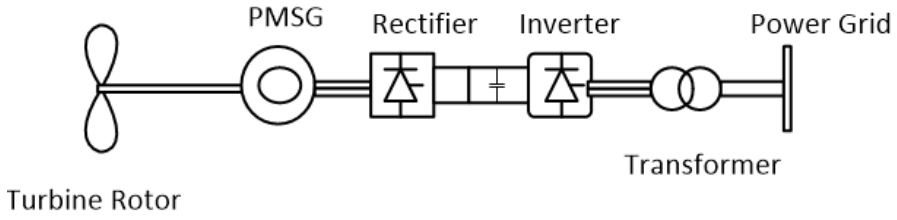

Figure 3. 1 A scheme of the wind turbine works with the PMSG, [28, 29,]

On the other hand, induction motors run at a velocity less than the synchronous velocity which is decreased when the electric load based on the self-starting torque is increased. The induction motor is classified as a single machine where the field of the stator winding is excited using an AC source, and it works under a lagging power factor. The Doubly Fed Induction Generator (DFIG) is the most common of the induction motor series that is used in small wind turbines. The DFIG is a wound rotor machine, in which the rotor circuit is connected to an external variable voltage, and the frequency source via slip rings with the stator is connected to the grid network. Figure 3.2 depicts the wind turbine works with the induction generator; whereas, the stator winding of the induction generator is

connected directly to the grid, and the rotor of the induction generator is driven by the gearbox of the wind turbine. In order to produce power, there are two important requirements that should be considered. First, the speed of the induction generator must be slightly above the synchronous speed. Second, reactive power is required to establish the air gap magnetic flux. A capacitor bank or synchronous condenser is used to provide the induction generator with reactive power in the case of a standalone system. In the case of a grid connection, the reactive power is drawn from the grid in order to maintain the air gap magnetic flux [29]. In order to understand the electrical and mechanical deficiencies within existing generators, it is instructive to examine archetypes of these generators. The structures of the synchronous and induction generators are demonstrated in the following sections.

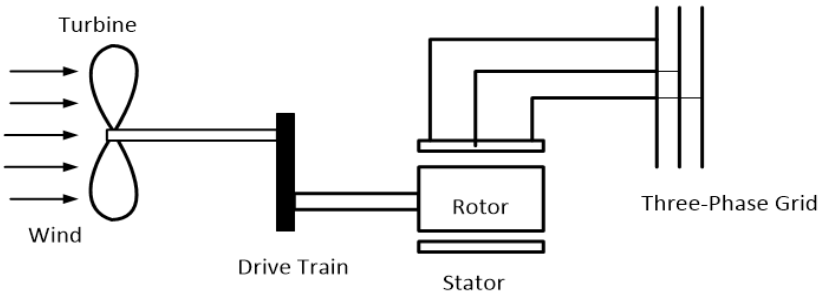

Figure 3. 2 A scheme of the wind turbine works with the induction generator, [28, 29,]

3.2. Synchronous Generator Main Structure.

The synchronous generator is an AC rotating machine, the speed of which is proportional to the frequency of the current in the generator's armature under a steady state

condition. The magnetic field is created by the armature currents, which rotate at the same velocity as the rotor field current. The rotor, in turn, rotates at the synchronous speed and produces a regular torque. The synchronous generator can be categorized as a rotating-armature generator, where the armature winding is on the rotor and a field system is on the stator, or it can be categorized as a rotating-field type where the armature winding is placed on the stator and the field system is on the rotor. Figure 3.3 displays a section of the synchronous generator structure.

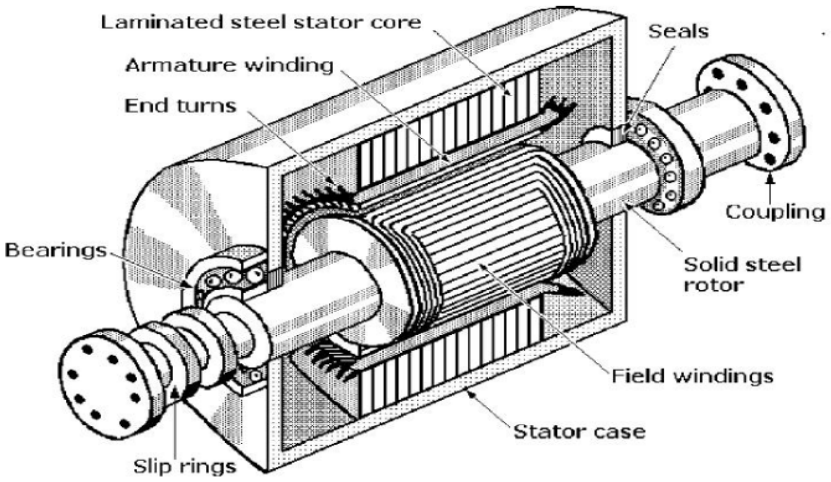

Figure 3. 3 A section of the synchronous generator structure, [28, 29,]

The windings in the synchronous generators produce the magnetic field (rotor windings for synchronous machines), and the armature windings of the synchronous generators induce the voltage (stator windings for synchronous machines). Figure 3.4 displays the construction of a PMG in a cross sectional view. The PMSG is made by using Neodymium Iron Boron or Samarium Cobalt, since they can be classified as high-energy

rare earth materials. In order to maintain the permanent magnet on the shaft, a high strength metallic or composite containment ring is used. The static iron core is made of laminated electrical grade steel. The electrical windings are made from high purity copper conductors. The entire armature assembly is impregnated by using high temperature resin or epoxy.

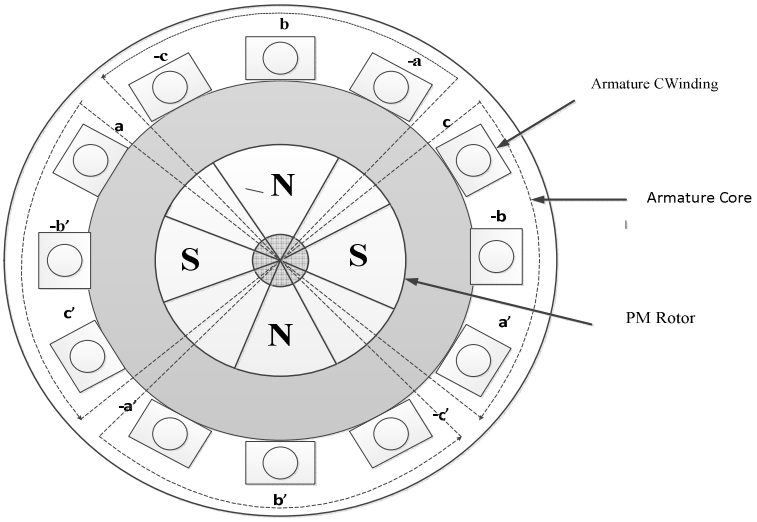

Figure 3. 4 Permanent magnet generator cross-sectional view, [28, 29,]

The most important parts of the synchronous generators, which generally face collapse, can be presented very briefly as follows:

3.2.1. The Stator

The armature winding of a classic synchronous generator is attached to the stator and is usually a three phase winding. The stator frame is made of thick steel plates to prevent distortion during operation as shown in Fig. 3.5. The stator frame should be robust

and ruffed in order to bear the mass of a stator core and resist the bending stresses and deflections. The frame bore is designed to ensure a uniform air gap between the rotor and stator, thereby minimizing the unbalanced magnetic pull.

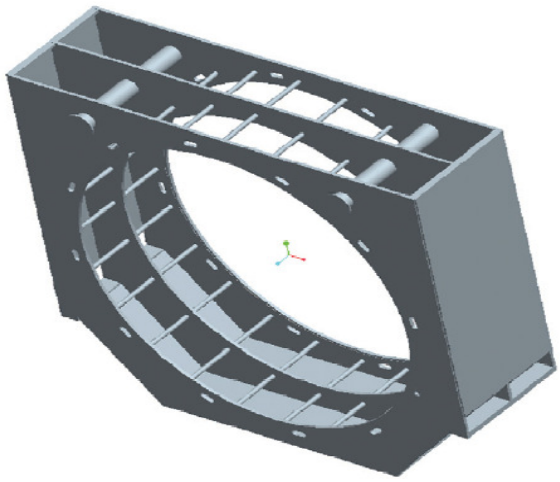

Figure 3. 5 The stator frame of the permanent magnet synchronous generator, [28, 29,]

The stator core consists of segmented and insulated laminations of cold-rolled low-loss silicon steel, which is clamped between substantial side plates. Laminations are stacked up with a controlled burr in order to ensure insignificant losses. Lamination steel is selected based on project requirements. The core is built inside a structural cage, which is then inserted into the frame. Figure 3.6 illustrates the shape of the stator core. The internal boundary of a three-phase stator has an integer number of slots and three identical coils of wire, which is distributed in multiple stator slots with many turns. Figure 3.7 shows an assembly stator picture of a PMSG.

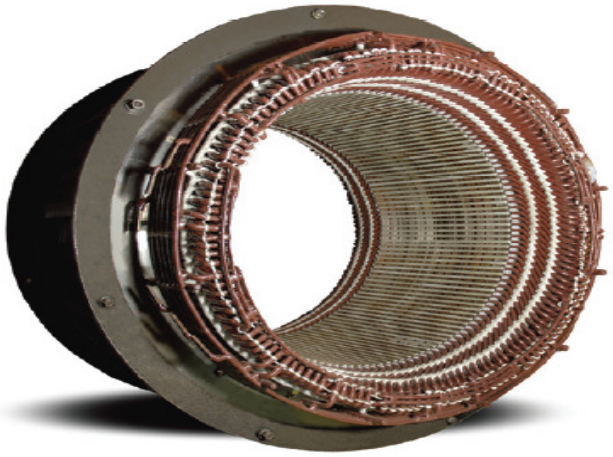

Figure 3. 6 The stator core of the permanent magnet synchronous generator, [28, 29,]

Figure 3. 7 Stator of a 3-phase PMSG, [28, 29,]

3.2.2. The Rotor

There are two types of rotor structures, which are related to the PMSG: the round or cylindrical rotor and the salient pole rotor. The round rotor structure type is used for

high speed synchronous machines, while salient pole structure is used for low speed applications. The rotor of a synchronous machine is designed to rotate satisfactorily at a continuous synchronous speed according to certain standards involving the application of the generator. The central part is the shaft, which has journals to support the rotor assembly in the bearings. In the axial mid-section, the rotor core is located, which is embodying the magnetic poles. Figure 3.8 shows a picture of a PMSG rotor.

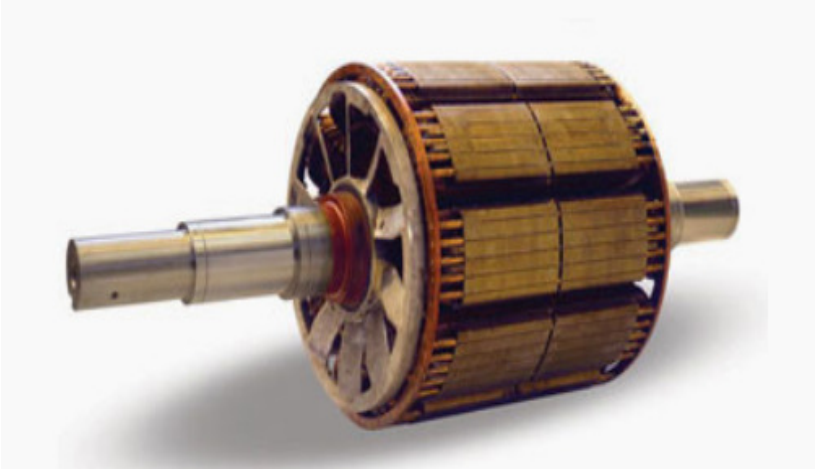

Figure 3. 8 Rotor of a 3-phase PMSG, [28, 29,]

When the rotor is round it is called ‘‘nonsalient pole’’, and when the rotor has protruding pole assemblies it is called ‘‘salient pole’’ construction. The nonsalient pole construction has magnetic poles, which is created by direct current, and located in the slots at the outside diameter of the rotor. The coils are restricted in the slots by the slot wedges and at the ends by rings on the large high-speed rotor. This construction is not appropriate for use on a motor requiring self-starting since the rotor surface, wedges, and rings are

overheated and melted from the high currents of self-starting. Figure 3.9 shows the anatomy of a rotor with shaft-mounted out board exciter. The salient pole construction can also be integral with the rotor lamination and mounted directly to the shaft. The excitation current is transmitted by using the salient poles, which have exciting coils around them. An appropriate cage winding in the face of the rotor poles usually with pole-to-pole connections is employed to dampen the shaft torsional oscillation and repress the harmonic variation in the magnetic waveform. Usually, on the shaft there are two axial or radial fans to supply airflow in order to maintain the machine temperature within the limits specified and to ensure the temperature distribution across the field and the stator windings is uniform.

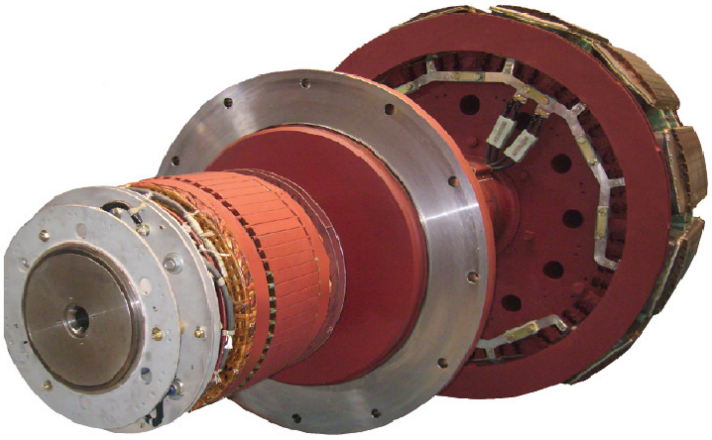

Figure 3. 9 The anatomy of the rotor with shaft-mounted out board exciter, [28, 29,]

3.2.3. The Bearing

Bearings are a critical component and their design is very significant for all rotating machines in order to resist the mechanical, electrical, and thermal stresses. The generator

is equipped with two ball bearings, which are mounted at both ends of the shaft for rotor support. The bearing metal is of sleeve type made of cast steel lined with Babbitt metal [47]. In order to prevent the inflow of the shaft current insulated metal, which is located opposite the coupling side is adopted for the bearing. The estimation of the bearings wear with suitable installation and running conditions is always possible since the easiness of dealing with them. In addition, bearings are usually renewed when the machine is serviced. Early breakdown of the bearings results in excessive vibration and even rotor eccentricity to the point of contact between the stator and the rotor on the small air-gap machines. Figure 3.10 shows a bearing picture of a PMSG.

Figure 3. 10 Bearing of a 3-phase PMSG, [28, 29,]

3. 3. Induction Generator Main Structure

The structure of the induction generators (asynchronous generators) is less intricate than the construction of the synchronous generators. The asynchronous generators require

no brushes and relatively complicated electronic controllers. They require energized connection to the electric power grid in order to operate unless they are designed to work with energy storage system.

In general, the main parts of the synchronous and asynchronous generators that are faced to collapse are similar. Like any electric motor, Induction motor has a stator holds three phase winding, and rotor holds short-circuit winding. Figure 3.11 displays the structure of an induction motor.

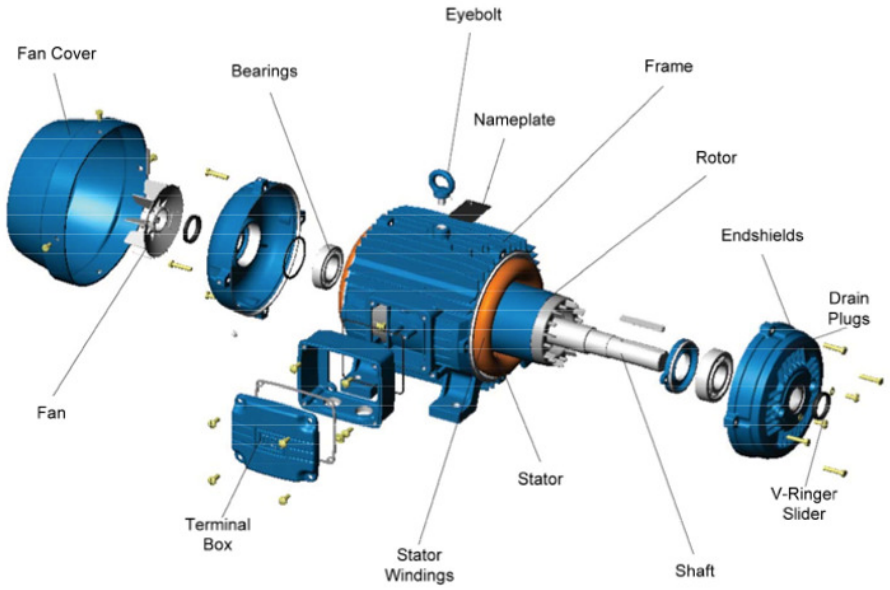

Figure 3. 11 A structure of induction motor, [28, 29,]

Induction generator also has two electromagnetic fields: the rotating magnetic field, which is produced due to high conductivity, high strength bars located in the slotted iron

core, and the stationary armature winding, which is similar to the one described previously. Figure 3.12 shows a scheme of an induction generator in a cross sectional view.

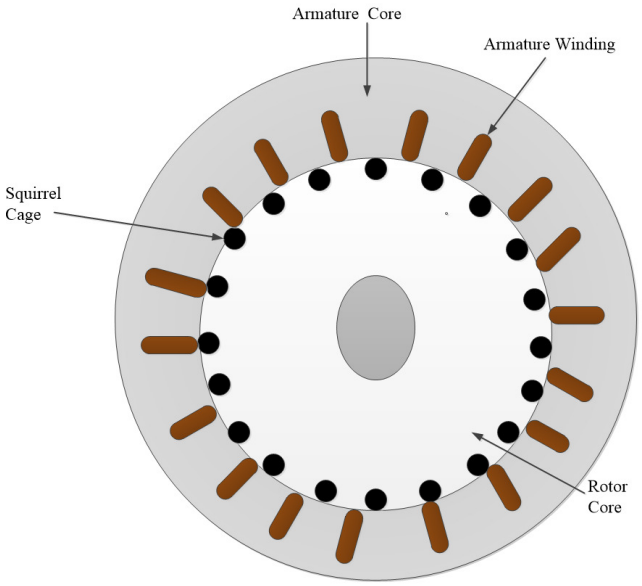

Figure 3. 12 Induction generator cross-sectional view, [28, 29,]

The generator output voltage is regulated with three phase and the voltage control is accomplished in a closed loop operation. Furthermore, the excitation current is adjusted to produce constant output voltage regardless of the fluctuations of the speed and load current. The magnitude of the excitation current, and frequency are determined by the control system. The excitation current is supplied to the stationary armature winding, which is induced from the secondary short circuited squirrel cage winding in the rotor.

3. 4. Wind Generators Failure Modes

The electrical generators consist of many mechanical and electrical parts, such as a rotor bar, rotor magnet, stator ending, end-ring, and bearing. In order to implement proper CMS on the electrical generators, understanding the nature of the fault in each part is very necessary. In many situations, the failure magnitude in the wind generators depends on the wind turbine size. For instance, the bearing failures of the 2MW wind turbines are more than the small wind turbines by roughly 200%. In addition, failures due to the generator rotor in the small wind turbines (less than 1 MW) are much more than the large wind turbines by roughly 900% [38]. Failure of such wind generators probably causes power losses besides the repair costs. The early detection of impending failure of such wind generators; therefore is very important in order to improve the reliability of the power systems. The majority of electric failures in wind turbine generators are due to bearing, stator, and generator rotor. Previous research confirms that about 40% 0f the electric failures are related to the bearings, 38% to the stator and 10% to the generator rotor [20, 26,]. The reasons of causing failures in the wind generators can be summarized in the following points:

1- Wrong rated power, unstable supply voltage, and current source.
2- Overload or unbalanced load.
3- Electrical stress from the fast switching inverters or unstable ground.
4- Improper routine maintenance.

5- Harsh environmental conditions (dust, water, leaks, environmental vibration, chemical pollution, high outside temperature).

There are many types of the electrical generator faults, which can be categorized to electrical faults, mechanical faults, and outer drive system defects as shown in Table 3.1.

Table 3. 1 The type of faults of the electrical generators, [20, 26, 31,]

Type of Fault	Fault Description
Electrical Faults	Open/short circuit in the windings due to winding insulation failure. Inappropriate connection of windings. High resistance contact to the conductor. Unstable ground.
Mechanical Faults	Broken rotor bars. Broken magnet/Partial demagnetization. Cracked end-rings. Bent shaft. Bolt losing Bearing failure. Air-gap irregularity.
Outer Generator Drive System Failures	Inverter system failure. Unstable voltage/current source. Shorted/Opened supply line.

The shorted winding coil is a very common electrical fault for which immediate preservation action should be taken. Shorted coil reduces the generator reactance, whereas the mechanical torque is directly proportional with the angular speed of the high speed shaft and inversely proportional with the generator reactance. The ratio of the mechanical torques to the angular speed of the high speed shaft is increased dramatically when the shorted winding coil condition is occurred [26]. Moreover, the signal behavior of the

generator voltage, current, and power can be utilized to identify the situations of the shorted-coil. Same methodology can be used to detect the faults that occur due to the generator rotor imbalance. The design of the electrical generator is prepared to have electrical and mechanical symmetry in the stator and the rotor for better coupling and higher efficiency. The aforementioned faults damage the symmetrical characteristic and induce abnormal symptoms during operation, which can be categorized as follows:

1- Mechanical vibration.
2- High temperature.
3- Irregular air-gap torque.
4- Change in the line voltage.
5- Change in the line current.
6- Speed variations.
7- Acoustic noise.
8- Instantaneous output power variation.

The faults that occur in the synchronous and induction generators will be demonstrated in details through the following sections.

3.4.1. Synchronous Generator Faults

There are some faults, such as stator inter-turn faults, rotor inter-turn faults and bearing faults are widespread in all synchronous generators. However, some faults like

rotor winding faults, broken damper bars, or end-rings are related to the wound rotor synchronous generators. The demagnetization faults are specified in the PMSGs. Synchronous generators are subject to many different types of the mechanical and electrical faults, which can be classified as follows:

- Open or short circuit in one or more turns of the stator winding.
- Open or short-circuited rotor winding in the wound rotor synchronous machines.
- Broken damper bars or end-rings.
- Eccentricities faults.
- Rotor's mechanical faults, which might result bearing damage, bent shaft, or misalignment.
- Demagnetization faults, which are related to the permanent magnet synchronous machines [26, 31,].

There are specific symptoms appear when the synchronous machines suffer from the faults, which are mentioned previously during their operation as follows:

- Unbalanced line currents and air-gap voltages.
- Excessive heating and redundant temperature.
- Heard noise and motor mechanical vibration.
- Low average torque.
- High torque pulsations.
- Increased power losses and reduced efficiency.

- Harmonics in the stator current/voltage/flux [26, 31, 48,].

The most significant faults that occur in the synchronous generators can be demonstrated wider as follows:

3.4.1.1. Stator Inter-Turn Fault

Stator inter-turn fault is one of the most widespread faults in the synchronous machines and cause due to the effect of the electrical, mechanical, thermal, and ecological exertions. In other words—this fault is represented in the inter-turn short circuit, which occurs in one of the stator's coils due to the electric and thermal stresses—whereas the increase in the thermal stress causes degradation in the winding insulation. Inter-turn fault in the stator winding results decrease in the output torque and loss in the current due to asymmetry in the generator, therefore; monitoring the stator current is important to detect the stator inter-turn faults. Stator inter-turn faults in the salient pole synchronous generator can be discovered by testing the field current of the machine. There are different types of the stator winding faults, which can be summarized as follows:

- Inter-turn short circuits between turns of the same phase and winding short circuits, short circuits between winding and stator core. The short circuits on the connections and between phases are commonly caused by the stator voltage transients, and abrasion.

- Burning of the winding insulation leads to winding short circuits of all phase windings. The burning of the winding insulation is usually caused by the motor overloads and blocked rotor. Further, the burning of the winding insulation is caused due to the sub-rated voltage and over rated voltage power supplies, which produce stator energization. The damage in the insulation of the stator windings also occurs due to the frequent starts and rotation reversals.

- Inter-turn short circuits can also be occurred due to the consecutive reflection of the voltage transmission, which produced from the long cable connection between the motors and AC drives. Such AC drives produce extra voltage causes high stress on the stator windings due to the inherent pulse width modulation of the voltage, which are applied to the stator windings.

- Entire short circuits of one or more phases can take place in the series of the stator winding faults due to the phase loss, which is caused inasmuch to an open fuse, contactor or breaker failure, connection failure, or power supply failure [26, 31], [48-51].

In general, short circuits in one phase usually occurs due to an unbalanced stator voltage, which is caused by an unbalanced load in the power line, bad connection of the motor terminals, or bad connections in the power circuit. The unbalanced voltage condition

confirms that at least one of the three stator voltages is under or over the value of the other phase voltages. Figure 3.13 shows typical insulation damage, which leads to inter-turn short circuit of the stator windings in the three-phase synchronous motors.

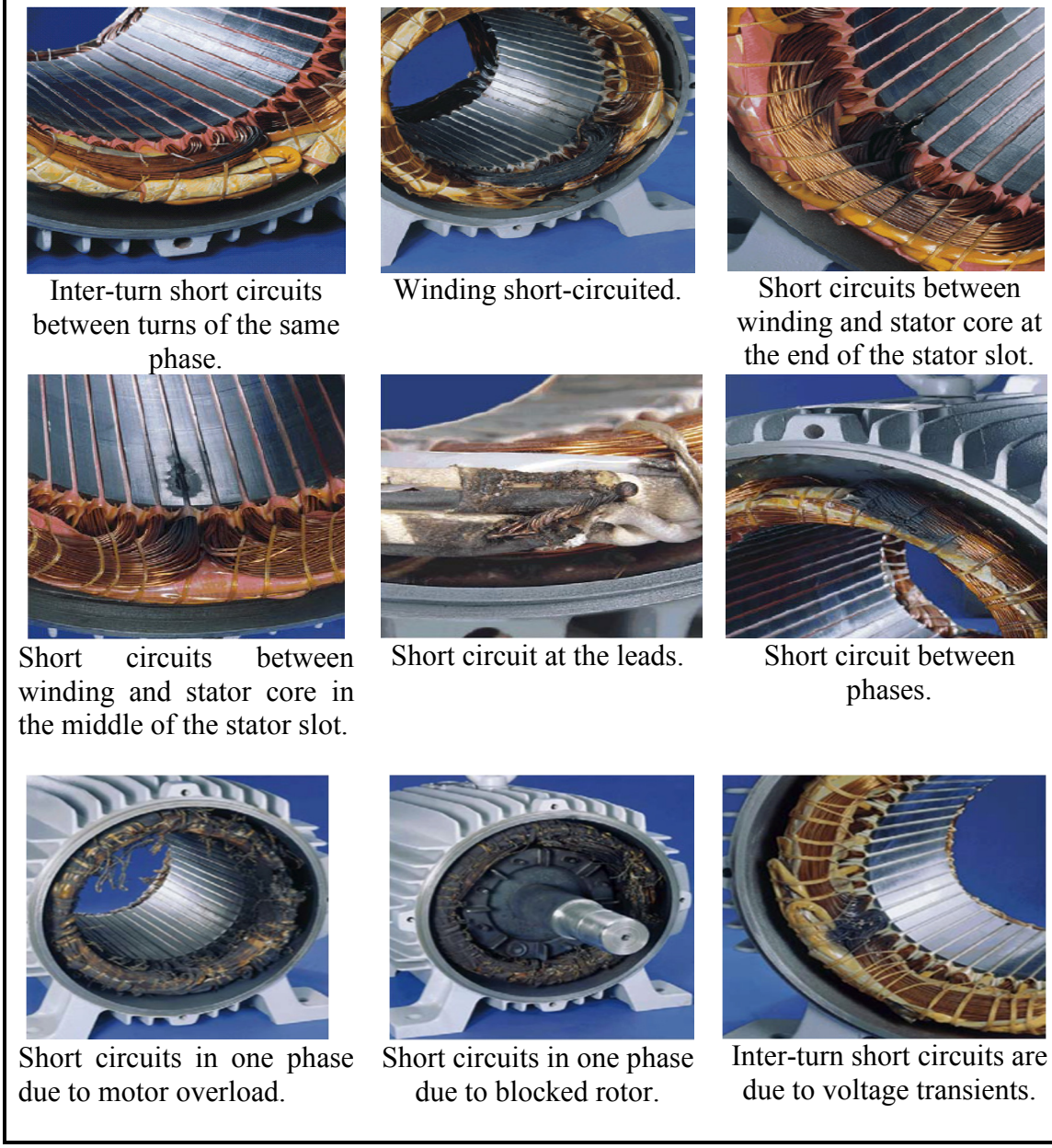

Figure 3. 13 Atypical insulation damage leading to inter-turn short circuit of the stator windings, [52]

In order to analyze the internal phase and the ground faults in the stator winding, different mathematical models for the synchronous machines can be utilized. For instance, Inter-turn faults of synchronous machines can be modeled on the actual winding arrangements by using a function computes the machine inductances from the machine winding distribution and considering the produced harmonics by the machine winding [26, 27, 31, 48, 49,]. In addition, a model for simulation of inter-turn faults in the stator ending of the permanent magnet synchronous machines is proposed by Abdullah et al. [48]. The proposed method is based on the coupled magnetic circuit technique, which make no hypothesis about the sinusoidal and symmetric distribution of the machine windings and, therefore, considers for the whole magnetomotive force harmonics. The machine inductances are estimated from the geometric data and winding design. The time-stepping finite element is another analysis technique to study the inter-turn faults of the synchronous generators. Vaseghi et al. presents this method for detecting the inter-turn fault of a surface-mounted permanent magnet synchronous generators. The proposed method is based on the study of the magnetic field, and the estimation of the machine parameters under various faults [51].

3.4.1.2. Rotor Inter-Turn Fault

Rotor winding inter-turn fault is very common in the synchronous generators and caused significant problems, such as high winding temperature, deformed voltage waveform, mechanical vibration….etc. Rotor winding inter-turn fault because of some

reasons, such as deformation of the high-speed rotor winding due to centrifugal force, overheating, bad insulation…etc.

Researchers have published several methods and techniques to diagnose the rotor inter-turn fault. One method is based on indirect measurement of the impedance of the rotor field winding during running. This method is beneficial when the number of the shorted turns increases dramatically [53]. Another approach uses the detection of the flux asymmetry, which is created by the shorted turns based on applying the alternative current to the field [54]. The drawback of this method is represented in the difficulty of removing the rotor from the bore. Some reliable methods are based on the direct measurements of the air-gap magnetic flux during operation. The flux cam be measured by using a search coil, which is installed in the air gap [55]. Furthermore, the neural network models of machines can be utilized to detect the rotor turn faults. Training data are required to implement this technique through the simulation and mathematical models of the machine are needed to simulate the data [26, 27, 31, 48, 49,]. Streifel et al. propose a method, which is based on traveling wave [56]. The proposed technique along with the neural network extraction by creating detection algorithm for the short-circuited windings in any rotating machinery. Figure 3.14 displays damage in a rotor of wind generator due to the rotor winding inter-turn fault.

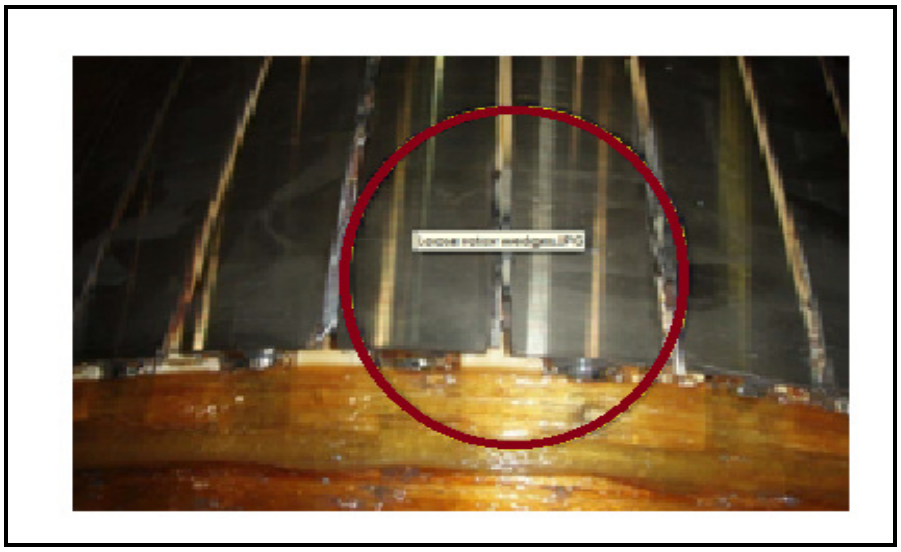

Figure 3. 14 Damage in a rotor of wind generator, [52]

The damage in the rotor's lead can occur due to an increase in the harmonic current during the operation. The power converter is linked directly with the rotor winding through lead wires, which pass the cavity rotor shaft where the bearing inside housing is fitted. The harmonics and the peak voltage could be higher than the rated voltage and would cause bearing harmonic current be larger and stronger than the normal running conditions. Consequently, the bearing temperatures will increase, which creates enough heat and damages the rotor's lead as shown in Fig. 3.15.

3.4.1.3. Bearing Fault

Bearing is the most part of the synchronous generator that is exposed to damage and its failures have frequently reported in the wind energy industry. The failures in this important component take place when the flaking of the bearing occurs due to overstress.

Bearing failures in the wind generators are typically caused by some misalignments in the drive train, which increase the abnormal loading and decrease the bearing wear [26, 31, 32, 36,]. When an outer-race or inner-race bearing fault occurs in an electric motor, the rotating shaft of the motor will suffer from mechanical vibrations, which lead to eccentricity and produce abnormal flux density in the air-gap. Further, these vibrations have private attributes, which are linked with the shaft rotating speed and affect the bearing negatively. Figure 3.16 indicates an outer-race bearing fault of an electric motor [32, 36,].

Figure 3. 15 Rotor lead failure, [38]

Bearing fault detection techniques in the wind generators need mechanical sensors, such as vibration sensors (accelerometers), which are mounted on the surface of the wind generator. Different methods for a joint time frequency analysis and experimental study of detection and fault diagnosis of damaged bearing on a PMSG were investigated by Rosero

et al. [57]. When the machine operates under nonstationary conditions, the use of some traditional signal processing methods, such as Fast Fourier transform (FFT) in the motor current signature analysis does not work well. In such conditions, the stator current can be analyzed by means of Short Time Fourier Transform (STFT) and Gabor Spectrogram (GS) for detecting the bearing fault. Pacas et al. propose another fault diagnosis technique for detecting the bearing faults in the permanent magnet synchronous machines based on the frequency response analysis [58]. The torque and velocity signals of the machine will be regularly disturbed when the bearing is damaged. This leads to changing the frequency response of the mechanical system. The frequency response of the machine in the closed loop speed control can be derived by utilizing the velocity of the motor and the torque-generating component of the stator current. Figure 3.17 displays anatomy of bearing failure.

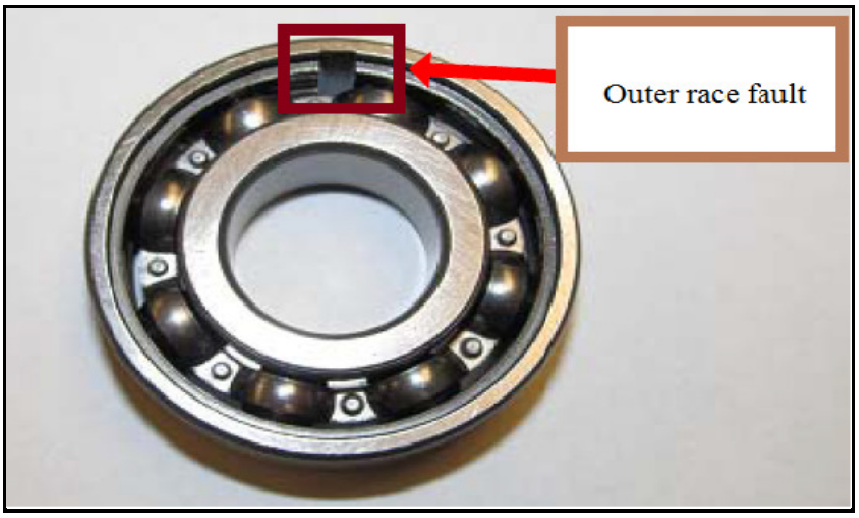

Figure 3. 16 An outer-race bearing fault, [33]

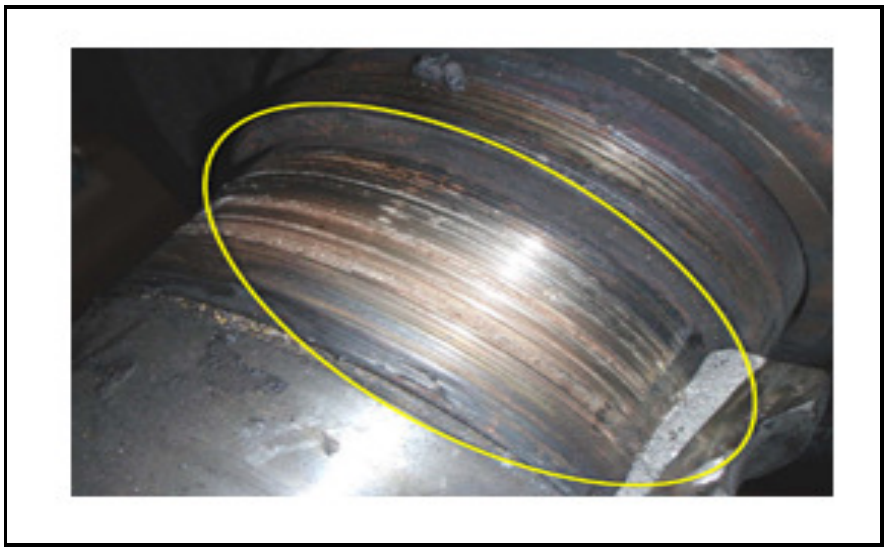

Figure 3. 17 Anatomy of bearing failure [52]

3.4.1.4. Damper Winding Fault

The damper winding is commonly used in the synchronous machine since it provides smooth starting and compensating the transient effect or the unbalanced condition. Damper windings consist of heavy copper bars with the two ends shorted together installed in the rotor slots. Figure 3.18 shows a schema of a damper winding in a salient pole machine.

The rotor must be turning in the stator field at the synchronous speed to produce torque in the synchronous generators. At any other speed, the rotating field of the stator poles will not be synchronized with the rotor poles. This condition produces no average torque and the machine will not start. Damper windings can increase the generators' speed to reach the synchronous speed. The induced current in the bars is interacted by the rotating

air-gap field and produces torque. When the load is suddenly changed, an oscillatory motion will be superimposed on the normal synchronous rotation of the shaft. The damper windings help to damp out these oscillations. During the transient time, when the machine accelerates from zero speed to the synchronous speed, a significant current flows to the damper windings. Excessive start-stop cycles, frequent load or speed changes can cause the breakage of the damper bars [52, 59,].

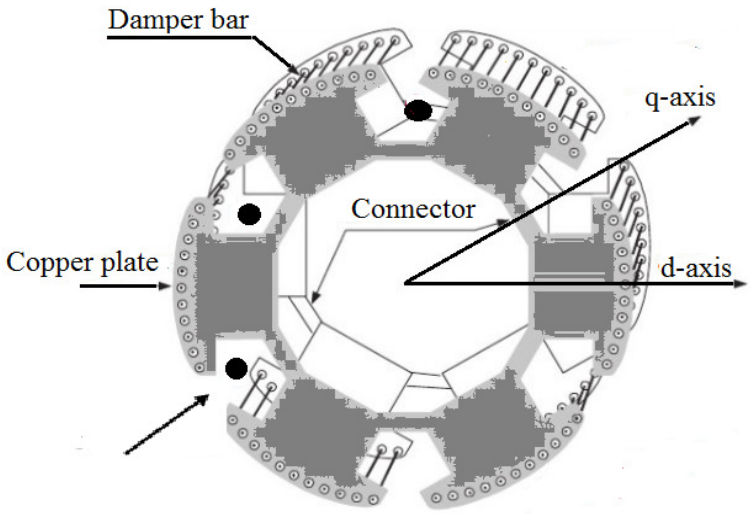

Figure 3. 18 Damper winding in salient pole synchronous generators, [52, 59,]

Several methods have been reported for detecting the broken damper bars. For instance, flux probes can be attached to the stator bore surface for the measurement of the air-gap flux waveform during the acceleration from the starting speed to the rated speed [59]. Furthermore, separation of pole voltages of the field winding according to its polarity can be used as an effective technique for detecting the broken damper bars [60]. First, the difference of the pole voltages must be determined. Then, the main field of a symmetrical

machine disappears in the difference voltage. Meanwhile, the difference voltage that is produced by the perturbed field of the missing damper bar will remain. The winding function analysis and the time-stepping finite element analysis have been used to study the broken damper bars and end-rings [59-61].

3.4.1.5. Demagnetization Fault in the PMSGs

The demagnetization phenomenon occurs due to the armature reaction, especially in the high torque conditions. During the normal operation, the inverse magnetic field, which is produced by the stator current opposes the permanent magnets' remnant induction. When this phenomenon is repeated, the permanent magnets will be demagnetized. This demagnetization can be all over the pole or on a part of the pole. The high temperature also demagnetizes the magnet. Stator winding short-circuit fault may partially demagnetizes a surface mount magnet. Partial demagnetization causes magnetic force harmonics, noise, and mechanical vibration, and creates unbalanced pull effects in the generator [26, 62,].

The demagnetization effects on the parameters of the motor, such as cogging torque, ripple torque, and load angle curve were investigated by Ruiz et al. [63]. For steady-state analysis under demagnetization conditions, Fast Fourier Transform (FFT) of the stator current is used for the frequency analysis. Time-frequency analysis methods have been used for nonstationary conditions. The methods, such as Short-Time Fourier Transform (STFT), Continuous Wavelet Transform (CWT), and Discrete Wavelet Transform (DWT)

require a suitable selection of the parameters, such as the window size and the coefficients. Field Reconstruction Method (FRM) can also be utilized to detect the demagnetization fault in PMSGs. The fault can be monitored by estimating the flux linkages of the stator phases [64].

3.4.2. Induction Generator Faults

Induction motors are commonly associated with small wind turbines and widespread due to different reasons, such as the simplicity, long life time, high power per unit mass of materials, and can be employed as motor or generator. However, in many situations they are liable to many types of faults that cause production shutdowns, and waste of raw material. The causes and symptoms of the faults that occur in the induction generators are approximately similar to the synchronous generators faults. Induction motor faults can be also detected in the initial phases in order to prevent the complete failure of the system. This section presents the most common failures that occur in the induction generators, and some of the fault diagnosis methods.

3.4.2.1. Stator Faults

Much of the previous research emphasizes that the stator faults bring about 30% to 40% of all electric generators failures [26, 37, 38,]. Stator faults in the indication generators can be classified to frame faults and stator winding faults. The frame faults occur due to core defect—circulation current, and ground fault—whilst the stator winding faults take

place due to winding insulation damage or displacement in the conductors. Figures 3.19 and 3.20 show the winding insulation and frame damage of the stator in an indication generator respectively.

Winding insulation plays a significant role to protect stators from failures since the insulation should bear the electric, mechanical and environmental stresses. Therefore, winding insulation must be robust and should meet the system requirements to resist all stresses modes. There are many causes affect the lifetime of the winding insulation, such as the electromagnetic vibration at twice the power frequency, differential expansion forces due to the temperature variations following load changes, and impact forces due to electrical/mechanical asymmetries.

The increase in the stator temperature affects the stator material. In this context, failure might occur due to the internal chemical interactions that make the winding insulation material brittle, which causes the melting of the stator material in a short time. The thermal stress—which caused due to the copper losses, reverse current—and stray load losses in the copper conductors, also influences the stator winding insulation negatively. The thermal stress increases the temperature of the copper conductor and this increase in temperature spread rapidly on the ground wall insulation [9, 12, 18, 33,].

Figure 3. 19 Winding insulation damage of the stator, [52]

Figure 3. 20 Stator frame damage, [63]

Another significant effect on the winding insulation aging is the partial discharges, which are small electric sparks that occur within air bubbles in the winding insulation

material due to irregular electric field distribution. The partial discharges cause progressive deterioration in the insulation material, which leads to electrical breakdown. On the other hand, the stator winding insulation is exposed to high voltage stress when used with the inverter. The high voltage stress is caused by the interaction of the rapid raising voltage pulses of the drive with the transmission line effects in the cable [65, 66,]. Furthermore, there are additional causes can be accounted as accelerating effects on the aging of the winding insulation, such as delamination discharges, moisture impacts, abrasive material influences, chemical decomposition, and radiation [67].

Motor and generators winding insulation failures during the operation can lead to costly outage, which decreases the revenues of the wind energy projects. In the literatures [67, 68]—the partial discharge is taken as a symptom of isolation aging, which begins within voids or cracks—then progressive deterioration of the insulating material occurs, which leads to electrical breakdown. When a partial discharge occurs, the case may be detected as a slight change in the drawn current. It is very difficult to measure the current of the partial discharge because of the small magnitude of this current and the short duration to detect it. Therefore, it is very complicated to investigate the partial discharge phenomena in the electrical generators before the breakdown.

There are several methods for condition monitoring of the generator stator winding. Monitoring the temperature of the stator winding is very essential to determine the degree of the thermal deterioration. Fixing thermocouples or thermal cameras is very proper to

conserve the stator winding insulation and monitor the cooling system temperature. Phase and ground fault relays can be installed to prevent the damage in the winding insulation [69]. On-line monitoring of the partial discharge is another method that warns the user before the damage. This approach can be done either by monitoring differential line current or using some specific sensors, such as antenna, high voltage capacitors on the generator terminals, or radio frequency current transformers at the generator neutral [67].

Ozone gas generation occurs, as a result, of the partial discharge on the stator coil. The surface partial discharges are the cause of the deterioration from defective slot and end-winding stress relief coating as well as conductive pollution. The failure mechanisms that give rise to the surface partial discharge can be detected by monitoring the ozone gas concentration over time. Furthermore, ozone monitoring in the early stages of deterioration is not complicated and can regularly be done with inexpensive chemical and electrical detectors [70].

3.4.2.2. Bearing Faults

Large number of the wind turbine failures are associated with the bearing faults in the induction generators. Bearing faults cause more than 40% of all generator's failures [26, 27, 38,]. Most of the bearings operate under nonstationary conditions and are subject to many technical problems, such as fatigue, overloading misalignment, ambient mechanical vibration, current fluting, corrosion, and incorrect lubrication. Bearing faults

can be classified to inner raceway fault, outer raceway fault, ball defect, and cage defect. The defects spread from the inner raceway to the outer raceway and generate mechanical vibrations causing vocal noise and inconsiderable rotor displacements as shown in Fig. 3.21.

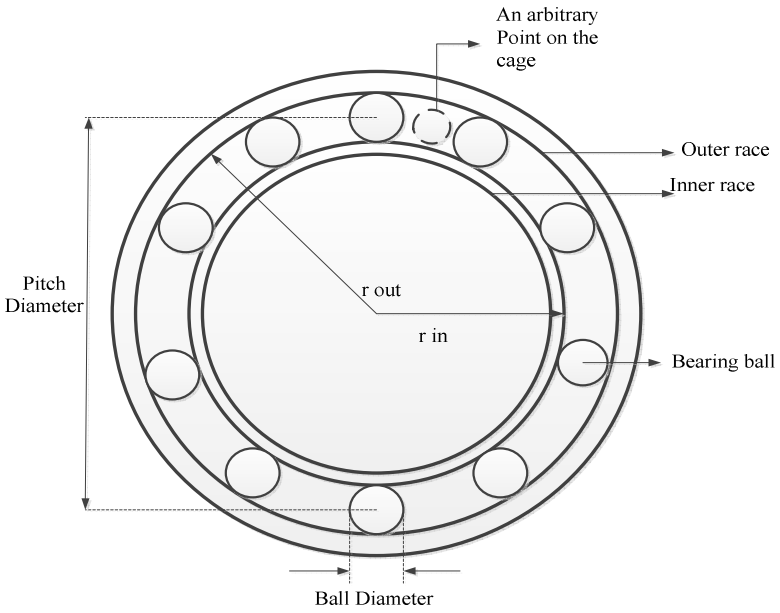

Figure 3. 21 A typical bearing sketch, [26]

In order to apply an effective CMS due to the bearing faults of the wind generators—mechanical vibration, infrared—thermal, and acoustic analyses are used based on sensors or thermal transducers that are installed on the generators. Further, monitoring the generator current is an alternate approach to perform CMS on the bearing of the wind generators with minimal additional cost. The mechanical vibration frequency component of the bearing faults are different according to the fault type. In this context, the mechanical pulsations that are caused by the bearing faults change the air-gap similarity and the

generator inductances. The generator inductance variations are reflected the line current in terms of the current harmonics, which are the sign of the bearing faults associated with the mechanical oscillation in the air-gap [26, 38, 48,], [71-73].

A fault diagnosis method of detecting the bearing faults based on a distinctive energy function is presented by J. Ilonen et al. In this context, the proposed energy function is employed to detect the frequency-domain regions where the failures are specified [74]. Schoen et al. present on-line system for the induction motor based on the line current. The proposed system uses the artificial neural networks to study the spectral characteristics of a perfect motor operating online [75]. An amplitude modulation detector is developed to detect the bearing faults before causing damage in Ref. [76]. Knowledge of the bearing characteristic fault frequencies is required to apply the proposed method. In addition, computer simulations and machine vibration data from the bearings containing outer race faults are requisite to obtain suitable results. Yazici et al. suggest an adaptive statistical time-frequency method for detecting the broken motor bars and bearing faults in the induction motors [77]. The proposed method is based on training approach in which all the different normal operating modes of the motor are learned before the actual testing starts.

3.4.2.3. Broken Rotor Bar Faults

Broken rotor bar or cracked faults cause more than 5% of all generators failures in the wind energy industry [26]. These faults are caused due to different stresses, such

magnetic stress, thermal stress, dynamic stress, and mechanical stress, which remain within the tolerance band-width and the motor operates properly for years. An incipient broken rotor bar condition aggravates itself almost exponentially in time as the redundant current flow is concentrated on the adjacent bars instead of the broken one, which leads to increasing the electrical stress in the adjacent area. The broken rotor bar is considered as a rotor asymmetry that causes high torque pulsation, low average torque, and unbalanced line currents. The electric and magnetic asymmetry increases the left sideband of supply frequency. Figure 3.22 displays a broken rotor bar in an induction generator [26, 31, 38, 48, 72, 73, 78,].

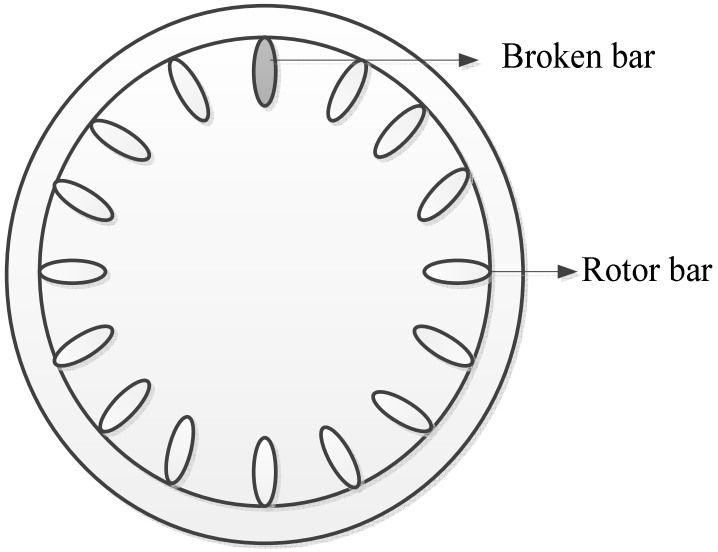

Figure 3. 22 Broken Rotor Bar, [18]

The broken rotor bar fault can be detected by the time and frequency domain analysis of the induced voltage in search coils placed in the motor [79]. During the steady

operation, asymmetrical stator winding excited at frequencyf_e and creates rotor bar currents at sf_e frequencies. When the asymmetry occurs in the rotor structure, the backward rotating negative sequence $-sf_e$ component starts the spectrum electrical and the mechanical interactions between the rotor and the stator of the motor. In the beginning, stator electromotive force at frequency $(1-2s)f_e$ is induced, which causes ripple torque. Then, the ripple torque reflects the stator as a line current oscillation at frequency $(1+2s)f_e$. The $(1+2s)f_e$ component induces rotor current at$\pm 3sf_e$, and this chain reaction goes until entirely being filtered by the rotor inertia. K. R. Cho et al. propose a detection method of broken rotor bars faults, based on the use of the harmonics at the stator terminal voltages after switching off the motor [80]. To detect the broken rotor bars, measurements, such as stator voltage, stator current, stator excitation frequency, and rotor velocity are available over a small range of velocity. The near least square error estimator is utilized to process these measurements and results estimated motor states and parameters.

3.4.2.4. Eccentricity Faults

This fault occurs when the distance between the rotor and stator in the air-gap is not uniform, which causes unbalanced magnetic flux in the air-gap. Harmonics in the line current will be created, which is specified in the spectrum. There are two types of eccentricity faults, static eccentricity fault and dynamic eccentricity fault. The static eccentricity fault occurs when the shaft axis is at a constant offset from the center of the stator or when the rotor is misaligned along the stator cavity. On the other hand, the

dynamic fault occurs when the shaft axis is at a variable offset from the center of the stator or the minimum air-gab revolves with the rotor. Figures 3.23 and 3.24 display the both types of the eccentricity faults. When the distance between the stator bore and the rotor is not equal throughout the entire generator, different magnetic flux in the air-gap produces imbalance in the current line, which causes rotor unbalances or misalignment.

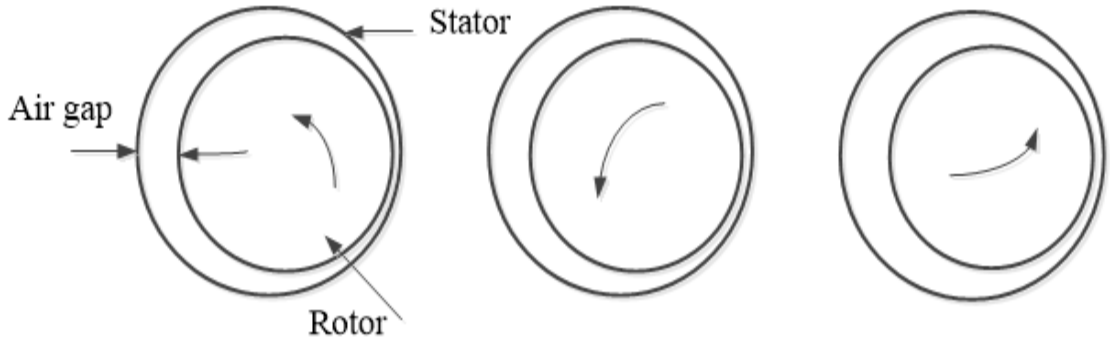

Figure 3. 23 Static eccentricity, [26]

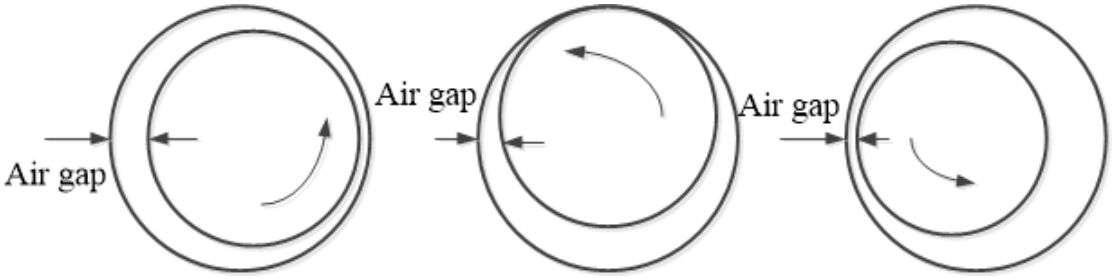

Figure 3. 24 Dynamic eccentricity, [26]

There are several fault diagnosis methods of the eccentricity based on the line current measurement [26, 29, 31, 48, 71, 72,]. Because both static and dynamic

eccentricities incline to live together in practices, only mixed eccentricity considered showing the effects of inverter harmonics. Since the flux linkages in the air-gap wave with the synchronous frequency, any further harmonics oscillating at the speed due to non-uniform structure are expected to take place at the rotating frequency sideband of the synchronous frequency.

Chapter 4. The First Method: Condition Monitoring System of the Wind Generators Based on Study the Effects of the Electrical Torque Pulsations, Temperature of the Generator, and Temperature of the Permanent Magnet

This literature provides various techniques and methods in order to apply an effective CMS on wind turbines' generators. The proposed methods are based on mechanical, electrical, thermal, mathematical, statistical, and reliability analyses. Further, the proposed methods are very different from the previous techniques since the majority of them are based electrical approaches to performing CMS on the wind generators.

The current chapter presents the first method in this research, which is based on studying the effect of the electrical torque pulsations and the temperature of the generator and the permanent magnet on the wind turbine generators under different conditions to define the generators health. Different methodologies have been adopted to develop a proper CMS on the wind generators, such as evaluating the generator electrical torque based on the mechanical torque with taking into account the acceleration torque, which has not been considered in previous work. The mechanical, thermal, and electrical analyses can be utilized to detect the faults, which are coming from the wind generators by monitoring the changes in their characteristics under different (normal and abnormal) operation conditions. Therefore, in order to specify the generator faults, the trend of the electrical

torque with respect to the rotor angular speed of the wind generator under different operation conditions is analyzed. Further, the rate of change in the generator temperature is considered as well an indicator to define the health of the wind generators with respect to the induced electrical torque, because of the negative effect of the elevated generator temperature on the induced electrical torque. Describing the behavior of the rotating permanent magnet of the generator also is very beneficial to apply CMS on the wind generators. The torque of the permanent magnet of the generator is affected by the Oscillation of the magnet temperature. Therefore, monitoring the torque of the permanent magnet with respect to the rate of change in the permanent magnet temperature indicates the generator health. Case study, which is based upon collected data from actual measurements is presented in this work in order to demonstrate the adequacy of the proposed model.

4.1. Introduction

The generated wind power can be increased dramatically by performing modern condition monitoring on the parts that are faced to failures, such as the gearboxes and generators. Further, the operation and maintenance costs of the wind turbines will be reduced when implement the CMS efficiently, which increases the reliability of the wind energy industry, particularly when the turbines deployed offshore. CMS provides detailed information about the wind turbine components' condition by analyzing measured signal to predict and avoid the imminent failure in the wind turbines components [5-7], [81]. The

failures that occur in the wind turbines due the generators have been shown to be significant, which leads to increased attention to avoid the technical problems that are caused by the wind generators during operation. The most important components of the wind generator, which experience likely failures are the bearing—stator, and rotor—and certainly the failures ratios are different in every single component [38]. The mechanical, thermal, and electrical properties can be combined to detect the faults are coming from the wind turbine generators by analyzing their behavior under different operation conditions.

There are various symptoms that appear when the wind generators suffer from faults during operation, such as unbalanced in line currents and air-gap voltages, low torque average, high power losses, and turbulent torque pulsations [26, 31,]. This proposed work presents an application of condition monitoring system on the wind generators based on data collected from actual measurements and Matlab simulation in order to demonstrate the adequacy of the proposed model. The proposed model consists of three algorithms, which link the mathematical, thermal, and mechanical analyses with the electrical methodology. For instance, the high oscillation of the electrical torque pulsations with respect to the rotor angular speed of the generator can be used to implement CMS by combining the mechanical and electrical analyses together. The acceleration torque is considered to evaluate reliable electric torque values and apply proper condition monitoring on the wind generators under different operation conditions. Further, the thermal and electrical analyses can be integrated to study the effect of the elevated generator temperature on the induced electrical torque in order to estimate the rate of the

change in the generator temperature with respect to the induced electrical torque. In this context, the system operation condition can be defined under different loads to apply a proper CMS [82-84]. Finally, the approach of determining the torque of the permanent magnet of the generator with respect to the temperature of the permanent magnet, which is slightly higher than the generator temperature is significant to implement CMS on the wind generators. Based on the mathematical analysis of the differential equations, the permanent magnet torque can be estimated with respect to the magnet temperature with the aim of Matlab simulation.

The rest of this chapter is arranged as follows: Section 4.2 presents the influences of the ripple torque, cogging torque, and the elevated generator temperature on the induced electrical torque. Section 4.3 explains the effect of the elevated generator temperature on the produced electrical torque. In Section 4.4, the influence of the permanent magnet temperature on the driving torque of the rotating permanent magnet is demonstrated by introducing a set of partial differential equations, which is devolved for the characterization of the rotations of the permanent magnet. Section 4.5 provides knowledge about the selected wind turbine, synchronous generator, the model parameters and the available SCADA. This information is necessary to test the validity of the proposed algorithms through a case study and Matlab simulation. The analysis of the proposed algorithms to apply CMS on the wind generators is illustrated in Section 4.6. In order to demonstrate the utilization of the proposed method and its capability, case study is provided in Section 4.7. The obtained results of the proposed models are showed in Section 4.8. Finally, discussion,

conclusions and suggestions for further research are presented in Section 4.9. Figure 4.1 illustrates the mechanism of work for the three proposed different methodologies of the present work.

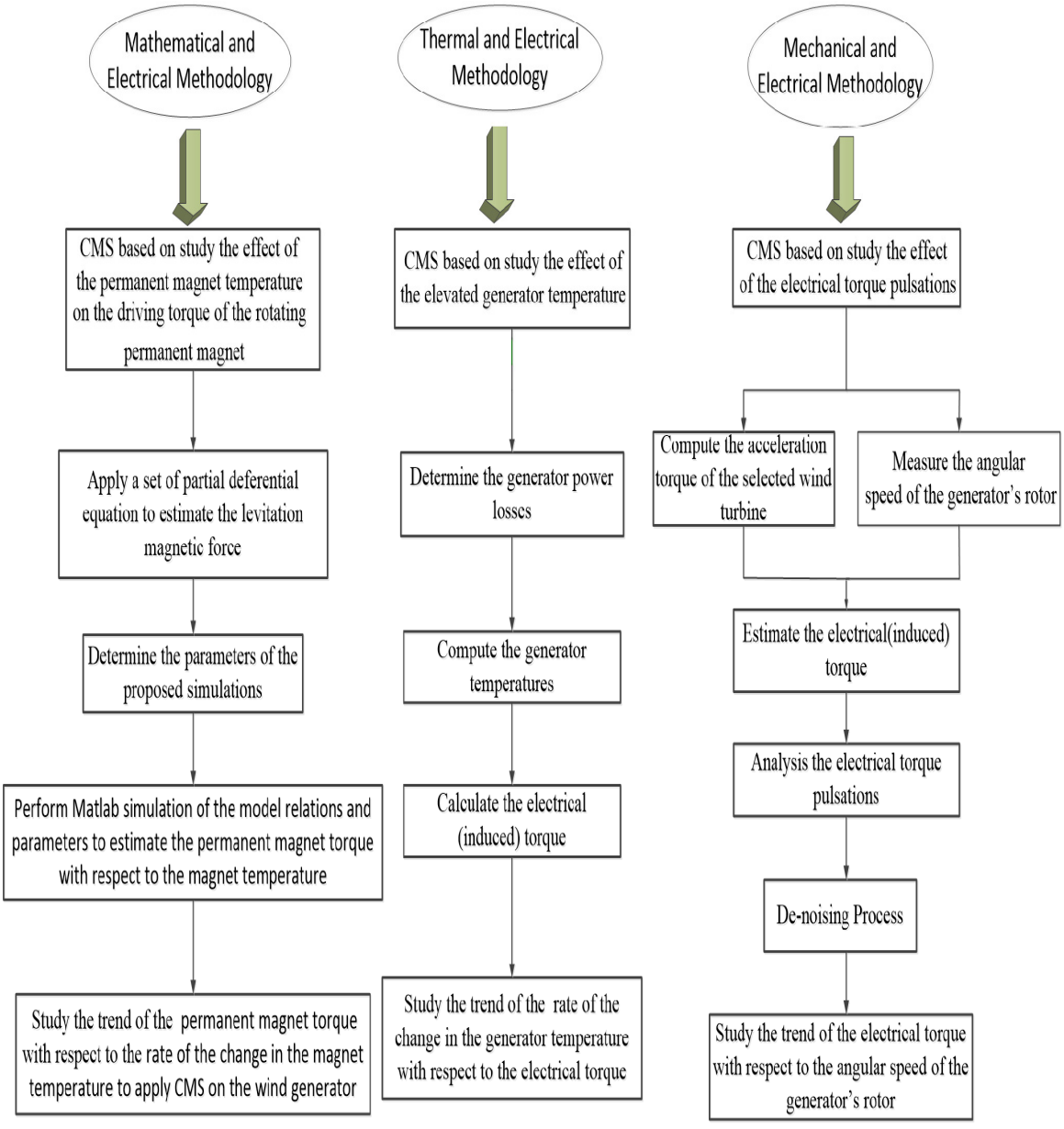

Figure 4. 1 The proposed methodologies' flowchart of the first method to apply CMS on the wind generators.

4.2. The influence of the Ripple Torque, and Cogging Torque, on the Induced Electrical Torque.

The failures, which occur due to different faults, such as bearing faults, stator inter-turn faults, and eccentricities are related to all types of synchronous machines. While some faults are related to the wound rotor machines, such as rotor winding faults, broken damper bars, or end-rings [82-84]. One major drawback to the permanent magnet machines is the ripple torque and its accompanying torque, which is called the cogging torque. The electrical torque pulsation is represented in the summation of the ripple and cogging torque with zero mean value and produces vibration and phonic noise, which might grow in the variable speed drives. In this context, the induced electrical torque will be affected negatively in the case of the ripple and cogging torques.

The ripple torque is undesirable and leads to mechanical vibration, acoustic noise, and problems in the drive systems, which reduce the lifetime of generators. This torque is created by the interaction between the magnetomotive force (MMF) due to the stator windings and the MMF due to the rotor magnets. Ripple torque can be calculated from the next formula:

$$T_{ripp} = \text{Ripple Torque} = (T_{max} - T_{min})/T_{avg} \quad (4.1)$$

where:

T_{max} is the maximum electrical torque,

T_{min} is the minimum electrical torque, and

T_{avg} is the average electrical torque [80-82].

Ripple torque changes according to the relative magnet width of the machine, which is partly reflected in the harmonics of the air-gap flux density. Figure 4.2 displays the ripple torque behavior, which indicates a dramatic irregular change in the torque path through the time. The electromagnetic designer of the permanent magnet synchronous generators assure that the ripple torque beneath 1%, guaranteeing regular operation, low noise and extended gear and machine lifetime [82-84].

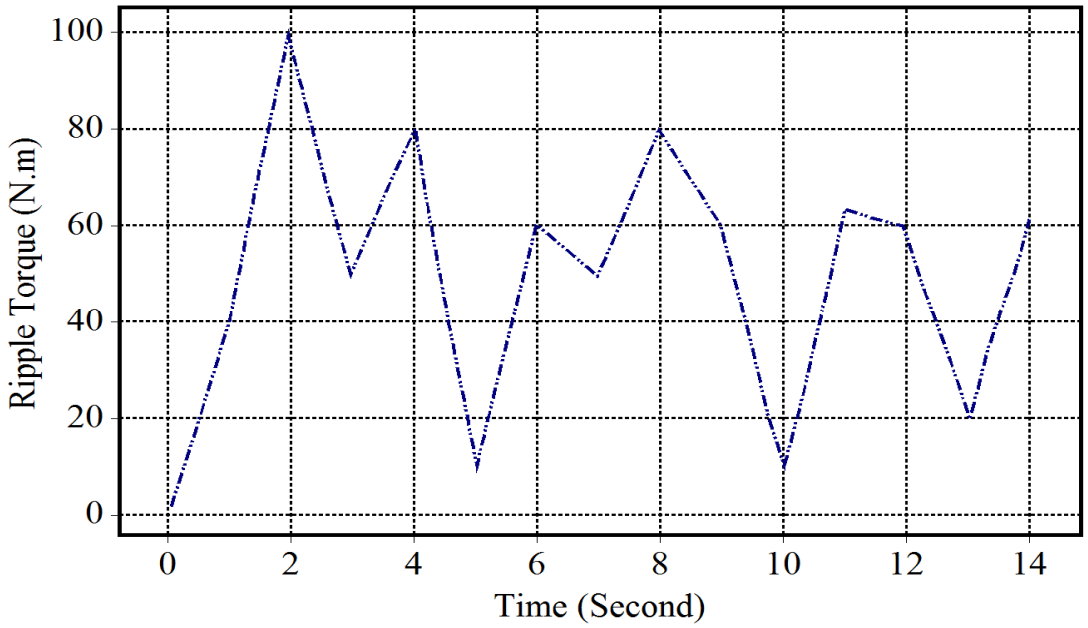

Figure 4. 2 Ripple torque trend, [82-84]

On the other hand, cogging torque is caused due to the interaction between the permanent magnets and the stator slots. This interaction causes an uneven air-gap

permeance resulting in the magnets regularly seeking a position of minimum reluctance [83-85]. In other words, when the rotor of a generator rotates with respect to the stator at no electrical load, cogging torque is created. Many undesirable effects are produced from the cogging torque, such as noise and mechanical vibration on the wind turbines, which affects the self-start running negatively. The cogging torque can be calculated for different rotor positions when the stator winding carries no current and the magnetic field is available. Reaching low cogging torque is necessary because of lower mechanical vibrations, less noise and longer operational life of the gearing and other mechanics. [82-85]. For small wind turbines in the low wind speed, noise and mechanical vibration may be excited by the cogging torque, which threaten the safety of the whole structure. While, in high wind speed, there is enough of torque and the kinetic energy, which stored in the turbine rotor leads the cogging torque to be insignificant. The cogging torque (T_{cog}) can be expressed in the general form:

$$\mathrm{T_{cog}} = -\frac{1}{2}\,\emptyset_{\mathrm{g}}^{2}\frac{\mathrm{d}R_g}{\mathrm{d}\varphi} \tag{4.2}$$

where, $\emptyset_g$ is the air-gap flux, R_g is the air-gap reluctance, and φ is the position of the rotor. The cogging torque can be canceled by forcing the air-gap reluctance to be stable with respect to the rotor position [82-84]. Figure 4.3 shows a typical cogging torque waveform for synchronous wind generator. It can say that during the start-up process— cogging torque is low, which is desirable— while the wind turbine may never start with the high cogging torque.

In order to perform an efficient condition monitoring system on the wind generators, the approach of analyzing the electrical torque pulsations at different generator's speeds in the normal and abnormal conditions is adopted based on intergrading the mechanical and electrical methodologies together. The proposed algorithm is based on the acceleration torque, which is taken into account at different rotational speed of the generator's rotor. This assumption leads to accurate results, which will be presented later. In the following section, the effects of the elevated generator temperature on the induced electrical torque is demonstrated.

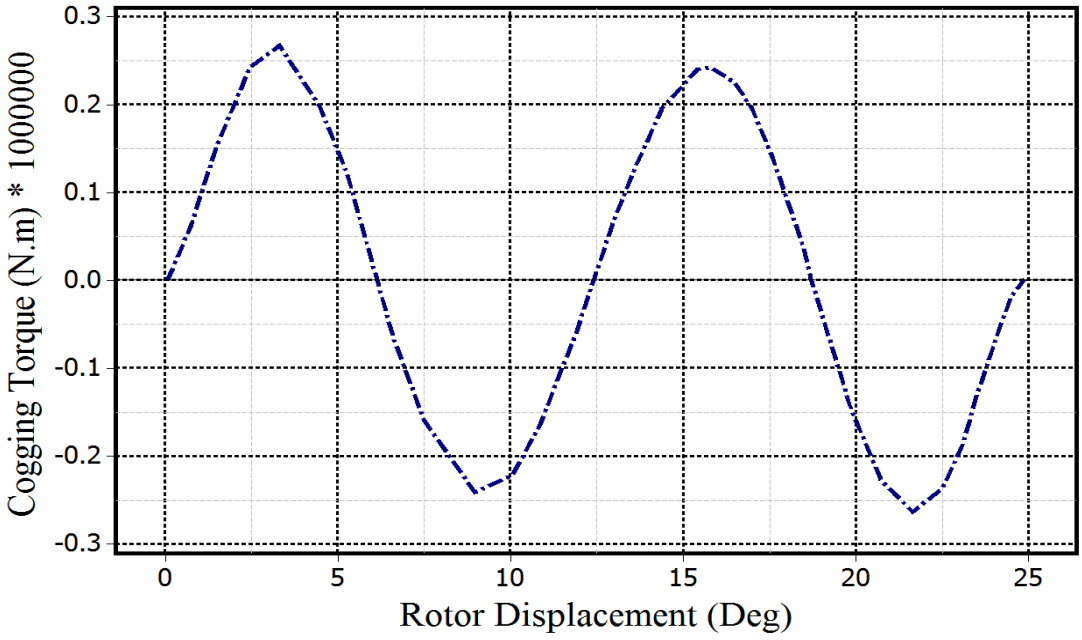

Figure 4. 3 Typical cogging torque waveform [82-84]

4.3. The Effect of the Elevated Generator Temperature on the Produced Electrical Torque.

The elevated generator temperature plays a remarkable role in decreeing the induced electrical torque, which affects negatively the efficiency of the system. When the temperature reaches high values in the permanent magnet generators, a reversible demagnetization effects the torque capability and reduces the efficiency of the entire system. Therefore—the stator winding temperature, which is assumed the generator temperature itself— can be considered an important indicator to define the system operation condition. The residual flux density and the field intensity of the magnet decline with the increase of the generator temperature and return to the initial value with the decrease in the generator temperature. This change in the residual flux density of the magnet along and the change in the armature resistance of the motor with respect to the temperature affect the torque capacity and the efficiency of the system [86]. The nature of the reversible demagnetization is due to the low values of the force of the field intensity and the remanent flux density. The relationship between the generator temperature and both remanent magnetic flux density and the forced field intensity can be determined respectively as follows:

$$B_r = B_{r_{amb}}[1 + \frac{\alpha_B}{100} \cdot (T_G - T_{amb}) \tag{4.3}$$

$$H_c = H_{c_{amb}}[1 + \frac{\alpha_H}{100} \cdot (T_G - T_{amb}) \tag{4.4}$$

where, T_G and T_{amb} are the generator and ambient temperatures respectively, B_r and $B_{r_{amb}}$ are the remanent magnetic densities at the operation and ambient temperature respectively, H_c and $H_{c_{amb}}$ are the forced or coercive field intensities at the operation and ambient temperature respectively, and α_B and α_H are the temperature coefficients for the remanent magnetic density and for the coercive field intensity respectively [86].

In AC synchronous generators, the electrical power P_{el} can be converted to mechanical power P_{mech} by adding the frictional losses power P_{loss} as follows:

$$P_{el} = P_{mech} + P_{loss} \tag{4.5}$$

In order to determine the effects of the generator temperature on the induced electrical torque, the frictional losses power must be defined. The frictional losses power P_{loss} for the AC generators can be determined as follows [87]:

$$\begin{aligned}\text{The frictional losses power} \\ = \text{Stray losses } P_{SL} + \text{Friction and windage losses } P_{F\&W} \\ + \text{Core losses } P_{CL} + \text{ copper losses } P_{cu}\end{aligned} \tag{4.6}$$

$$P_{loss} = P_{SL} + P_{F\&W} + P_{CL} + P_{cu} \tag{4.7}$$

The mechanical power loss, stray losses, and core losses can be ignored in the advanced synchronous generators at the rated condition. In this proposed work, the copper loss is only considered, and changed based on the armature current flow and the armature resistance. The copper loss in the three phase synchronous generators is defined as follows:

$$C_{cu} = 3\, I_A^2\, R_A \tag{4.8}$$

where, I_A, R_A are the armature current flow and armature resistance respectively. The Eq. (4.7) can be formulated as follows:

$$P_{loss} \approx 3\, I_A^2\, R_A \tag{4.9}$$

The heat resulting from the copper losses in the coil is diffused by conduction through the generator components and airflow in the air gap. The dissipated heat is a function of the generator type, insulation system, operation conditions, and construction. The generator manufacturers typically provide an indication of the generator's ability to diffuse heat by providing thermal resistance values. The thermal resistance is a measure of the resistance to the transfer of heat through a given thermal path. In the case of the AC generators, there is a thermal channel from the generator windings to the generator case and a second between the generator case and the generator environment (ambient air). Some generator's manufacturers define the thermal resistance for each of the two thermal channels while others define only the sum of the two as the total thermal resistance of the generator. The thermal resistance is specified in the temperature increase per the unit of the power loss. The generator temperature can be determined based on the power loss and the thermal resistances as follows [86]:

$$T_G = P_{loss} \cdot (R_{th1} + R_{th2}) + T_{amb} \tag{4.10}$$

where, R_{th1} is thermal resistance from the windings to the case (C°/Watt), and R_{th2} is the thermal resistance from the case to the ambient (C°/Watt). Consequently, the generator temperature can be expressed as follows:

$$T_G = [(3\, I_A^2\, R_A) \cdot (R_{th1} + R_{th2})\,] + T_{amb} \tag{4.11}$$

In the AC generators, the induced electrical torque τ_{el} can be determined as follows:

$$\tau_{el} = I_A \cdot K_M \tag{4.12}$$

where, K_M is the generator torque constant. By substitution of Eq. (4.12) into Eq. (4.11), the generator temperature will equal to the next relation:

$$T_G = [\ (3 \cdot (\tau_{el}^2/K_M^2)\ R_A) \cdot (R_{th1} + R_{th2})\,] + T_{amb} \tag{4.13}$$

The previous equation indicates that the relationship between the electrical torque and the generator temperature is curvilinear. Based on Eq. (4.13), the induced electrical torque for the AC generators can be defined as follows:

$$\tau_{el} = \left[\frac{(T_G - T_{amb}) \cdot K_M^2}{3R_A \cdot (R_{th1} + R_{th2})}\right]^{1/2} \tag{4.14}$$

The effect of the generator temperature on the induced electrical torque can be determined based on Eq. (4.14). The induced electrical torque is based on two variables, the generator temperature, and the armature resistance since the rest of the terms are constants. The frequency response of the generator is reduced due to the decreasing in the

torque capability. Further, the magnet flux density comes down at higher generator temperature, which affects the induced electrical torque as shown in Fig. 4.4.

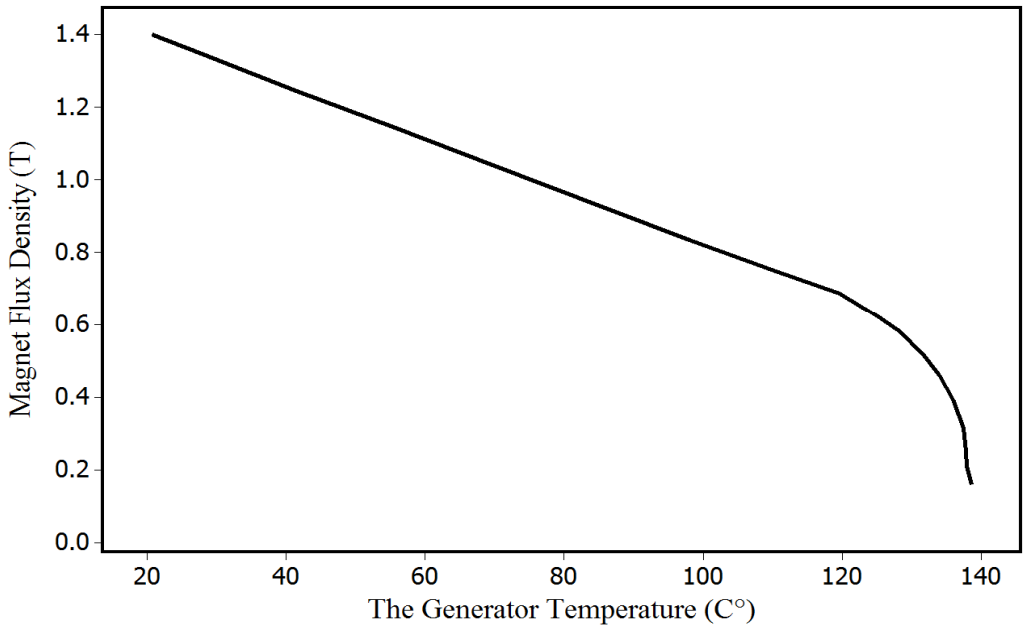

Fig. 4. 4 The measured magnet residual flux density.

4.4. The Effect of the Permanent Magnet Temperature on the Driving Torque of the Rotating Permanent Magnet

Due to the increase in the permanent magnet temperature, the driving torque of the rotating permanent magnet oscillates with increasing the amplitude based on the change in the magnetization angle of the permanent magnet. An important reason for the driving torque of the permanent magnet is the temperature dependence of the magnetization since the temperature range decreases with the magnetization increases [88]. In this context, defining the behavior of the rotating permanent magnet is significant to apply CMS on the

wind generators. The permanent magnet model should describe the rotating permanent magnet condition during operation in the normal and abnormal situations. This section presents a set of partial differential equations, which is devolved for the characterization of the rotations of the permanent magnet. Suppose the permanent magnet has a cylindrical shape and volume ∀ as shown in Fig 4.5. The length of the cylinder is L and the radius is r. Thus, the volume of the cylindrical shape (∀) is $\pi r^2 L$. The density of the permanent magnet is considered to be constant (ρ); consequently, the total mass of the permanent magnet (m) is $\pi r^2 L\, \rho$. A coordinate system is determined in such a way that the axis of the cylinder corresponds with the z-axis. Therefore, the z-coordinator of the cylinder is in the range $[0, L]$. In the case of the two-dimensional setting, a cross section of the cylinder, such as a circle is considered. The cross section area of the circle is A in the xy-plane with radius r and center (0,0). The normal vector at a point of the boundary ∂A is denoted by n and assumed to reference into the surrounding air.

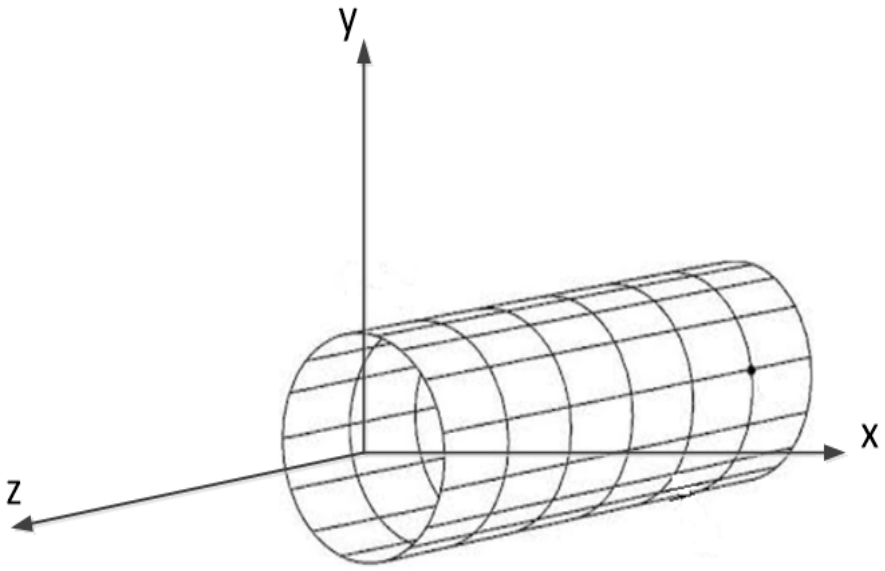

Fig. 4. 5 The cylindrical shape of the permanent magnet.

Assuming the temperature in the limited volume of the cylindrical shape (∀) does not change in the z-direction and the heat flux through the bottom and the top surface of the cylinder is negligible. The temperature distribution $T = T(t, x, y)$ is governable by the two-dimensional time dependent heat equation [89, 90,]:

$$\rho c \frac{\partial T}{\partial t} - \nabla \cdot (\lambda \nabla \mathrm{T}) = 0 \tag{4.15}$$

The term $\rho c \frac{\partial T}{\partial t} - \nabla \cdot (\lambda \nabla \mathrm{T})$ equals to zero since there are no heat sources. The specific heat is denoted with c, and λ is the thermal conductivity. This equation has to be completed with an initial condition $T(0, x, y) = T_0(x, y)$ and the boundary conditions. By applying the Newton's law of cooling at the boundary ∂A, the heat flux can be assumed as follows:

$$n \cdot (\lambda \nabla \mathrm{T}) = \alpha \cdot (T_0 - T) \tag{4.16}$$

where the temperature $T_0 = T_0(x, y)$ of the surrounding air, which can be estimated from the measurements and α is the heat transfer coefficient. The coordinate system is fixed and not rotating with the magnet. Therefore, the point (x, y) moves with the velocity $\omega(-y, x)^T$. Further, the convective heat transfer should be taken into account, which modifies the heat equation as follows:

$$\rho c \left[\frac{\partial T}{\partial t} + \omega \begin{pmatrix} -y \\ x \end{pmatrix} \cdot \nabla T\right] - \nabla \cdot (\lambda \nabla T) = 0 \quad \text{In the cross section area (A)} \tag{4.17}$$

With respect to the boundary conditions, the time dependent heat equation equals to:

$$h\frac{\partial T}{\partial n} + T = T_0 \quad \text{On } \partial A \tag{4.18}$$

where h is the heat transfer coefficient by convection and T_0 is continuously differentiable on ∂A.

In order to estimate the torque on the permanent magnetic, a detailed consideration of the magnetic forces is necessary. Since the permanent magnet is levitated above the superconductor, the total levitation force in the three dimension is defined as follows:

$$F = \begin{pmatrix} 0 \\ \pi r^2 L\rho g \\ 0 \end{pmatrix} \tag{4.19}$$

The permanent magnet consists of a spatial homogeneous volume density. Let B is the magnetic field due to the induced current, then the magnetic force of the permanent is defined as follows:

$$F = \int_{\forall} \nabla(m \cdot B) d\forall = \int_{\forall} (m \cdot \nabla) B d\forall \tag{4.20}$$

The permanent magnet mass has components in the z-direction m_z (the permanent magnet axis), thus:

$$F = \int_{\forall} (m \cdot \nabla) B d\forall = m_z \cdot \frac{\partial B}{\partial z} \tag{4.21}$$

Using that $\frac{\partial}{\partial y} B_z = \frac{\partial}{\partial z} B_y$, the y-component of the magnetic force F_y is defined as follows:

$$F_y = \int_{\forall} m_z \frac{\partial}{\partial y} B_z \, d\forall = \int_0^l \int_A m_z \frac{\partial}{\partial y} B_z \, da \, dz = L \int_A m_z \frac{\partial}{\partial y} B_z \, dA = L \int_A m_z \nabla B_z \, dA \tag{4.22}$$

Since the diameter of A is small, linearization of B in A is beneficial, which means ∇B_z is constant in A:

$$\nabla B_z = \begin{pmatrix} 0 \\ g_B \\ 0 \end{pmatrix} \tag{4.23}$$

Based on a suitable constant g_B, the x – and z–components are zero due to the fact of the total force has zero x– and z–components. Thus, the y–component of the force is given by:

$$F_y = L \, g_B \int_A m_z \, (x, y) \, dA \tag{4.24}$$

where F_y is the levitation force at the limit temperature and will modify as follows:

$$F_y = L\pi r^2 \rho \, g \tag{4.25}$$

According to the Bloch $T^{3/2}$ relation [91], a linear function of the permanent magnet mass in the z-direction can be introduced before the torque is calculated as follows:

$$m_z = u + qT \tag{4.26}$$

where u and q are parameters and can be determined by using specific relations. The levitation force will define as follows:

$$F_y = L \int_A m_z \frac{\partial}{\partial y} B_z \, dA = L \int_A (u + qT) g_B \, dA \tag{4.27}$$

The torque of the permanent magnet τ_{pm} around the z-axis can be estimated in a similar way:

$$\begin{aligned} \tau_{pm} = L \int_A x \, m_z \frac{\partial}{\partial y} B_z \, dA = \; & L \int_A x \, (u + qT) \, g_B \, d \\ = \; & \rho g_B L \int_A x \, dA + q g_B \, L \int_A x \, T \, dA \end{aligned} \tag{4.28}$$

Since $\int_A x \, dA = 0$, the final version for the torque of the permanent magnet τ_{pm} as follows:

$$\tau_{pm} = \; q \; g_B L \int_A x \, T \, dA \tag{4.29}$$

Where g_B can be calculated according to the next relation:

$$g_B = \frac{\rho \, g}{u + q \, \bar{T}} \tag{4.30}$$

where $\bar{T}$ is the mean temperature of the permanent magnet and the parameter q is computed as follows:

$$q = \frac{\mu_r}{J_{pm}} \tag{4.31}$$

where μ_r is the friction coefficient and J_{pm} is the moment of inertia for the cylindrical permanent magnet, which can be defined as follows:

$$J_{pm} = \pi L \rho r^4/2 \tag{4.32}$$

The parameter u is estimated from the next formula [91]:

$$u = 2.5\ x\ 10^{-6} F_y\ /J_{pm} \tag{4.33}$$

The mean temperature of the permanent magnet can be estimated based on the time-dependent equation (4.17) in the polar coordinates ($x = a\ cos\varrho,\ y = a\ sin\varrho$) as follows:

$$\frac{\partial T}{\partial t} + \omega \frac{\partial T}{\partial \gamma} - \lambda \left(\frac{\partial^2}{\partial a^2} + \frac{1}{a} \frac{\partial}{\partial a} \right) T - \frac{\lambda}{a^2} \frac{\partial^2}{\partial \gamma^2}\ T = 0 \tag{4.34}$$

where $a \in (0, r)$ and γ is the magnetization angle of the permanent magnet. By integrating the last equation from 0 to 2π. It can obtain:

$$\int_0^{2\pi} T(t, a, \varrho) d\gamma + \omega \int_0^{2\pi} \frac{\partial}{\partial \varrho} T(t, a, \gamma) d\gamma$$
$$-\lambda \left(\frac{\partial^2}{\partial a^2} + \frac{1}{a} \frac{\partial}{\partial a} \right) \int_0^{2\pi} T(t, a, \gamma) d\gamma - \frac{\lambda}{a^2} \int_0^{2\pi} \frac{\partial^2}{\partial \gamma^2}\ (t, a, \gamma) d\gamma = 0 \tag{4.35}$$

Suppose the abbreviation $\xi(t, a) = \int_0^{2\pi} T(t, a, \gamma) d\gamma$ the integrals with partial derivatives with respect to γ modify the singular differential equation to:

$$\frac{\partial}{\partial t}\ \xi(t, a) - \lambda \left(\frac{\partial^2}{\partial a^2} + \frac{\partial}{a \partial a} \right) \xi(t, a) = 0 \quad for\ a \in (0, r), \tag{4.36}$$

For the boundary condition we get similarly:

$$h\frac{\partial \xi}{\partial a} + \xi \mid_{a=r} = \int_0^{2\pi} T_0 \, d\gamma \tag{4.37}$$

Setting the time derivative to zero, Eq. (4.36) becomes a stationary heat equation to obtain rotational symmetric solution. For this situation, the solution of $\xi(a)$ becomes constant [90, 92,], so that:

$$\pi r^2 T = \int_0^r \xi(a) a \, da = \frac{1}{2} r^2 C = \frac{1}{2} r^2 \int_0^{2\pi} T_0 \, d\gamma \tag{4.38}$$

Thus,

$$\bar{T} = \frac{1}{2\pi} \int_0^{2\pi} T_0 \, d\gamma \tag{4.39}$$

The previous mathematical analysis can be utilized to find the effect of the permanent magnet temperature on the driving torque of the rotating permanent magnet to define the generator operation condition based on Matlab simulation of the model relations and parameters.

4.5. Knowledge about the Selected Wind Turbine, Generator, Available SCADA, and the models parameters

Actual data was obtained from a variable speed wind turbine with rated power of 600 KW, 60Hz, two blades, 43.3m rotor diameter, and rated speed 12.7 m/s with upwind horizontal axis. The turbine height is 36.6m and has a permanent magnet synchronous

generator with 1800 rpm rated synchronous speed and gearbox ratio 1:43. The combined generator rotor and wind turbine moment of inertia (J) is equal to 2252 kg. m^2 [93]. The collected data represent two operation conditions of the selected wind turbine, normal and abnormal conditions. The SCADA system offers sufficient knowledge about the system's condition during running based on many parameters that are measured and recorded over 600 seconds. The mechanical torque is measured by the SCADA system, which represents the high speed shaft torque. The angular speed of the high speed shaft is balanced with the rotor rotational speed of the synchronous generator and measured over time based on the gearbox ratio. Figure 4.6 displays the pulsations behavior of the estimated electric torque with respect to the rotor rotational speed of the selected synchronous generator (rpm) in the normal and abnormal conditions according to the measured data. The synchronous generator shows different torque-speed attributes in the normal and abnormal conditions, which confirms that the torque-speed relationship could be a significant indicator for applying condition monitoring on the wind generators.

As was mentioned previously, the first method involves three different methodologies. The first methodology is based on the acceleration torque, which is estimated in order to obtain accurate electric torque to perform a proper condition monitoring on the selected wind generator. The main concept of the second methodology is determining the rate of change in the generator temperature with respect to the electrical torque provides knowledge to defining the operation condition of the system. The third methodology confirms that CMS on the wind generators can be applied also based on

evaluating the driving torque of the rotating permanent magnet with respect to the magnet temperature by processing the parameters of the proposed algorithm. The parameters of the simulations should be known in order to estimate the other characters, which govern the permanent magnet torque with respect to the permanent magnet temperature. Table 4.1 summarizes the third methodology parameters, which are significant to process the data of the proposed algorithm.

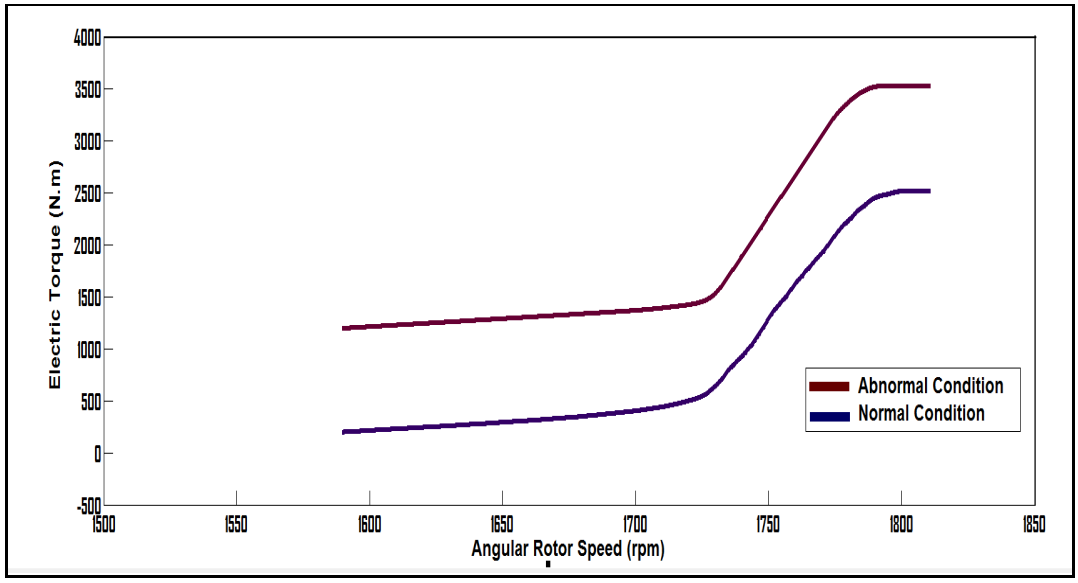

Figure 4. 6 The electric torque trend with rotor rotational speed, [93].

Table 4. 1 The third methodology's parameters of the first method, [93]

Geometry and Mechanical Properties	
g	$9.81\ m/s^2$
r	$0.2\ m$
L	$0.34\ m$
ρ	$8236\ kg/m^3$
μ_r	$1.04635\ x\ 10^{-10} N.m\ s$
λ	$8\ W/(m.K)$
$\propto$	$50\ W(m^2K)$
T_0	$18\ C^{\circ}$

4.6. The Proposed Models Analysis of the First Method

Mechanical parameters are easily measured and more available than the electric parameters. In addition, it is very tricky and complicated to use the electrical methodology in order to estimate the electric torque. Consequently, the electromagnetic torque τ_e can be estimated easily from the mechanical aspect. When a synchronous machine is operated as a generator, the prime mover drives the generator at synchronous speed ω_s. The mechanical torque of the prime mover τ_m can be defined from the next relation:

$$\tau_m = \tau_{el} + \tau_{acc} \tag{4.40}$$

where, τ_{acc} is the acceleration torque which can be determined as follows:

$$\tau_{acc} = J \cdot \frac{d\omega_r}{dt} \tag{4.41}$$

where J is the combined inertia coefficients for the generator's rotor and the wind turbine during the steady-state (constant speed), and $\frac{d\omega_r}{dt}$ is the change in the rotational angular speed of the high speed shaft per time which is equal to the change in the rotational angular speed of the generator rotor shaft per time [16, 94,]. The mechanical torque τ_m that produced by the wind accelerates the wind turbine and counterbalances with the torque of the low speed side shaft τ_{Ls} (the torque produced by the torsional movement of the low speed side shaft). From Fig. 4.7, the relation between τ_m and τ_{Ls} can be estimated as follows:

$$\tau_{\mathrm{m}} - \tau_{\mathrm{Ls}} = \mathrm{J}_{\mathrm{B,H}} \cdot \frac{\mathrm{d}\omega_{\mathrm{t}}}{\mathrm{dt}} \tag{4.42}$$

where, ω_{t} is the rotational angular speed of the low speed shaft, and $\mathrm{J}_{\mathrm{B,H}}$ is the total moment of inertia for both the blades and hub of the wind turbine$(\mathrm{kg.\,m^2})$, which can be calculated as follows:

$$\mathrm{J}_{\mathrm{B,H}} = \mathrm{J}_{\mathrm{B}} + \mathrm{J}_{\mathrm{H}} \tag{4.43}$$

$$\mathrm{J}_{\mathrm{B}} = \frac{3}{12}\left[\, l^2 + b^2 + \, cos^2\,\theta^2 + 3\, m_B\, d^2\right] \tag{4.44}$$

$$J_H = \, m_H \cdot \mathrm{D}_1^2/8 \tag{4.45}$$

where J_{B} is the turbine's blades moment of inertia, J_{H} is the turbine' hub moment of inertia, l is the blades measured length, b is the average width the blades, θ is the blade angle, d is the center of mass displacement of the blades, m_H is the weight of the hub, and $\mathrm{D}_1$is the diameter of the hub [16, 94,].

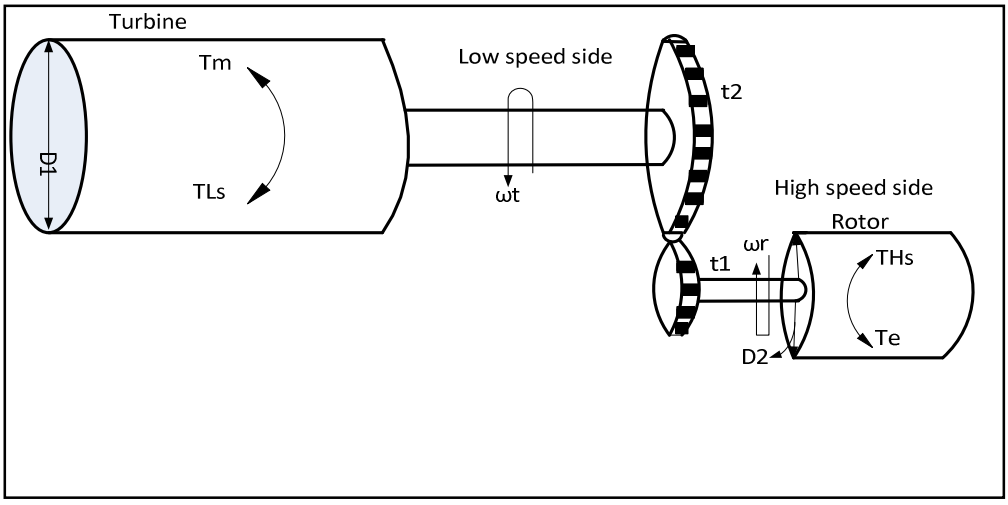

Figure 4. 7 Wind Turbine Drive Train [16, 94,].

Similarly, the torque that produced by the high-speed shaft τ_{Hs} accelerates the rotor of the synchronous generators and equalizes with the electromagnetic torque τ_{e} that produced by the generator. The relation between the electromagnetic torque τ_{e} and high-speed side torque τ_{Hs} is determined as follows:

$$\tau_{\mathrm{Hs}} - \tau_{\mathrm{el}} = \mathrm{J_g} \cdot \frac{\mathrm{d}\omega_{\mathrm{r}}}{\mathrm{dt}} \tag{4.46}$$

where $\mathrm{J_g}$ is the moment of inertia of the generator's rotor, which depends on the weight m_g and diameter D_2 of the generator, and ω_{r} is the angular speed of the generator's rotor. The gear ratio is defined as follows:

$$\frac{\tau_{\mathrm{Ls}}}{\tau_{\mathrm{Hs}}} = \frac{\omega_{\mathrm{r}}}{\omega_{\mathrm{t}}} = \frac{\mathrm{t_1}}{\mathrm{t_2}} = \text{Gear ratio} \tag{4.47}$$

where $\mathrm{t_1}$ is the number of teeth on the output gear, $\mathrm{t_2}$ is the number of teeth on the input gear, and ω_{r} is the rotational angular speed of the generator rotor's shaft. The rotational angular speed of the turbine ω_{t} can be defined such as:

$$\omega_{\mathrm{t}} = \omega_{\mathrm{r}} \cdot \frac{\mathrm{t_2}}{\mathrm{t_1}} \tag{4.48}$$

With the help of the previous relations, the electromagnetic torque can be determined as follows [16, 94,]:

$$\tau_{\mathrm{el}} = \tau_{\mathrm{m}} \cdot \frac{\mathrm{t_1}}{\mathrm{t_2}} - \mathrm{J_g} \cdot \frac{\mathrm{d}\omega_{\mathrm{r}}}{\mathrm{dt}} - [\mathrm{J_m} \frac{\mathrm{d}\omega_{\mathrm{r}}}{\mathrm{dt}} \cdot [\frac{\mathrm{t_2}}{\mathrm{t_1}}]^2] \tag{4.49}$$

The use of Eq. (4.49) provides an estimation of the induced electrical torque based on the operation condition and the design of the manufacture.

As was mentioned before, estimating the electromagnetic torque is not complicated when the information of the mechanical and thermal parameters are available by SCADA system. In order to derive a proper algorithm to apply a CMS on the wind generators depending on the study of the electrical torque pulsations, following the electrical analysis on the generator part is very beneficial. There are two magnetic fields in the synchronous machine under normal condition. One produced from the rotor circuit and another from stator circuit. The electric torque is produced due to the interaction between those magnetic fields. In a three-phase non-salient pole synchronous generator, the electromagnetic torque τ_e that produced by the generator can be determined as follows:

$$\tau_{el} = 3\, E_a \cdot \frac{V_{\emptyset}}{\omega_s X_s} \sin\delta \tag{4.50}$$

where E_a is the internal voltage that produced in one phase of a synchronous generator, $V_{\emptyset}$ is the output voltage of a particular phase, X_s is synchronous reactance of the generator, ω_s is the generator synchronous rotational speed, and δ refers to the torque angle of the synchronous generator and can be defined as the angle between the internal generated voltage and output voltage [16], [82-84]. The simple generator electrical circuit is shown in Fig. 4.8.

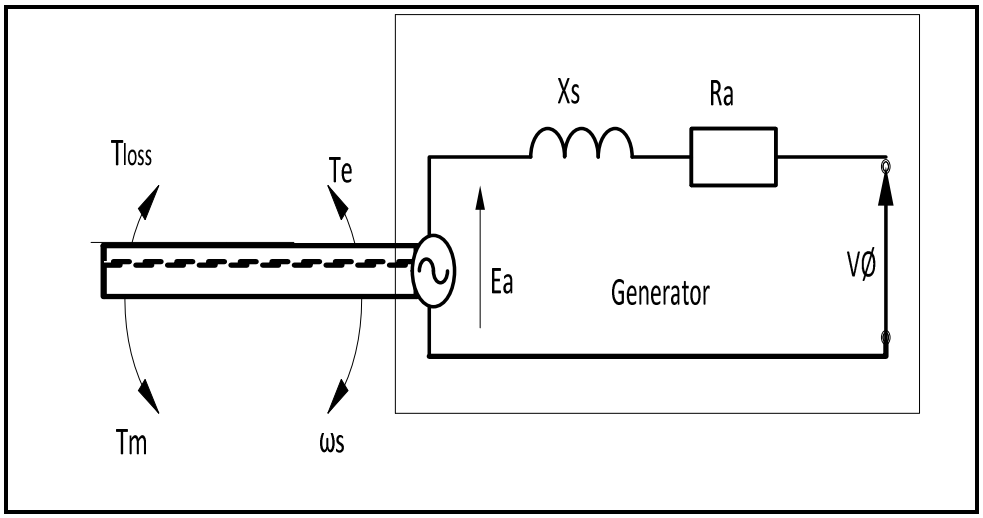

Figure 4. 8 Synchronous machine operated as a generator [16]

The Kirchhoff's voltage law equation for this electrical circuit can be derived as:

$$V_{\emptyset} = E_a - (j X_s + R_A) I_A \tag{4.51}$$

where, R_A is the resistance of the generator's stator, and I_A refers to the state phase current [14, 87,]. The winding resistance R_a can be ignored in the large synchronous generators since it is very small value. Consequently, the synchronous voltage can be written as follows:

$$V_{\emptyset_a} \approx E_a - (jX_s)I_A \tag{4.52}$$

Then, the electrical torque can be estimated in different formula as follows:

$$\tau_{el} = 3E_a \cdot \frac{E_a - (j X_s)I_A}{\omega_s X_s} \sin\delta \tag{4.53}$$

The internal voltage that produced in one phase of a synchronous generator E_a can be written in another form as follows:

$$E_a = \sqrt{2}\,\pi\, N_C\, \emptyset\, f_e \tag{4.54}$$

where $\emptyset$ is the magnetic flux, N_C is the coil turns of the stator, and f_e is the electrical frequency in hertz. The internal voltage also can be written in another form:

$$E_a = \frac{\sqrt{2}}{4}\, N_C\, \emptyset\, \omega_r\, p \tag{4.55}$$

From Eq. (4.51) it becomes clear that:

$$E_a - (j\, X_s + R_A)\, I_A \propto {E_a}^2 \tag{4.56}$$

With the aid of EQs. (4.55) and (4.56) should be modified as follows:

$$E_a - (j\, X_s + R_A)\, I_A \propto {E_a}^2 = N_c^2\, \emptyset^2\, \omega_r^2\, \frac{p^2}{8} \tag{4.57}$$

By substitution of Eq. (4.50) into Eq. (4.57), the electrical torque will be equal to the next relation:

$$\tau_{el} = 3\, \frac{N_c^2\, \emptyset^2\, \omega_r^2\, \frac{p^2}{8}}{\omega_r X_s} \sin\delta \tag{4.58}$$

Consequently, the final formula of the electrical torque is as follows:

$$\tau_{el} = 3\, \frac{N_c^2\, \emptyset^2 \omega_r\, \frac{p^2}{8}}{X_s} \sin\delta \tag{4.59}$$

Because N_C, and p are constant parameters, the relationship between the electrical torque and rotational angular speed of the generator's rotor can be written as follows:

$$\tau_{el} \alpha \frac{\omega_r}{X_s} \quad (4.60)$$

The previous equation used when the torque angle δ and magnetic flux ∅ are stable. A condition monitoring criterion C is proposed in [16] as an indicator to apply a monitoring technique on the wind generators. The electrical torque is directly proportional with the angular rotational speed of the high speed shaft, which is approximately balanced with the generator's rotor angular speed. Therefore, computing the electric torque with respect to the angular speed values of the generator's rotor at each data point is very proper to apply a condition monitoring on the wind turbine generator. When a generator suffers from a specific fault like stator winding fault or rotor imbalance fault, the corresponding reactance of the generator X_S will decrease. Consequently, high electrical torque pulsations created with reference to the angular speed of the generator's rotor in this condition. A case study is presented in the following section in order to confirm the validity of the proposed algorithm.

On the other hand, the high generator temperature affects the induced electrical. According to Eq. (4.14), the induced electrical torque is based on two variables, the generator temperature, and the armature resistance. Therefore, CMS of the wind generators cam be applied based on the simulation of the obtained data of the model. The behavior of the rotating permanent magnet also gives powerful indication about the generator health. According to Eq. (4.29), the permanent magnet temperature plays a significant role also to govern the driving torque of the rotating permanent magnet, which changes the

magnetization angle of the permanent magnet automatically. A case study is presented in the following section in order to confirm the validity of the proposed algorithms.

4.7. Case Study

In order to utilize the proposed models to develop a proper condition monitoring on the generator of the selected wind turbine, the collected data by SCADA system are categorized and analyzed according to the operation conditions. First, with the aid of EQs. (4.40) and (4.41) the electric torque can be calculated based on the acceleration torque. Further, the electric torque can be estimated from the thermal aspect based on the generator temperature and the armature resistance by using Eq. (4.14). The calculated values of the electric torque for both aspects are very similar. The rotational angular speed of the generator's rotor can be estimated from Eq. (4.47), which depends on the wind turbine gear ratio and the rotational angular speed of the low speed shaft. The SCADA system submits enough details for the rotational angular speed of the low speed shaft, high-speed shaft torque, and low-speed side shaft torque every 0.01 second. The collected data present two conditions, the first condition is a stator winding fault condition (abnormal condition), and the second condition is a normal operating condition [93].

Study the trend of the electric torque pulsations can be considered an indicator to perform a condition monitoring system on the wind generators. Based on Fig. 4.6, there is a linear proportional relationship between the electric torque of the synchronous generator

and the rotor angular speed in both conditions. The electrical torque in the abnormal condition is higher than the electrical torque in the normal condition, which implies that the generator reactance X_S changes according to the operation condition. In order to compare and analyze the electrical torque pulsations through the normal and abnormal conditions, the duration time of each operation conditions was divided to 200 seconds. Table 4.2 demonstrates the data classification over time for both conditions.

Table 4. 2 Data conditions classification over time, [93]

Time Interval (Second)	The Operation Condition
0 - 200	Normal
200 - 400	Abnormal
400 - 600	Normal
600 - 800	Abnormal
800 - 1000	Normal
1000 – 1200	Abnormal

In addition, de-noising process was required since the torque and the angular speed signals were very noisy. With the aid of Matlab software, the electrical torque and rotor angular speed signals are de-noised efficiently. The time-waveforms of the electrical torque and angular speed of the generator's rotor signals are shown in Figs. 4.9 and 4.10.

On the other hand, an additional indicator can be utilized to define the generator health and the operation condition by tracking the change in the generator temperature with respect to the induced electrical torque. The elevated generator temperature reduces the generator reactance and increases the rate of change in the generator temperature, which affects the induced electrical torque negatively. The influence of the generator temperature on the induced electrical torque with respect to the armature resistance is illustrated in Fig.

4.11 based on the collected data of this proposed work. The high generator temperature due to different reasons, such as improper cooling system or high power losses, reduce the electrical torque remarkably.

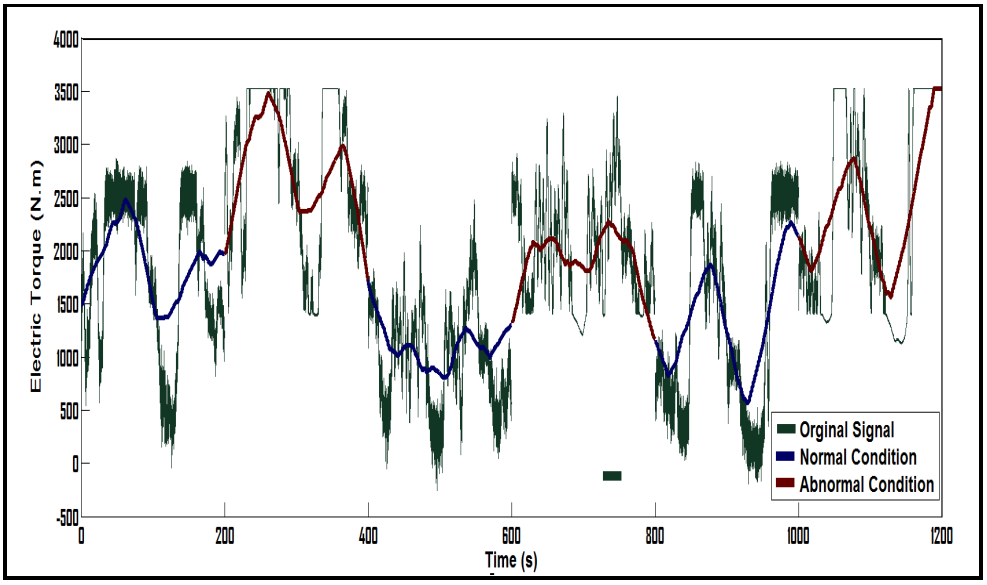

Figure 4. 9 The time-waveform of the electrical torque.

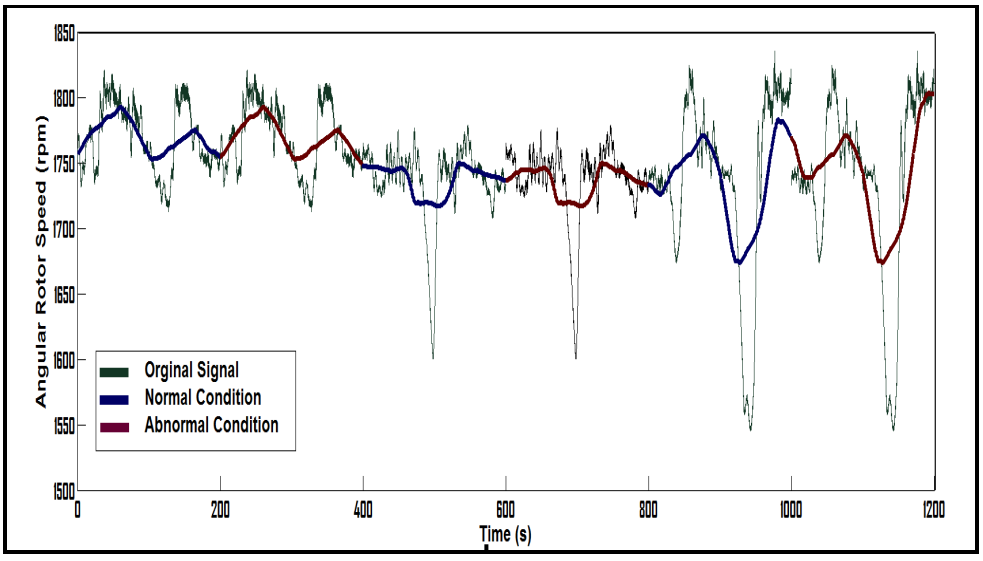

Figure 4. 10 The time-waveform of the angular rotor speed.

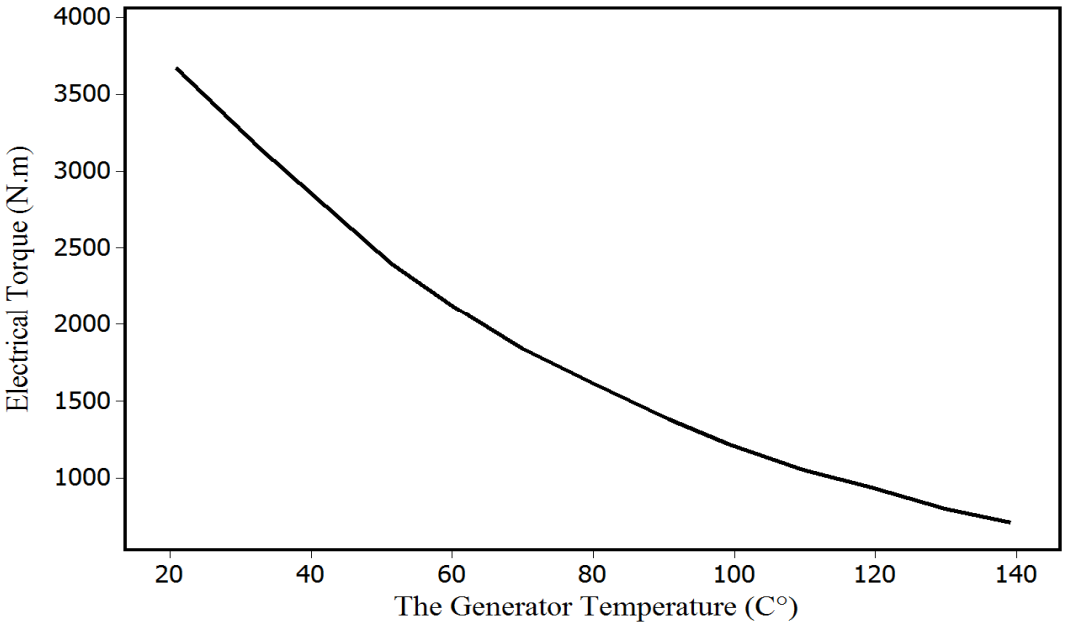

Fig. 4. 11 The induced torque trend with respect to the generator temperature

The last indicator, which aims to define the operation condition of the generator, is studying the behavior of the driving torque of the rotating permanent magnet. The magnetization angle of the permanent magnet changes when the permanent magnet torque oscillates due to the fluctuation in the permanent magnet temperature. Figure 4.12 illustrates the trend of the permanent magnet torque with respect to the magnetization angle of the permanent magnet. When the magnetization angle is within the range (0 to 15 rad), the permanent magnet torque is increased. The reason of this situation is due to a decrease in the permanent magnet temperature. After that, a sudden decrease in the permanent magnet torque when the magnetization angle is within the range (0.15 to 0.46 rad), which confirms the increase in the temperature of the permanent magnet torque. Finally, the

permanent magnet torque regularly increases with respect to the magnetization angle ($\gamma > 0.45\ rad$) and the decrease in the temperature of the permanent magnet.

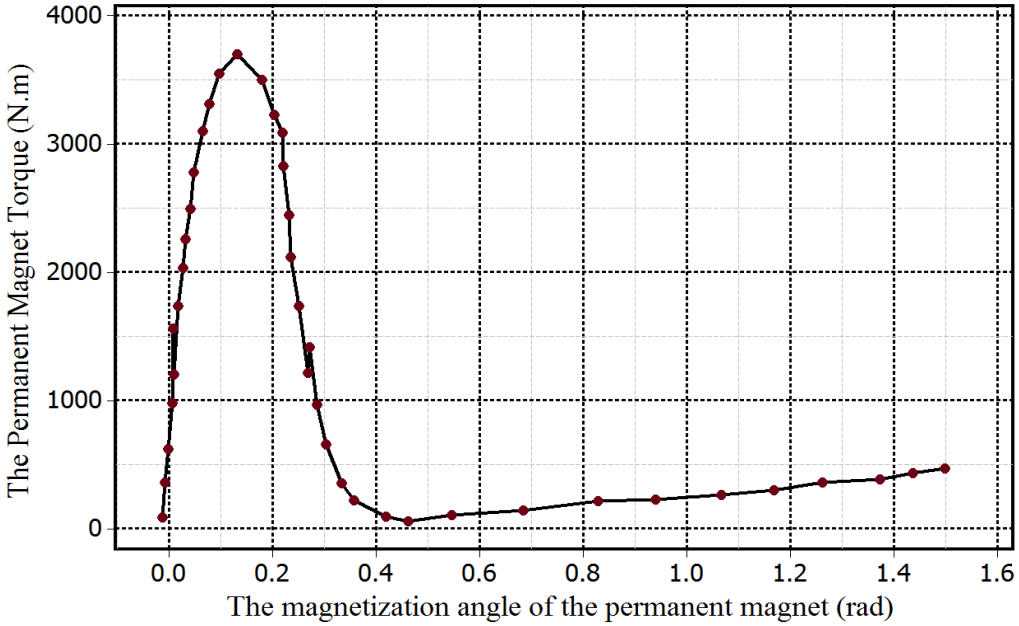

Fig. 4. 12 The driving torque of the rotating permanent magnet trend with respect to the magnetization angle.

According to the manufacturer's handbook, the abnormal operation condition will be considered when the generator temperature exceeds 110 Cº or the permanent magnet temperature overtakes 112 Cº. One of the most significant goals of this work is to determine the effect of the high generator temperatures on the induced electrical torque and the high temperature of the permanent magnet on the permanent magnet torque, which aims to identify the generator health. Table 4.3 presents the operation conditions of the selected wind turbine based on the generator temperature and the permanent magnet temperature.

Table 4. 3 The operation conditions of the selected wind turbine based on the generator temperature and the permanent magnet temperature, [93]

The Operation Condition	The Generator Temperature	The Permanent Magnet Temperature
Normal	$T_G < 110\ C°$	$T_{PM} < 112\ C°$
Abnormal	$T_G > 110\ C°$	$T_{PM} > 112\ C°$

4.8. The Obtained Results of the First Method

As was mentioned previously, there is a significant change in the trend of the torque-speed signal over time. This confirms that the torque-speed curve behavior can be used as an obvious indicator with a view to perform a suitable CMS on wind generators during running. The fluctuation in the electric torque pulsations through the normal and abnormal conditions is due to the ripple and cogging torque. The value of $\left(\frac{T_e}{\omega_r}\right)$ can be utilized to figure out the presence of the electrical faults in the wind generators, e.g. stator winding fault or rotor imbalance fault. Further, the proposed monitoring model is based on the parameters that control the operation condition, such as the generator reactance. The change of the generator reactance X_S, which is corresponding to the operation condition, is one of the most significant effects that lead up to electrical faults in the generator. Figure 4.13 shows the dramatic changes over time in the signal of the criterion $\left(\frac{T_e}{\omega_r}\right)$ during the operation. When the generator suffers from an electric fault, such as stator inter-turn fault, the generator reactance decreases automatically, which increases the variable $\left(\frac{T_e}{\omega_r}\right)$

remarkably. Therefore, high values of the criterion $\left(\frac{T_e}{\omega_r}\right)$ represent a real impression of the abnormal operation condition of the generator.

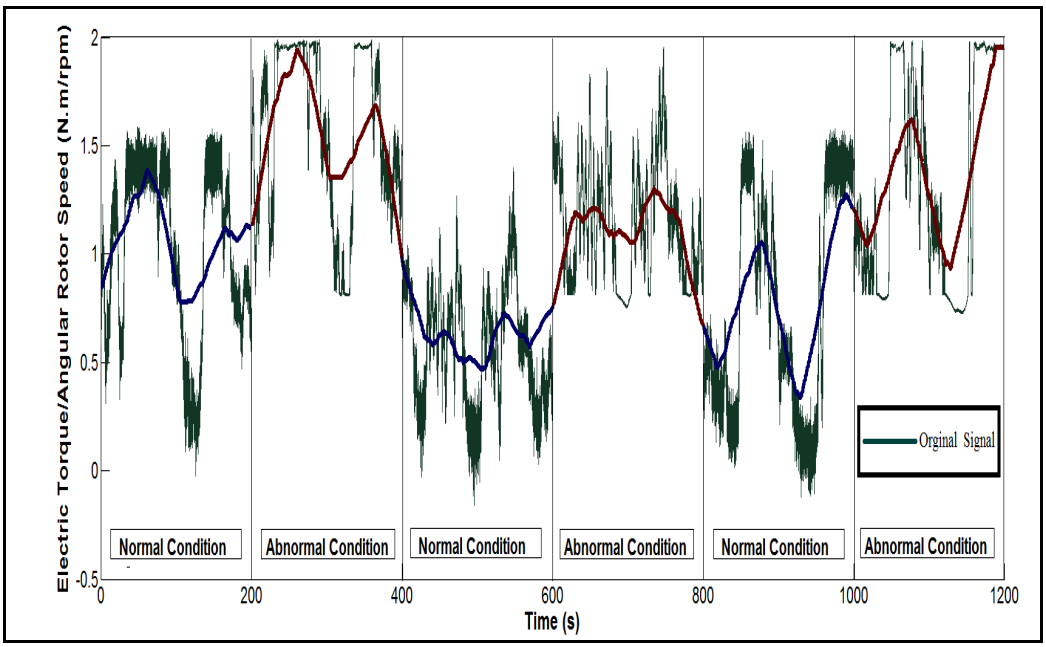

Figure 4. 13 The proposed indicator $\left(\frac{\tau_{el}}{\omega_r}\right)$ trend.

Likewise, the excitation flux in the core of the generator and connected power transformers are directly proportional to the ratio of the voltage to the frequency on the terminals of the equipment. The losses that are due to the eddy currents and hysteresis rise the temperature and hence increase in proportion to the level of excitation. In the abnormal operation condition, the generator reactance X_S might rapidly decrease, and the ratio of the change in the generator temperature increases with respect to the electrical torque and rotor rotational speed. Therefore, the ratio of the change in the generator temperature could be considered an indicator to detect the faults in the generators. Figure 4.14 illustrates the

behavior of the rate of change in the generator temperature with respect to the rotor rotational speed in the normal and abnormal conditions respectively.

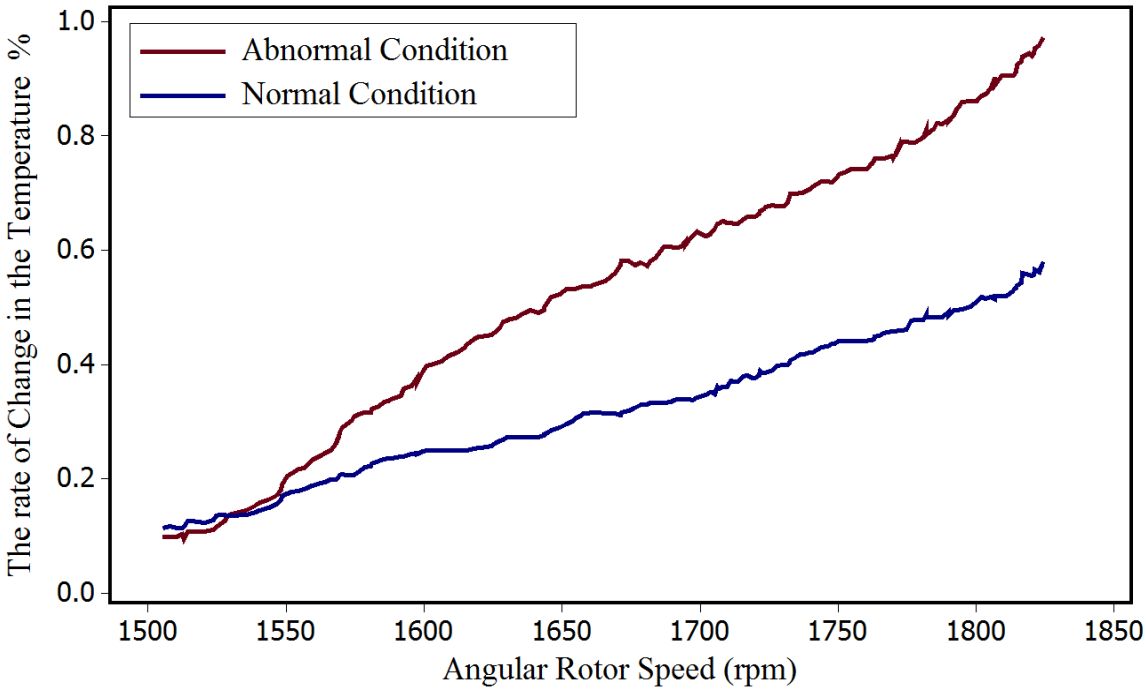

Fig. 4. 14 The rate of change in the generator temperature with respect to the angular rotor speed.

Further, Fig 4.15 shows the rate of change in the generator temperature trend with respect to the electrical torque in the normal and abnormal conditions respectively. The increase in the generator temperature shows high values in the abnormal condition with respect to the generator output power as shown in Fig. 4.16, which illustrates the scatterplot of the generator temperature rise against the relative power output (%) in the normal and abnormal conditions. This figure clearly presents the contrast in the rise of the generator temperature with respect to the relative power output between these conditions.

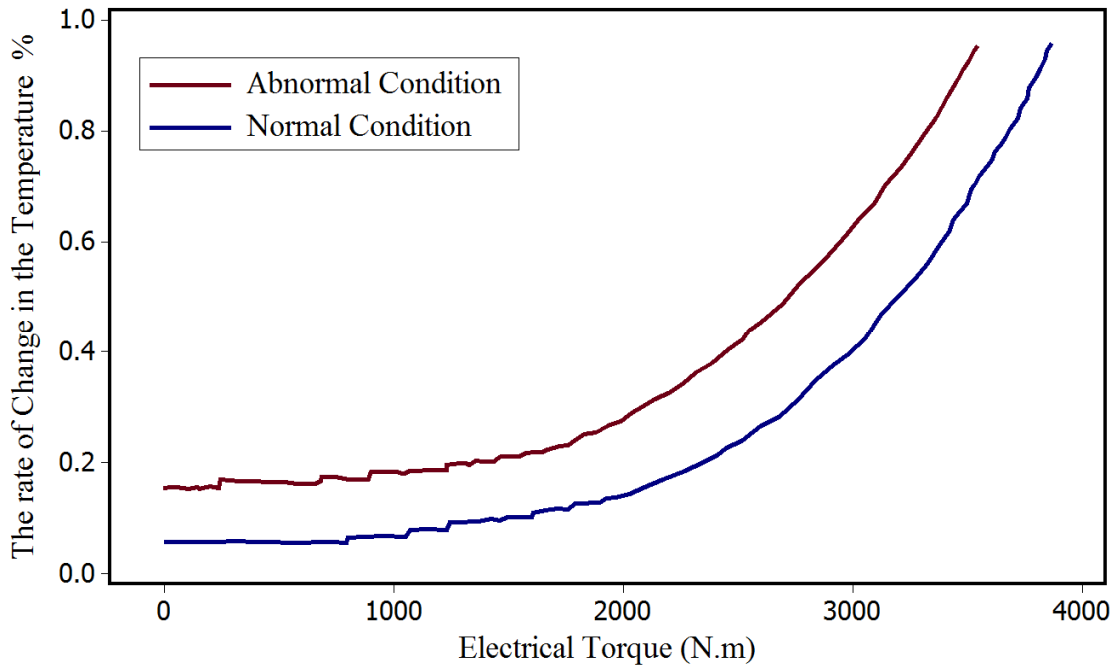

Fig. 4. 15 The rate of change in the generator temperature with respect to the electrical torque.

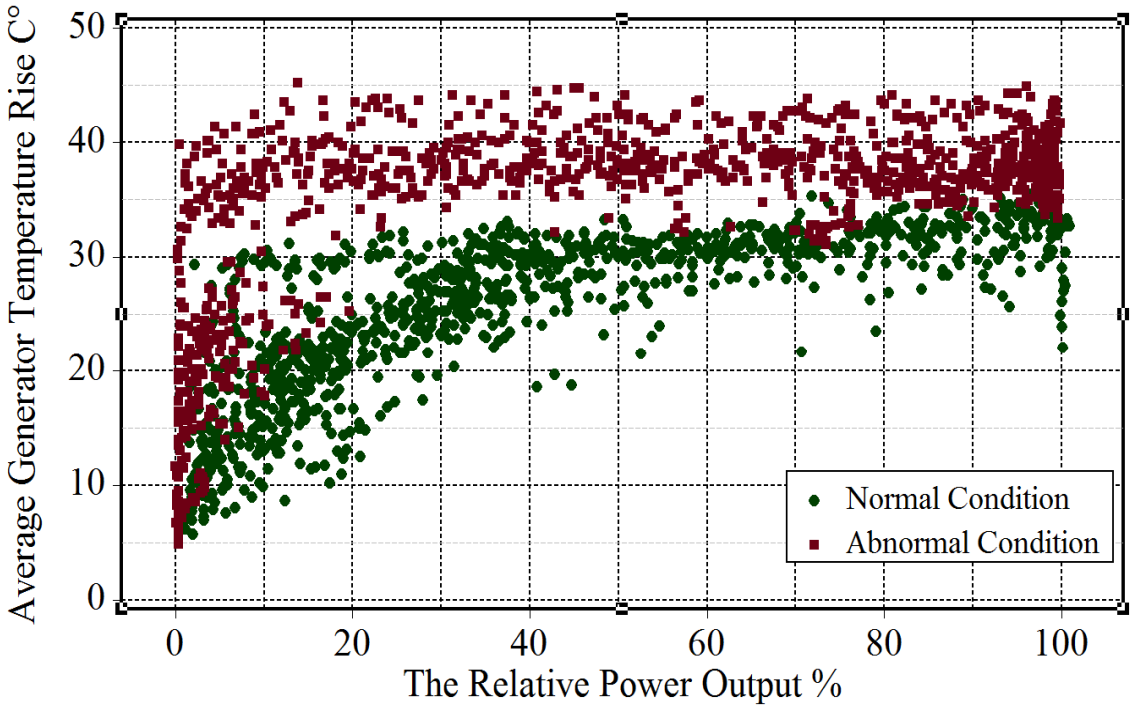

Fig. 4. 16 The generator temperature rise against the relative output power.

The average generator temperature rise for each 50kW increment of the output power in the normal and abnormal conditions is illustrated in Fig. 4.17. The transition condition represents the transit from the normal to the abnormal situation.

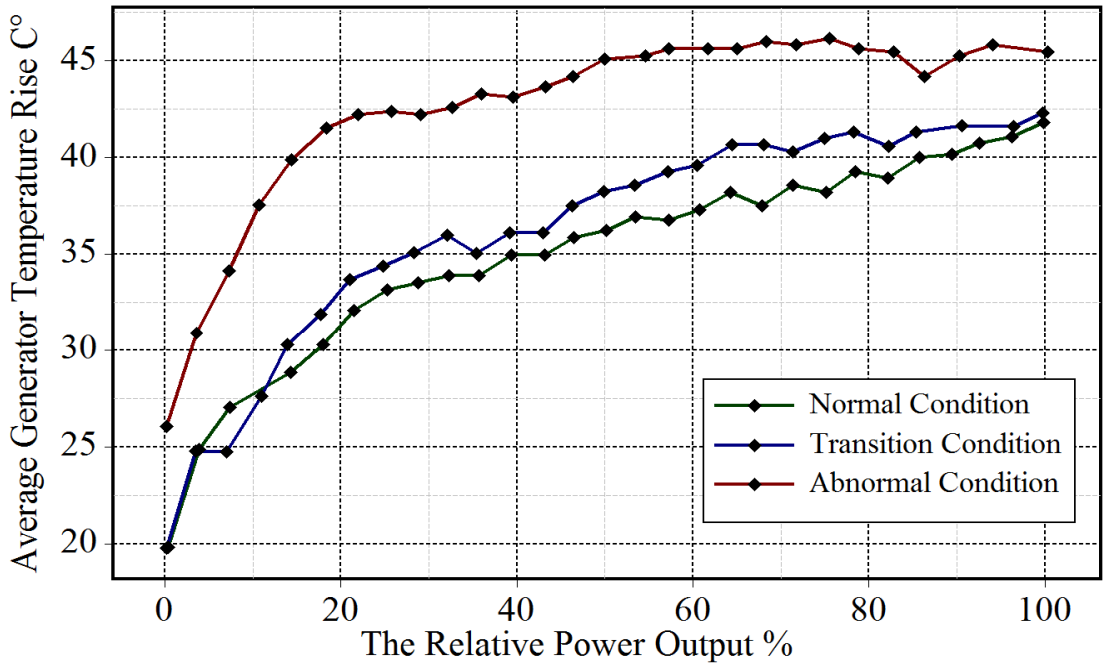

Fig. 4. 17 The generator temperature rise trends against the relative output power.

The simulation results of the induced driving rotating permanent magnet torque show low values in the abnormal condition with respect to the rate of change in the rotating permanent magnet temperature as shown in Figs. 4.18, 4.19. The figures illustrate the trend of the of the permanent magnet torque of the wind generator in the normal and abnormal conditions with respect to the rate of change in the rotating permanent magnet temperature and the magnetization angle of the permanent magnet. The influence of the permanent magnet temperature on the driving permanent magnet torque and the magnetization angle is very obvious in the normal and abnormal conditions.

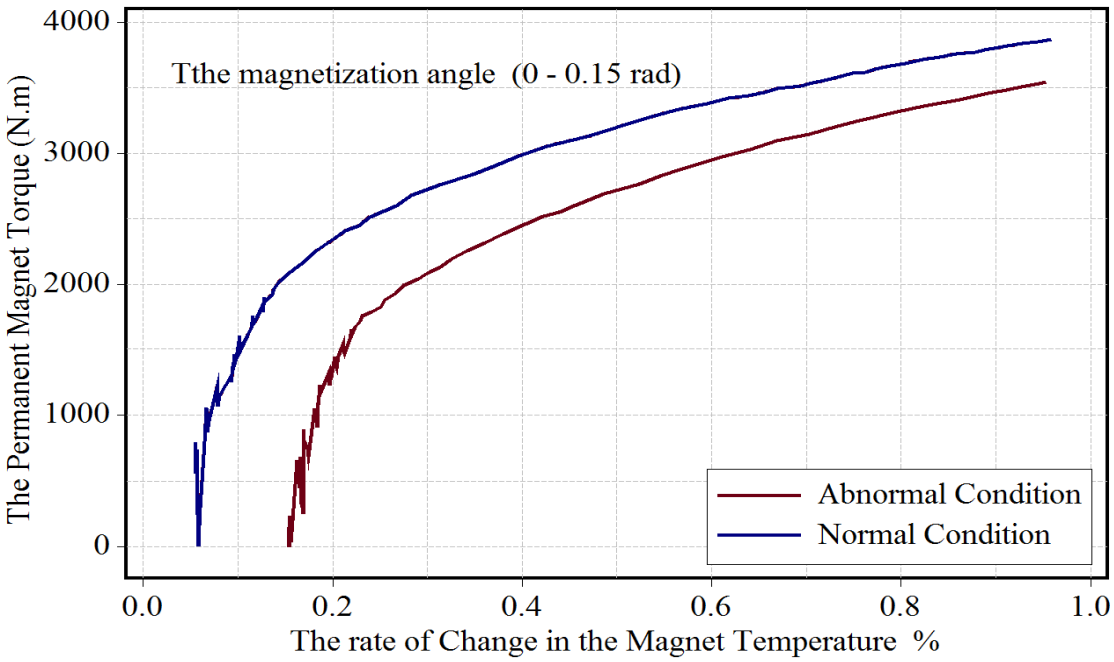

Fig. 4. 18 The trend of the permanent magnet torque with respect to the rate of change in the magnet temperature when the magnetization angle is within (0 – 0.15 rad).

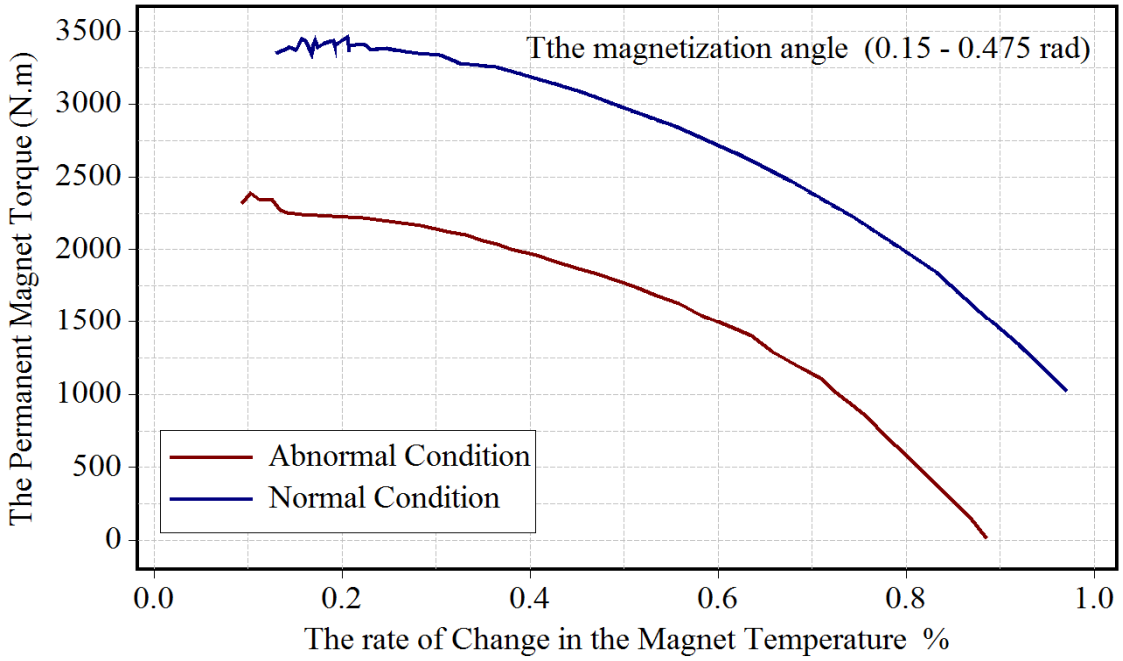

Fig. 4. 19 The trend of the permanent magnet torque with respect to the rate of change in the magnet temperature when the magnetization angle is within (0.15 – 0.475 rad).

The high-driving permanent magnet torque with respect to the rate of change in the magnet temperature represents the normal operation condition when the magnetization angle is within the range (0 to 0.15 rad). In this situation, the wind generator produces proper torque in the normal condition. For instance, when the rate of change in the magnet temperature reaches 0.8, the generator produces approximately 3800 N. m and 3300 N. m in the normal and abnormal conditions respectively. The contrast in the induced torque between the normal and the abnormal is very obvious when the magnetization angle is within the range (0.15 to 0.475 rad). For instance, when the rate of change in the magnet temperature reaches 0.8, the generator produces approximately 2000 N.m and 650 N.m in the normal and abnormal conditions respectively. In the both cases, the high-rotating permanent magnet torque indicates that the wind generator does not suffer from any improper magnet temperature even though the magnetization angle is different.

4.9. The Conclusion of the First Method

The proposed work indicates that the mechanical, electrical and thermal characteristics can be used to diagnose the faults that can occur in wind generators. High electric pulsations torque can be considered a significant indicator to identify the generator operation condition. Electric torque pulsations consist of the sum of cogging torque and ripple torque. Therefore, the behavior of the electric torque pulsations is considered an effective approach for a condition monitoring system on the wind generators. In the abnormal condition, the generator faults cause decreases in the generator reactance, and

the value of the proposed model $\left(\frac{T_e}{\omega_r}\right)$ increases remarkably. On the other hand, the rate of change in the generator temperature with respect to the induced electrical torque is also considered an indicator to define the generator health. Potential electrical faults might occur due to a decrease in the generator reactance X_S, and an increase in the generator temperature, which influence the induced torque immediately with respect to the armature resistance of the generator. The last indicator, which can employ to implement a proper CMS on the wind generators is the behavior of the driving torque of the rotating permanent magnet with respect to the permanent magnet temperature. In the abnormal condition, which indicates that the permanent magnet temperature during operation is higher than the design permanent magnet temperature, the permanent magnet torque decreases dramatically with respect to the magnetization angle of the permanent magnet. Future work is required to apply the proposed method on the wind generators that suffer from different electrical faults. Furthermore, the proposed model could be applied on different parts of the wind turbines, such as gearboxes, to confirm the validity of the proposed method.

Chapter 5. The Second Method: The Application of Heat Transfer Analysis through Wind Generators Heat Exchangers to Apply Condition Monitoring System on the Wind Generators

This chapter presents the second method that can be utilized to apply CMS on wind generators due to high power loss, which leads to increase generator temperature. A new methodology has been proposed based on the use of the heat transfer and fluid mechanics analysis through the heat exchangers of the wind generators, which use water to air cooling system. The proposed technique can indicate the operation condition of the wind generators during operation and detect the potential faults that occur due to an increase in the temperature of the wind generators. Case study based on data collected from actual measurements demonstrates the adequacy of the proposed model.

5.1. Introduction

Wind turbine capacity, particularly for the offshore turbines continues to increase each year in the range of 5-10 MW, and the number of the wind turbine failures due to high generator temperatures has been shown to be significant [94-97]. Certain advances in the wind generator heat exchangers play a significant role to remove the released heat from the wind generator active parts like generator stator and rotor. Although the traditional air-air heat exchangers of the wind generators have a lower cost than the water-air heat

exchangers, the water to air heat exchangers are widely applied to cool the rotor and stator windings efficiently in the large wind generators. The reason for applying the water-air heat exchangers in the wind industry is the high cooling capability of water, which is much larger than air and the availability of the water, especially for the offshore wind turbines where the water is more available. The water-air heat exchangers can be employed to cool the generators, by circulating hot air inside the heat exchanger to soak up the heat by the cold fluid and then transferring the absorbed heat to another area outside the generator. The electro-magnetic losses within the wind generators are a significant source of the heat, which warms up the generator and cause a temperature rise in stator bars reducing the life-span of the insulation materials [15-17], [20, 27, 54,]. This fact leads the wind turbine manufacturers to create and construct an efficient cooling system to cool down the active parts inside wind generators and attracts engineers to develop a proper condition monitoring on the wind generators.

Many efforts have been made and employed to apply CMS on the wind generators due to the high temperature. However, the most of these efforts used the analytical electrical and statistical methodologies and theories to derive suitable algorithms for proper CMS on the wind generators. In this chapter, a new application of CMS on the wind generators due to high power losses, which lead to increasing the generator temperatures is presented. The proposed methodology is constructed on the heat transfer analysis and fluid mechanics techniques, based on data of 5 MW offshore wind turbine collected from actual measurements. Using the heat transfer and fluid techniques relations of the heat

exchangers is very efficient in this application. The main concept of the proposed model depends on evaluating the heat exchange between the hot air due to the high temperatures of generator parts and the cold water inside the heat exchangers. The obtained results of the proposed method define the generator health while running in the normal and critical conditions. The rest of this chapter is arranged as follows, Section 5.2 provides knowledge and specifications about the selected wind generator, heat exchanger, cooling system mechanism, and the measured data, which are used in this method to test the proposed model. In section 5.3, the heat transfer and fluid mechanics analysis through the wind generator heat exchangers is explained to find the proper thermal model for implementing an effective CMS on the wind generators due to an increase in generator temperature. Section 5.4 provides a case study to experience the validity of the proposed condition-monitoring algorithms on the wind generators. Then, in Section 5.5 the collected results and the capability of the proposed algorithms are presented. Section 5.6 submits discussion, conclusions, and suggestions for future research.

5.2. Information about the Selected Wind Turbine, Generator, Cooling System Mechanism, and the Available SCADA

Actual data was collected from a variable speed offshore wind turbine with rated power of 5 MW, 60Hz, three blades, 126m rotor diameter, and rated rotor speed 12.1 rpm. The wind turbine has SPMG with rated speed 1500 rpm and efficiency equals to 94.4%. The cooling-system of the generator is based on water-air counterflow heat exchanger with six cold fluid pipes. The generator cooling-system is schematically shown in Figure 5.1,

where the inlet air transfers the heat from the generator parts (generator rotor and stator winding) to the water-air heat exchanger. This step is the first cooling process in the system. There are two axial fans, one to draw the outside air inside the generator (fan 1) and the other to recycle the cold air that comes from the heat exchanger to transmit it through the system (fan 2). The airflow is separated directly by using valves after passing both fans. The design of the cooling system compels about 25 % of the airflow leaving both fans and flows through the stator's end-windings to cool them. The rest of airflow (75%) enters the rotor region in an axial trend through the slots between the rotor poles, which direct the air in a radial direction towards the stator-core. The air-gap space between the rotor and the stator is about 15mm, and airflow leaves the air-gap rapidly and enters the cooling- ducts of the stator-core. After leaving the stator-core, both airflows (stator-core airflow and stator's end-windings airflow) are mixed to become one stream. Then the mixed stream is directed to the water-air counterflow heat exchanger to cold it by the water. Finally, the cold mixed flow will return to the circuit at the inflow-sides of both axial fans to cool the generator parts (second cooling process) [98].

There are several temperature sensors installed within the generator in order to measure the stator winding temperatures or stator-core temperatures. The manufacturer handbook emphasizes that the generator temperature should not exceed 100 C° to protect the electric generator, and the wind turbine will shut down when the generator temperature reaches 135 C°. More additional temperature and pressure measuring devices are available to measure the water inlet and outlet temperatures and pressure drop through the heat

exchanger [98]. These measuring devices can be installed to define the cold fluid (water) conditions at the inlet and outlet slots of the heat exchanger.

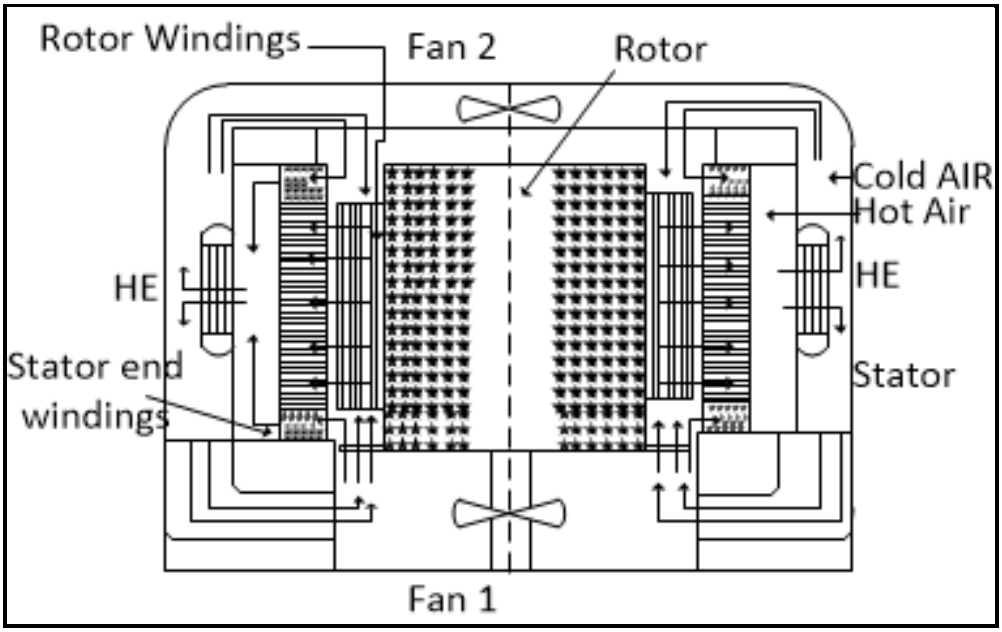

Figure 5. 1 Wind generator cooling system, [98, 99].

The SCADA system provides enough details about the generator stator temperature, which are considered as the generator temperature itself, and the generator power values. Moreover, the temperature of the inlet air to the rotor and the stator winding can be measured, which is based on the outside temperature. There is a valve to control the inlet mass flow rate of the water to the heat exchanger, which is roughly 2.6 kg/s according to the manufacturer's handbook. In addition, the air mass flow rate into the rotor winding and the stator end windings is designed to equal almost 4.7 kg/s. The collected data of the applied experiment represent three conditions: normal, warning, and critical conditions—

and the information of each condition is available based on the SCADA system. The recorded data represent the wind turbine operation condition in different days [98]. Table 5.1 classifies the operation condition of the selected wind turbine based on the generator temperature.

Table 5. 1 The wind turbine operation conditions, [98].

Operation Condition	Generator Temperatures
Normal condition	$T < 90\ C°$
Warning condition	$90\ C° < T < 110\ C°$
Critical condition	$110\ C° < T < 135\ C°$

In order to apply the heat transfer and fluid mechanics analysis—which will explain in the following sections, the thermal properties of the cold fluid (water) and the hot fluid (air) are available according to the collected data of each condition.

5.3. Heat Transfer and Fluid Mechanics Analysis for the Heat Exchangers of the Wind Generators

In order to transfer the heat from the hot fluid into the cold fluid, heat exchangers are used for this process. It could neglect the losses of the heat between the heat exchanger and surroundings since it is very low in comparison with the exchanged heat between the cold and hot fluids. Therefore, heat exchangers are considered as adiabatic devices (no heat exchange with the surrounding through the heat exchangers). They are classified according to the flow configuration and the system construction. Many types of the heat exchangers are used in the wind generators to provide a suitable cooling system. Counterflow tube heat

exchanger is the most common and desirable heat exchanger, which is used in the wind generators cooling system [7], [100-102]. Figure 5.2 displays the mechanism of work in the cross-flow case of the tube heat exchanger model.

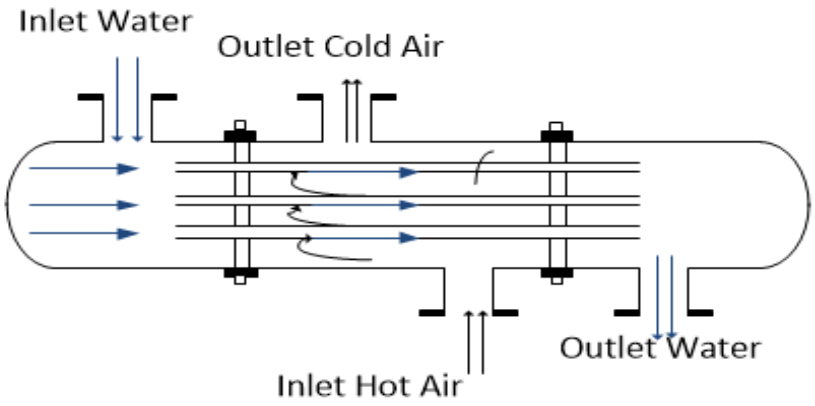

Figure 5. 2 Tube counterflow heat exchanger mechanism of work, [102, 103,]

The previous figure shows that one flow moves inside set of tubes and other through the outer shell in the opposite direction. Based on this design, the heat exchanges between the hot and cold fluids for proper cooling process. The hot and cold fluid temperatures distribution with respect to the counterflow heat exchanger length is shown in Figure 5.3. The temperature of the hot fluid decreases dramatically because of the heat exchange process. On the other hand, the cold fluid earns heat from the hot fluid through the heat exchanger causes increase in its temperature.

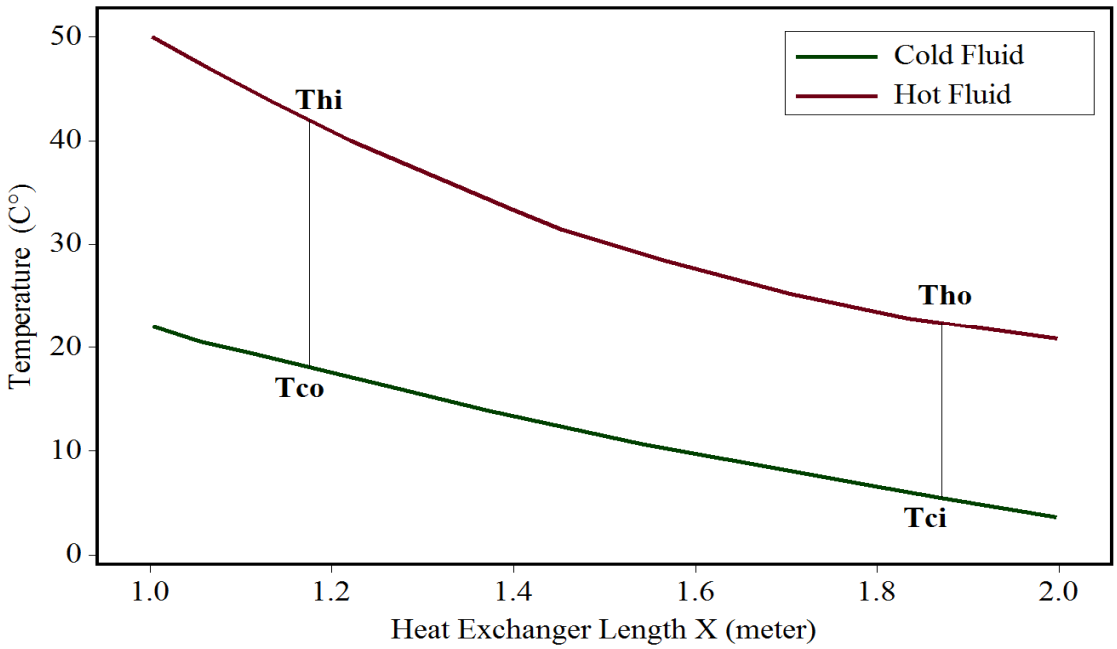

Figure 5. 3 Temperature distribution for a counterflow heat exchanger, [102, 103,]

By applying the energy balance to each fluid (the cold and hot fluid), which states that the heat losses from the hot fluid equal to the heat gains for the cold fluid, the following relations can be obtained:

$$Q_h = Q_c \tag{5.1}$$

$$\dot{m}_h \cdot c_{p,h} \left(T_{h,i} - T_{h,o} \right) = \dot{m}_c \cdot c_{p,c} \left(T_{c,o} - T_{c,i} \right) \tag{5.2}$$

Assuming that the potential and kinetic energy are negligible and the specific heat values for each fluid over the time are constant. Q_h and Q_c are the loss in the heat of the hot fluid and the heat gain of the cold fluid, respectively. $T_{h,i}$ and $T_{c,i}$ are the hot and cold fluid inlet temperatures, respectively. $T_{h,o}$ and $T_{c,o}$ are the hot and cold fluid outlet temperatures, respectively. Finally, $c_{p,h}$ and $c_{p,c}$ are the hot and cold fluid specific heat, respectively. It

should mention that the specific heat of the hot or the cold fluid is not constant and changes according to the temperature condition at the inlet and outlet points. These expressions may be integrated across the heat exchanger to obtain the overall energy balance given by Equations 5.1, 5.2. The heat transfer across the surface area dA may also expresses as:

$$dq = U\,\Delta T\,dA \tag{5.3}$$

Where $\Delta T = T_h - T_c$ is the local temperature difference between the hot and cold fluid. To determine the integrated from of Eq. 5.3, substituting EQs. 5.1, and 5.2 into the local temperature difference ΔT as follows:

$$d(\Delta T) = dT_h - dT_c \tag{5.4}$$

$$d(\Delta T) = -dq\left(\frac{1}{c_h} - \frac{1}{c_c}\right) \tag{5.5}$$

Substituting for dq from Eq. 5.3 and integrating across the heat exchanger, the next relation can be obtained:

$$\int_1^2 \frac{d(\Delta T)}{\Delta T} = -U\left(\frac{1}{c_h} - \frac{1}{c_c}\right)\int_1^2 dA \tag{5.6}$$

$$\ln\frac{\Delta T_2}{\Delta T_1} = -UA\left(\frac{1}{c_h} - \frac{1}{c_c}\right) \tag{5.7}$$

Substituting for c_h and c_c from Eq. 5.1 and Eq. 5.2, respectively, it follows that

$$\ln\frac{\Delta T_2}{\Delta T_1} = -UA\left(\frac{\mathrm{T_{h,i}} - \mathrm{T_{h,o}}}{\mathrm{q}} + \frac{\mathrm{T_{c,o}} - \mathrm{T_{c,i}}}{\mathrm{q}}\right) = \Delta T_m \tag{5.8}$$

To simplify the calculations, the average temperature of the inlet and outlet points of the hot or cold fluid is assumed to represent the hot and cold fluid inlet temperatures [100-102]. For the countercurrent flow heat exchanger, commonly is referred in the high exchangers design to the LMTD, which is called the logarithmic average of the temperature difference between the hot and cold streams at each end of the heat exchanger with a constant flow. In other words, the LMTD is defined as the maximum mean temperature difference that can be achieved for any given set of the inlet and outlet temperatures through the heat exchangers [100-102].

$$\mathrm{LMTD} = \frac{\left[\left(\mathrm{T_{h,i}} - \mathrm{T_{c,o}}\right) - \left(\mathrm{T_{h,o}} - \mathrm{T_{c,i}}\right)\right]}{\ln\left[\frac{\left(\mathrm{T_{h,i}} - \mathrm{T_{c,o}}\right)}{\left(\mathrm{T_{h,o}} - \mathrm{T_{c,i}}\right)}\right]} = \tag{5.9}$$

In addition to the energy balance, the heat transfer can be described based on the logarithmic average of the temperature difference as follows:

$$\mathrm{Q} = \mathrm{U} \cdot \mathrm{A} \cdot \mathrm{LMTD} \tag{5.10}$$

whereas, A is the heat exchanger area and U is the overall heat transfer coefficient, which can be calculated from the next formula:

$$\mathrm{U} = \frac{1}{\frac{1}{\mathrm{h_i}} + \frac{1}{\mathrm{h_o}}} \tag{5.11}$$

where, $\mathrm{h_i}$ and $\mathrm{h_o}$ are the internal and external heat coefficients respectively [93-96]. In order to apply an efficient CMS on the wind generators due to the increasing in the

generator temperature, the trend of the heat transfer through the generator's heat exchangers over time, and the logarithmic average of the temperature difference of the hot fluid, could be considered as indicators. This because the heat exchange through the generator's heat exchangers and the LMTD are related directly to the winding stator temperatures. It could take into consideration that the stator winding temperature is the generator temperature itself. Further, the thermal properties of the air that is used to cool the stator winding a flows through the heat exchanger are related to the change in the thermal properties of the cold or the hot fluid [27, 85]. The generator heat losses increase directly the generator temperature and can be computed as follows [87, 99,]:

$$\begin{aligned}\text{Generator losses} &= \text{Air friction losses} + \text{Generator bearing losses} \\ &+ \text{Iron losses} + \text{stator winding losses} \\ &+ \text{Harmonic losses in the generator rotor}\end{aligned} \tag{5.12}$$

However, the generator heat losses could be calculated from the thermal aspect since the generator heat losses are equal to the air heat gains, which flow through the heat exchanger. Therefore, the water heat gain through the heat exchanger is supposed equal to the generator heat loss. In addition, study the trend of the heat loss or the heat gain is beneficial to define the generator conditions. Based on EQs. 5.2 and 5.9, a criterion S_1 , which is a versatile function for monitoring the running condition of wind turbine is proposed as follows:

$$S_1 = \frac{Q_h}{LMTD} \tag{5.13}$$

In general, the criterion S_1 can be used to detect the electrical faults of the wind generators due to high temperature. Furthermore, the criterion S_1 is demonstrated according to the linear relationship between Q_h , LMTD in all operation conditions. Figure 5.4 presents the linear relationship between Q_h , LMTD in the three conditions. This figure shows the heat loss trend with respect to the logarithmic temperature difference through the heat exchanger of the generator of the 5MW wind turbine in three different conditions.

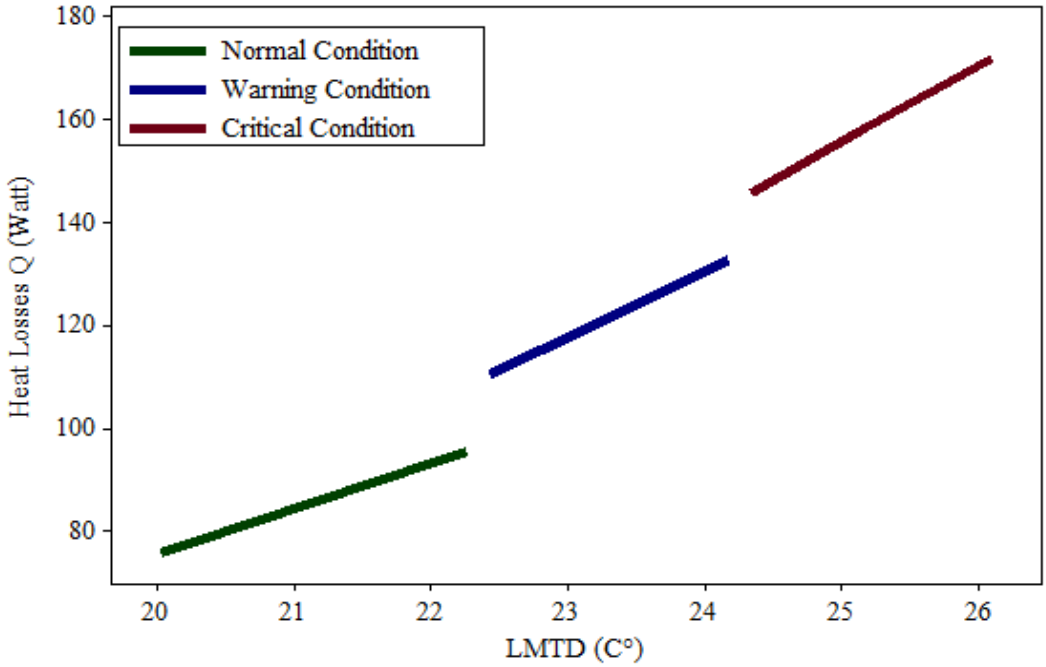

Figure 5. 4 The trend of the heat losses with respect to the LMTD through heat exchanger in three different conditions.

One more parameter that can be used to implement CMS on the wind generators due to the increasing temperature is the pressure drops of the flow streams through the heat exchanger. The pressure drops of the flow streams is a considerable indicator to determine

the generator health since it is based on the change in the fluid condition, which are used to cool the. The cooled fluid pressure drop can be calculated from the next relations [95-98]:

$$\Delta P = \frac{0.184 \cdot R_e^{-\frac{1}{5}} \cdot \rho_c \cdot V_c^2 \cdot L}{2d} \cdot N \text{ ... ... For turbulent flow} \quad (5.14)$$

$$\Delta P = \frac{0.316 \cdot R_e^{-\frac{1}{4}} \cdot \rho_c \cdot V_c^2 \cdot L}{2d} \cdot N \text{ ... ... For laminar flow} \quad (5.15)$$

where, L is the effective pipe length of the heat exchanger, d is the pipe internal diameter, N is the number of pipes, V_C is the cold fluid velocity, ρ_c is the cold fluid density, and R_e is the shell-side Reynolds number, which can be calculated as follows:

$$R_e = \frac{4\dot{m}}{\pi \cdot \mu_T \cdot d} \quad (5.16)$$

where, μ_T is the cold fluid viscosity, which depends on the average fluid temperature and can be determined as follows:

$$\mu_{T=2.414 \cdot 10^{-5}} \cdot 10^{(247.8)/(T-140)} \quad (5.17)$$

The cold fluid density changes with the change in the fluid temperature, and can be determined as follows:

$$\rho = \frac{\rho_0}{1 + 0.002 \cdot (T - T_0)} \quad (5.18)$$

where, T is the average temperature of the cold fluid and ρ_0 is the cold fluid density at T_0, which is assumed to equal 20C° in this application. [95-98].

The pressure drop of the cold fluid in the heat exchanger over the logarithmic average of the temperature difference is a suitable parameter to apply CMS on the wind generators since the pressure drop of cold fluid is related directly to the hot fluid temperature and heat loss. Consequently, any change in the generator temperatures leads to change in the hot fluid temperatures, which affects the pressure differences of the cold fluid. Therefore, it can use this parameter as another criterion and versatile function for monitoring the operation condition of the wind generators as follows:

$$S_2 = \frac{\Delta P}{LMTD} \tag{5.19}$$

The linear relationship between the pressure drop and the logarithmic average of the temperature difference is plotted in Fig. 5.5, which shows the trend of the pressure drop with respect to the logarithmic temperature difference through the heat exchanger under the three different conditions. The diagram emphasizes that when the wind generator works under ideal condition (normal case), the pressure drop of the cold fluid stream through the heat exchange increases dramatically with respect to the logarithmic temperature difference. On the other hand, when the wind generator operates under improper condition (critical case), the pressure drop of the cold fluid stream through the heat exchange decreases significantly with respect to the logarithmic temperature difference. Case study will be presented to demonstrate the validity of the proposed technique in the following section.

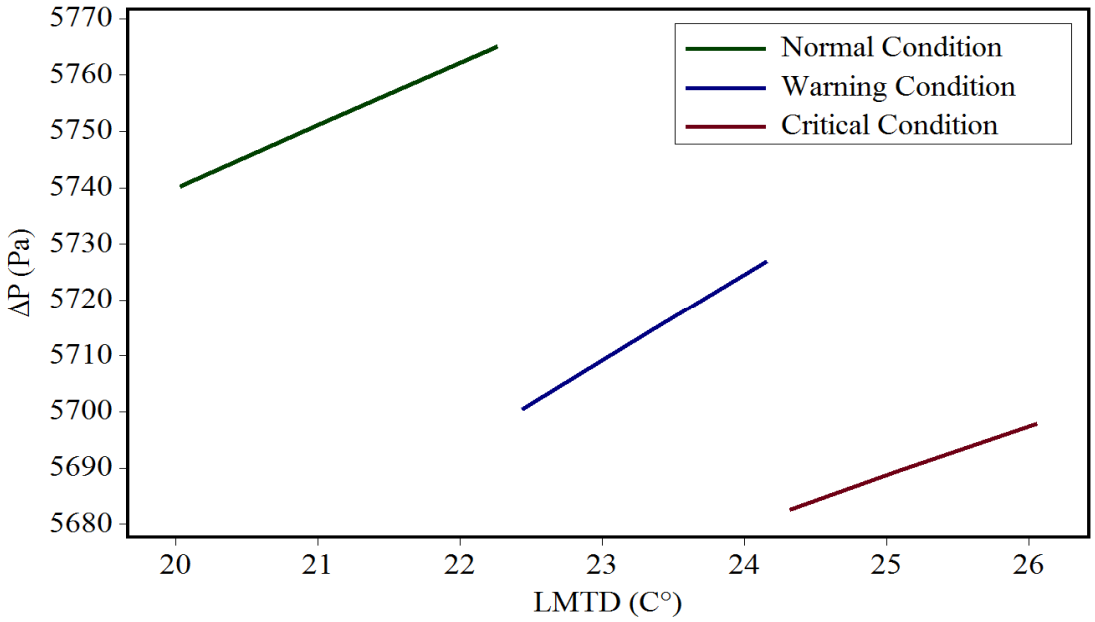

Figure 5. 5 The trend of the drop pressure differences with respect to the LMTD through heat exchanger in three different conditions.

5.4. Case Study

Actual data was collected and used to test the validity of the proposed technique for applying CMS on the selected wind generator. As mentioned before, the collected data present three different conditions: the normal condition, warning condition, and critical condition [9]. The LMTD between the hot and cool streams with respect to the heat loss should determine the generator condition. The thermal properties of the hot and cool streams that flow through the heat exchanger are based the generator temperature during operation. By computing the LMTD and the exchange heat between the hot and cold streams at each end of the heat exchanger with a constant flow, a powerful indication emphasizes that an expected fault could be detected due to high temperature of the generator. Further, by evaluating the pressure drop of the cold fluid in the three conditions

with respect to the LMTD, an additional sign gives enough details about the generator health condition. The data size is 60,000 generator temperatures in the three different conditions within 10 minutes and all cold and hot fluids thermal properties are known. Figures 5.6 and 5.7 show the losses in the heat and logarithmic average of the temperature difference trends over time in the three different conditions respectively.

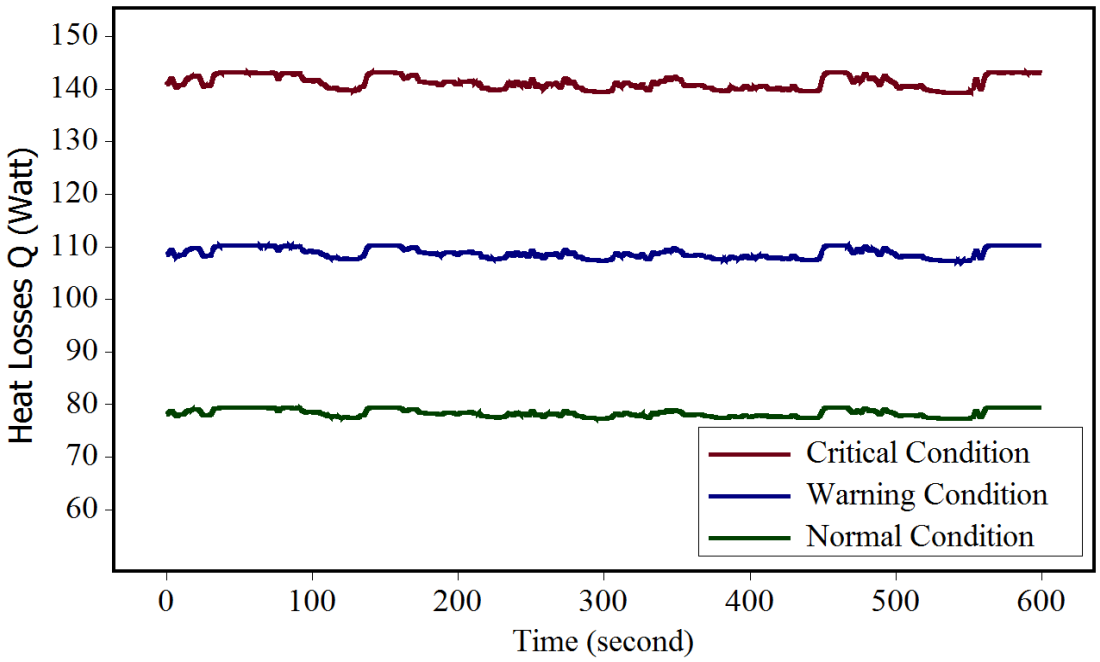

Figure 5. 6 The heat losses trends over time through three different conditions.

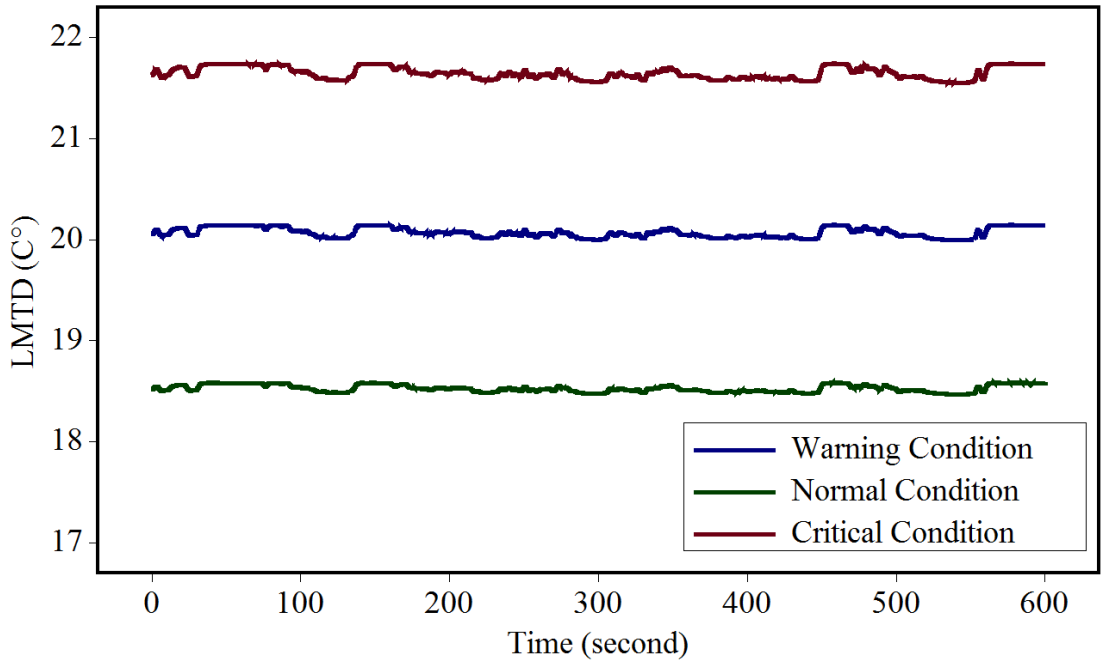

Figure 5. 7 The LMTD trends over time through three different conditions.

The previous figures show that when the generator suffers from high temperatures (critical case) due to some reasons, such as overload—winding insulation failure, and core insulation failure [95], the amount of heat losses rises dramatically. In this case, the logarithmic average of the temperature difference between the hot and cold streams will increase at each end of the heat exchanger. Therefore, the increase in the component of the generator temperature is expected and the critical condition is imminent. The normal condition presents smooth performance of the wind generator, and it could see the heat losses, and the LMTD values become small over the time. The warning condition is transition stage between the critical and normal conditions and occurs when the generator temperature trend increases gradually and exceeds the safe operation temperature limit due to the heat losses. The electrical power loss, which is the loss in the heat of the wind

generator can be determined from two aspects, electric and thermal aspects. In this work, the estimation of the loss in the heat, which is roughly equal to the gained heat of the air that used to cool the wind generator is based on the thermal aspect. In fact, there is few difference in the loss values of the heat between the thermal and electrical aspects, but in many situations estimating the loss in the heat of the wind generators from the electric analysis represents a difficult challenge. Therefore, it is very reasonable to use the thermal anatomies to estimate the loss in the heat of the wind generators due to the simplicity and flexibility of the heat transfer relations.

5.5. The Obtained Results of the Second Method

The obtained results confirm that the use of the heat transfer relations is very powerful to perform CMS on the wind generators due to high temperatures under abnormal and normal conditions. Using the heat transfer analysis gives an alternative way to detect the generator faults that occur due to the elevated temperature by utilizing some of the thermal parameters. Figure 5.8 displays the trend of the criterion S_1 as a versatile function for monitoring the operating condition of the wind generator. The criterion S_1 depends on the linear relationship between the loss in the heat from the generator and the logarithmic average of the temperature differences through the heat exchanger in three different conditions. The results indicate that the high value of criterion S_1, which represents the heat loss with respect to the LMTD is not desirable since this situation occurs when the loss in the heat of the generator increases, which raises the generator temperature gradually. This

situation confirms that the generator health is not adequate, and the operation condition of the generator is risky. The increase in the generator temperatures occurs due to different causes, such as the environment and nacelle temperatures. However, the loss in the generator power is the most significant cause that increases the generator temperature dramatically.

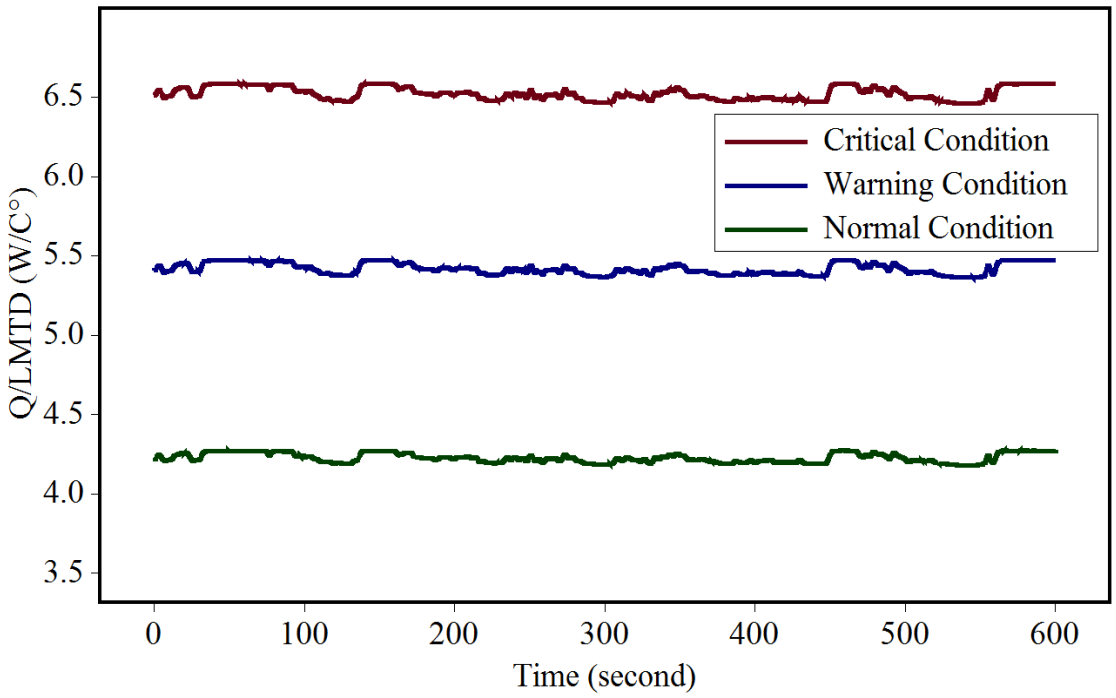

Figure 5. 8 Criterion S_1 trends through three different conditions.

Reynolds number, which is widely used in the fluid mechanics applications can be considered an indicator to investigate the generator health. This variable is directly related to the loss in the heat of the generator and the LMTD through the heat exchanger. The Reynolds values in Fig. 5.9 show a significant trend through the three different conditions. The high value of the Reynolds variable for the coolant fluid represents a deterioration in

the operating conditions of the system due to the high temperature since Reynolds variable is based on the coolant fluid viscosity, which decreases dramatically with the increase in the generator temperatures.

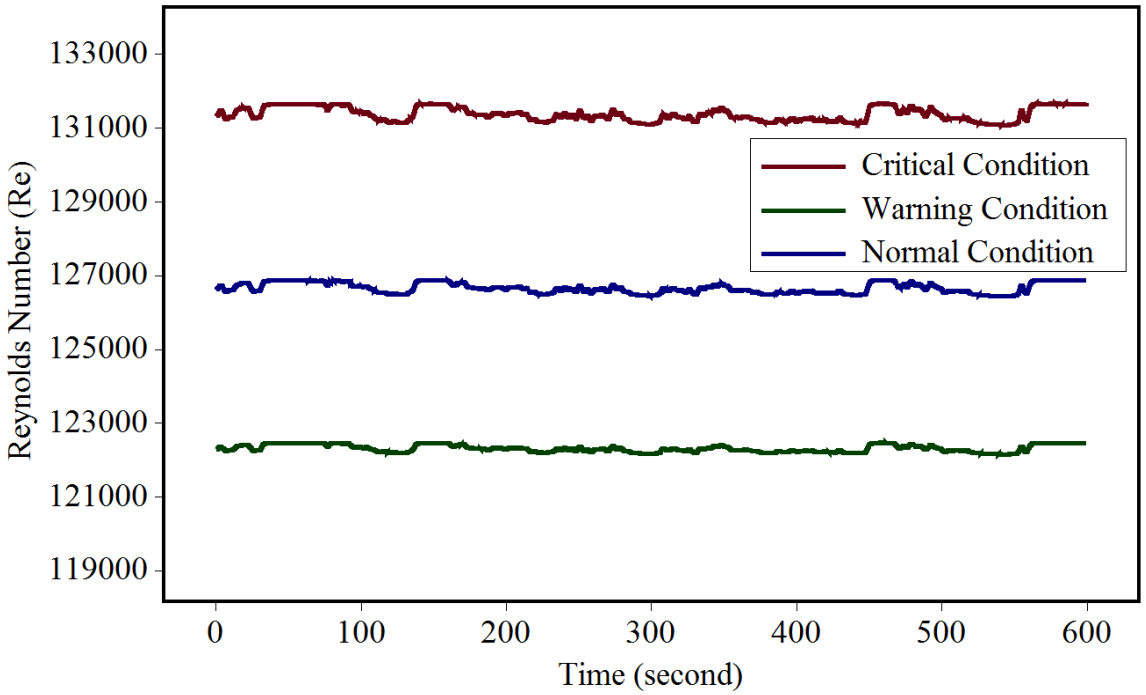

Figure 5. 9 Reynolds values trends through three different conditions.

Finally, the pressure drop through the generator's heat exchanger as well is worthy parameter and could be used as an indicator to investigate the generator health. The obtained results confirm that when the generator suffers from high temperature, the pressure drop of the coolant fluid decreases remarkably since the coolant fluid density increase with the high generator temperature and Reynolds values increase obviously. Therefore, the criterion S_2 is considered another scale for monitoring the operating condition of the wind generator because it is directly linked to the pressure drop and LMTD

through the heat exchanger. Figure 5.10 shows the trend of the criterion S_2 over 600 seconds in the three different conditions and emphasizes that when generator condition in the critical mode, the pressure drop with respect to the LMTD of the generator heat exchanger is lower than normal mode [100-103].

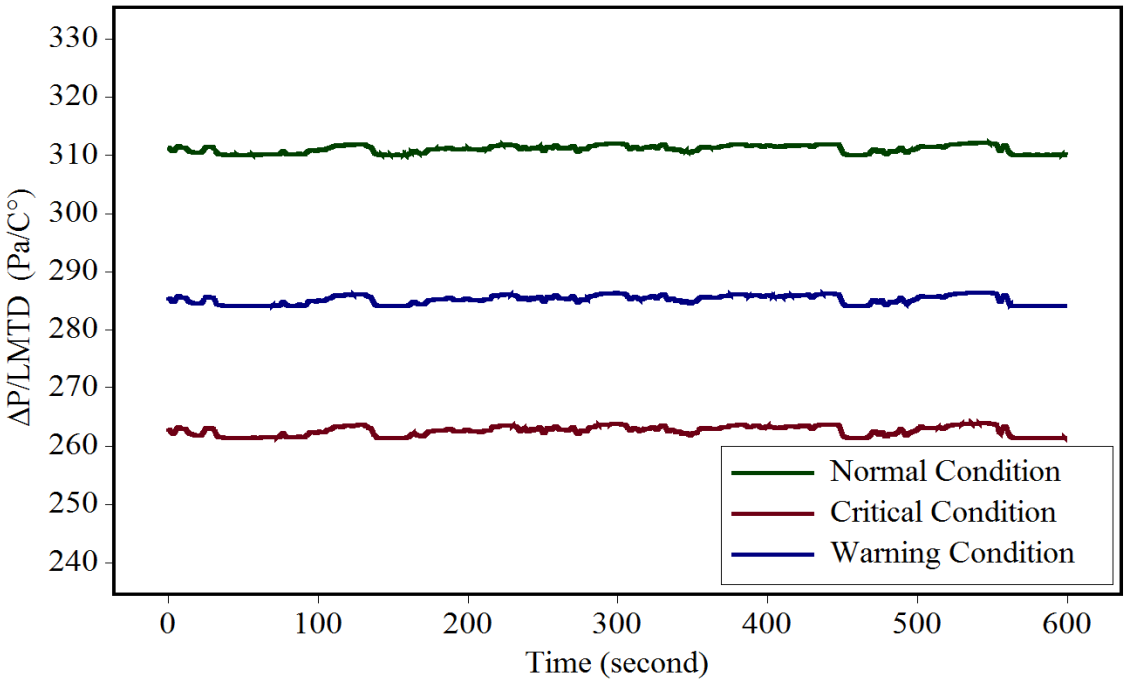

Figure 5. 10 Criterion S_2 trends through three different conditions.

5.6. The Conclusion of the Second Method

In this proposed work, the heat transfer analysis and fluid mechanics relations are employed to developing a proper CMS on the wind generators due to the increasing in the generator temperature. The performance of the heat exchangers plays an effective role to

avoid the failures and maintain the wind turbines to be protected. New methodology has been applied in the CMS of the wind generators that work with the water-air heat exchanger to provide proper cooling system to the generator. The obtained results of the proposed model show that high values of the loss in the heat of the wind generator with respect to the LMTD of the generator's heat exchanger is not desirable. In this situation, the performance of the cooling system is affected negatively, which creates inappropriate operation conditions due to the increasing in the generator temperature. Reynolds number of the coolant fluid is a good indicator as well to define the operation condition of the system since it depends on the coolant fluid viscosity, which decreases rapidly with the increase in the generator temperature. In addition, the obtained results demonstrate that the pressure drop through the generator heat exchanger is indicator to identify the operation condition of the wind generator with respect to the LMTD. The high value of the pressure drop with respect to the LMTD indicates that the generator temperature is suitable. The cool fluid pressure drop is based on the cold fluid density, which increases with the high generator temperature. Future work should take into account to apply this method on the wind generators that work with the air-air heat exchangers and confirm the validity of the proposed algorithm.

Chapter 6. The Third Method: Hazard Model Reliability Analysis Based on a Wind Generator Condition Monitoring System

This chapter presents an application of the hazard model reliability analysis on wind generators, based on CMS. The hazard model techniques are most widely used in the statistical analysis of the electric machine's lifetime data. The model can be utilized to perform appropriate maintenance decision-making based on the evaluation of the mean time to failures that occur on the wind generators due to high temperatures. The knowledge of the CMS is used to estimate the hazard failure, and survival rates, which allows the preventive maintenance approach to be performed accurately. A case study is presented to demonstrate the adequacy of the proposed method based on the condition monitoring data for two wind turbines. Such data are representative in the generator temperatures with respect to the expended operating hours of the selected wind turbines. In this context, the influence of the generator temperatures on the lifetime of the generators can be determined. The results of the study can be used to develop the predetermined maintenance program, which significantly reduces the maintenance and operation costs.

6.1. Introduction

The CMS for wind turbine components is critical to developing an effective maintenance program. An inclusive monitoring system provides diagnostic information on

the health of the turbine components, and issues warnings to the maintenance crew that potential failures or critical malfunctions might be imminent. CMS; therefore, can be used to schedule maintenance tasks or repairs before a technical problem causes downtime in the whole wind turbine [104, 105,]. The CMS technique can be divided into two categories: off-line monitoring and on-line monitoring. The wind turbine must be taken out of service in order to allow the maintenance crew to inspect the conditions through the off-line monitoring. Usually this monitoring technique is applied as routine or scheduled maintenance at regular intervals. The maintenance includes verification of the oil condition, and an inspection of the functioning of the system components, and the control systems. The on-line monitoring, on the other hand, provides enough details about the performance of the turbine subsystems performance while they rotate under different loading conditions. The Supervisory Control and Data Acquisition systems (SCADA) in turn, present the performance of the turbine subsystems. In the recent years, many advanced on-line monitoring systems have been introduced to wind turbines. The most common ones are vibration monitors, temperatures monitors, electrical current monitors and fluid contamination monitors [104-108].

In wind generators— the temperature is extensively monitored— i.e., the temperature sensors are designed to monitor specific areas of the stator core and the cooling fluids of large electrical machines— such as wind turbine generators. The generator temperature has a direct relationship with the electrical loads, cooling systems, and ambient conditions— consequently, when the temperature measurement is combined with the

information of the system conditions— the effective condition monitoring can be achieved [15]. Such monitoring systems increase the reliability of the generator component and reduce the operation and maintenance expenses.

The nature of the maintenance needs to determine which methods must be applied. There are two methods available: the calendar-based method (the component needs to be replaced after a specified time), and the condition-based method (the component needs to be replaced based on its physical condition). To improve the reliability of wind energy systems, the Condition-Based Maintenance (CBM) approach is one of the most effective methods that can be applied. Based on CBM, the collected data can be summarized and analyzed, such as oil analysis, vibration analysis, acoustic emission analysis, and temperatures trend analysis. Furthermore, CBM can be applied to determine the appropriate time to replace a component, such as the wind generator. [15], [104-110,].

Many Researchers have improved several condition-monitoring techniques that can increase the reliability of the wind energy industry. Rajesh Karki and Po Hu present a simplified approach for reliability evaluation of wind power systems [111]. The main idea of their work is to define the minimum multistate representation for a wind farm generation sample with respect to the estimated reliability of the power systems. Haitao Guoa and Simon Watson propose three-parameter Weibull failure rate function to perform life tests on wind turbine components, by utilizing two techniques: maximum likelihood and least-squares [112]. In Ref. [108] a life cycle cost approach is considered in order to estimate the

financial interest by using CMS as a tool to implement the CBM strategy. Ref. [109] presents an approach to evaluate the wind turbine degradation process based on an optimal maintenance program, which develops the reliability analysis of the system. Hall and Strutt present an application of physics-of-failure models of component lifetimes in the existence of parameter and model uncertainties [110]. The selected random variables and the characteristic life-time of the systems are described by using the knowledge of Weibull distribution. Then, the Monte Carlo technique is utilized to estimate the probability of failure of the selected component. In this paper, a hazard reliability technique for wind generators based on CMS is employed to develop a proper maintenance strategy, which aims to extend the system life-time and reduce potential failure during operation due to high generator temperatures.

Monitoring the trend of the generator temperatures with respect to the expended working hours is beneficial. Reliability analysis of the wind generators can be performed based on generator temperature data in order to make appropriate decisions concerning generator maintenance. In order to estimate the failure and survival rates of the wind generators, the hazard rate function statistical method can be utilized. The main objective of this work is to estimate the Mean Time to Failure (MTTF) of wind generators, and estimate the failure and survival rates of the wind generators. Consequently, the proper time to replace the generators can be determined, and the appropriate maintenance approach can be implemented. This leads to reduce the maintenance cost and improve the reliability of the wind energy system remarkably. Based on the collected generator

temperature data of two wind turbines, a case study is presented to demonstrate the proposed approach.

This chapter is arranged as follows: the theoretical background about the proposed hazard failure rate model is introduced in Section 6.2. To model the failure time of the wind generators, the hazard technique based on the Weibull distribution function is presented in this section. Then, the estimation of the mean time to failure for wind generators is described in Section 6.3. For the sake of testing the validity of the proposed method, a case study is provided in Section 6.4. The obtained results of the research work and discussions are presented in Section 6.5. Concluding remarks are given in Section 6.6.

6.2. Theoretical Background on the Proposed Hazard Failure Rate Model

Years of experience with wind energy systems and machines in general, have provided the failure rate characteristic curve of wind turbines as shown in Fig. 6.1 [112-118]. This curve is called the life curve or bathtub curve, and it can be applied widely in reliability engineering applications for any component, such as a wind generator. It characterizes the hazard function, thus illustrating the component failure stages. The initial failures might occur during operation in the early life period of wind generators (first stage) due to many reasons, such as improper design, defective raw material, poor quality of work, and poor quality control. The failure rates in this stage are called the infant mortality or rapidly declining failure rates since the generator will be replaced once the fault is detected. During the operating period (second stage), the failure rates are relatively constant. In the

third stage of the aging period, the wearout occurs due to operation conditions and/or electrical/thermal stress. The expended working hours also determine to a great extent the increase in the failure rates of wind generator. The failure rate through this phase is dramatically increased; consequently, the reliability analysis on wind generators should be applied through this critical period. Furthermore, the models for such failure rate functions are required, when the life cycle of the system is studied.

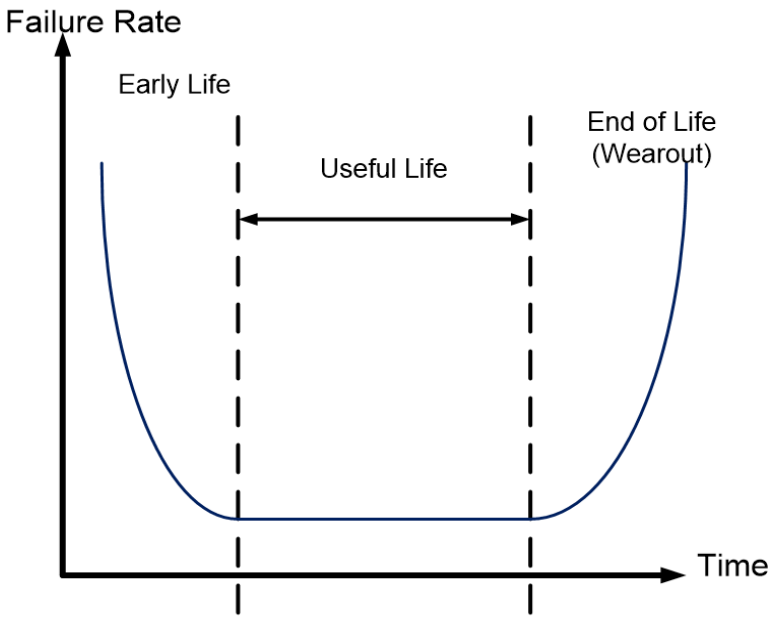

Fig. 6. 1 The life curve of wind generator [112-118].

In order to estimate the failure rates, survival rates, and the MTTF, several methods based on the reliability analysis can be utilized. The hazard analysis technique is one of the most effective approaches that can be used for this purpose. The failure rate is called the hazard rate, and can be represented by the hazard function h(t), which measures the risk

or the probability that the generator can still survive after time t+ δt as follows [94,116-122,]:

$$h(t) = \lim_{\delta t \to 0} \frac{P(t \leq \underline{T} < t + \delta t) \,|T \geq t}{\delta t} \tag{6.1}$$

where, T is the failure time of the wind generator.

The knowledge of CMS can be employed to estimate the hazard failure rate function, which is the most widely used statistical analysis tool of the lifetime data. The failure rates data of wind generators can be acquired in several forms, such as the historical failure rate data about the generator under monitoring, handbooks of failure rate data, which are available from commercial sources. In addition, the failure data can be obtained by exposing the generator to abnormal operation conditions in the lab.

To model the failure time, Weibull distribution function can be utilized, which is one of the most efficient functions that can represent the distribution of the lifetime data accurately. Furthermore, Weibull distribution has the advantage of flexibility in modeling the failure time data; consequently, accurate risk prediction for the component can be obtained. Therefore, Weibull distribution can is a guaranteed method to model the wind generators' time to failure. The Weibull hazard function h(t) at time t is defined as follows [94], [116-122]:

$$h(t) = \frac{f(t, \alpha, \beta)}{R(t, \alpha, \beta)} = \frac{\beta\, t^{\beta-1}}{\alpha^{\beta}} \tag{6.2}$$

where, β is the shape parameter; α is the scale parameter or characteristic life; $f(t,\alpha,\beta)$ is the Weibull probability density function; and $R(t,\alpha,\beta)$ is the Weibull survival function [94], [116-124]. The shape and scale parameters of the Weibull distribution function are defined as follows:

$$\beta = [\frac{\sigma_x}{\mu_x}]^{-1.086} \tag{6.3}$$

$$\alpha = \mu_x\,[0.568 + 0.433/\beta]^{-1/\beta} \tag{6.4}$$

where,

σ_x is the stander deviation of the group of data (x);

μ_x is the avarge value of the group of data (x)

Notice that:

$$h(t) \text{ is: } \begin{pmatrix} \text{a decreasing function of t when } \beta < 1 \\ \text{a constant when } \beta = 1 \\ \text{an increasing function of t when } \beta > 1 \end{pmatrix}$$

Therefore, the failure rate can be determined based on the Weibull probability density function, and reliability function. For distributions, such as Weibull distribution, the hazard function is not stable with respect to time. When the shape parameter increases, the mean of the distribution approaches the scale parameter value, and the variance approaches zero. The survival function $S(t)$ is the probability of survival until time *t* but not beyond time *t*. It is the reliability function that operates at time *t,* and can be estimated as follows [94], [116-124]:

$$S(t) = P(T \geq t), \quad t \geq 0 \tag{6.5}$$

The Weibull survival function is constructed as follows:

$$S(t) = R(t,\alpha,\beta) = 1 - F(t,\alpha,\beta) = e^{-(t/\alpha)^{\beta}} \quad (6.6)$$

The survival analysis is also an essential part for studying the period between the entry to the study of the fault, and the subsequent event. It is limited to the following ranges [94], [117-120]:

$$S(t) = 1 \; when \; t = 0$$
$$S(t) = 0 \; when \; t \to \infty$$

The Weibull probability density function of failure time for the wind generator can be defined as follows:

$$f(t,\alpha,\beta) = \frac{d}{dt} F(t,\alpha,\beta) = \frac{\beta \cdot e^{[-(t/\alpha)^{\beta}]} \cdot (t/\alpha)^{\beta-1}}{\alpha} \quad (6.7)$$

The mean and standard deviation of the Weibull probability density function are defined respectively as follows [94], [117-120]:

$$E(T) = (1/\alpha)^{1/\beta} \Gamma(1 + 1/\beta) \quad (6.8)$$

$$S.D = \left(\frac{1}{\alpha}\right)^{\frac{1}{\beta}} [\Gamma\left(1 + \frac{2}{\beta}\right) - \Gamma^2(1 + \frac{1}{\beta})]^2 \quad (6.9)$$

The cumulative distribution function $F(t)$ describes the continuous probability distribution of a random variable, such as the time in survival analysis. It can be defined as follows [48], [113-116]:

$$F(t) = P(T < t) = 1 - S(t) \quad (6.10)$$

The Weibull cumulative distribution function that characterizes the likelihood of failure prior to time *t* is estimated as follows [94], [117-120]:

$$F(t,\alpha,\beta) = 1 - e^{[-(t/\alpha)^{\beta}]} \tag{6.11}$$

In general, the cumulative distribution function is constructed to interpret the probability of the variable T, which will be lower than or equal to the probability of any value of t

To estimate the MTTF of wind generators, the types of maintenance that can be applied for any wind turbine should be understood first. For wind energy systems, two main types of maintenance are usually performed, the preventive maintenance (PM), and the corrective maintenance (CM) as shown in Fig. 6.2, which illustrates the classification of the maintenance types.

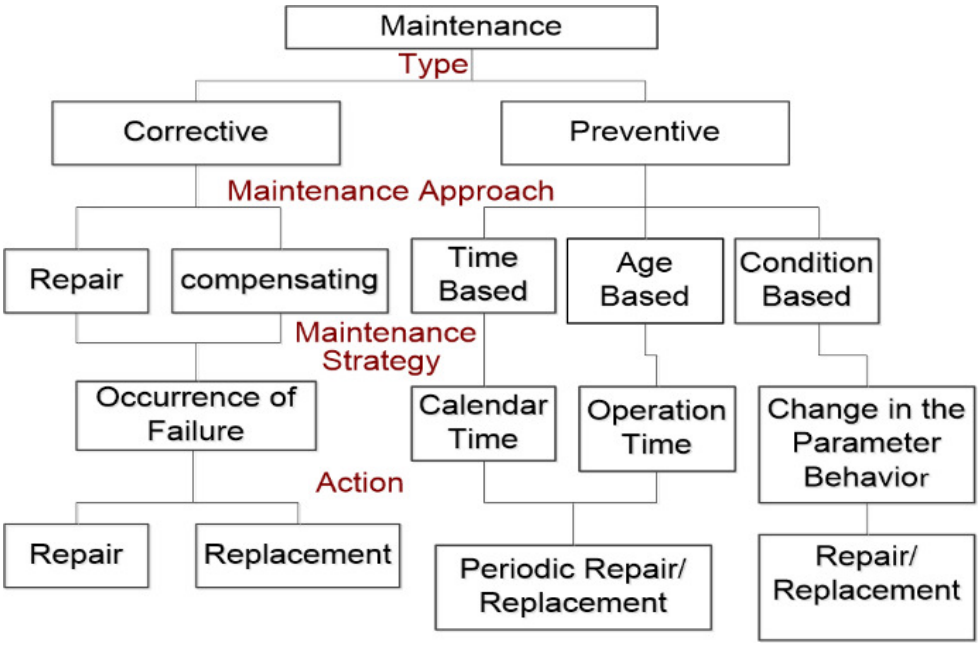

Fig. 6. 2 The maintenance strategy application [34], [105-109], [116].

In this context, PM is further divided into the time-based maintenance, the usage or age-based maintenance, and condition based maintenance. In the time-based maintenance approach, the maintenance schedule is predetermined depending on the calendar time strategy. While the age-time maintenance method is implemented based on the expended operation hours of the entire system, which represent the component age. The application of the condition based maintenance technique is based on data, which can be analyzed to acquire knowledge about the physical operation conditions. The CM, on the other hand, is applied when failure occurs according to unexpected operation or surrounding conditions. The classical replacement policy, however, is performed for both PM and CM due to failure or a certain age [34], [105-109], [116]. The most important considerations that should take in the account when determining the proper maintenance program are the age of the component, and the performance history of this component until the moment of decision making. The use of reliability analysis, such as failure rates and MTTF can minimize the costs for inspections and repairs as well as the costs due to component downtime. The estimation of MTTF is presented in the following section.

6.3. The Estimation of the Mean Time to Failure of Wind Generators

The MTTF of a component in wind energy systems, such as the generator is a reliability term based on methods for lifecycle predictions. It is a numerical statistical value based on analyzing a group of data to identify the failure rate and determine the expected operation time. It can be defined as the expected mean time until the first failure occurs. Suppose the likelihood for a random variable T (lifetime) to take on a given value (density

function) is $f(t)$, and the reliability of the maintained system with no maintenance is $R(t)$. In many instances, the PM approach is the most applicable maintenance type in the wind energy systems. After such a maintenance action is taken, the system is repaired to reach a condition "as good as new." Figure 6.3 indicates the effect of the PM on a wind generator [116].

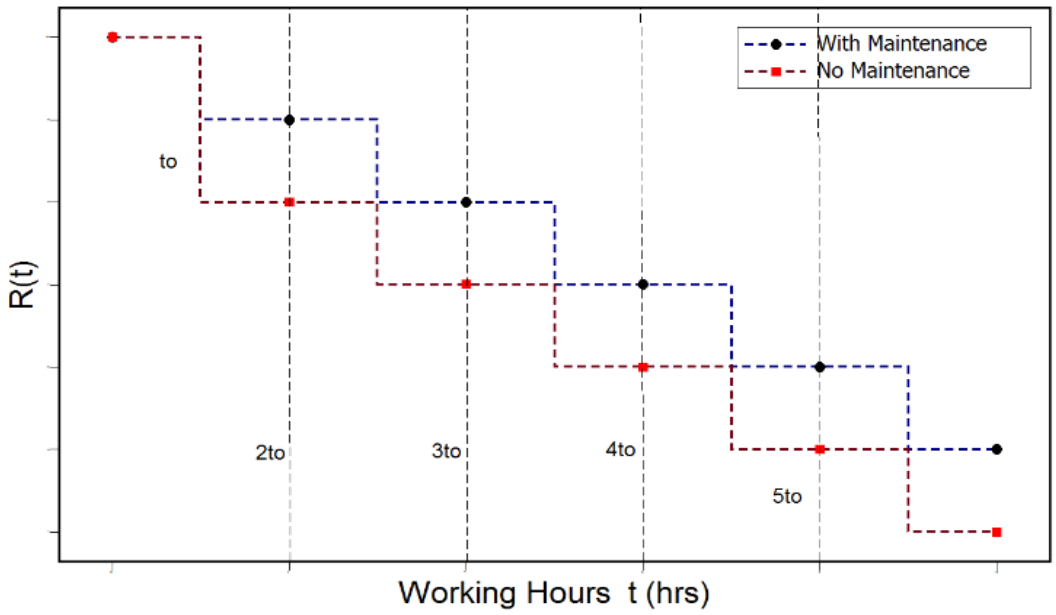

Fig. 6. 3 The reliability of a wind generator with and without preventive maintenance (PV), [116].

As shown in this figure, no maintenance action is taken until $t = t_o$, and the reliability of the maintained system $R_m(t)$ through the interval $0 \leq t \leq t_0$ can be stated as follows [105, 106, 112, 116,]:

$$R_m(t) = R(t); \quad 0 \leq t \leq t_0 \tag{6.12}$$

At any time during the next interval of time $t_0 \leq t \leq 2t_0$, the reliability of the maintained system is defined as follows [34, 106, 116, 119, 124,]:

$$R_m(t) = R(t_0)\, R\,(t - t_0); \quad t_0 \leq t \leq 2t_0 \tag{6.13}$$

Consequently, the reliability of the maintained system during the interval $it_0 \leq t \leq (i+1)t_0$ can be expressed as follows [105, 106, 112, 116, 117, 119,]:

$$R_m(t) = R^i(t_0)R(t - it_0); \quad it_0 \leq t \leq (i+1)t_0\ ;\ i = 0, 1, 2, \ldots.. \tag{6.14}$$

The MTTF of a maintained system is determined as follows [106, 112, 116, 117, 119, 124,]:

$$MTTF = \int_0^{\infty} R_m(t)dt = \int_0^{t_0} R_m(t)dt + \int_0^{2t_0} R_m(t)dt + \cdots \int_{it_0}^{(i+1)t_0} R_m(t)dt \tag{6.15}$$

$$MTTF = \sum_{i=0}^{\infty} \int_{it_0}^{(i+1)t_0} R_m(t)dt \tag{6.16}$$

By substituting Eq. (6.14) into Eq. (6.16), we have

$$MTTF = \sum_{i=0}^{\infty} R^i(t_0) \int_{t=it_0}^{(i+1)t_0} R_m(t - it_0)dt \tag{6.17}$$

Assuming $\tau = t - it_0$; Then, Eq. (6.17) can be rewritten as follows:

$$MTTF = \sum_{i=1}^{\infty} R^i(t_0) \int_{\tau=0}^{t_0} R_m(\tau)d\tau \tag{6.18}$$

In general, the MTTF is defined as follows:

$$MTTF = \frac{1}{1 - R(t_0)} \int_0^{t_0} R_m(\tau) d\tau \quad (6.19)$$

In the Weibull distribution, the MTTF can be estimated by using the next formula [105, 106, 112, 116, 117, 119,]:

$$MTTF = \frac{1}{\beta} \Gamma\left(\frac{1}{\beta}\right) \cdot \alpha \quad (6.20)$$

The variance of MTTF is defined as follows:

$$MTTF_{var} = \alpha^2 \left[\Gamma\left(1 + \frac{2}{\beta}\right) - \left(\Gamma(1 + \frac{1}{\beta})\right)^2 \right] \quad (6.21)$$

In addition, the Median Life (ML) of the MTTF is quite significant as it shows the sufficient information about the failure trend of the wind generator, which can be estimated as follows [106, 111, 112, 116, 117, 119,]:

$$MTTF_{ML} = \alpha \cdot (\ln 2)^{1/\beta} \quad (6.22)$$

The proposed methodology of Maintenance Decision – Making approach is described in the flowchart shown in Figure 6.4. First, the recorded generator temperature data must be inserted to the model in order to compute the number of faults due to high temperature. Based on specifying the expended operating hours at each recorded fault, the previous step can be achieved. Then, defining the distribution of the failure data is significant to identify the model parameters and apply the reliability analysis. The survival and hazard failure rates with respect to the expended operating hours are required to analyze the system condition. When hazard rate nears to one and the survival rate approaches zero, the corrective maintenance process must be implemented immediately,

and the wind generator has to be replaced. On the other hand, the MTTF at a particular expended operating hour t must be determined when $S(t) \gg 0$, and $H(t) \ll 1$, which means that the system does not suffer from any severity at the moment in which the data are collected. Finally, determining the need of preventive maintenance for the system is based on the estimation of MTTF. When MTTF exceeds the expended operating hours (t), the preventive maintenance must be applied immediately; otherwise, the maintenance approach should apply according to the maintenance calendar method. A case study will be presented in the following section, to demonstrate the mechanism of using the hazard failure rate model. The case study will explain how to use the condition monitoring data to estimate the MTTF based on the expended working hours of wind turbines.

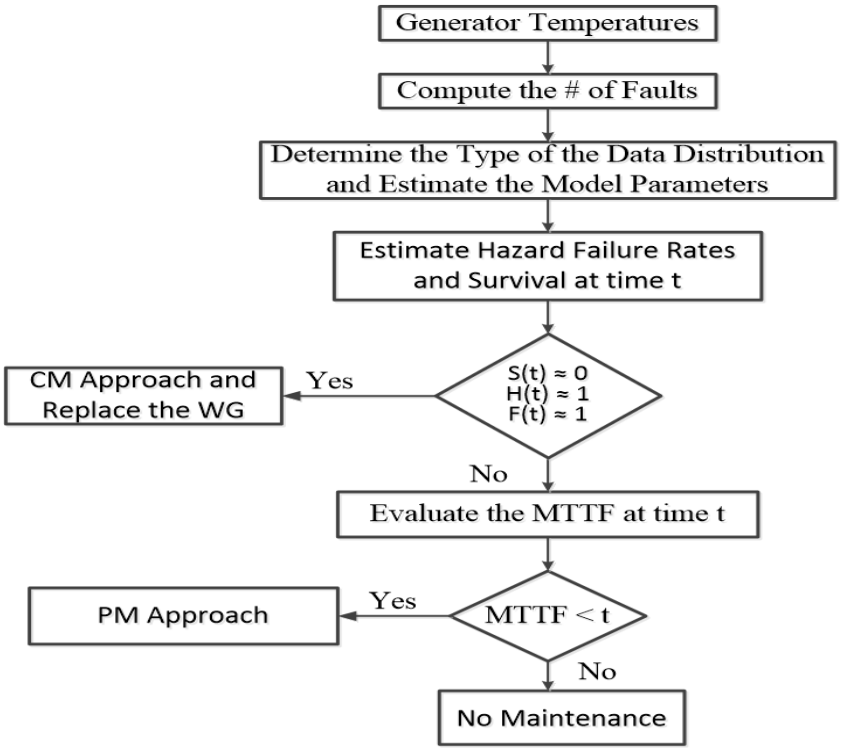

Fig. 6. 4 The proposed methodology of Maintenance Decision – Making approach.

6.4. Case Study

In this section, a case study is provided in order to explain how to employ the proposed hazard approach to estimate the MTTF, failure rates, and survival rates of two wind generators at any specific running time. Actual data are collected from the two variable speed wind turbines, which are installed in different wind farms in order to test the validity of the proposed model. The brand of each wind turbine is different, and each has a synchronous permanent magnet generator with the rated speed of 1500 rpm. The ratings of the two wind turbines are 750 kW, 60 Hz, and they have three blades upwind with 46 m rotor diameter. The SCADA system provides enough details about the generator stator temperature, which is considered in this work as the generator temperature for both wind turbines. Moreover, the generator temperatures are recorded since the first operation hour for both wind turbines.

According to the manufacturer's handbooks /manuals, the wind turbines will shut down when the generator temperature reaches 140Cº over a continuous period of 60 seconds, and restart when the generator temperature drops to 120Cº. The operation conditions of the wind turbines are classified as shown in Table 6.1. In this work, the fault condition will be considered when the generator temperature exceeds 100Cº, because the operation condition below 100Cº is normal [125, 126,]. The main goal of this work is to determine the effect of the high generator temperatures on the generator age, which can identify the failure rate and reliability of the wind generators and suggest the proper time to replace or repair the wind generator based on estimating the MTTF.

Table 6. 1 The operation conditions of the study [125, 126,].

State	Generator Temperatures
Normal condition (No Fault)	$T_G < 100$ C°
Warning condition (Fault)	100 C° $< T_G < 135$ C°
Critical condition	$T_G > 135$ C°

The recorded historical generator temperatures for both wind turbines are measured every 60 seconds, i.e., there are sixty recorded generator temperature values for each wind turbine in an hour. In order to simplify the proposed work, the average of the recorded generator temperatures for every 60 minutes (each working hour) is calculated [125, 126,]. Consequently, through 50,000 working hours; for instance, there are 50,000 generator temperature values available to apply the proposed analysis. The recorded faults due to high generator temperatures (more than 100Cº) through the specific working hour intervals for both wind turbines are classified as shown in Tables 6.2, and 6.3 respectively.

Table 6.2 The recorded faults vs. the expended working hours for Turbine A [120, 121,]

Working Hours * 10^3 (hrs.)	Up to 25	25-30	30–36	36 - 46	46– 54
Number of Faults	426	522	1212	4789	7211

Table 6.3 The recorded faults vs. the expended working hours for Turbine B [120, 121,]

Working Hours * 10^3 (hrs.)	Up to 25	25-30	30– 36	36 - 46	46– 60
Number of Faults	343	487	967	2103	7124

The available recorded generator temperatures for Turbine A represent 54,000 expended working hours, while for Turbine B represent 60,000 expended working hours. The distribution of the number of faults due to high generator temperatures with respect to

the expended working hours (the failure time distribution) of both wind turbines is shown in Figs. 6.5, and 6.6 respectively.

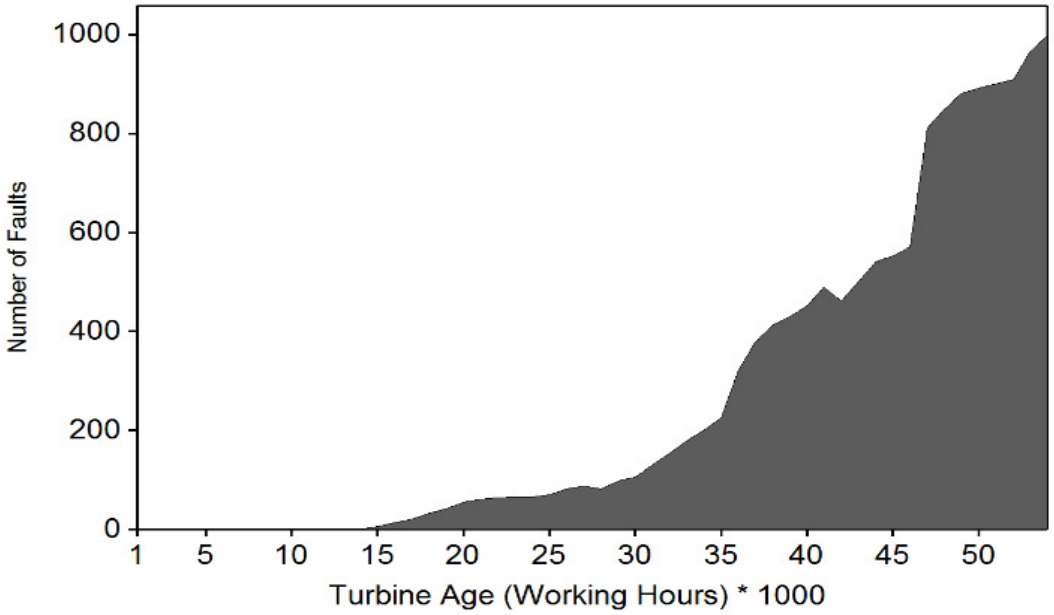

Fig. 6. 5 The area fault graph for Turbine A

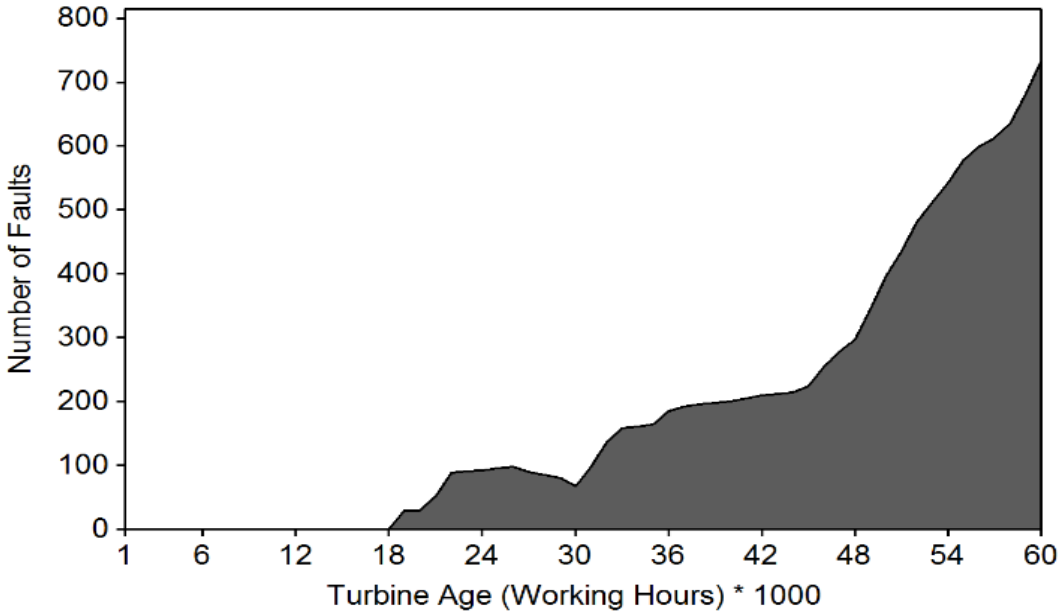

Fig. 6. 6 The area fault graph for Turbine B

Based on the area fault graphs for both wind turbines, the number of times that the generator temperature exceeds 100Cº at Turbine A are greater than that at Turbine B; although, the interval of the expended operating hours of Turbine B is bigger. This is due to the fact of the operation conditions and thermal stress were different, which causes variations in generator temperatures. Figure 6.7 shows the comparison of both wind turbines regarding the number of faults with respect to the expended operation hours.

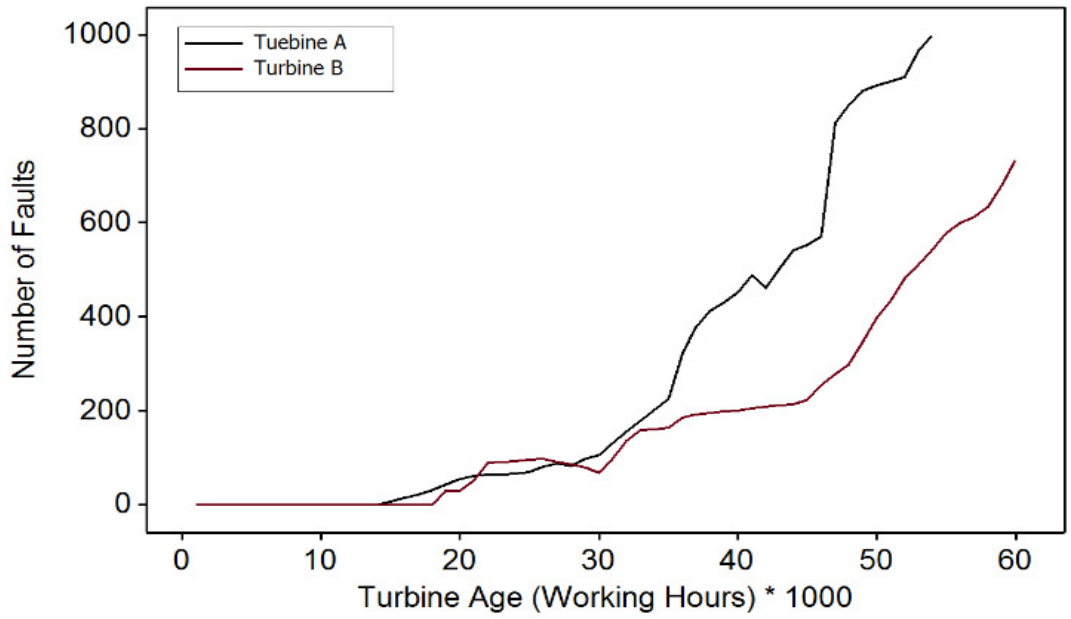

Fig. 6. 7 The number of faults trend of the Turbine A, and B

The previous figure illustrates that the number of faults increases dramatically in the last period of study for both wind turbines with respect to the expended working hours. Further, the inequality in the generator temperature values for both wind turbines is apparent. This indicates that the estimated working life of both wind generators will be

unequal. The increase of the number of faults is occurred due to high temperatures, which reduces the average age of both wind generators. The Weibull distribution can be utilized to obtain more accuracy on the reliability analysis of wind turbines than other distributions. This fact is confirmed by inserting the recorded generator temperatures of both wind generators into the EasyFit software, which deals with a wide range of distributions and selects the best model that fits the collected data in seconds. Table 6.4 shows the best five distributions, which are categorized according to Chi-Squared, Anderson Darling, and Kolmogorov Smirnov statistical tests of the collected data.

Table 6.4 The best five distributions of the collected data for Turbines A, and B.

Turbine	Distribution Type	Kolmogorov Smirnov		Anderson Darling		Chi-Squared	
		Statistic	Rank	Statistic	Rank	Statistic	Rank
A	Pert	0.09812	3	2.2164	1	29,684	3
B	Pert	0.09652	3	2.176	1	34.611	4
A	Weibull	0.10488	4	2.3891	2	25.753	1
B	Weibull	0.0872	2	2.221	2	24.672	1
A	Inv. Gaussian	0.0778	1	2.6511	3	29.709	4
B	Triangular	0.0674	1	2.485	3	38.812	5
A	Cauchy	0.07952	2	2.9	4	26.153	2
B	Log-Gamma	0.1875	4	3.0761	5	29.276	3
A	Normal	0.10564	5	3.0349	5	29.724	5
B	Lognormal	0.19732	5	2.752	4	25.986	2

Based on the Chi-Squared test, the Weibull distribution has the smallest Chi-Squared statistical value for both wind turbines, which means that the Weibull distribution model fits the generator temperature data perfectly [127]. The Weibull probability plots of the generator temperatures for both wind turbines are required in order to confirm the fact of the Weibull distribution is appropriate to represent the data. Figures 6.8, and 6.9 respectively illiterate that there are acceptable Weibull probability plots in which the majority of the temperature points lie approximately along a straight line.

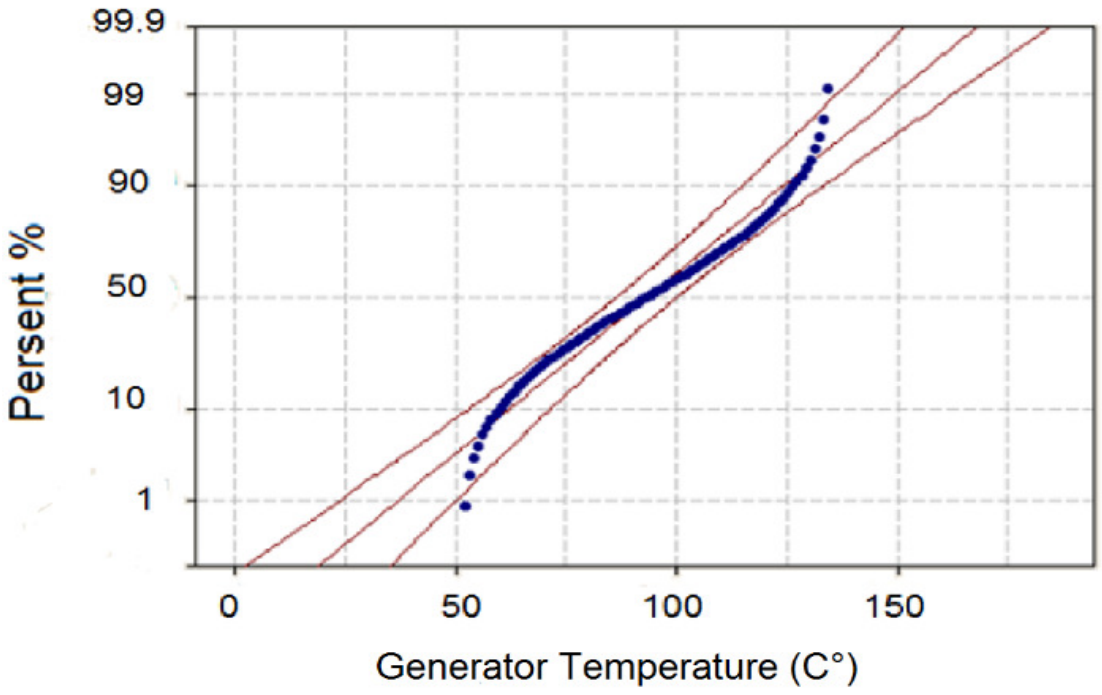

Fig. 6. 8 The Weibull probability plot of the generator temperatures for the wind Turbine A.

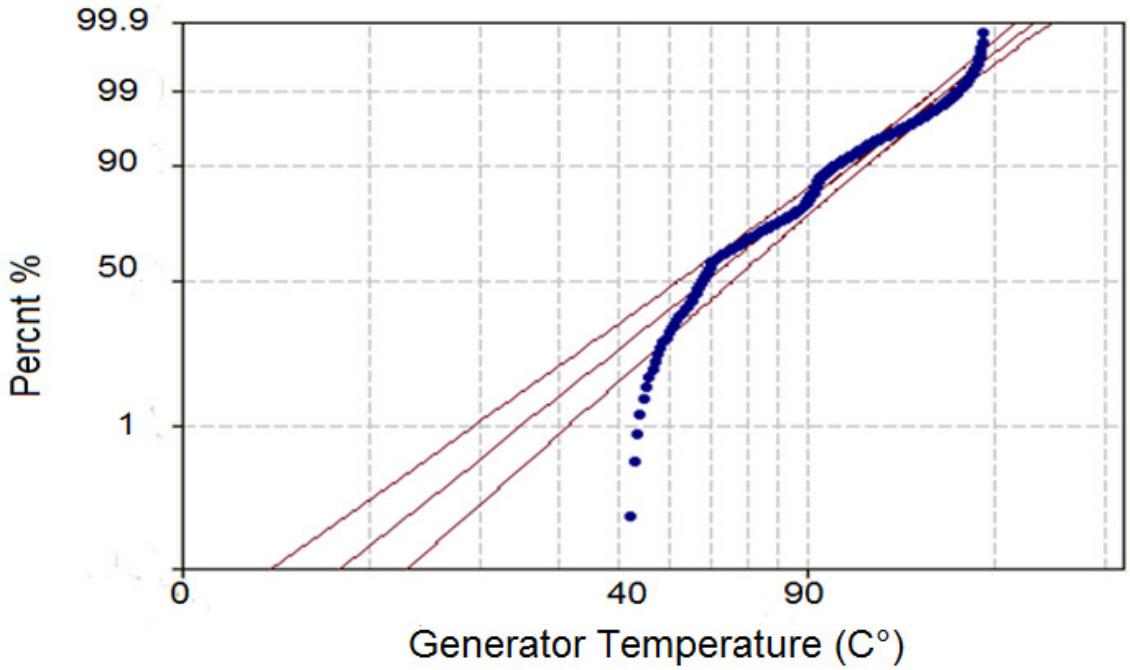

Fig. 6. 9 The Weibull probability plot of the generator temperatures for the wind Turbine B.

In order to estimate the generator failure rate and survival rate, the Weibull probability density function (PDF) is required for both wind turbines according to the recorded generator temperatures, and the expended working hours as shown in Figure 6.10. The density function of the Weibull distribution is to present the frequency of the failure time when the generator temperature is above 100Cº. Furthermore, the PDF chart describes the relative likelihood of the generator temperatures as random variable varies with the change in the operation conditions [94, 120, 121, 127, 128,]. Note each wind turbine has a different shape and scale parameter due to the variation in the generator temperatures of both wind turbines. The shape and scale parameters affect the obtained results, which are presented in the following section.

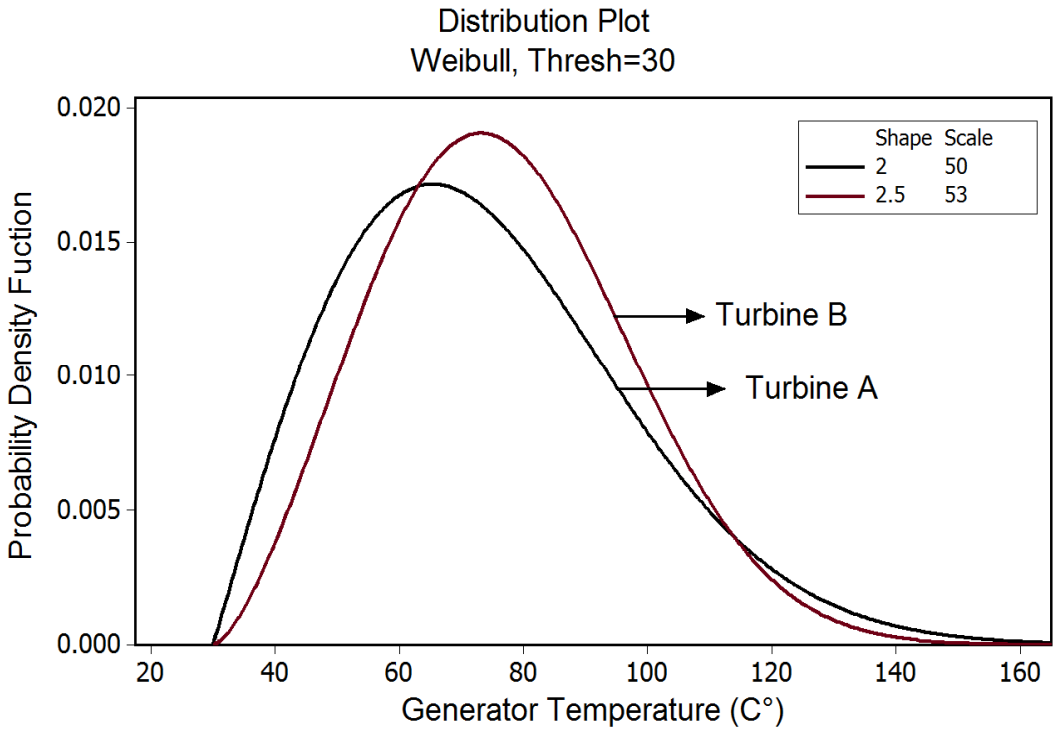

Fig. 6. 10 The Weibull PDF According to the generator temperatures

6.5. The Obtained Results of the Third Method

In order to search the of effect the generator temperature on the wind turbine reliability with respect to the generator expended working hours, the data of Turbine B are taken as an example. This because Turbine B has longer expended working hours than Turbine A, which helps to extend the analysis size of the current study. Figure 6.11 shows several survival rate curves for Turbine B, based on the expended operating hours and the generator temperatures. It is found that the survival rate decreases when the expended operating hours increase at any generator temperature. Furthermore, when the generator

temperatures increase, the survival rate or the generator decreases at any range of the expended operating hours.

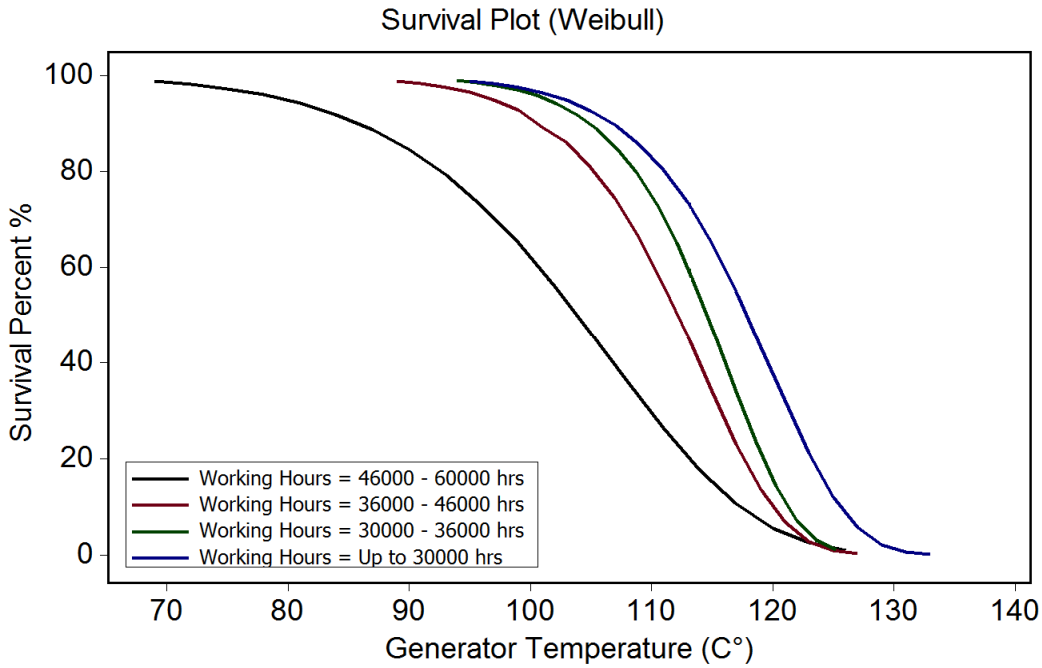

Fig. 6. 11 The Weibull survival plot with respect to the generator temperatures and generator ages for Turbine B.

The cumulative distribution function $F(t)$ can utilize to determine the likelihood of failure that occurs at any generator temperature, with respect to the expended operating hours as shown in Fig. 6.12. The influence of the generator temperature on the probability of failure prior to any specific time based on the generator ages is confirmed by this figure. Figure 6.13 illustrates different failure rate curves for Turbine B based on the expended operating hours, and the generator temperatures.

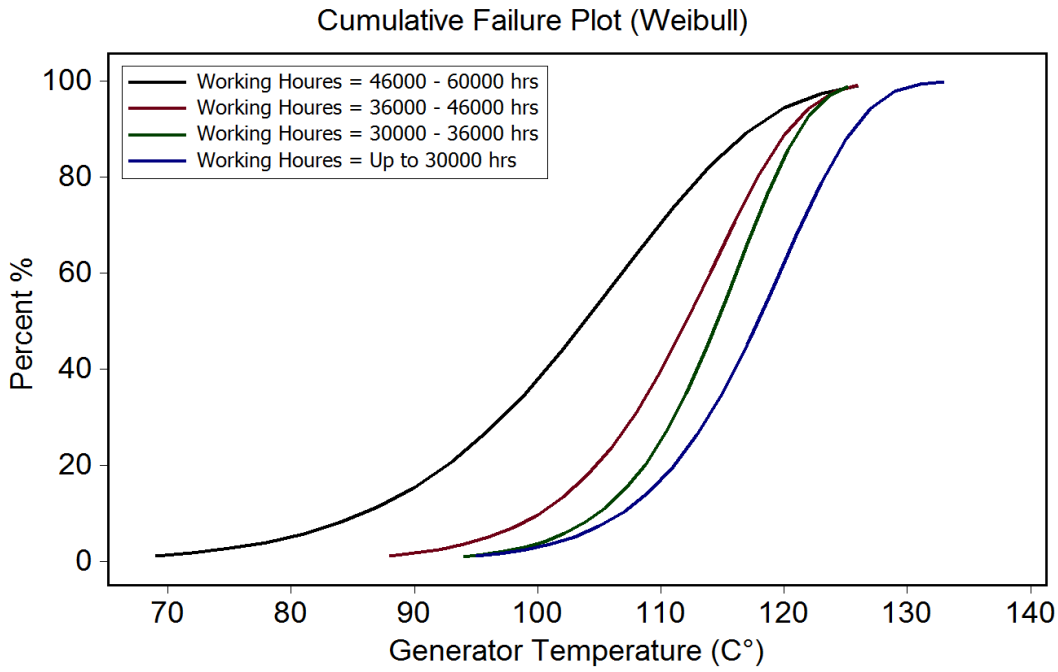

Fig. 6. 12 The Weibull cumulative failure plot with respect to the generator temperatures and generator ages for Turbine B.

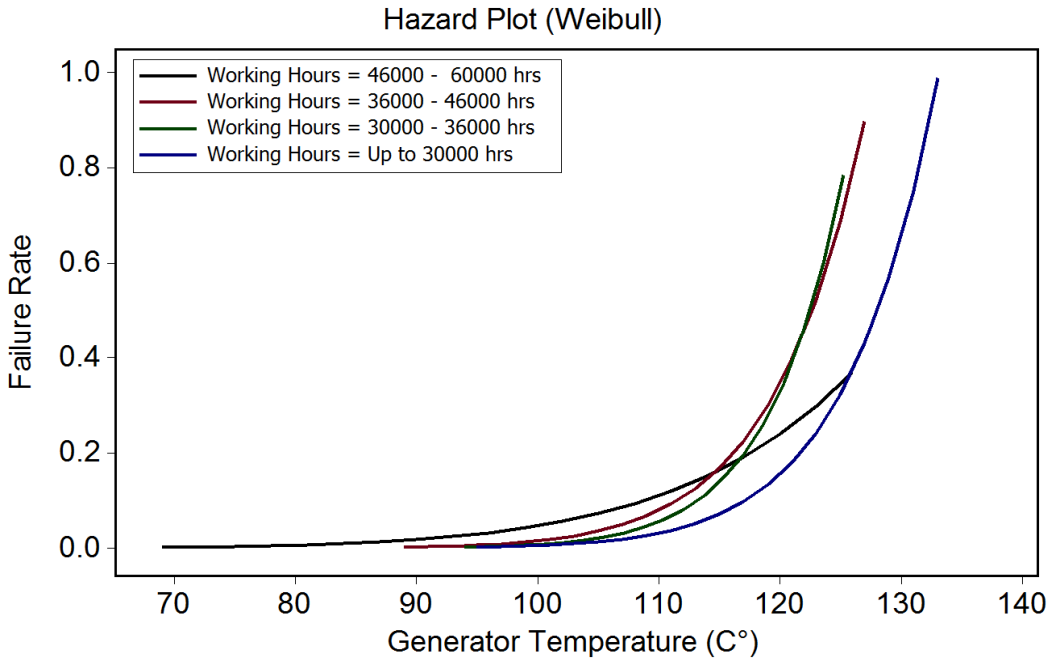

Fig. 6. 13 The Weibull failure rate plot with respect to the generator temperatures and generator ages for Turbine B.

As shown in Fig. 6.13, the Hazard failure rates show higher values with higher expended operating hours; however, the increases of the hazard failure rates become dramatic till the generator temperature reaches 115.8 Cº. After that, the Hazard failure rates fluctuate with increasing the generator temperatures and generator ages. This gives, indication about the presence of additional causes affecting the Hazard failure rates in addition to the generator temperature.

Figures 6.14—6.15, and 6.16 show the general reliability analysis for Turbines A— and B according to the expended generators working hours, and the number of faults that considered due to high generator temperatures. Based on the simulation analysis of the collected operation data, it can conclude that the reliability of the generator of Turbine B is better than the generator of Turbine A, which further indicates that the surrounding operation conditions of Turbine A were different from Turbine B. There are several reasons that heighten the generator stator winding temperature, such as the increase of the electrical loads or inappropriate cooling systems in the generator. This leads to increases the thermal and electrical stresses and decrease the wind generator age, and thus have a negative effect on the overall system performance [15].

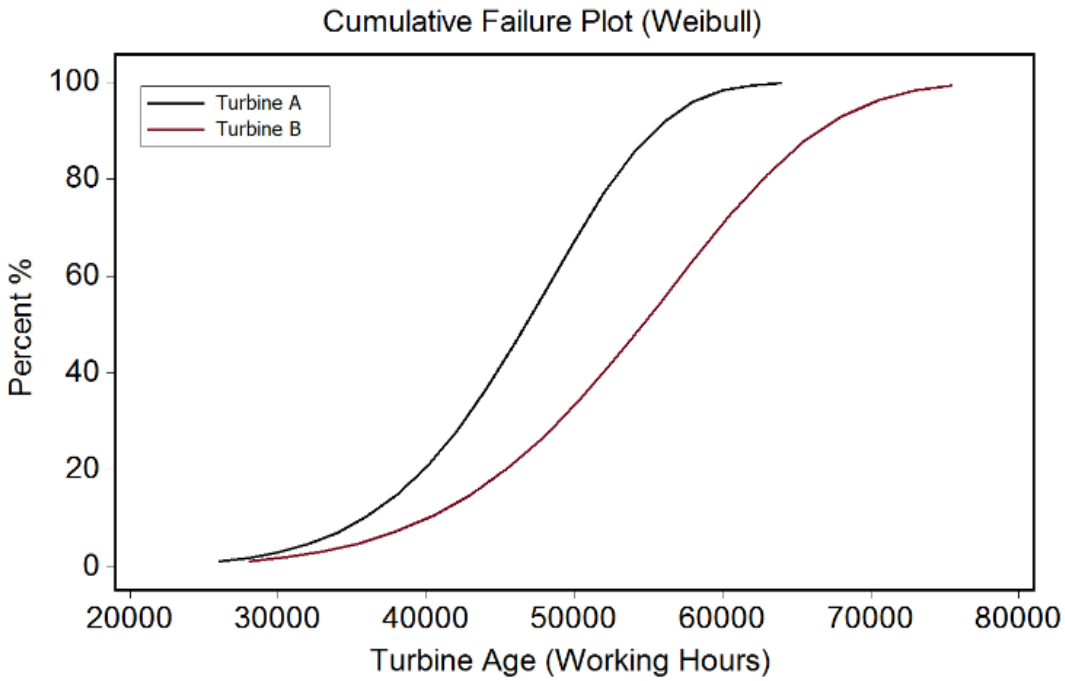

Fig. 6. 14 The Weibull cumulative failure plots with respect to the generator operation hours and the number of faults for Turbines A, B.

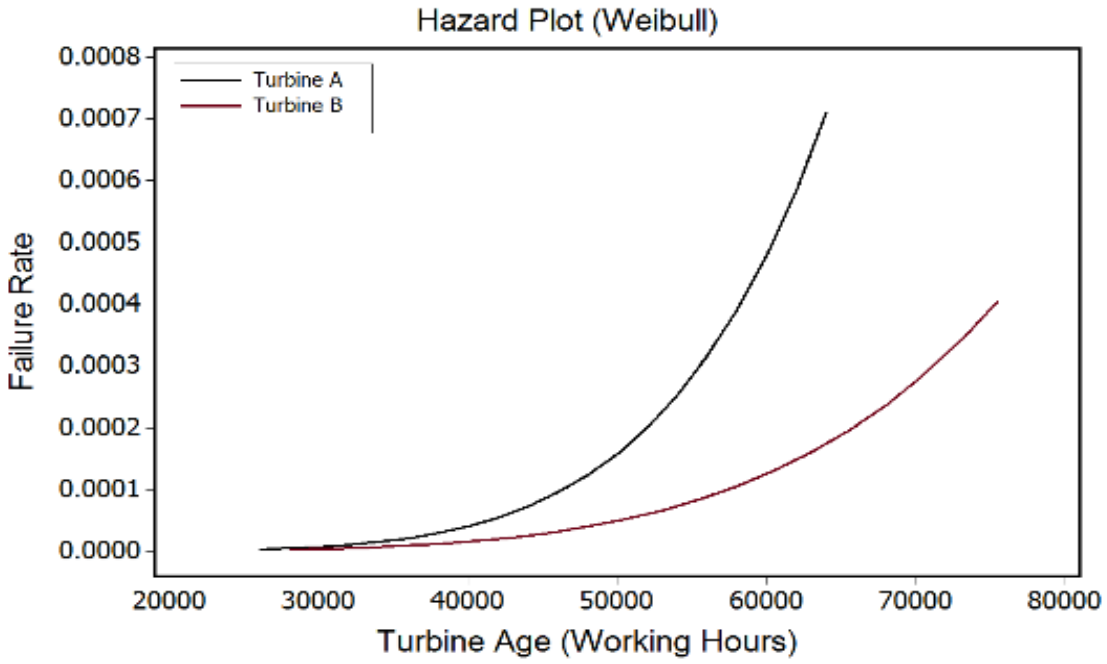

Fig. 6. 15 The Hazard plots with respect to the generator operation hours and the number of faults for turbines A, B.

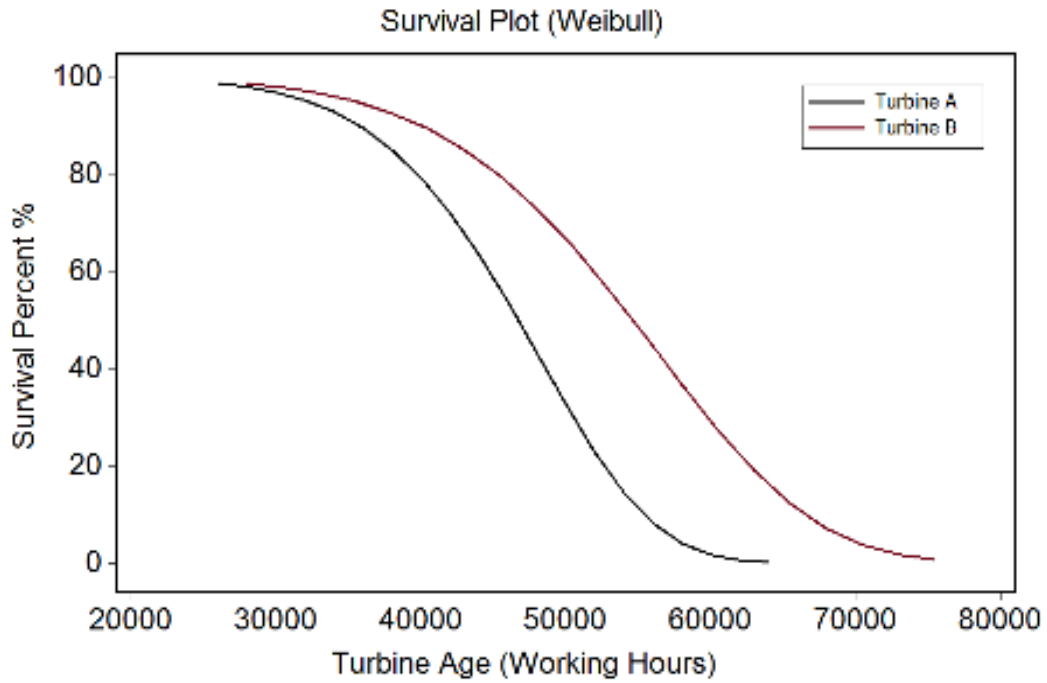

Fig. 6. 16 The SR plots with respect to the generator operation hours and the number of faults for Turbines A, B.

Figures 6.17 and 6.18 respectively show the probability plot graphs of the failures that are occurred due to the high generator temperatures, with respect to the operating hours of each wind turbine. These figures present acceptable Weibull probability plots, in which the majority of the failure points lie approximately along a straight line [94], [119-121], [127]. Tables 6.5 and 6.6 summarize the general reliability analysis results of both wind turbines, which indicate that the estimated life of the generator for Turbine A is approximately 64,000hrs, while the generator for Turbine B is 75,500 hrs. The obtained reliability information helps to reduce the shutdown events, and to implement a suitable maintenance program.

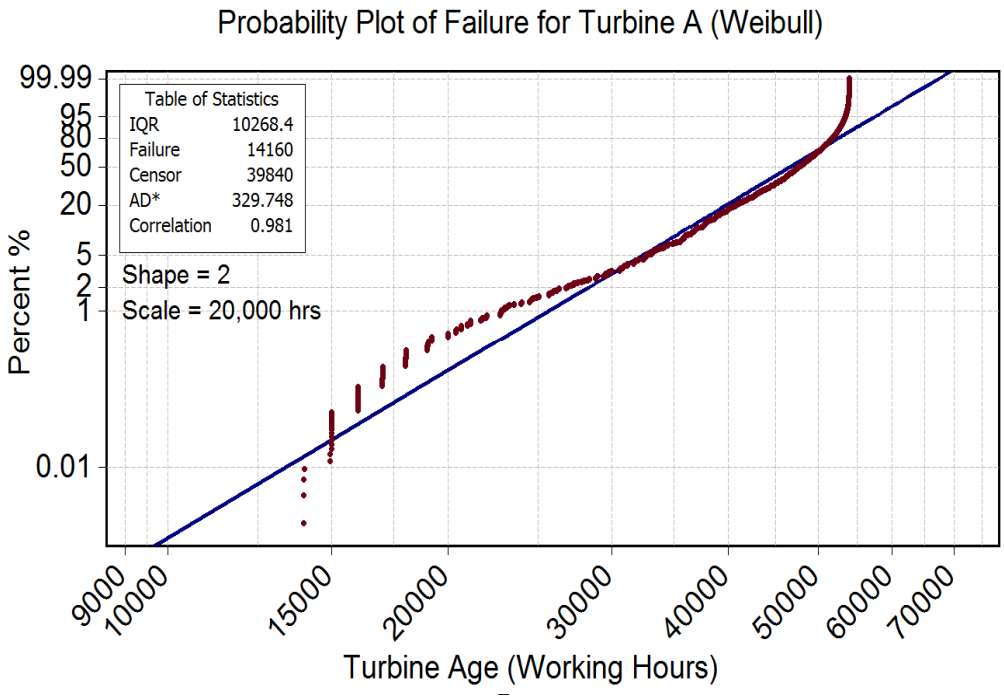

Fig. 6. 17 The Weibull probability plot of the failure points for Turbine A

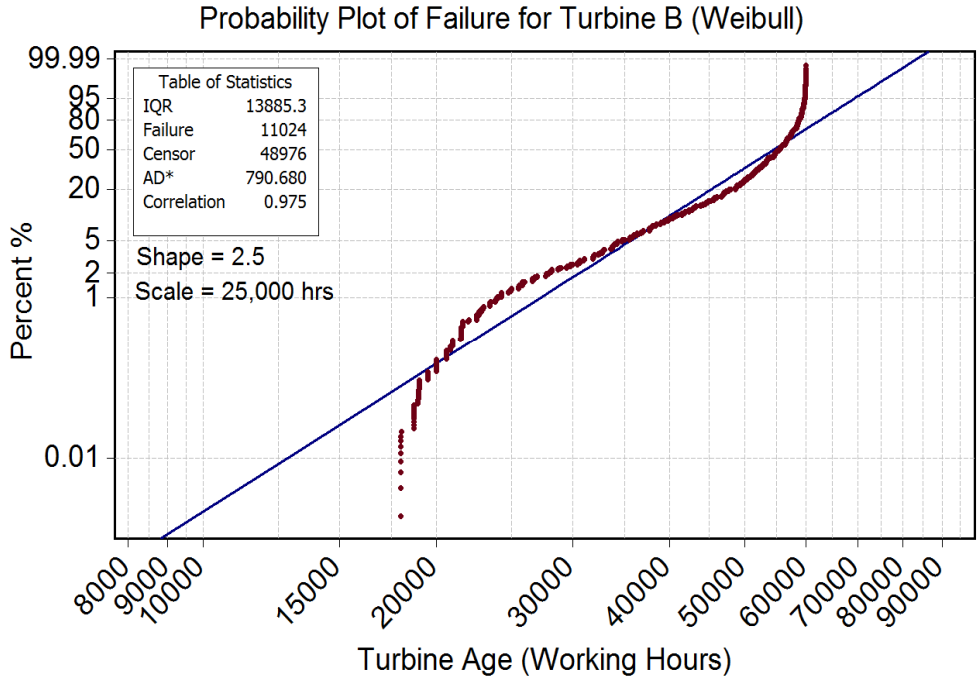

Fig. 6. 18 The Weibull probability plot of the failure points for Turbine B

Table 6.5 The reliability analysis for Turbine A

Working Hours x 10^3	26	34	44	54	64
Hazard Failure Rate x 10^{-4}	0.03	0.15	0.73	2.6	7
Survival Percent	98.9	92.96	63.6	14.5	0.16
Cumulative Failure Percent %	1.1	7.04	36.4	85.5	99.8

Table 6.6 The reliability analysis for Turbine B

Working Hours x 10^3	30.5	45.5	55.5	65.5	75.5
Hazard Failure Rate x 10^{-4}	0.04	0.31	0.84	1.96	4.05
Survival Percent	98.1	97.7	46.6	12.2	0.67
Cumulative Failure Percent %	1.95	20.3	53.4	87.8	99.3

With the increase of the number of faults (the number of times that the generator temperature exceeds 100Cº), the survival rates of both turbines decrease. The results show that the survival rate of Turbine B is more than that of Turbine A, due to the high temperatures that the generator of Turbine A had experienced. In addition, there are other influencing factors lead to increased generator temperatures, such as the electrical loads, and efficiency of the generator cooling systems [15]. This further results an increase in the thermal and electrical stresses on the generators; consequently, the number of faults (the failure rate) grows as the wind generator ages, which eventually affects the reliability. The surface plots for Turbines A and B are shown in Figs 6.19, and 6.20 respectively. These figures clearly present the relationship between the failure rate, and the survival rate, with respect to the turbine operating hours graphically in three dimensions.

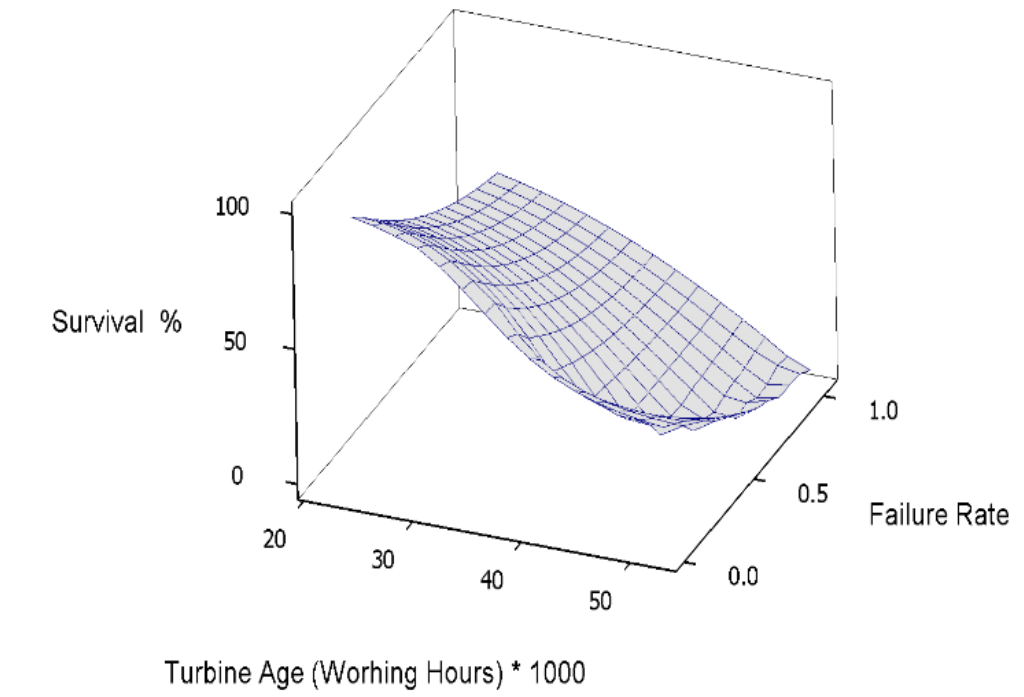

Fig. 6. 19 The surface plot of Turbine A

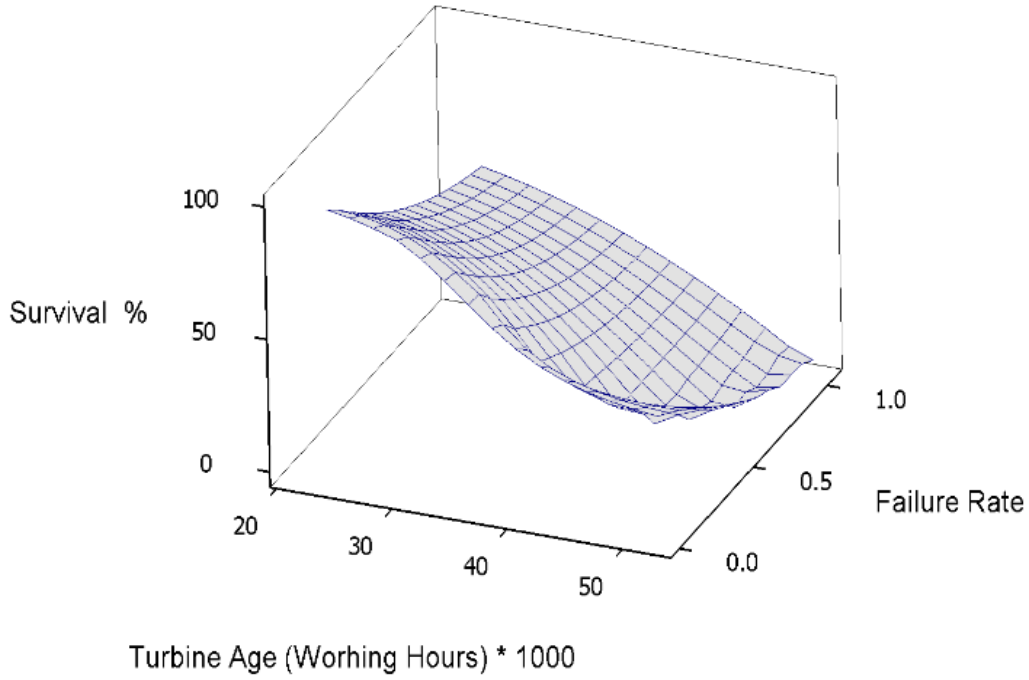

Fig. 6. 20 The surface plot of Turbine B

According to Eq. (6.20), the Weibull mean time to failure MTTF for both generators can be estimated. Table 6.7 indicates that the average of the predicted operating hours of Turbines A and B before the first failure occurred is 17,725 hrs and 27,700 hrs respectively. In other words, the first fault that is occurred due to the high generator temperature (above 100C^{o}) is recorded at the average time of 17,725 hrs for Turbine A, and 27,700 hrs for Turbine B. Note that the estimation of the MTTF is based on the Weibull scale and shape parameters. The preventive maintenance for both wind turbines is scheduled every 3000 working hours, and the inspection time (t), which was recorded since the previous maintenance was 2000 working hours. In this context, the $\mathrm{MTTF}_{A,B} > t =$ 2000 hrs—which confirms that the preventive maintenance is not immediately required, and the scheduled maintenance is accurate and proper.

Table 6.7 The statistical properties of the MTTF for Turbines A, and B

Turbine	Statistical Parameter α (Hrs)x 10^3	Statistical Parameter β	MTTF (Hrs)x 10^3	$\mathrm{MTTF}_{S.D.}$ (Hrs)x 10^3	MTTF_{ML} (Hrs)x 10^3
A	≈20	≈ 2	17.725	9.265	16.651
B	≈25	≈2.5	27.727	9.492.	21.591

6.6. The Conclusion of the Third Method

In this proposed method, an application of Hazard model reliability analysis based on a CMS of wind generators is proposed. The proposed technique can be utilized to address the technical problems that are related to wind generators, which leads to reduce

maintenance and operation costs. The CMS knowledge can be employed to estimate the hazard failure and survival rate functions, which are the most widely used statistical analysis tools of the lifetime data. In order to perform a proper preventive maintenance on wind generators, the estimation of the mean time to failure (MTTF) is required, and the method of estimating this parameter is proposed in this paper. A case study is presented to demonstrate the proposed method based on condition monitoring data of two wind turbines. The purpose of the research is to investigate the influence of the high generator temperatures on the estimated generators age, which helps to plan a suitable maintenance program, and improves the system reliability. The reliability analysis is performed for each wind turbine, and the hazard lifetimes are estimated based on the Weibull distribution with respect to the generator temperatures, and expended working hours of both wind turbines. It is found that with the increase of the number of faults (the number of times that the generator temperature exceeds 100C^{o}), the survival rate of both turbines decreases. The hazard life time, failure and survival rates, are deferent in each generator of the turbines. The two turbines show variations in the reliability analysis results, because the operation conditions of both wind turbines, such as electrical loads, and the generator cooling systems are dissimilar. By estimating the MTTF, the failure and survival rates of wind generators, an optimal maintenance decision can be made. The future work will be focused on estimating the age of wind generators and the MTTF by inserting additional covariates to the model, such as the generator voltage or frequency to indicate their effects. Furthermore, constructing an optimized cost model by using the hazard model techniques or different degradation models will be beneficial.

Chapter 7. The Fourth Method: A Condition Monitoring System for Wind Turbine Generator Temperature by Applying Regression Models

A modern statistical approach to perform CMS on the wind generators based on the regression models is presented in this chapter. Two types of the regression models are demonstrated through the derivation of the proposed algorithm. The first one is the standard multiple linear regression model, which can be used in the linear pattern between the response and the independent variables of the model. The second one is the polynomial regression model, which can be applied when a curvilinear relationship is existent between the response and the model's independent variables. The proposed technique are used to construct the normal behavior model of the electrical generator temperature based on the historical generator temperatures, and to study the influence of the heat loss on a wind generator's temperatures.

Monitoring the wind generator temperatures is a significant for efficient operation and plays a key role in an effective CMS. Many techniques, including prediction models can be utilized to reliably forecast a wind generator's temperature during operation and avoid the occurrence of a failure. The regression models can be used to construct a normal behavior model of an electrical generator's temperatures based on recorded data. Many independent variables affect a generator's temperature; however, the degree of influence

of each independent variable on the response is dissimilar. In many situations, adding a new independent variable to the model may cause unsatisfactory results; therefore, the selection of the variables should be very accurate. A generator's heat loss can be considered a significant independent variable that greatly influences the wind generator with respect to the other variables. A generator's heat loss can be estimated in intervals by analyzing the exchange in the heat between the hot and cold fluid through the heat exchangers of wind generators. A case study built on data collected from actual measurements demonstrates the adequacy of the proposed model. A case study built on data collected from actual measurements demonstrates the adequacy of the proposed model.

7.1. Introduction

Wind generator failure caused by high temperatures, which can occur as a result of various reasons, has increased remarkably. External vectors, such as harsh climatic situations and variable electrical loads cause abnormal operation conditions. However, wind energy reliability is growing as a result of recently implemented advanced monitoring systems. Applying modern condition monitoring to wind generators increases the generated wind power and helps reduce operation and maintenance expenses, especially in wind turbines deployed offshore. CMS can provide detailed information about a wind generator's condition by analyzing measured signals to predict and avoid an impending failure in the wind turbine's components. The temperature of a wind generator is one of its most important operating characteristics, and it needs to be monitored. In wind generators,

the electromagnetic losses produce a significant amount of heat, which in turn warms up the generator and causes a temperature increase in the stator bars that reduces the life span of the insulation materials. This problem challenges engineers to develop proper CMSs for wind turbine generator parts [20, 31, 94,].

Monitoring the wind generator temperatures is a significant for efficient operation and plays a key role in an effective CMS. Many techniques, including prediction models can be utilized to reliably forecast a wind generator's temperature during operation and avoid the occurrence of a failure. The regression models can be used to construct a normal behavior model of an electrical generator's temperatures based on recorded data. Many independent variables affect a generator's temperature; however, the degree of influence of each independent variable on the response is dissimilar. In many situations, adding a new independent variable to the model may cause unsatisfactory results; therefore, the selection of the variables should be very accurate.

The heat loss of wind generators is a very significant independent variable that affects the generator temperature; therefore, it is worthwhile to focus on the wasted heat of wind generators. The heat loss of wind generators can be estimated from the thermal aspect by computing the heat exchange between the hot air that comes from the high temperatures of a generator's parts and the cold fluid inside a generator's heat exchangers [26, 99,]. The proposed method studies and evaluates the effect of heat loss on a generator's temperatures by employing regression models. Regression models are formulated in several ways, such

as the standard multiple regression model (MLRM) or the polynomial regression model (PRM). The regression model is an effective approach that can be utilized to predict and monitor temperatures inside wind turbine generators by evaluating the correlation between the observed values and the predicted values of the criterion variables based on recorded generator temperatures. The rest of the paper is organized as follows: Section 7.2 introduces background information about the MLRM and describes how model validation can be detected. Section 7.3 presents the statistical tests that can be applied to measure the standard MLRM adequacy. The transformation process to the PRM is explained in Section 7.4. To demonstrate the estimation of wind generator heat losses from the thermal side, Section 7.5 provides heat transfer analysis for the heat exchangers of wind generators. A case study is provided in Section 7.6 to demonstrate the methodology of the present work. Section 7.7 presents the results of the proposed method. Finally, the conclusion of the proposed work is given in Section 7.8.

7.2. Theoretical Background on the Standard MLRM

The MLRM is one of the most popular statistical techniques used to predict the behavior of a response (dependent variable) by modeling a group of explanatory variables (independent variables) [26, 128, 129,]. The independent variables that affect the generator temperature can be defined as follows [15]:

- *Generator power (GP):* A generator's power has a direct effect on a generator's temperature. The stator current in a generator rises when the electrical load is high,

which leads to an increase of the generator's output power and the temperature of the generator.

- *Ambient or outside temperature (OT):* The considerable and frequent rise in the outside temperature leads to an increase in a generator's temperature.
- *Nacelle temperature (NT):* A nacelle's temperature is closely related to a generator's temperature, because the generator itself is located inside the nacelle component.
- *Cooling temperature (CT):* There is a strong relationship among the temperatures of the cold fluids inside the heat exchangers, which are used to cool a generator and the temperature of the generator. Heat exchangers that are used in wind generators play a remarkable role in providing proper operating conditions for the generator components.
- *Heat loss (HL):* The heat loss of a wind generator is a very significant variable that can be added to the proposed model as an independent variable because the heat loss warms up the active parts of a generator and causes an increase in the generator's temperature [26, 41, 42, 99,].

There are three parts of the generator their temperature can be measured easily and represented the generator temperature in general. These parts are the generator frame, the stator windings, and the generator rotor. Figure 7.1 presents the measured temperatures of the selected generator parts through 600 seconds. It can see that the generator winding temperature trend lies between the temperature trends of the rotor and frame of the

generator. Therefore, the stator winding temperature represents the generator temperature (T_G). Further, the windings are the machine parts that are most likely to be damaged by excessive heating and their temperature identify the generator health. Through this proposed work the generator temperature (T_G) represents the dependent variable (response) and strongly correlates to the previous independent variables of the model [41-43], [94].

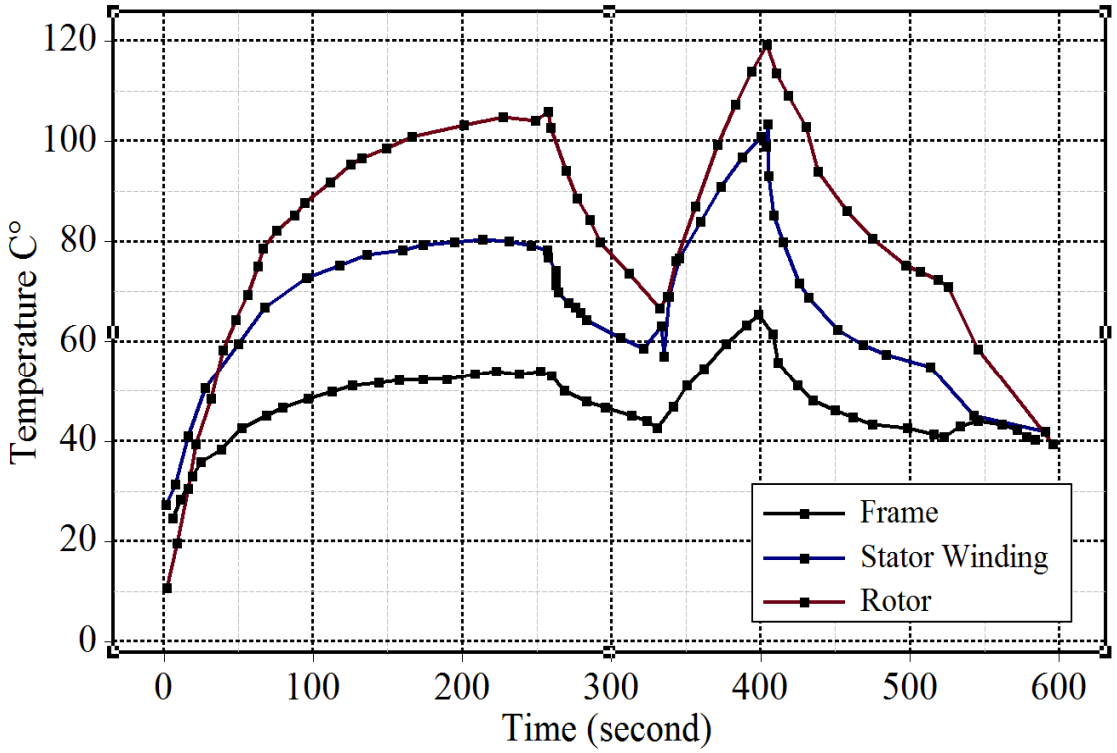

Fig. 7. 1 The temperature trend of the generator parts [130].

The multiple regression model might describe the relationship between the dependent variable (GT) and the independent variables as follows [128-131]:

$$T_G = \beta_0 + \beta_1 \cdot CT + \beta_2 \cdot GP + \beta_3 \cdot HL + \beta_4 \cdot NT + \beta_5 \cdot OT + \varepsilon \quad (7.1)$$

where:

- β_i $(i = 1,2, \dots, n)$ is the i[th] regression coefficient β corresponding to the independent variables, and n is the number of the independent variables.
- ε is the residual, defined as the difference between the experimental and predicted value.

The response *GT,* which is related to the predictor variables (independent variables X) and the regression coefficients $\beta = [\beta_0, \beta_1, \beta_2, \dots \dots, \beta_n]$ can be estimated by using the method of least squares, as follows:

$$\beta = \begin{pmatrix} \beta_1 \\ \beta_2 \\ : \\ : \\ \beta_n \end{pmatrix}, \quad \text{X=} \quad \begin{pmatrix} 1 & CT_1 & CT_2 \dots \dots CT_n \\ 1 & GP_1 & GP_2 \dots \dots GP_n \\ 1 & HL_1 & HL_2 \dots \dots HL_n \\ 1 & NT_1 & NT_2 \dots \dots NT_n \\ 1 & OT_1 & OT_2 \dots \dots OT_n \end{pmatrix} \tag{7.2}$$

$$y = \begin{pmatrix} T_{G_1} \\ T_{G_2} \\ : \\ : \\ T_{G_N} \end{pmatrix}, \quad \varepsilon = \begin{pmatrix} \varepsilon_1 \\ \varepsilon_2 \\ : \\ : \\ \varepsilon_N \end{pmatrix}, \quad \beta = (X' X)^{-1} \cdot (X' y) \tag{7.3}$$

Then the predicted generator temperature ($\widehat{GT}$) can be formulated as follows:

$$\widehat{T_G} = \beta_0 + \beta_1 \cdot CT + \beta_2 \cdot GP + \beta_3 \cdot HL + \beta_4 \cdot NT + \beta_5 \cdot OT \tag{7.4}$$

The residuals ε (the difference between the observed values of T_G and the corresponding predicted values $\widehat{T_G}$) play an important role in evaluating the adequacy of the fitted regression model and the shape of the model. The model deficiencies show up clearly by

analyzing the relationship between the residuals ε and the corresponding fitted values $\hat{y}$, [128-130]. The error variance of term y is σ^2, which can be determined by using the following equation:

$$\sigma^2 = \frac{SS_{Res}}{N - p} \tag{7.5}$$

where, N is the number of observations (experimental data points) and SS_{Res} is the residual sum of squares, which can be given as follows [26, 128, 129,]:

$$SS_{Res} = y' y - \beta' X' y \tag{7.6}$$

The term $N - p$ is the residual degree of freedom, and $p = k - 1$, where k is the regression degree of freedom. The residual mean square can be determined as follows [128-131]:

$$MS_{Res} = \frac{SS_{Res}}{N - p} \tag{7.7}$$

The total sum of squares SS_T is a statistical term that is partitioned into the sum of squares as a result of regression SS_R and the residual sum of squares SS_{Res}. Thus,

$$SS_T = SS_R + SS_{Res} \tag{7.8}$$

$$SS_R = \sum_{i=1}^{n} (\hat{y}_i - \bar{y})^2, \ \bar{y} = \frac{1}{N} \sum_{i=1}^{N} y_i \tag{7.9}$$

The regression mean square can be defined as follows:

$$MS_R = \frac{SS_R}{k} \tag{7.10}$$

The regression and residual mean squares are utilized to determine the existence of the linear relationship between the response and any of the independent variables based on the test for the regression significance. The model's coefficients must be within a range determined by utilizing the next formula [128-131]:

$$\beta_i - \left[t_{\frac{1-\gamma}{2},N-p}\right] \cdot \sqrt{\vartheta^2 \cdot C_{jj}} \leq \beta_{jj} \leq \beta_i + \left[t_{\frac{1-\gamma}{2},N-p}\right] \cdot \sqrt{\delta^2 \cdot C_{jj}} \quad (7.11)$$

where, ϑ^2 is the residual mean square, γ is the confidence interval percent ($\gamma = 95\%$ in the model assumption), and C_{jj} the j^{th} diagonal element of the $(X'\,X\,)^{-1}$ matrix.

To determine the importance level for each independent variable in the model, the length-scaling method can be used. The model coefficients are the criteria that are used to detect the importance level for each independent variable. The differences in the dimensions of the dependent variables and model coefficients affect the response values. To address this problem, it is beneficial to create dimensionless regression coefficients by utilizing the length-scaling method. The corrected sum of squares for an independent variable X_i:

$$S_{jj} = \sum_{i=1}^{k}(X_{ij} - \bar{X}_i)^2, \quad (7.12)$$

where, *i = 1, 2,..,n, j= 1, 2,..,N,* and X_{ij} is the independent variable i at a specific observation *j*. The average value of the dependent variable $\bar{X}_i = \frac{1}{N}\sum_{j=1}^{N} X_{ij}$ for the duration of the window of observation.The corrected sum of squares for the dependent variable GT_i:

$$S_{ii} = \sum_{i=1}^{n} (T_{G_{ij}} - \overline{T_{G_i}})^2, \tag{7.13}$$

The simple correlation between X_i and X_j is r_{ij}:

$$r_{ij} = \frac{S_{ij}}{(S_{ii}S_{jj})^{1/2}} \tag{7.14}$$

In this scaling, each new regressor is w_i. Based on the correlation matrix $w'w$ and the standardized regression coefficients matrix, $\hat{b}$ can be estimated as follows:

$$w'w = \begin{pmatrix} 1 & r_{12} & r_{13} \dots\dots r_{1n} \\ r_{12} & 1 & X_{23} \dots\dots X_{2n} \\ r_{13} & r_{23} & 1 \dots\dots X_{3n} \\ : & : & : \quad : \\ r_{1N} & r_{2N} & r_{3N} \dots\dots 1 \end{pmatrix} \tag{7.15}$$

$$\hat{b} = (w'w)^{-1} \cdot r_{iy} = \begin{bmatrix} \hat{b}_1 \\ \hat{b}_2 \\ : \\ : \\ \hat{b}_n \end{bmatrix} \tag{7.16}$$

Estimating the standardized regression coefficients for each independent variable is essential for measuring the reliability of each independent variable. Such estimations indicate the significance of each variable and term in the model [128-131]. The following section presents the required test that can be applied to measure the model adequacy.

7.3. Measure of Model Adequacy

Several techniques can be utilized to determine the validity of the proposed model. They can be summarized as follows:

7.3.1. Test of Individual Regression Coefficients

This test is helpful in selecting the best independent variables for the model. The variance of the response probably increases with more independent variables; therefore, the model might be more efficient with the deletion of some of the independent variables in the model. Determining the correlation coefficients and the degree of significance for each variable are both beneficial to defining the proper independent variables in the model. The hypothesis for testing any regression coefficient is as follows: If the significance of the regression coefficient's statistical value for a particular independent variable (t_0) is more than the proposed t value (t_{TABLE}), then the hypothesis of H_0: $\beta_i = 0$ is rejected and the independent variable strongly contributes to the model. This hypothesis can be interpreted as follows [127-131]:

$$t_0 \text{ should be} > t_{(1-\gamma)/2,n,N-n-1},$$

where:

$$t_0 = \beta_i / \sqrt{SS_{Res} \cdot C_{jj}} \tag{7.17}$$

7.3.2. Test of Significance of Regression

A test of significance of regression is required to investigate whether a linear relationship between the response and any of the regressor variables is present. The statistical concept of this test emphasizes that at least one of the independent variables is

clearly related to the model. The hypothesis of this test is as follows: If the significance of the regression statistical value (F_0) is more than the proposed F value (F_{TABLE}), then the hypothesis of H_0: $\beta_1 = \beta_2 = \cdots = \beta_n = 0$ is rejected, which means [127-132]:

$$F_0 \text{ should be} > F_{1-\gamma,n,N-n-1},$$

where:

$$F_0 = MS_R/MS_{Res} \tag{7.18}$$

7.3.3. The Test for Lack of Fit

This test can be considered as an overall test of the model adequacy. The lack-of-fit test is helpful to determine whether the linear relationship fits the obtained data. The requirements of this test refer to the normality in the distribution of the model's residuals, the independence of the regressor, and the constant-variance in the model. Fulfilling these requirements confirms whether the tentative model adequately describes the data. To perform this test, the lack-of-fit sum of squares SS_{LOF} and the pure-error sum of squares SS_{PE} can be estimated as follows [127-132]:

$$SS_{LOF} = SS_{RES} - SS_{PE} \tag{7.19}$$

$$SS_{PE} = \sum_{i=1}^{m}\sum_{j=1}^{ni}(T_{G\,ij} - \overline{T_{G\,i}})^2, \tag{7.20}$$

where, $\overline{T_{G_i}}$ is the generator temperature average of the i row of the generator temperature matrix, and $T_{G_{ij}}$ is the generator temperature of the observation j at row i of the generator temperature matrix. The hypothesis of this test says that if the model adequately describes the data, then the assumption of (Lack-of-fit F test $F_{LOF} > F_{\gamma,df_{LOF},df_{PE}}$) will be rejected, where F_{LOF} can be calculated from the next relation:

$$F_{LOF} = \frac{mean\ square\ of\ lack\ of\ fit}{mean\ square\ of\ pure\ erroe} = \frac{SS_{LOF}/df_{LOF}}{SS_{PE}/df_{PE}} \tag{7.21}$$

where, df_{LOF} is the lack of fit degree of freedom, and df_{PE} is the pure-error degree of freedom.

7.3.4. Predicted Residual Sum of Squares Statistic Test

The Predicted Residual Sum of Squares (PRESS) is a measure of the regression model validity and the prediction of potential performance. The PRESS statistical value can be defined as the sum of the squared residuals. An observation that falls outside of the general trend of the data should be considered as adversely affecting the model. The presence of this variation can be exposed by computing the PRESS statistic value and comparing that value to the residual sum of squares. Therefore, the PRESS statistic is considered as a measure of how well the regression model will be able to predict new data. To compare PRESS to the residual sum of squares, a small value of PRESS is desirable in the proposed model. The PRESS value can be computed as follows [127-132]:

$$PRESS\ \ statistic\ value = \sum_{i=1}^{n} (\frac{T_{G\,i-}\widehat{T_{G\,i}}}{1-h_{ij}})^2 \tag{7.22}$$

where, h_{ij} is the leverage for the ij^{th} element of the hat matrix (H), H=$X\ (X'X)^{-1} \cdot X'$.

7.3.5. The Coefficient of Multiple Determination

The coefficient of determination R^2 also measures the goodness of fit of the proposed model. The high value of R^2, however, does not necessarily denote that the regression model is suitable. In many cases, adding a new independent variable to the model may causes worse results. This situation occurs when the mean squared error for the new model is larger than the mean squared error of the old model—even though the new model will show an increased value of R^2. The coefficient of determination is defined as follows [125-132]:

$$R^2 = \frac{SS_R}{SS_T}, \tag{7.23}$$

7.3.6. Multicollinearity Test

Multicollinearity is an undesirable case that might occur in the regression models when one or more of the independent variables are robustly correlated to each other. This condition negatively affects the obtained results. The high multicollinearity among the independent variables results in a large variance and covariance for the least-squares estimators of the regression coefficients. High multicollinearity causes the coefficients to

be insignificant because the model coefficients will be unstable, and their standard errors will become large. A very simple way to measure the multicollinearity is to calculate the inflation factors (VIFs), which can be obtained from the following formula [128, 129, 132, 133,]:

$$VIF_j = (1 - R_i^2)^{-1} \tag{7.24}$$

where, R_i^2 is the coefficient of determination obtained when a particular independent variable regressed with a degree of freedom equals the total number of variables (T_G and *Xs*) -1. Many experts confirm that when the VIFs values exceed 5 (high multicollinearity), the regression coefficients of the model will be unreliable [128, 129, 132, 133,]. SPSS and Minitab statistical software [134-135] automatically perform a tolerance analysis and will not adopt the model results with tolerance < 0.2 for each variable inserted into the regression model.

$$Tolerance = \frac{1}{VIF} \tag{7.25}$$

A transformation process, which is presented in the following section will be required when the proposed MLRM fails to exceed the previous statistical tests.

7.4. The Transformation Process to the Polynomial Regression Models.

When the proposed model fails to exceed the statistical hypothesis tests that were explained previously, a transformation process on the independent variables is required.

Even though the condition of the normal distribution is satisfied—i.e., the residual is almost normally distributed—this transformation process is needed because the relationship between the dependent variable *GT* and some of the independent variables is nonlinear. Therefore, a nonlinear function is required to fit the collected data [127-132]. Many nonlinear functions can be used for this purpose. PRMs are widely used in situations when the relationships between the response and the independent variables are curve-linear. For example, the second-order polynomial model with two variables would be:

$$y = \beta_0 + \beta_1 \cdot X_1 + \beta_2 \cdot X_2 + \beta_3 \cdot X_1^2 + \beta_4 \cdot X_2^2 + \beta_5 \cdot X_1 X_2 \tag{7.26}$$

One of the most common transformation methods that works well with PRMs is the mean-centering technique. The methodology of this technique involves first calculating the mean of each independent variable. Then, by subtracting the old independent variable value at each observation from its mean, new data can be created for each variable as follows [127-133]:

$$X_{i_{NEW}} = X_{i_{old}} - \bar{X}_{i_{old}} \tag{7.27}$$

In addition to the applicability of this technique, the multicollinearity problem disappears because the mean-centering technique reduces the correlation between the independent variables and the variance for the least-squares estimators of the regression coefficients [26], [27-131]. Section 7.5 presents the mathematical analysis that is used to estimate the heat loss of a wind generator.

7.5. The Estimation of the Heat Loss of the Wind Generators.

A generator's heat losses, which directly increase a generator's temperature, can be estimated based on the air friction losses, generator bearing losses, iron losses, stator winding losses, and harmonic losses in the rotor of the generator [41-43], [99,]. However, a generator's heat losses can be evaluated from the thermal aspect because the heat losses are equal to the heat gains of the fluid that flows through the heat exchanger of the wind generator. As mentioned in Chapter 5, the heat gain of the cold fluid through the heat exchanger is supposedly equal to the generator's heat loss. Heat exchangers are used to transmit the heat from the hot fluid into cold fluid. The losses of the heat between the heat exchanger and surroundings could be neglected because such losses are very low compared to the heat exchange between the cold and hot fluids; therefore, heat exchangers are considered adiabatic devices—i.e., no heat is exchanged with the surrounding through the heat exchangers. Heat exchangers are classified according to their construction and the flow configuration. Many types of heat exchangers are used to provide a suitable cooling system in wind generators. Counterflow tube heat exchangers are the most widespread type that are used in wind generator cooling systems [100-102]. Based on Chapter 5, the estimation of the heat loss of the wind generator is possible by applying heat transfer analysis through the heat exchanger. By utilizing Eq. (5.4), the heat loss can be determined with the aid of Eq. (5.3). Heat loss, can be considered as significant independent variable that affects the generator temperature. Therefore, the first step of the proposed work is estimating the heat loss variable, and insert it to the regression model as one of the most

independent variables that influence the generator temperature. Figure 7.2 presents a flowchart that illustrates the methodology of the present work. The flowchart indicates that a transformation process might be required if the model is not linear. A case study is presented in the following section to confirm the validity of the proposed technique.

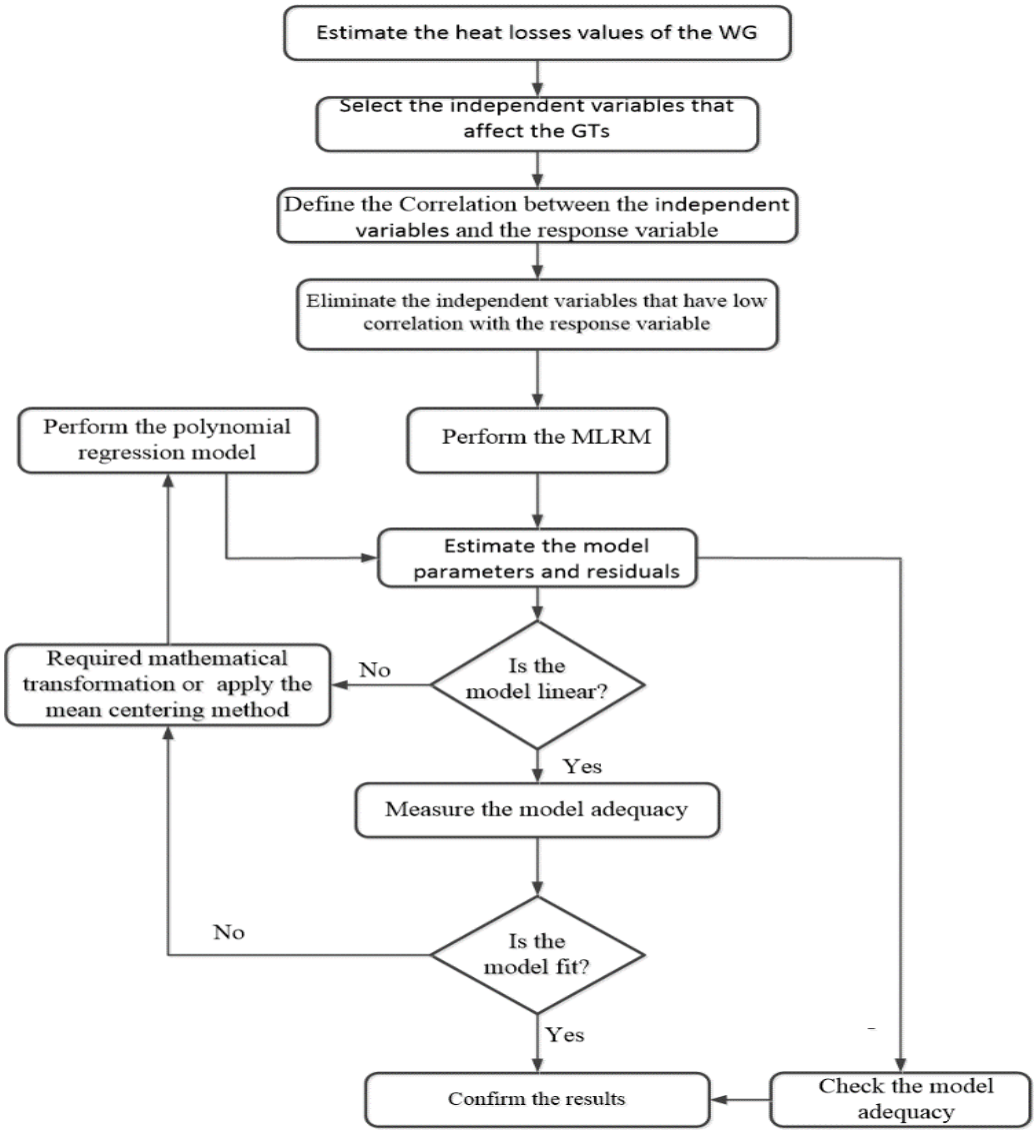

Fig. 7. 2 The methodology of the proposed regression model

7.6. Case Study.

This case study involves actual data collected from a variable-speed offshore wind turbine with rated power of 5 MW, 60 Hz, three blades, 126 m rotor diameter, and rated rotor speed of 12.1 rpm. The wind turbine has a synchronous permanent magnet generator with a rated speed of 1,500 rpm; generator efficiency is 94.4% [130]. The cooling system of the generator includes a water-air counterflow heat exchanger with six cold-fluid pipes. Several temperature sensors are installed within the generator to measure the stator winding temperatures, or stator-core temperatures. The manufacturer handbook emphasizes that the generator temperature should not exceed 110 C° to protect the electric generator, and the wind turbine will shut down when the generator temperature reaches 135 C°. More additional temperature- and pressure-measuring devices are available to gauge the water inlet and outlet temperatures and pressure drop through the heat exchanger [130]. These devices can be installed at the inlet and outlet slots of the heat exchanger.

The required SCADA system provides enough details about the collected variables that are needed to be inserted into the proposed model. Further, the temperature of the air that enters the rotor and stator winding region can be measured based on the outside temperature. There is a valve to control the inlet mass flow rate of water to the heat exchanger, which is roughly 2.6 kg/s according to the manufacturer handbook. In addition, the air mass flow rates into the rotor and stator end windings are designed to equal almost 4.7 kg/s [130]. This information is necessary to estimate the heat loss values. The recorded data employed to test the validity of the proposed model represents 740 working days and

the turbine's life during from 25,000 to 35,000 operating hours. The change in the data for each variable is very small every single day; therefore, the average of each day's collected data (gauged each second) is representative of the selected variables.

As mentioned previously, the variance of the predicted generator temperature increases as the number of independent variables increases. A variable selection process, therefore, is required to reduce and eliminate the variables that have the least correlation coefficient to the generator temperature. In addition, the significance of the regression coefficients for each independent variable in the model must be estimated to finally select the independent variables. By using Minitab or SPSS statistical software and inserting the related data into the model, the correlation coefficients and the degree of significance for each variable can be determined, as shown in Table 7.1.

Table 7. 1 The correlation coefficients and the degree of significance for the model's variables.

The Variables		T_G	CT	HL	OT	NT
CT	Corr. Coeff.	0.95				
	P-Value	0.00				
HL	Corr. Coeff.	0.93	0.87			
	P-Value	0.00	0.00			
OT	Corr. Coeff.	0.56	0.72	0.42		
	P-Value	0.14	0.06	0.14		
NT	Corr. Coeff.	0.51	0.45	0.47	0.88	
	P-Value	0.15	0.13	0.19	0.00	
GP	Corr. Coeff.	0.96	0.83	0.95	0.87	0.95
	P-Value	0.00	0.00	0.00	0.00	0.00

As shown, the outside temperature and nacelle temperature variables have the least correlation coefficients with respect to the generator temperature; moreover, they are not

highly significant because the *P*-value for both of them $> 0.05,$ where $\mathrm{P} = (1 - \gamma)$ is the degree of significance and $\gamma = 95\%$ according to the assumption of this present work. In this context, when the degree of significance for any independent variable is less than 5%, the contribution of that variable in the model is very strong [127-132].

The significance of the regression coefficient statistical values (t_0) for the independent variable (t_0) are also very helpful in determining the best independent variables for the proposed model in terms of the accuracy of the results. Table 7.2 clarifies low values of (t_0) for the outside temperature variable and the nacelle temperature variable. The (t_0) values for both variables are less than the standard t value (t_{TABLE}), which is equal to 1.960 [127-132]; therefore, the outside temperature and nacelle temperature variables must be eliminated and removed from the proposed model because they do not influence the response strongly.

The initial analysis of variance for this model is shown in Table 7.3. The coefficient of determination R^2 is high (92%), which indicates that adding a new term may make the regression model worse. This situation occurs when the mean squared error for the new model $MS_{Res_{New}}$(when adding new independent variables to the model) is larger than the mean squared error of the older model $MS_{Res_{old}}$ (without adding new independent variables to the model).

Table 7. 2 The significance of regression coefficients statistical values.

The Independent Variables	CT	HL	OT	NT	GP
Significance of the Regression Coefficients Statistical Value t_0	3.9	3.5	1.8	1.7	3.6

Table 7. 3 The initial analysis of variance of the proposed model.

Analysis of Variance					
Source	DF	SS	MS	F	P
Regression	3	16,866.24	5,622.1	3026	
Residual Error	736	1,367.53	1.858		
Lack of Fit	371	812.83	2.190	1.46	0.000
Pure Error	369	554.7	1.5		
Total	739	18,233.77			

PRESS = 1368.78 R-Sq. = 92.5%

To determine the model adequacy, the PRESS and the lack-of-fit statistic values are very useful. First, it must be determined that the PRESS statistic value is greater than the residual sum of square. Second, the significance of the regression statistical value $F_0 = 3026 \gg F_{1-\gamma,n,N-n-1} = 2.60$, which means that at least one of the independent variables is strongly related to the model. In addition, the lack-of-fit statistic value $F_{LOF} = 1.46 > F_{\gamma,df_{LOF},df_{PE}} = 1$. The initial regression equation is as follows:

$$\widehat{T_G} = 1.14733 + 0.438984\ CT + 0.0149205\ GP + 0.0345665\ HL$$

Figures 7.3 and 7.4 present the three-dimensional surface plots that correlate the nominated independent variables to the generator temperature. It seems that the relationships between the independent variables and the dependent variable are not linear, which means that the transformation process is required.

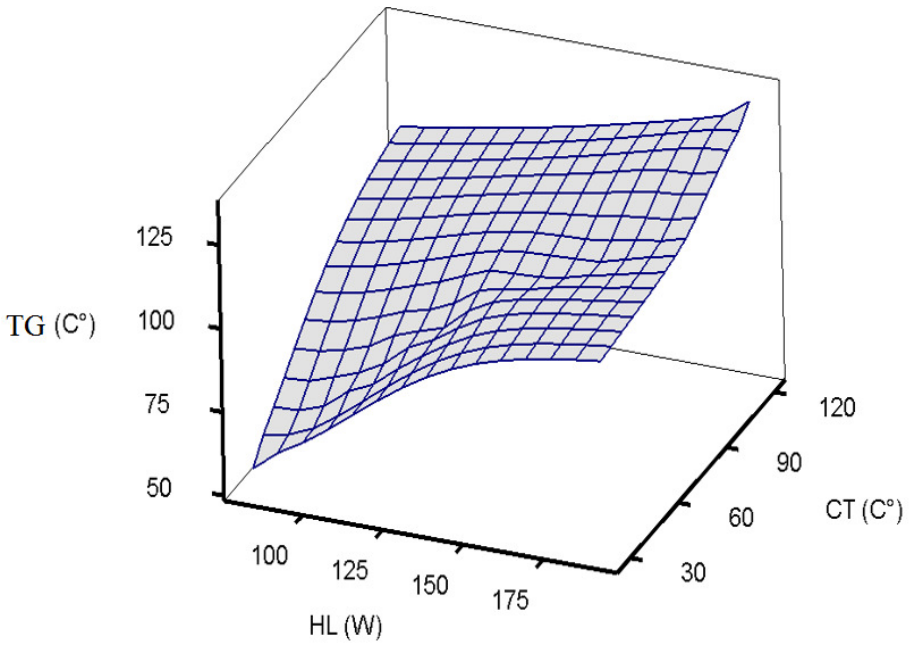

Fig. 7. 3 The surface plot of CT, HL with GT [130]

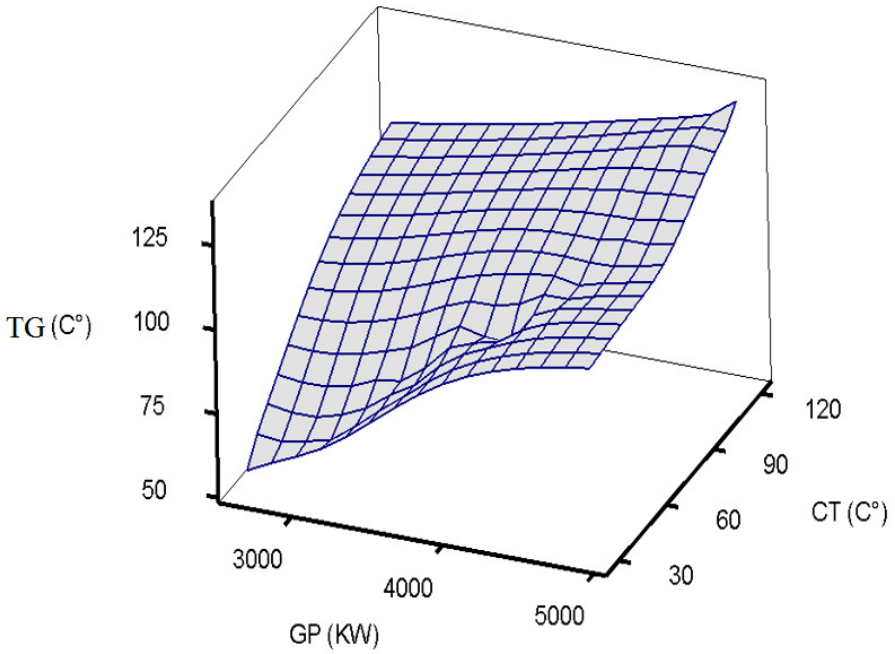

Fig. 7. 4 The surface plot of CT, GP with GT [130]

Further, the initial results indicated that the model does not fit the data, which means that the standard MLRM is not proper to the collected data because the relationship between the generator temperature and the nominated independent variables is not linear. The shape of the regression model can be clarified by defining the relationship between the generator temperature and each independent variable, as shown in as shown in Figs 7.5, and 7.6. The antecedent graphical relations confirm that there are curve-linear relationships between the independent variables and the response. Further, it appears that the third-degree order is the proper form for the proposed regression model that can be adopted to achieve logical results. Analysis of the residuals is an effective way to discover several types of model inadequacies.

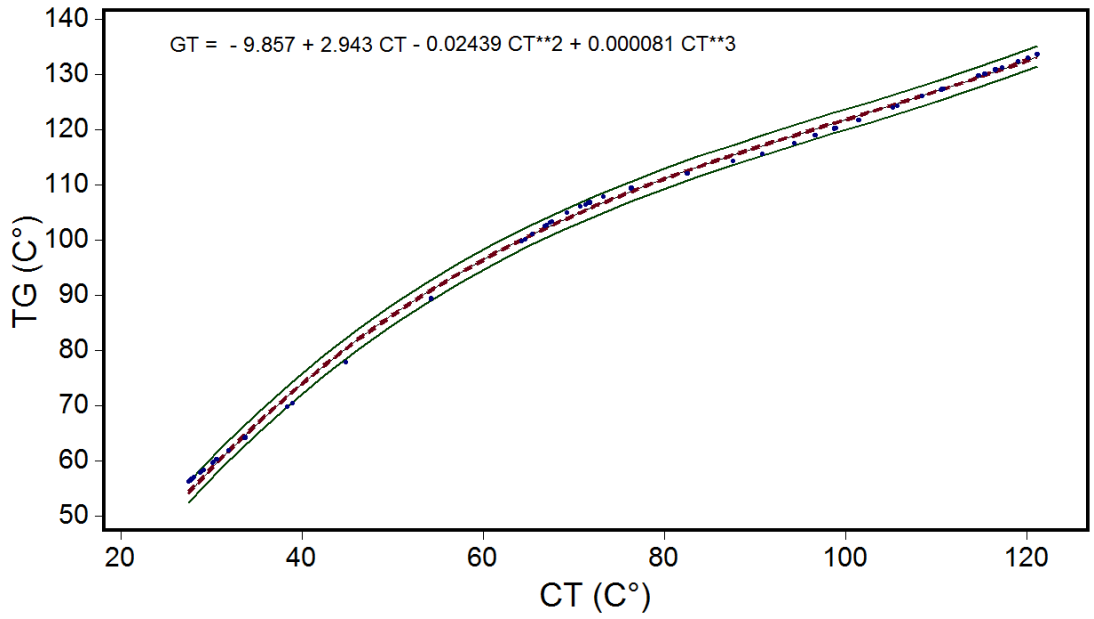

Fig. 7. 5 The fitted curve between CT, GT variables

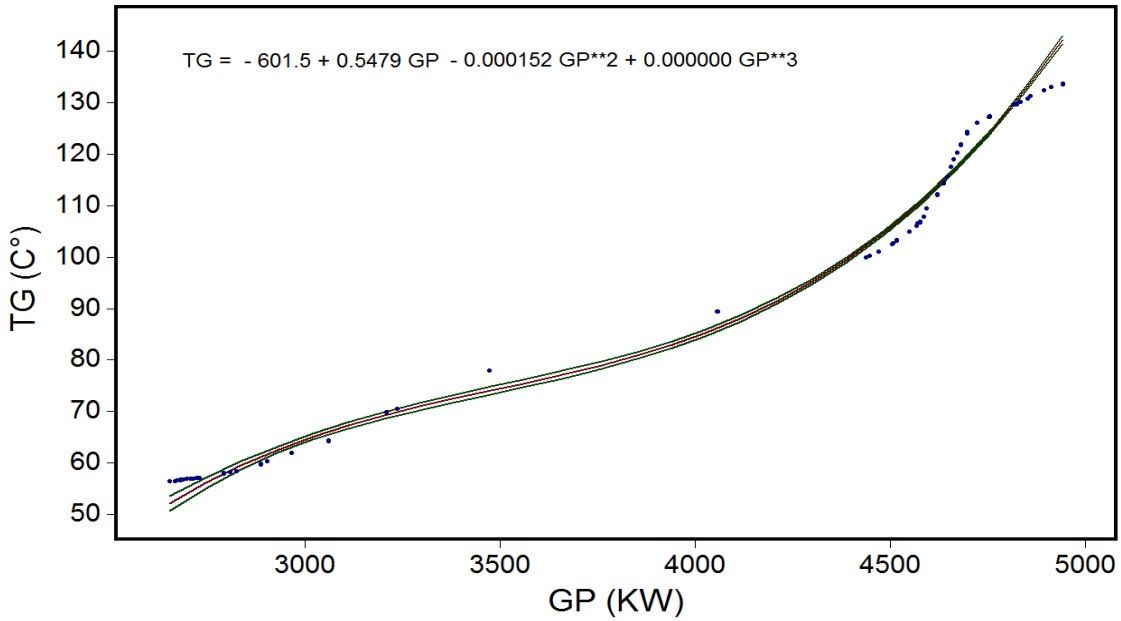

Fig. 7. 6 The fitted curve between GP, GT variables

Figure 7.7 confirms that the pattern of the residuals versus the fitted values of the generator temperature is not contained in a horizontal band, which confirms that there are obvious defects in the model and a cubic term needs to be added to the model [127-132]. Therefore, the appropriate transformation process is necessary to let the model exceed the proposed statistical tests. Polynomial models are very beneficial and widely used when the curve-linearity depicts the true response function. The fitting PRM of the third-order response surface in three independent variables is as follows:

$$\widehat{T_G} = \beta_0 + \beta_1(CT) + \beta_2(GP) + \beta_3(HL) + \beta_4(CT^2) + \beta_5(GP^2) + \beta_6(HL^2) + \beta_7(CT \cdot GP) + \beta_8(CT \cdot HL) + \beta_9(GP \cdot HL) + \beta_{10}(CT^3) + \beta_{11}(GP^3) + \beta_{12}(HL^3) + \beta_{13}(CT \cdot GP \cdot HL) \quad (7.28)$$

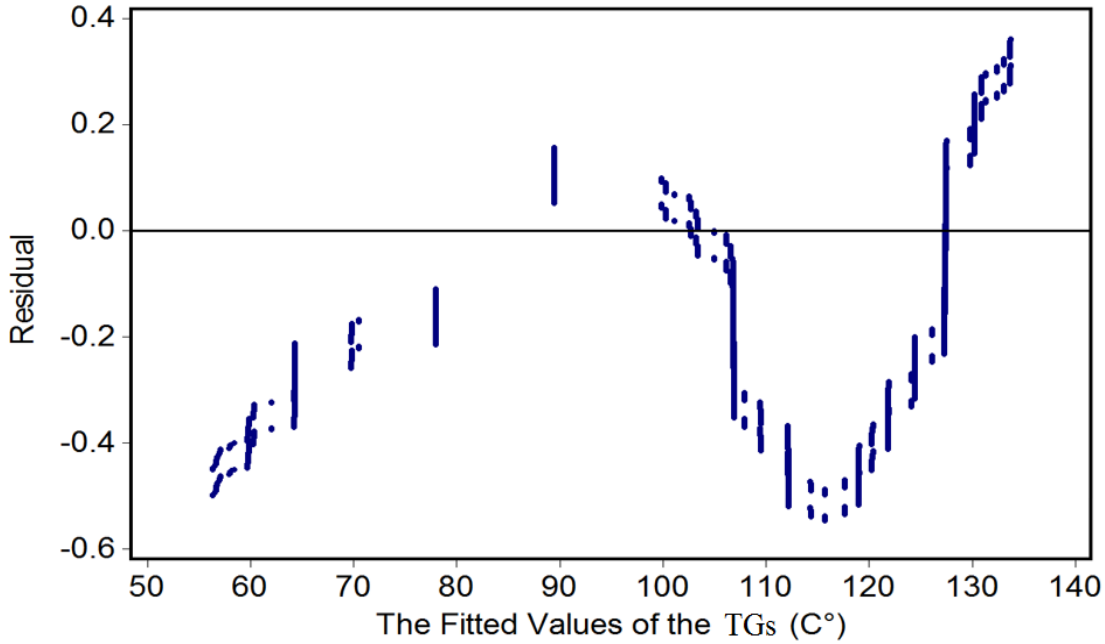

Fig. 7. 7 The scatterplot of the residual versus the fitted values of the GTs.

The mean-centering method works perfectly with PRMs, where each independent variable is subtracted from its mean, and the new values of each variable are inserted into the PRM [125-129]. The final obtained results are presented in the following section.

7.7. The Obtained Results of the Fourth Method.

To measure the adequacy and normality of the proposed PRM, the model's residual should be analyzed. Figure 7.8 shows that the error term ϵ is almost normally distributed, and it is very close to the ideal normal probability plot because the majority of the residual points are approximately distributed along a straight line. Few points fall outside the fitting line (regression line); these can be neglected because they do not affect the general trend of the model.

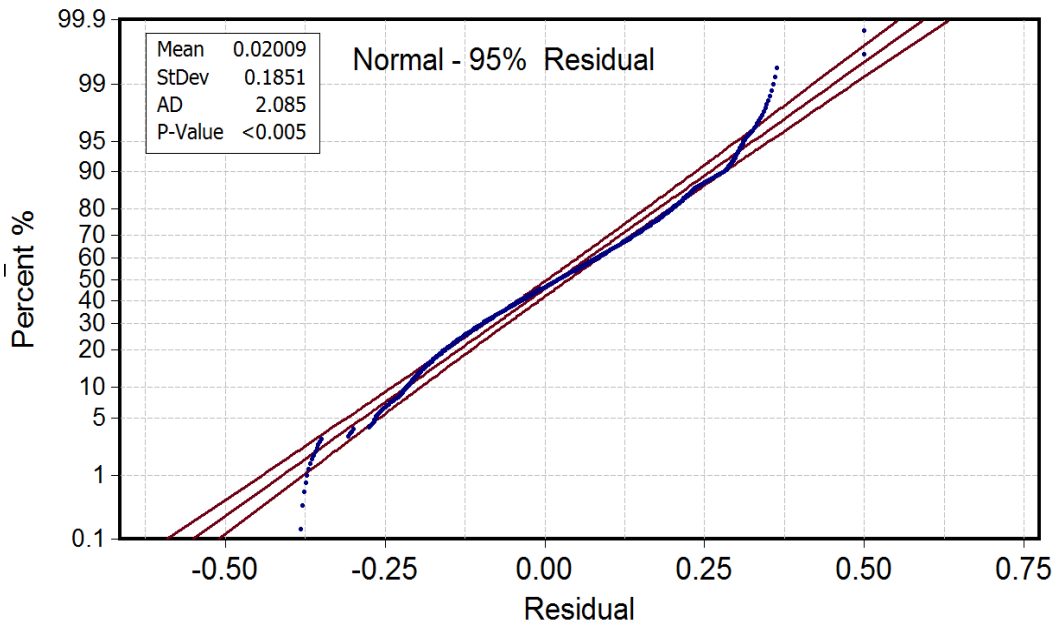

Fig.7. 8 The residual normal probability plot.

Figure 7.9 presents the residuals plot versus the predicted generator temperatures $\widehat{TG_i}$. The graph emphasizes that the residual distribution is perfectly normal because the majority of the points are contained in a horizontal band. Table 7.4 presents the final analysis of variance (ANOVA) for the proposed PRM. The PRM that can be used to predict the generator temperature is as follows:

$$\begin{aligned}\widehat{T_G} = {} & 108.57 + 0.78CT - 0.0024GP + 47.45HL + 0.012CT^2 \\ & +4.27X10^{-5}GP^2 + 5943.31HL^2 - 5.34X10^{-5}CT^3 \\ & -2.85X10^{-7}GP^3 - 149805HL^3 - 0.0014GP \cdot CT \\ & -0.16GP \cdot HL - 8.84CT \cdot HL + 0.0135GP \cdot CT \cdot HL\end{aligned}$$

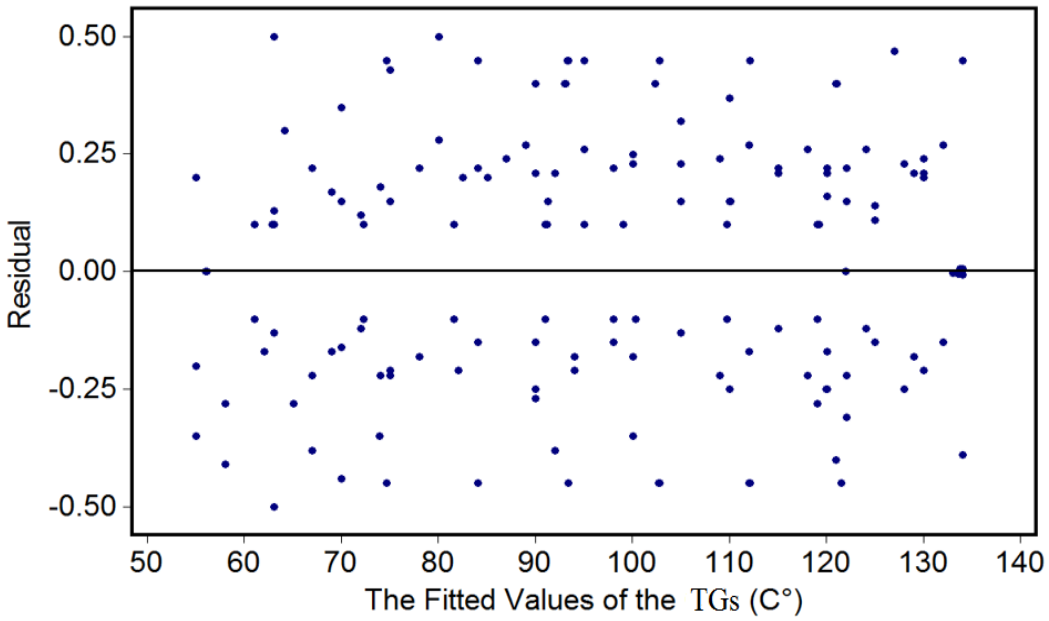

Fig. 7. 9 The fitting GTs. values versus the residual plot.

Table 7. 4 The final analysis of variance (ANOVA) of the proposed model.

ANOVA					
Source	DF	SS	MS	F	P
Regression	13	10,473.71	805.67	633.4	
Residual Error	726	923.5	1.272		
Lack of Fit	483	595.86	1.234	0.92	0.000
Pure Error	239	320.902	1.343		
Total	743	11,397.21			

PRESS = 914.87 R-Sq. = 94.86%

The ANOVA table indicates that the model does not suffer from lack of fit with the data. It can consider that the proposed PRM describes the data because the statistic value $F_{LOF} = 0.92 < F_{\gamma,df_{LOF},df_{PE}} = 1$, and the PRESS statistic value = 914.87 < SS_{Res} = 923.5. Further, there is an improvement in the coefficient of determination R^2 value, which indicates that the PRM is more proper than the standard multiple regression model. The high value of the coefficient of determination confirms that there is no need to add

independent variables to the mode and the selected variables are adequate. Finally, the results confirm that at least one of the independent variables relates strongly to the model because the significance of regression statistical value F_0 = 633.4 is still much larger than the $F_{1-\gamma,n,N-n-1} = 2.60$.

The length-scaling method is required to determine the most important independent variable that strongly affects the proposed model [127-132]. Table 7.5 presents the most significant terms of the proposed PRM because they have the highest standardized coefficients values. The main purpose of determining the standardized coefficients of the model is specifying the most important terms in the model that strongly influence the generator temperature. For instance, increasing the standardized value of the heat loss variable by one unit increases the standardized value of the generator temperature by 9.86 units (dimensionless regression coefficient). In addition, the standardized value of the generator temperature increases by 4844.3 units when increasing the standardized value of the third order of the heat loss variable by one unit. The high influence of the heat loss's third order term on the generator temperature can be seen. This indicates that the most significant variable that controls the generator temperature is the heat loss variable. The other independent variables differ in their impact on the model based on the weight of the standardized coefficient value of each term. Moreover, the table presents the coefficients' confidence intervals of the most significant terms in the model, which confirm that the coefficient of each term must be within the specified interval. The last issue that should be mentioned in the ANOVA table analysis is the multicollinearity problem. The obtained

results of the proposed model indicate that the model does not suffer from the multicollinearity problem because the variance inflation factors (VIFs) for the model's terms are very low (< 5), and the tolerance values are > 0.2. In addition, the degrees of significance for the model terms are less than 0.05, which confirms that all terms are significant and contribute strongly in the model [122-127]. Table 7.6 presents the VIFs for the most important terms in the proposed model. The obtained VIFs emphasize that the independent variables are not correlated to each other, which increases the model reliability.

Table 7. 5 The standardized coefficients of variance of the proposed model.

Coefficients			
Parameter	95% Confidence Interval		*Stand. Coeff.*
	Lower Value	Upper Value	
HL	28	67	9.86
HL^2	5522	6364	214.46
HL^3	-159315	-140294	4844.3
CT	0.565	0.924	6.87
CT^2	0.009	0.024	2.25
GP	-0.0035	-0.00124	1.45
CT.HL	-10.00	-8.00	0.43
GP.HL	-0.180	-0.142	0.03
GPCTHL	0.0098	0.0162	0.0001

Table 7. 6 VIF, tolerance, and the significant values for the most important terms in the model.

Parameter	Tolerance	VIF	P
HL	0.645	1.550	0.0014
HL^2	0.540	1.85	0.0012
HL^3	0.427	2.342	0.0018
CT	0.805	1.242	0.00185
CT^2	0.873	1.145	0.0019
GP	0.922	1.085	0.00194
CT.HL	0.404	2.476	0.00196
GP.HL	0.443	2.256	0.00198
GPCTHL	0.459	2.178	0.00199

Contour plots are very beneficial and can be utilized to study the effect of the heat loss variable on the predicted generator temperatures. Figures 7.10, 7.11, and 7.12 display graphic representations of the relationships among three numeric variables. These figures present the influence of the heat loss on the predicted generator temperature with respect to the generator power variable. The predicted generator temperature is for contour levels, which are plotted as curves. As shown, the effect of the heat loss with respect on the generator power is approximately regular in the first, second, and third order of the polynomial model.

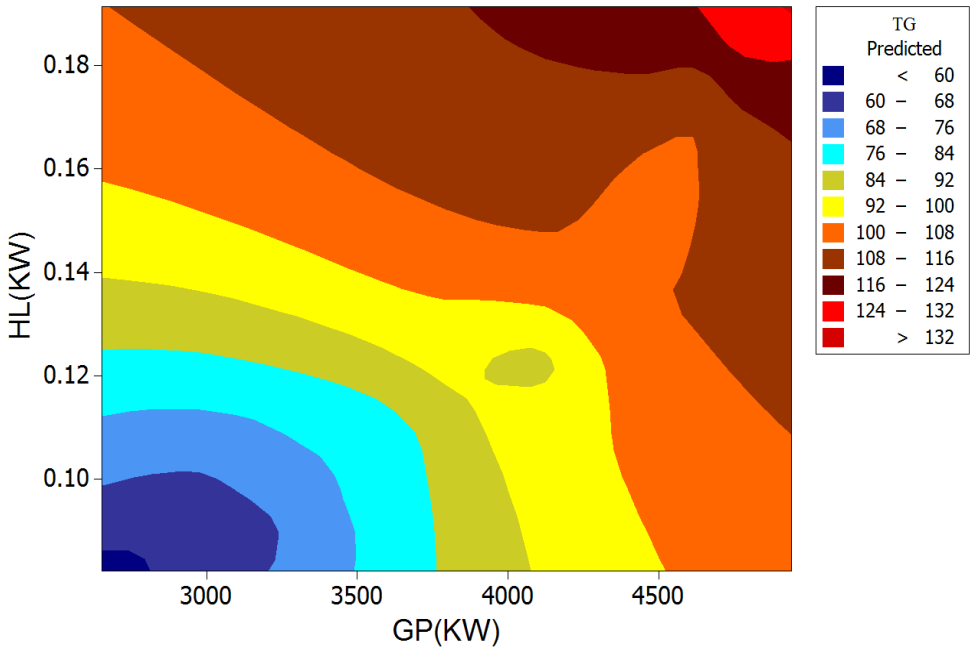

Fig. 7.10. The contour plot of the $\widehat{T_G}$ based on the first order of the hat loss in the PRM with respect to the GP.

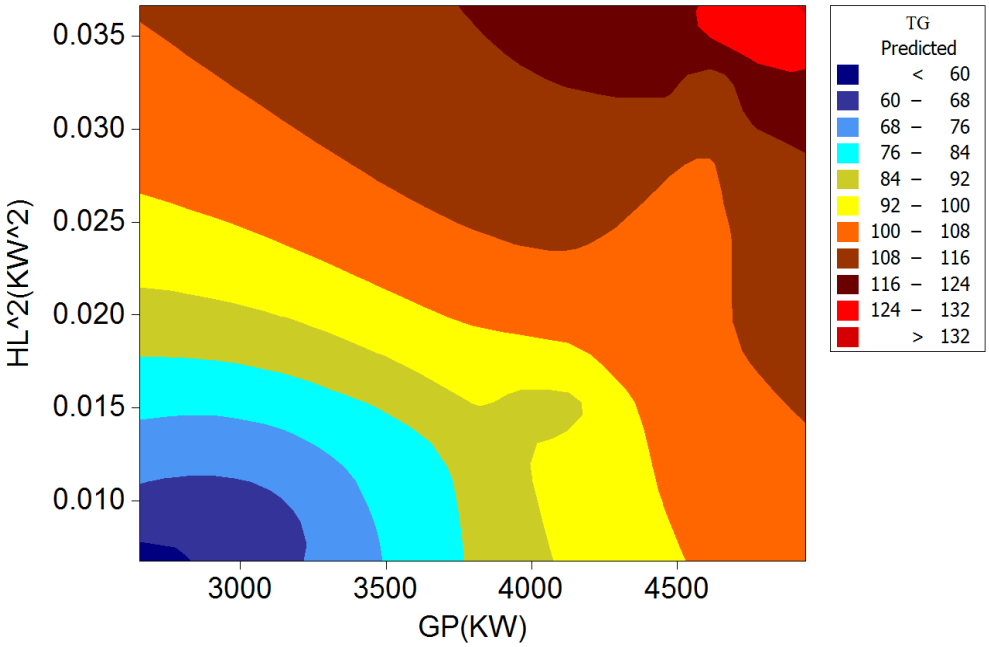

Fig. 7.11. The contour plot of the $\widehat{T_G}$ based on the second Order of the heat loss in the PRM with respect to the GP.

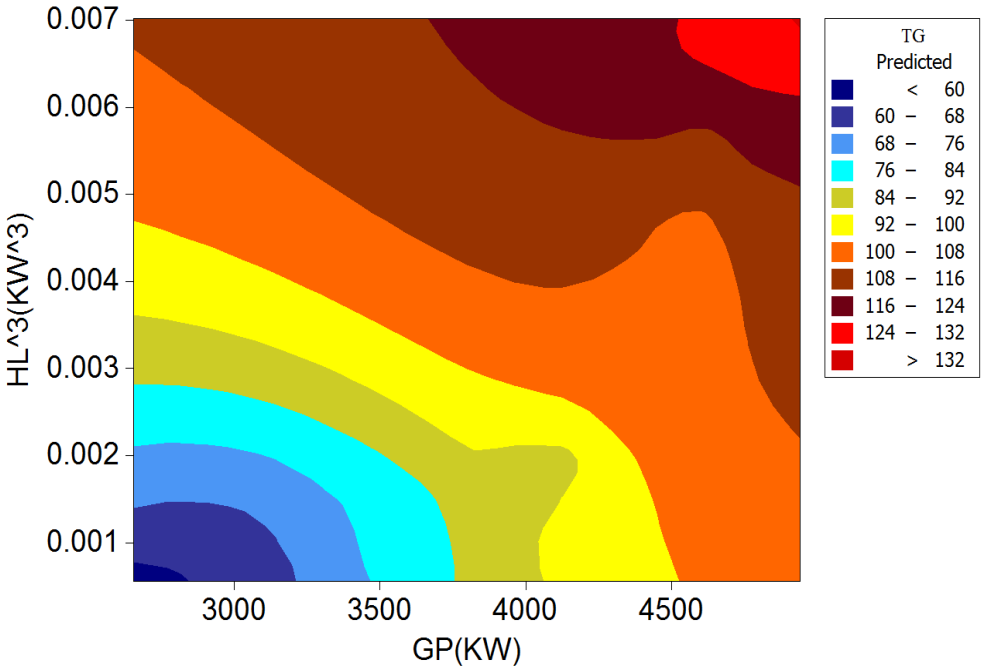

Fig. 7.12. The contour plot of the $\widehat{T_G}$ based on the third order of the heat loss in the PRM with respect to the GP.

On the other hand, there is a very obvious increase in the zones of the predicted generator temperature when it exceeds 124 C° as result of the influence of the heat loss with respect to the cooling temperature as shown in Figs 7.13, 7.14, and 7.15. The effect of the heat loss with respect to the cooling temperature is visible through the zones that present the high predicted generator temperature, compared to the effect of the heat loss with respect to the generator power on the predicted generator temperature. It is very obvious that each term in the proposed PRM controls the predicted generator temperature based on the weight of its coefficient. The statistical results confirm that the influence of the heat loss variable on the predicted generator temperature is higher than the influence of the cooling temperature variable according to the standardized coefficients of both variables. Therefore, the increase in the predicted generator temperature due to the influence of the heat loss variable is more than the influence of the cooling temperature variable. Further, the obtained results indicate that the heat loss term in the third order is the most significant term, which influences the predicted generator temperature strongly since the standardized coefficient of this term is very high and approximately equal to 4844.3 unit. Figure 7.16 present a surface contour plot in 3-dimensional, which how does the predicted generator temperature changes as a function of the heat loss term in the third order and cooling temperature term in the first order.

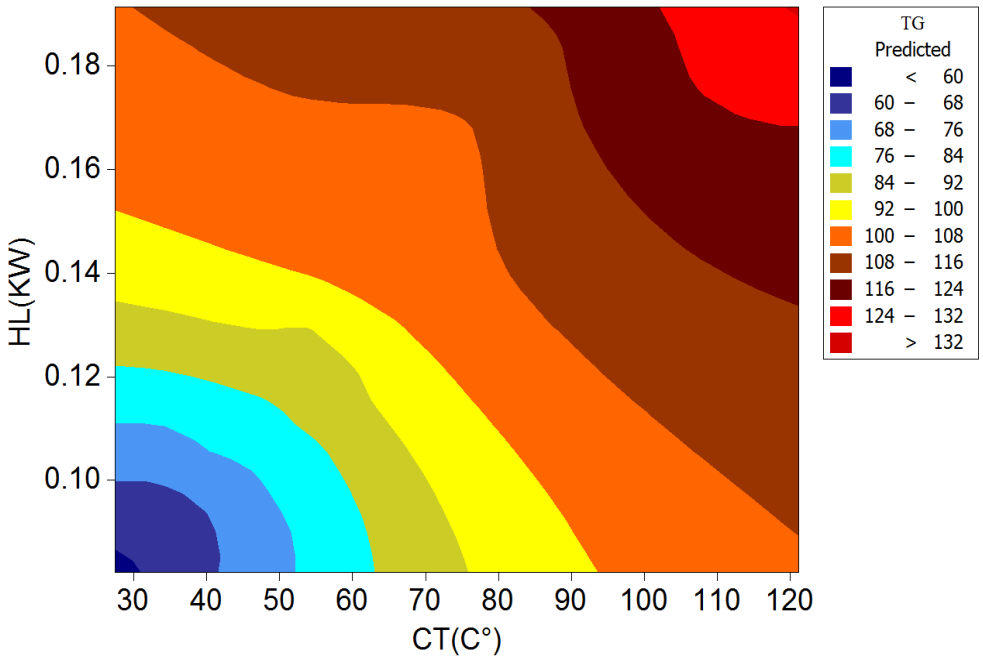

Fig. 7.13. The contour plot of the $\widehat{T_G}$ based on the first order of the heat loss in the PRM with respect to the CT.

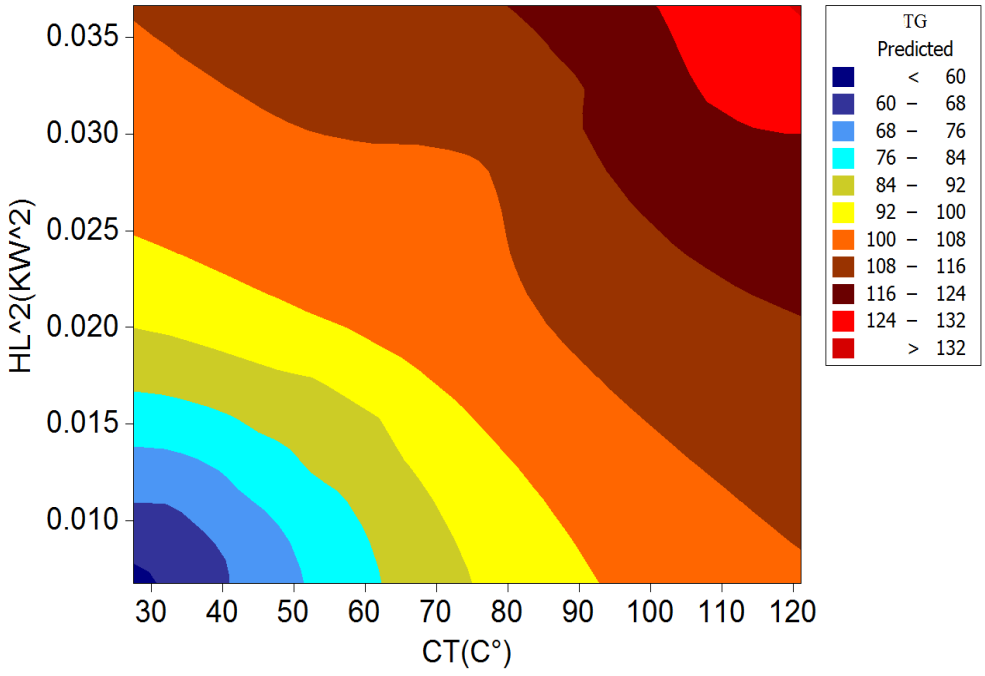

Fig. 7.14. The contour plot of the $\widehat{T_G}$ based on the second order of the heat loss in the PRM with respect to the CT.

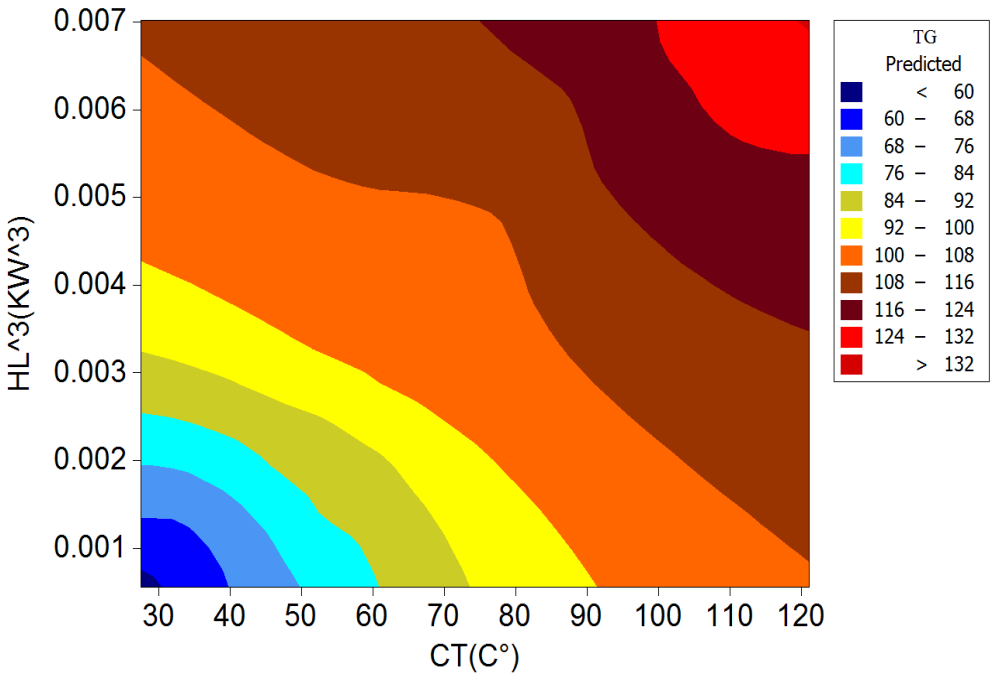

Fig. 7.15. The contour plot of the $\widehat{T_G}$ based on the third order of the heat loss in the PRM with respect to the CT.

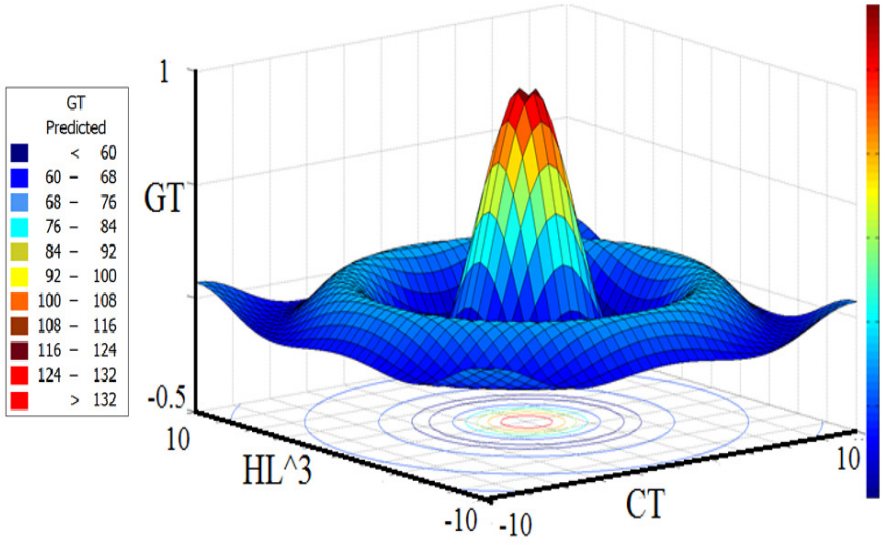

Fig. 7.16. A surface contour plot in 3-dimensional represents the change in $\widehat{T_G}$ due to the effect of HL^3 and CT.

7.8. The Conclusion of the Fourth Method.

To perform an effective CMS on the wind generators, this paper presents an application of the regression models based on the study of the heat loss's influence on a wind generator's temperatures. The proposed method can be utilized to address the technical problems resulting from high temperatures on wind generators. This leads to reduced maintenance and operation costs and increased wind generators' reliability. The knowledge of CMS can be employed with the aid of regression techniques to create a prediction model for generator temperatures. The heat loss, cooling temperature, and generator power variables are the most significant variables that strongly affect generator temperature, according to the correlation coefficients and the degree of significance for each variable with the response. The transformation process to the PRM was required because the relationships between the response and the independent variables were curve-linear. The data behavior controls the regression model type and the need for the transformation process. The main concept of the proposed technique is measuring the correlation between the observed values and the predicted values of the criterion variables based on historical data. The obtained results confirm that the heat loss variable is the most influential variable on generator temperatures based on the standardized coefficients of the model. However, the other nominated independent variables obviously affect generator temperatures based on the weight of their coefficients. Future work is required to apply this method to different data with other operational wind turbines to detect faulty conditions and advance the prediction of potential failures.

Chapter 8. Summary and Future Research

8.1. Summary

The practicalities and challenges of the CMS on the wind generators have been presented in this thesis. Due to the remarkable increase in the failures of the wind generators this literature is concentrated on the implementation of the CMS on the wind turbine generators. Synchronous and induction generators are the most common generators that are used in the wind energy industry, and their electrical and mechanical faults frequently occur. The most general faults, which are related to the induction generators are the stator winding faults, inner and outer raceway faults in the bearing, ball defect in the bearing, and broken rotor bar or cracked faults in the rotator. While, the stator inter-turn fault and the rotor inter-turn fault are the most common faults, which are related to the synchronous machine. Further, the bearing, damper winding, and demagnetization faults occur as well in the synchronous generators.

The knowledge of the faults that are related to the wind generators is indispensable to apply the CMS on the generator parts accurately. There are many methods can be utilized to identify the faults, such as the observer-based approach, signal analysis approach, artificial intelligent and expert systems approach, and system identification approach. In

this proposed work, the analysis approach monitoring technique is adopted to identify the faults that occur in the wind generators. The faults of the wind generators are related to different causes, such as unbalanced line currents and air-gap voltages, high torque pulsations, undesirable noise, and motor mechanical vibration. However, the increase in the generator temperature during operation is one of the most significant reason that makes deep technical problems in the wind generators. Therefore, this present work is focused on the problem of the elevated generator temperature and its negative effects on the wind generator systems.

Many techniques are employed to avoid the failures of wind generators. The majority of the previous techniques that are applied to monitor the wind generator conditions are based on the electrical and mechanical concepts and theories. This thesis presents an advanced CMS of the wind generators based on statistical, thermal, reliability analysis, electrical and mechanical analyses. Four modern methods are presented in this research based on different data to implement CMS on wind generators. The first method introduces three different algorithms link the mathematical, thermal, and mechanical analyses with the electrical methodology to apply CMS on the wind generators. The first algorithm is based on studying the effect of the electrical torque pulsations and the high generator temperature on the wind turbine generators under different conditions to apply proper condition monitoring. According to the first algorithm, a different methodology has been adopted to develop a proper CMS on the wind generators by evaluating the generator electrical torque based on the mechanical torque and the acceleration torque. The proposed

technique indicates the generator health based on the use of the electric torque with respect to the rotor angular speed of the generator as indicator to apply CMS on the wind generators when they operate under different operation conditions. When the generator suffers from electric faults, such as stator inter-turn fault or rotor inter-turn fault, the generator reactance decrease automatically and the use of the proposed technique is very powerful to identify the fault. Further, the rate of change in the generator temperature with respect to the induced electrical torque is utilized to determine the faults of the wind generators based on the use of the second algorithm. The obtained results indicate that the trend of the rate of the change in the generator temperature with respect to the induced electrical torque is an indicator to define the generator health because of the negative effect of the elevated generator temperature on the induced electrical torque. The last proposed algorithm of the first method derives the driving torque of the rotating permanent magnet with respect to the permanent magnet temperature to implement a proper CMS on the wind generators. Due to the increase in the permanent magnet temperature, the driving torque of the rotating permanent magnet oscillates with increasing the amplitude based on the change in the magnetization angle of the permanent magnet. The obtained results confirm that the permanent magnet torque decreases dramatically based on the magnetization angle of the permanent magnet when the permanent magnet temperature during operation is higher than the design permanent magnet temperature (abnormal condition).

The second method presents a new approach to apply CMS on the wind generators based on the heat transfer and fluid mechanics analysis through the heat exchangers of the

wind generators, which uses water to air cooling system. The proposed technique can indicate the operation condition of the wind generators while running to avoid the potential faults that occur due to the increasing in the generator temperature. The obtained results of the proposed model show that high value of the loss in the heat of the wind generator with respect to the LMTD of the generator's heat exchanger leads to increasing the generator temperature. Reynolds number of the coolant fluid is a good indicator as well to detect the system operation condition since it depends on the coolant fluid viscosity, which decreases dramatically with the increase in the generator temperatures. Furthermore, the results of the proposed method emphasize that the pressure drop through the generator heat exchanger is a significant indicator to identify generator health with respect to the LMTD. The high value of the pressure drop with respect to the LMTD indicates that the generator temperature is suitable. The cool fluid pressure drop is based on the cold fluid density, which increases with the high generator temperature.

The third method proposes an application of hazard model reliability analysis based on the CMS of the wind generators. The proposed model can be utilized to perform appropriate maintenance decision-making based on the evaluation of the mean time to failures that occur on the wind generators due to high temperatures. The knowledge of the CMS is used to estimate the hazard failure and survival rates to perform the preventive maintenance approach accurately. The main goal of this method is to investigate the influence of the high generator temperatures on the estimated generators age to improve the system reliability by adopting a suitable maintenance program. The obtained results of

the proposed method confirm that the survival rate of the wind turbines decreases with the increase of the number of faults (the number of times that the generator temperature exceeds 100C^{o}). The hazard lifetime is estimated based on the Weibull distribution with respect to the generator temperature and the expended working hours of the wind turbines. Estimating the MTTF parameter of the wind generators helps to determine the maintenance approach that should be taken.

Finally, the fourth method proposes an application of the regression models based on the study the influence of the loss in the heat on the wind generator temperature. The proposed method shows two types of regression models that can be employed to apply CMS on the wind generators due to the high temperature. The first type is the standard multiple linear regression model, which can be used in the linear pattern between the response and the independent variables of the model. The second type is the polynomial regression model, which can be applied when a curvilinear relationship is existent between the response and the model's independent variables. The proposed technique can be utilized to address the technical problems resulting from high temperatures on the wind generators. The knowledge of the CMS can be employed with the aid of the regression techniques to create a prediction model for the generator temperatures. The heat loss, cooling temperature, and generator power variables are the most significant variables that strongly affect the generator temperature according to the correlation coefficients and the degree of significance for each variable with the response. The transformation process to the PRM was required because the relationships between the response and the independent

variables were curve-linear. The data behavior controls the regression model type and the need for the transformation process. The obtained results confirm that the heat loss variable is the most influential variable on the generator temperature based on the standardized coefficients of the model. However, the other nominated independent variables obviously affect generator temperatures based on the weight of their coefficients.

8.2. Future Areas for Investigation and Development

There are many different topics that can be utilized and contributed to developing the implementation of the CMS on the wind generators. For instance, the cost analysis of the hazard reliability approach can be taken into account to determine the minimal maintenance cost. The analysis cost can be performed by evaluating the life cycle cost with strategies where CMS improved the maintenance planning for the wind turbines. Further, the age of the wind generators and the MTTF can be estimated by inserting additional covariates to the model, such as the generator voltage or frequency to indicate their effects.

Second, condition based maintenance optimization for the faulty wind generator under continuous monitoring is an extensive topic that can be applied. An optimization technique can be used to solve the preventive maintenance problem for the wind generator system. The proposed technique must be utilized to build an optimal maintenance action providing system working with the required level of the availability or reliability during the system lifetime with minimal maintenance cost rate.

Third, the normal behavior models can be integrated for condition assessment of wind turbine generator systems. The monitoring parameters, which are selected by SCADA of wind farms can be used to establish an assessment index system. In this context, the neural network can be used to establish the normal behavior models for the parameters closely related to the natural environment. Then the probability density function of the normal distribution must be computed to determine the health degrees of the wind generator components. For the other monitoring parameters, normal behavior models can be developed based on the Parzen estimation, a common non-parametric estimation method.

Finally, cost-sensitivity analysis of the CMS for the wind generators is another proposed work to decrease the operation and maintenance costs of the wind turbines. A cost-benefit study must be applied to determine what the required performance of the CMS should be considered in order to implement it on the wind generators beneficially. Based on Monte Carlo and the cox proportional-hazards regression simulations, the generator maintenance cost and the cost-sensitivity analysis can be determined.

References

[1] Olimpo Anaya-Lara, Nick Jenkins, Janaka Ekanayake, Phill Cartwright, and Mika Hughes, "Wind Energy Generation Modeling and Control," Library of Congress Cataloguing-in-Publication Data, 1st Edition. United Kingdom, Wiley, 2009.

[2] Bredan Fox, Damian Flynnm Leslie Bryans, Nick Jenkins, David Milborrowm, Mark O'Malley, Richard Watsn, and Olimp Anaya-Lara, "Wind Power Integration," IET Power and Energy Series 50, The Institution of Engineering and Technology, 1st Edition, London, United Kingdom 2007.

[3] Pramod Jain, "Wind Energy Engineering," McGraw-Hill, 2011.

[4] Hamed Babazadeh, Wenzhong Gao, and Kurtis Duncan, "A New Control Scheme in a Battery Energy Storage System for Wind Turbine Generators," Power and Energy Society General Meeting, 2012 IEEE. Date: 22-26 July 2012.

[5] Milovanþeviü, Miloš, and Boban Anÿelkoviü. "Modern Techniques of Wind Turbine Condition Monitoring," iipp 2010.

[6] Sheng, S., H. Link, W. LaCava, J. van Dam, B. McNiff, P. Veers, J. Keller, S. Butterfield, and F. Oyague, "Wind Turbine Drivetrain Condition Monitoring During GRC Phase 1 and Phase 2 testing," Technical Report, NERL, October, 2011.

[7] Li Yanyong, "Discussion on the Principles of Wind Turbine Condition Monitoring System," In Materials for Renewable Energy & Environment (ICMREE), 2011 International Conference on, vol. 1, pp. 621-624. IEEE, 2011.

[8] Khaled B. Abdusamad, Wenzhong David Gao, Xiaodong Liang, and Jun Zhang, "Hazard Model Reliability Analysis Based on a Wind Generator Condition Monitoring

System," Journal of Energy and Power Engineering ISSN 1934-8975, USA, vol. 8 no. 7, pp. 1309-1322. July 2014, David Publishing Company, USA

[9] García Márquez, Fausto Pedro, Andrew Mark Tobias, Jesús María Pinar Pérez, and Mayorkinos Papaelias, "Condition Monitoring of Wind Turbines: Techniques and Methods," Renewable Energy 46 (2012): 169-178.

[10] Hyers, R. W., J. G. McGowan, K. L. Sullivan, J. F. Manwell, and B. C. Syrett, "Condition Monitoring and Prognosis of Utility Scale Wind Turbines," Energy Materials: Materials Science and Engineering for Energy Systems 1, no. 3 (2006): 187-203.

[11] Ackermann Thomas, "Wind Power in Power Systems," Vol. 140. Chichester, UK: John Wiley, 2005.

[12] Entezami, Mani, Stuart Hillmansen, and Clive Roberts, "Wind Turbine Condition Monitoring System," PhD Progress Report, University of Birmingham (2010).

[13] T. W. Verbruggen, "Wind Turbine Operation & Maintenance based on Condition Monitoring WT-Ω," Final Report, April, 2003.

[14] Laakso, Kari, Tony Rosqvist, and Jette L. Paulsen, "The Use of Condition Monitoring Information for Maintenance Planning and Decision-Making," Technical Report, NKS-80, 2002.

[15] Guo, Peng, David Infield, and Xiyun Yang, "Wind Turbine Generator Condition-Monitoring Using Temperature Trend Analysis," Sustainable Energy, IEEE Transactions on 3, no. 1 (2012): 124-133.

[16] Yang, Wenxian, P. J. Tavner, and Michael Wilkinson, "Condition Monitoring and Fault Diagnosis of a Wind Turbine with a Synchronous Generator Using Wavelet Transforms," In Power Electronics, Machines and Drives, 2008. PEMD 2008. 4th IET Conference on, pp. 6-10. IET, 2008.

[17] Watson, Simon Jonathan, Beth J. Xiang, Wenxian Yang, Peter J. Tavner, and Christopher J. Crabtree, "Condition Monitoring of the Power Output of Wind Turbine Generators Using Wavelets," Energy Conversion, IEEE Transactions on 25, no. 3 (2010): 715-721.

[18] Amirat, Yassine, Vincent Choqueuse, and Mohamed Benbouzid, "Wind Turbine Bearing Failure Detection Using Generator Stator Current Homopolar Component Ensemble Empirical Mode Decomposition," In IECON 2012-38th Annual Conference on IEEE Industrial Electronics Society, pp. 3937-3942. IEEE, 2012.

[19] Lu, Dingguo, Wei Qiao, Xiang Gong, and Liyan Qu, "Current-Based Fault Detection for Wind Turbine Systems via Hilbert-Huang Transform," In Power and Energy Society General Meeting (PES), 2013 IEEE, pp. 1-5. IEEE, 2013.

[20] Lu, Bin, Yaoyu Li, Xin Wu, and Zhongzhou Yang, "A Review of Recent Advances in Wind Turbine Condition Monitoring and Fault Diagnosis," In Power Electronics and Machines in Wind Applications, 2009. PEMWA 2009. IEEE, pp. 1-7. IEEE, 2009.

[21] Lu, Wenxiu, and Fulei Chu, "Condition Monitoring and Fault Diagnostics of Wind Turbines," In Prognostics and Health Management Conference, 2010. PHM'10. pp. 1-11. IEEE, 2010.

[22] Qiao, Wei, Ganesh K. Venayagamoorthy, and Ronald G. Harley, "Optimal Wide-Area Monitoring and Nonlinear Adaptive Coordinating Neurocontrol of a Power System with Wind Power Integration and Multiple FACTS Devices," Neural Networks 21, no. 2 (2008): 466-475.

[23] Kusiak, Andrew, Haiyang Zheng, and Zhe Song, "Models for Monitoring Wind Farm Power," Renewable Energy 34, no. 3 (2009): 583-590.

[24] Giebel, Gregor, Oliver Gehrke, Malcolm McGugan, and Kaj Borum, "Common access to wind turbine data for Condition Monitoring the IEC 61400-25 Family of Standards," In Proceedings of the 27th Risø International Symposium on Materials Science, Risø National Laboratory, Denmark, 2006.

[25] Han, Y., and Y. H. Song, "Condition Monitoring Techniques for Electrical Equipment-a Literature Survey," Power Delivery, IEEE Transactions on 18, no. 1 (2003): 4-13.

[26] Toliyat, Hamid A., Subhasis Nandi, Seungdeog Choi, and Homayoun Meshgin-Kelk, "Electric Machines: Modeling, Condition Monitoring, and Fault Diagnosis," CRC Press, 2012.

[27] Yang, Wenxian, P. J. Tavner, and M. R. Wilkinson, "Condition Monitoring and Fault Diagnosis of a Wind Turbine Synchronous Generator Drive Train," Renewable Power Generation, IET 3, no. 1 (2009): 1-11.

[28] Bang, D., H. Polinder, G. Shrestha, and J. A. Ferreira, "Review of Generator Systems for Direct-Drive Wind Turbines," In European Wind Energy Conference & Exhibition, Belgium, pp. 1-11. 2008.

[29] Peter Tavner, Li Ran, Jim Penman, and Howard Sedding, "Condition Monitoring of Rotating Electrical Machines," IET Power and Energy Series 56, Published by The Institution of Engineering and Technology, London, United Kingdom 2008.

[30] Simoes, M. Godoy, and Felix A. Farret, "Renewable Energy Systems: Design and Analysis with Induction Generators," CRC press, 2004.

[31] Avelino J. Gonzalez, M. Stanley, Balowin, J. Stein, and N. E. Nilsson, "Monitoring and Diagnosis of Turbine-Driven Generator," Electric Power Research Institute, Prentice Hall, Englewood Cliffs, New Jersey 07632, 1995.

[32] Gong, Xiang, and Wei Qiao, "Bearing Fault Detection for Direct-Drive Wind Turbines via Stator Current Spectrum Analysis," In Energy Conversion Congress and Exposition (ECCE), 2011 IEEE, pp. 313-318. IEEE, 2011.

[33] Damian S. Vilchis-Rodriguez, Sinisa Djurovic, Alexander C. Smith, "Wind Turbine Induction Generator Bearing Fault Detection Using Stator Current Analysis," IET Renewable Power Generation, Vol. 7, Iss. 4, pp. 330–340, 2013.

[34] Wu, Bairong, Zhigang Tian, and Mingyuan Chen, "Condition-Based Maintenance Optimization Using Neural Network-based Health Condition Prediction," Quality and Reliability Engineering International 29, no. 8 (2013): 1151-1163.

[35] Yang, Wenxian, Peter J. Tavner, Christopher J. Crabtree, and Michael Wilkinson, "Cost-Effective Condition Monitoring for Wind Turbines," Industrial Electronics, IEEE Transactions on 57, no. 1 (2010): 263-271.

[36] Popa, Lucian Mihet, Birgitte-Bak Jensen, Ewen Ritchie, and Ion Boldea, "Condition Monitoring of Wind Generators," In Industry Applications Conference,

2003. 38th IAS Annual Meeting. Conference Record of the, vol. 3, pp. 1839-1846. IEEE, 2003.

[37] Yazidi, A., H. Henao, G. A. Capolino, D. Casadei, F. Filippetti, and C. Rossi, "Simulation of a Doubly-Fed Induction Machine for Wind Turbine Generator Fault Analysis," In Diagnostics for Electric Machines, Power Electronics and Drives, 2005. SDEMPED 2005. 5th IEEE International Symposium on, pp. 1-6. IEEE, 2005.

[38] Alewine, Kevin, and William Chen, "A Review of Electrical Winding Failures in Wind Turbine Generators," In Electrical Insulation Conference (EIC), 2011, pp. 392-397. IEEE, 2011.

[39] Yang, Wenxian, Jiesheng Jiang, P. J. Tavner, and C. J. Crabtree, "Monitoring Wind Turbine Condition by the Approach of Empirical Mode Decomposition," In Electrical Machines and Systems, 2008. ICEMS 2008. International Conference on, pp. 736-740. IEEE, 2008.

[40] Khaled B. Abdusamad, Wenzhong David Gao, and Yan Li, "Condition Monitoring System of Wind Generators based on Effects of Electrical Torque Pulsations of Wind Turbine Generators, " IEEE Power & Energy Society General Meeting, July 27-31, 2014, Washington, DC.

[41] Khaled B. Abdusamad, Wenzhong David Gao, Linlin Wu, and Hui Liu, "Condition Monitoring System of Wind Generators based on the Effect of Electrical Torque Pulsations and Generator Temperature," IEEE Symposium on Power Electronics & Machines for Wind and Water Applications (PEMWA 2014), July 24-26, 2014, Milwaukee, WI, USA.

[42] Khaled B. Abdusamad, and Wenzhong David Gao, “The Application of Heat Transfer Analysis in Condition Monitoring System of Wind Generator,” IEEE PES Asia-Pacific Power and Energy Engineering Conference (APPEEC2013).

[43] Khaled B. Abdusamad, Wenzhong David Gao, and Eduard Muljadi, “The Influence of Heat Loss on Wind Generators to Implement Condition-Monitoring System Based on the Application of the Polynomial Regression Model,” International Journal of Renewable Energy Research, vol. 4, no. 2, pp. 401-412. June 2014.

[44] Khaled B. Abdusamad, Wenzhong David Gao, and Eduard Muljadi, “A Condition Monitoring System for Wind Turbine Generator Temperature by Applying Multiple Linear Regression Model, ” The 45th North American Power Symposium (NAPS 2013), IEEE September 2013.

[45] Garcia-Hernandez, Rubi, and Raul Garduno-Ramirez, “Modeling a Wind Turbine Synchronous Generator,” International Journal of Energy and Power 2.3 (2013).

[46] MASHIMO, Akihide, Masahiro HOSHI, and Mio UMEDA, “Permanent Magnet Synchronous Generator for Wind-Power Generation,” Energy Creation Technologies-Power Plants and New Energy 59, no. 2 (2013): 130.

[47] Cai, Hongwei, David Wood, and Qiao Sun, “Small Wind Turbine Generator Monitoring: A Test Facility and Preliminary Analysis,” In Quality, Reliability, Risk, Maintenance, and Safety Engineering (QR2MSE), 2013 International Conference on, pp. 1698-1701. IEEE, 2013.

[48] Penman, J., M. N. Dey, A. J. Tait, and W. E. Bryan, “Condition Monitoring of Electrical Drives,” Electric Power Applications, IEE Proceedings B 133, no. 3 (1986): 142-148.

[49] Djurovic, S., S. Williamson, P. J. Tavner, and W. Yang, “Condition Monitoring Artefacts for Detecting Winding Faults in Wind Turbine DFIGs,” In Proc. EWEC, pp. 16-19. 2009.

[50] Abdallah, A. Ali, J. Regnier, J. Faucher, and B. Dagues, “Simulation of Internal Faults in Permanent Magnet Synchronous Machines,” In Power Electronics and Drives Systems, 2005. PEDS 2005. International Conference on, vol. 2, pp. 1390-1395. IEEE, 2005.

[51] Vaseghi, Babak, Babak Nahid-Mobarakeh, Noureddine Takorabet, and Farid Meibody-Tabar, “Modeling of Non-Salient PM Synchronous Machines Under Stator Winding Inter-Turn Fault Condition: Dynamic Model-FEM Model,” In Vehicle Power and Propulsion Conference, 2007. VPPC 2007. IEEE, pp. 635-640. IEEE, 2007.

[52] Kevin Alewine, "Wind Turbine Generator Failure Modes, "Renewable Energy Services. Shermco Industries, http://www.nerl.gov/wind/pdfs/day1_sessioniv_04_shemco_alewine.pdf.

[53] Rotating Machinery Insulation Test Guide, Doble Engineering Company, 1985.

[54] Handbook to Assess the Insulation Condition of Large Rotating Machines, EPRI Power Plant Electrical Reference Series, vol. 16.

[55] Albright, D. R, “Interturn Short-Circuit Detector for Turbine-Generator Rotor Windings,” Power Apparatus and Systems, IEEE Transactions on 2 (1971): 478-483.

[56] Streifel, Robert J., R. J. Marks II, M. A. El-Sharkawi, and I. Kerszenbaum, "Detection of Shorted-Turns in the Feld Winding of Turbine-Generator Rotors Using Novelty Detectors-Development and Field Test," IEEE Transactions on Energy Conversion 11, no. 2 (1996): 312-317.

[57] Rosero, J., J. Cusido, A. Garcia Espinosa, J. A. Ortega, and L. Romeral, "Broken Bearings Fault Detection for a Permanent Magnet Synchronous Motor under Non-Constant Working Conditions by Means of a Joint Time Frequency Analysis," In Industrial Electronics, 2007. ISIE 2007. IEEE International Symposium on, pp. 3415-3419. IEEE, 2007.

[58] Pacas, Mario, Sebastian Villwock, and Ralf Dietrich, "Bearing Damage Detection in Permanent Magnet Synchronous Machines," In Energy Conversion Congress and Exposition, 2009. ECCE 2009. IEEE, pp. 1098-1103. IEEE, 2009.

[59] Kramer, and H.C. "Broken Damper Bar Detection Studies Using Flux Probe Measurements and Time-Stepping Finite Element Analysis for Salient-Pole Synchronous Machines," Diagnostics for Electric Machines, Power Electronics and Drives, 2003. SDEMPED 2003. 4th IEEE International Symposium on. IEEE, 2003.

[60] J. Bacher, "Detection of Broken Damper Bars of a Turbo Generator by the Field Winding," International conference on Renewable Energy Power Quality, JCREPC 2004.

[61] Rahimian, Mina M., and Karen Butler-Purry, "Modeling of Synchronous Machines with Damper Windings for Condition Monitoring," In Electric Machines and Drives Conference, 2009. IEMDC'09. IEEE International, pp. 577-584. IEEE, 2009.

[62] AKAR, Mehmet, and Mustafa EKER, "Demagnetization Fault Diagnosis in Permanent Magnet Synchronous Motors," Przegląd Elektrotechniczny 89 (2013): 229-233.

[63] Bonaldi, Erik Leandro, Levy Ely de Lacerda de Oliveira, Jonas Guedes Borges da Silva, Germano Lambert-Torresm, and Luiz Eduardo Borges da Silva, "Predictive Maintenance by Electrical Signature Analysis to Induction Motors," (2012).

[64] Khoobroo, Amir, and Babak Fahimi, "A Novel Method for Permanent Magnet Demagnetization Fault Detection and Treatment in Permanent Magnet Synchronous Machines," In Applied Power Electronics Conference and Exposition (APEC), 2010 Twenty-Fifth Annual IEEE, pp. 2231-2237. IEEE, 2010.

[65] Stone, Greg, Steve Campbell, and Serge Tetreault, "Inverter-Fed Drives: which Motor Stators are at Risk," Industry Applications Magazine, IEEE 6, no. 5 (2000): 17-22.

[66] Briz, Fernando, Michael W. Degner, Antonio Zamarron, and Juan M. Guerrero, "On-Line Stator Winding Fault Diagnosis in Inverter-Fed AC Machines Using High Frequency Signal Injection," In Industry Applications Conference, 2002. 37th IAS Annual Meeting. Conference Record of the, vol. 3, pp. 2094-2101. IEEE, 2002.

[67] Lee, Sang Bin, Karim Younsi, and Gerald B. Kliman, "An Online Technique for Monitoring the Insulation Condition of AC Machine Stator Windings," Energy Conversion, IEEE Transactions on 20, no. 4 (2005): 737-745.

[68] Stone, Greg, and Joe Kapler, "Stator Winding Monitoring," Industry Applications Magazine, IEEE 4, no. 5 (1998): 15-20.

[69] E. L. Brancato, “Insulation Aging a Historical and Critical Review,” Electrical Insulation, IEEE Transactions on 4 (1978): 308-317.

[70] G. C. Stone, “Advancements during the Past Quarter Century in On-Line Monitoring of Motor and Generator Winding Insulation,” Dielectrics and Electrical Insulation, IEEE Transactions on 9, no. 5 (2002): 746-751.

[71] Benbouzid, Mohamed El Hachemi, Michelle Vieira, and Céline Theys, “Induction Motors' Faults Detection and Localization Using Stator Current Advanced Signal Processing Techniques,” Power Electronics, IEEE Transactions on 14, no. 1 (1999): 14-22.

[72] Jung, Jee-Hoon, Jong-Jae Lee, and Bong-Hwan Kwon, “Online Diagnosis of Induction Motors Using MCSA,” Industrial Electronics, IEEE Transactions on 53, no. 6 (2006): 1842-1852.

[73] Tavner, P. J., B. G. Gaydon, and D. M. Ward, “Monitoring Generators and Large Motors,” Electric Power Applications, IEE Proceedings B 133, no. 3 (1986): 169-180.

[74] Ilonen, Jarmo, J-K. Kamarainen, Tuomo Lindh, Jero Ahola, Heikki Kälviäinen, and Jarmo Partanen, “Diagnosis Tool for Motor Condition Monitoring,” Industry Applications, IEEE Transactions on 41, no. 4 (2005): 963-971.

[75] Schoen, Randy R., Brian K. Lin, Thomas G. Habetler, Jay H. Schlag, and Samir Farag, “An Unsupervised, On-Line System for Induction Motor Fault Detection Using Stator Current Monitoring,” Industry Applications, IEEE Transactions on 31, no. 6 (1995): 1280-1286.

[76] Stack, Jason R., Ronald G. Harley, and Thomas G. Habetler, “An Amplitude Modulation Detector for Fault Diagnosis in Rolling Element Bearings,” Industrial Electronics, IEEE Transactions on 51, no. 5 (2004): 1097-1102.

[77] Yazici, Birsen, and Gerald B. Kliman, “An Adaptive Statistical Time-Frequency Method for Detection of Broken Bars and Bearing Faults in Motors Using Stator Current,” Industry Applications, IEEE Transactions on 35, no. 2 (1999): 442-452.

[78] Kiani, Morgan, and Wei-Jen Lee, “Effects of Voltage Unbalance and System Harmonics on the Performance of Doubly Fed Induction Wind Generators,” Industry Applications, IEEE Transactions on 46, no. 2 (2010): 562-568.

[79] Elkasabgy, Nagwa M., Anthony R. Eastham, and Graham E. Dawson, “Detection of Broken Bars in the Cage Rotor on an Induction Machine," Industry Applications, IEEE Transactions on 28, no. 1 (1992): 165-171.

[80] Cho, K. Rae, Jeffrey H. Lang, and Stephen D. Umans, “Detection of Broken Rotor Bars in Induction Motors Using State and Parameter Estimation,” Industry Applications, IEEE Transactions on 28, no. 3 (1992): 702-709.

[81] Lu, Dingguo, Xiang Gong, and Wei Qiao, “Current-Based Diagnosis for Gear Tooth Breaks in Wind Turbine Gearboxes,” In Energy Conversion Congress and Exposition (ECCE), 2012 IEEE, pp. 3780-3786. IEEE, 2012.

[82] E. Muljadi, and J. Green, “Cogging Torque Reduction in a Permanent Magnet Wind Turbine Generator,” In Proc. of the 21st American Society of Mechanical Engineers Wind Energy Symposium, pp. 1-8. 2002.

[83] W. Wu, V. S. Ramsden, T. Crawford, and G. Hill, "A Low Speed, High-Torque, Direct-Drive Permanent Magnet Generator for Wind Turbines," In Industry Applications Conference, 2000. Conference Record of the 2000 IEEE, vol. 1, pp. 147-154. IEEE, 2000.

[84] Z. Q. Zhu, and David Howe, "Influence of Design Parameters on Cogging Torque in Permanent Magnet Machines," Energy Conversion, IEEE Transactions on 15, no. 4 (2000): 407-412.

[85] Amirat, Yassine, Mohamed El Hachemi Benbouzid, Elie Al-Ahmar, Bachir Bensaker, and Sylvie Turri, "A Brief Status on Condition Monitoring and Fault Diagnosis in Wind Energy Conversion Systems," Renewable and Sustainable Energy Reviews 13, no. 9 (2009): 2629-2636.

[86] Lungoci, Carmen, and Dan Stoia, "Temperature Effects on Torque Production and Efficiency of Motors with NdFeB," parameters 2 (2008): 3.

[87] Li Bin, Xu Jianyuan, and Teng Yun, "Wind Farm Based on Double ANNs," Power and Energy Engineering Conference (APPEEC), 2010, pp: 1–4.

[88] Ma K. B., Liu J. R., McMichael C., Bruce R., Mims D., and Chu W. K., "Spontaneous and Persistent Rotation of Cylindrical Magnets Levitated," By Y-Ba-Cu-O superconductors. Journal of applied physics, 70(7), 3961-3963. (1991).

[89] Incropera F. P., and DeWitt D. P., "Fundamentals of Heat and Mass Transfer," John Wiley and Sons. Kays, WN and London, AL, Compact Heat Exchangers, MacGraw-Hill, New York. (1996).

[90] A. Tveito, and R. Winther, "Introduction to Partial Differential Equations," Springer, New York, 1998.

[91] Kittel C., and McEuen P., "Introduction to Solid State Physics," (Vol. 8). New York: Wiley. (1976).

[92] Kellog O. D., "Foundation of Potential Theory," Springer, Berlin, 1967.

[93] Data of a variable speed wind turbine 600 KW rated power, three phase permanent magnetic type 440/660 V 60 Hz. Provided by Dr. Kathryn, Colorado School of Mines and the National Renewable Energy Laboratory, 2013.

[94] J. F. Manwell, J. G. Mcgowan, and A. L. Rogers, "Wind Energy Explained Theory, Design, and Application," WILLY, Second edition 2009.

[95] Z. Hameed, Y. S. Hong, Y. M. Cho, S. H. Ahn, and C. K. Song, "Condition Monitoring and Fault Detection of Wind Turbines and Related Algorithms: A review." Renewable and Sustainable Energy Reviews 13, no. 1 (2009): 1-39.

[96] Frank S. Barnes, and Jonah G. Levine, "Large Energy Storage System Handbook," CRC Press, Taylor & Francis Group, 2011.

[97] Wilkinson, R. Michal, Fabio Spinato, and Peter J. Tavner, "Condition Monitoring of Generators & other Subassemblies in Wind Turbine Drive Trains," In Diagnostics for Electric Machines, Power Electronics and Drives, 2007. SDEMPED 2007. IEEE International Symposium on, pp. 388-392. IEEE, 2007.

[98] Data of a variable speed offshore wind turbine 5 MW rated power, three phase permanent magnetic type 440/660 V 60 Hz. Provided by Dr. Kathryn, Colorado School of Mines and the National Renewable Energy Laboratory, 2013.

[99] P. Preecha, and J. Dejvises, "The Power Losses Calculation Technique of Electrical Machines Using the Heat Transfer Theory," In Power Engineering Conference, 2007. IPEC 2007. International, pp. 297-301. IEEE, 2007.

[100] Incropera, DeWitt, Bergman, and Lavine, "Fundamentals of Heat and Mass Transfer," IET Renewable Power Generation, April 2008.

[101] J. H. Lienhard, "A Heat Transfer Textbook," Courier Dover Publications, 2011.

[102] Ramesh K. Shah, and Dušan P. Sekulić, "Fundamental of Heat Exchanger Design," Published Online, 2007.

[103] Yanyong Li, "Fluid Mechanics," Thermal Energy Dynamics Research Institute, IEEE, 2011.

[104] Nilsson, Julia, and L. Bertling, "Maintenance Management of Wind Power Systems Using Condition Monitoring Systems—Life Cycle Cost Analysis for Two Case Studies," Energy Conversion, IEEE Transactions on 22.1 (2007): 223-229.

[105] Amayri, Abeer, Z. Tian, and T. Jin, "A Condition Based Maintenance of Wind Turbine Systems Considering Different Turbine Types," Quality, Reliability, Risk, Maintenance, and Safety Engineering (ICQR2MSE), 2011 International Conference on. IEEE, 2011.

[106] T. Zhigang, J. Tongdan, B. Wu, and F. Ding, "Condition Based Maintenance Optimization for Wind Power Generation Systems under Continuous Monitoring," Renewable Energy 36.5 (2011): 1502-1509.

[107] S. Metwalley, and S. Abouel-seoud, "Condition Based Maintenance Optimization for Faulty Gearbox under Continuous Noise Monitoring," British Journal of Applied Science & Technology 3.2 (2013).

[108] H. Krokoszinski, "Efficiency and Effectiveness of Wind Farms—Keys to Cost Optimized Operation and Maintenance," Renewable Energy 28.14 (2003): 2165-2178.

[109] Byon, Eunshin, and Y. Ding, "Season-Dependent Condition-Based Maintenance for a Wind Turbine Using a Partially Observed Markov Decision Process," Power Systems, IEEE Transactions on 25.4 (2010): 1823-1834.

[110] D. Banjevic, A.K.S. Jardine, V. Makis, and M. Ennis, "A Control-Limit Policy and Software for Condition-Based Maintenance Optimization," INFOR-Ottawa- 39, no. 1 (2001): 32-50.

[111] R. Karki, Po Hu, and R. Billinton, "A Simplified Wind Power Generation Model for Reliability Evaluation," Energy Conversion, IEEE Transactions on 21.2 (2006): 533-540.

[112] H. Guo, S. Watson, P. Tavner, and J. Xiang, "Reliability Analysis for Wind Turbines with Incomplete Failure Data Collected from after the Date of Initial Installation," Reliability Engineering & System Safety 94.6 (2009): 1057-1063.

[113] P. L. Hall, and J. E. Strutt, "Probabilistic Physics-Of-Failure Models for Component Reliabilities Using Monte Carlo Simulation and Weibull Analysis: a Parametric Study," Reliability Engineering & System Safety 80.3 (2003): 233-242.

[114] E. Martinez, F. Sang, S. Pellegrinni, E. Jimenez, and J. Blanco, "Life Cycle Assessment of a Multi-Megawatt Wind Turbine," Renewable Energy 34.3 (2009): 667-673.

[115] Ş. Zekai, "Statistical Investigation of Wind Energy Reliability and its Application," Renewable energy 10.1 (1997): 71-79.

[116] S.S. Rao, "Reliability-Based Design," McGraw-HillM United States, 1992.

[117] W. Christopher, "Wind Turbine Reliability: Understanding and Minimizing Wind Turbine Operation and Maintenance Costs," United States. Department of Energy, 2006.

[118] M. Xie, Y. Tang, and T. N. Goh, "A modified Weibull Extension with Bathtub-Shaped Failure Rate Function," Reliability Engineering & System Safety 76.3 (2002): 279-285.

[119] M. Xie, and C. D. Lai, "Reliability Analysis Using an Additive Weibull Model with Bathtub-Shaped Failure Rate Function," Reliability Engineering & System Safety 52.1 (1996): 87-93.

[120] D. N. Prabhakar Murthy, M. Bulmer, and J. Eccleston, "Weibull Model Selection for Reliability Modelling," Reliability Engineering & System Safety 86.3 (2004): 257-267.

[121] Bagdonavicius Vilijandas, and Mikhail Nikulin, "Accelerated Life Models: Modeling and Statistical Analysis," CRC Press, 2010.

[122] T. Smith, B. Smith, and M. AK Ryan, "Survival Analysis Using Cox Proportional Hazards Modeling for Single and Multiple Event Time Data," Proceedings of the

Twenty-Eighth Annual SAS Users Group International Conference, SAS Institute, Inc, Cary, paper. 2003.

[123] David W. Coit, and Kieron A. Dey, "Analysis of Grouped Data from Field-Failure Reporting Systems," Reliability Engineering & System Safety 65.2 (1999): 95-101.

[124] A. J. Seebregts, L. W. M. M. Rademakers, and B. A. Van Den Horn, "Reliability Analysis in Wind Turbine Engineering," Microelectronics Reliability 35.9 (1995): 1285-1307.

[125] Data of a variable speed wind turbine (A), 750 KW rated power, three phase permanent magnetic type 440/660 V 60 Hz. Provided by Dr. Kathryn Johnson, Colorado School of Mines, and the National Renewable Energy Laboratory, 2013.

[126] Data of a variable speed wind turbine (B), 750 KW rated power, three phase permanent magnetic type 440/660 V 60 Hz. Provided by Dr. Kathryn Johnson, Colorado School of Mines, and the National Renewable Energy Laboratory, 2013.

[127] Achinity Haldar, and Sankaran Mahadevan, "Probability, Reliability, and Statistical Method in Engineering Design," WILLY 2000.

[128] P. J. Tavner, F. Spinato, G. J. W van Bussel, and E. Koutoulakos, "Reliability of Different Wind Turbine Concepts with Relevance to Offshore Application," European Wind Energy Conference & Exhibition, 2008.

[129] Douglas C. Montgomery, Elizabeth A. Peck, and Geoffrey Vining, "Introduction to Linear Regression Analysis," WILEY, Fifth edition 2012.

[130] Data of a variable speed wind turbine 5 MW rated power, three phase permanent magnetic type 440/660 V 60 Hz. Provided by Dr. Kathryn, Colorado School of Mines, and the National Renewable Energy Laboratory 2013.

[131] N.H. Bingham, and John M. Fry, "Regression Linear Models in Statistic," Springer-Verlag London Limited 2010.

[132] Ali S. Hadi, and Bertram Price, "Regression Analysis by Example," Third edition, Wiley Series in Probability and Statistics, 2000.

[133] Wold, Svante, Arnold Ruhe, Herman Wold, and W. J. Dunn, III, "The Collinearity Problem in Linear Regression. The Partial Least Squares (PLS) Approach to Generalized Inverses," SIAM Journal on Scientific and Statistical Computing 5, no. 3 (1984): 735-743.

[134] IBM SPSS software, http://www-01.ibm.com/software/ analytics/ products/statistics/index.html. Dec. 05, 2013.

[135] Minitab 16 software, http://www.minitab.com. Dec. 05, 2013.